Design and Evaluation of Novel Ophthalmic Drug Delivery Systems of Brimonidine Tartrate

THESIS

Submitted in partial fulfillment

of the requirements for the degree of

DOCTOR OF PHILOSOPHY

By

PRAKASH BHAGAY

Under the Supervision of

Dr. SAJEEV CHANDRAN

BIRLA INSTITUTE OF TECHNOLOGY AND SCIENCE

PILANI (RAJASTHAN) INDIA

2010

BIRLA INSTITUTE OF TECHNOLOGY & SCIENCE
PILANI, RAJASTHAN

CERTIFICATE

This is to certify that the thesis entitled, "**Design and Evaluation of Novel Ophthalmic Drug Delivery Systems of Brimonidine Tartrate**" and submitted by **Prakash Bhagav** ID.No. **2005PHXF414P** for award of Ph.D. degree of the Institute embodies original work done by him under my supervision.

Date: 26/12/2010

(Dr. SAJEEV CHANDRAN)
Senior Manager,
Advanced Drug Delivery Systems-R&D,
Pharma R&D,
Lupin Research Park (Lupin Ltd.)
Pune. Maharashtra.

Dedicated

to

my Parents

ACKNOWLEDGEMENTS

I would like to take this opportunity to thank my research supervisor Dr. Sajeev Chandran who guided me meticulously throughout my research work at each and every step. He stood by me and helped me during the highs and lows of this research work encouraging me where required and disciplining me where necessary like a thorough professional that he is. His zeal for perfection has inculcated in me a deep sense of excellence which will surely inspire me in all my future endeavours. I consider myself blessed to have got this opportunity to work under such a versatile perfectionist. Thank you very much sir!

I am grateful to Prof. Bijendra Nath Jain, Vice-Chancellor, BITS Pilani, Prof. L. K. Maheshwari, Advisor and Former Vice-Chancellor, BITS, Pilani, Prof G. Raghurama, Director, BITS Pilani- Pilani Campus, Prof. K. E. Raman, Acting Director, BITS Pilani- K K Birla Goa Campus and Prof. R. K. Mittal, Director, BITS Pilani- Dubai Campus for giving me an opportunity to pursue my doctoral research work in the Institute and for all the facilities made available for the work.

I would like to place on record my special gratitude to Prof. R. N. Saha, Deputy Director, Research and Education Development and Administration, for all his help and suggestions as my doctoral advisory committee member. He has been my mentor, a great teacher, a role model and a constant motivator for me.

My sincere thanks to Prof. Ravi Prakash, Former Dean, Research & Consultancy Division, BITS, Pilani and currently Vice-Chancellor, JUIT, Solan, Himachal Pradesh, for his support, cooperation and encouragement at every stage of this research work.

I am thankful to Dr. A.K Das, Dean, Research & Consultancy Division, BITS, Pilani, for his help and support and for allowing me to use the facilities of Biological sciences laboratory.

Special thanks to Prof. R. Mahesh, Former Group Leader, Pharmacy group and Chief, Community Welfare division, for providing the facilities required for the research work and his constant support and help.

I would like to thank Dr. Ninad Deshpanday, President, Pharma R & D, Lupin Ltd. and Dr. Shirish Kulkarni, Vice president- ADDS R&D, Lupin Ltd, for giving me an opportunity to work in the ADDS R & D Laboratory of Pharma R & D, Lupin Research Park, Pune.

I would like to express thanks to Dr. Shrikant Charde, Group Leader, Pharmacy Group, for his support and encouragement and advices throughout my research.

I also thank nucleus members of R & C specially Dr. Hemant Jadhav and Mr. Sharad Srivastava for the cooperation and help at every stage of this research work.

I sincerely acknowledge the help rendered by (past and present) faculty members of Pharmacy group especially Dr. Archna Roy, Dr. Punna Rao, Mrs. Purna, Mr. Murli Manohar Pandey, Mr. Gautam Singhvi, Mr. Jaipal, Mr. Baldev, Mr. Sunil, Mrs. Preeti Jain, and Mr. Shvetank Bhatt.

I am very much thankful to Dr. S. K. Yadav, Mr. Dilip Pandey and Mr. Vadiraj for their wonderful help in carrying out in vivo studies in animal house.

Also special thanks to Mr. Rajesh Kulkarni and Mr. Satish Dalal, Managers at ADDS R& D, Lupin Ltd. A very special thanks to members of Lupin Research Park starting with Ashish D, Pravin B, Ashish T, Shraddha, Pandarinath, Harshal, Kishor, Ganesh, Amith, Asmita, Sameer, Mayank, Abhayraj, Garima for a wonderful time at Lupin and making it memorable.

I express my thanks to our laboratory attendants Gokulji, Hariramji, Yasinji, Naveen for all their help. Thanks are also due to the other office staff of Pharmacy Group, BITS, Pilani, including M. P Soniji, Sitaramji, Mathuramji, Puran and a special thanks to Ram Sutar.

Special thanks to all the graduate students who did project under my supervisor who helped at various phases of my work starting from Roma, Imran, Vinay, Megha, Priyanka, Sujitha, Pandurang, Sourabh, Darshan, Vaibhav and Durlabh.

A special lot of love and thanks to all of my seniors, doctoral friends and colleagues at BITS especially Dr. Girish Bende, Dr.Venu Gopal, Dr. Snehalatha, Dr. Praveen Hiremath, Dr. Prashant Kole, Dr. Debjani, Dr. Dinakaran, Dr. Senthil, Dr. Ragavendran, Dr. Raj Kumar for all their encouragement and help at various phases of my work. A heartfelt gratitude to Dr. Laila Fatima for helping and motivating me at all stages of my research work at BITS, Pilani.

A special thanks to all of my friends at BITS, Subrata Kundu, Sunil, Pritesh, Thimmappa, Pradeep, Deepak, Ashwin, Narayan, Arvind, Pankaj, Naveen, Mallari, Kamesh, Manoj, Sidheshwar, Sathish, Vasant, Emil, Prashant, Garudachari, Sudarshan, Buchi for having been so kind to me and making my stay at Pilani a very memorable one.

Heartfelt thanks to staff members of Kannada Vedike Prof G. Raghurama, Prof. H. V. Manjunath, Dr. Usha Manjunath, Dr. Geetha B, Dr. Ishwar Bhat, Mr. Kiran DC and Mrs. Mahela Kiran for being so friendly and their wonderful support during my tenure as

member and President of Kannada Vedike. Also thanks to Dr. Nagendra Parashar, Dr. TSB Sudarshan and Dr. Shikha.

A special lot of thanks to Sidharth, Rajiv, Shreyas, Manoj, Narayan, Rajeev, Rahul, Gopal, Sharath for their love, care and making my stay at BITS a memorable moments of life. Also thanks to Krishna, Aurithro, Sandeep, Tarun, Chitra and other members of Kannada Vedike, BITS Pilani for their support.

Thanks to my teachers Prof. M. D. Karvakar, Dr. N. Udupa, Dr. Sureshwar Pandey, Prof. Thampi and Prof (Mrs). Sarla Thampi for their wonderful moral support, constant motivation and inspiration.

Thanks are also due-to my friends Shreekant, Harish, Kiran, Vathan, Manjunath, Santhosh, Mahantesh, Satya Prakash, Natraj, Shreenivas Reddy, Jayanthi, Sindhu, Sateesh, Vadivelan, Somashekar.

I am highly grateful to FDC Ltd, Mumbai, India for providing gift samples of brimonidine tartrate.

A very special loving thanks to my *father*, whose love, profuse inspiration, patience and determination brought me here. To my *mother* who taught me how to face life and sacrificed a lot for me and my career. Special loving thanks to my sister *Suma* and brother *Uday* for their generous love, tremendous encouragement, infinite moral support without which this journey wouldn't have been possible. Also, a special thanks to my *Dada* for his moral support, encouragement, care and inspiration.

Very special loving thanks to my friend, my life partner *Vanisha,* for her love, constant encouragement, patience and loving support throughout.

Special thanks to my *Dada*, *Kaki* and my cousins *Prasad*, *Sowmya* for their never ending love and care.

Also thanks to *Mama*, *Mami* and *Avinash* for their support and motivation.

I fall short of words when I attempt to acknowledge God Almighty for showering blessings on me and giving me an opportunity to progress in life. I pray for constant mercy so that I can use my research in the service of humanity.

Prakash Bhagav

List of Abbreviations / Symbols

% CDR	Percentage cumulative drug released
% RSD	Percentage relative standard deviation
% w/v	Percent weight per volume
% w/w	Percent weight per weight
μV	Micro volts (unit for UV absorbance)
μg/ml	Microgram per millliter
λ_{det}	Selected Wavelength of detection
ATC	Accelerated test conditions (40° C ± 2° C/ 75 ± 5% RH)
ANOVA	Analysis of variance
ARVO	Association for research in vision and ophthalmology
$AUC_{(\Delta IOP\ vs.\ t)}$	Area under the ΔIOP vs. time curve
AUC_{Rel}	Relative Area under the ΔIOP vs. time curve
BKC	Benzalkonium chloride
BP	British Pharmacopeia
BRT	Brimonidine Tartrate
C_{max}	Maximum serum concentration
CAP	Cellulose acetate phthalate
CI	Confidence interval
CMA	Carboxy methyl acrylate
CMC	Carboxymethyl cellulose
CMV	Cyto megalo virus
Conc.	Concentration
CP	Carbopol
cP	Centi poise
$Dynes/cm^2$	Dynes per square centimeter
CRT	Controlled room conditions (25 °C ± 2° C / 60 ± 5% RH)
CV	Coefficient of variance
DSC	Differential scanning calorimetry
EC-22	Ethyl cellulose, viscosity 22 cP
EC-50	Ethyl cellulose, viscosity 50 cP
EDTA	Ethylene diamine tetra acetic acid
EE	Entrapment efficiency
ERL 100	Eudragit RL100
ERS 100	Eudragit RS100
et al.	Co-workers
FTIR	Fourier transform infrared spectrometry
F	Shear stress
$F_{calculated}$	Calculated F value

$F_{critical}$	Critical of tabulated F value
GG	Gellan gum
G	Shear rate
HA	Hyaluronic acid
HCl	Hydrochloric acid
HP beta CD	Hydroxy propyl beta cyclodextrine
HPMC K4M	Hydroxypropylmethylcellulose 4000 cps
HPMC K15M	Hydroxypropylmethylcellulose 15000 cps
HPMC K100M	Hydroxypropylmethylcellulose 100000 cps
HPLC	High performance liquid chromatography
HQC	High quality control concentration
h	Hour
ICH	International conference on harmonization
IAEC	Institutional Animal Ethics Committee
IOP	Intra ocular pressure
ΔIOP	Decrease in intra ocular pressure ($IOP_{zero\ time}$ - $IOP_{time\ t}$)
IP	Indian Pharmacopeia
IR	Infrared
I_{max}	Time for maximum intra ocular pressure reduction
J/g	Joules per gram
K	Release rate constant
K_{deg}	Degradation rate constant
KCl	Potassium chloride
KH_2PO_4	Potassium dihydrogen phosphate
LOD	Limit of detection
log P_{App}	Log to base 10 of P_{App}
LOQ	Limit of quantification
LQC	Lower quality control concentration
LCT	Lecithin
LCST	Lower critical solution temperature
LE	Loading efficiency
M	Molar
MATP	Mono amine terminated poloxamer
MC	Methylcellulose
MQC	Medium quality control concentration
MSSR	Mean sum of squares
NaOH	Sodium hydroxide
N	Newtons
NIH	National Institute of Health
nm	Nanometer
NMR	Nuclear magnetic spectroscopy
^oC	Degree centigrade

P_{App}	Apparent partition coefficient
pH	Negative log to the base 10 of hydrogen ion concentration
PEG	Poly ethylene glycol
PEO 100 kD	Poly ethylene oxide, molecular weight 100 kD
PEO 400 kD	Poly ethylene oxide, molecular weight 400 kD
pKa	Negative log to base 10 of acid dissociation constant
PF 127	Poloxamer Pluronic F-127
PF 68	Poloxamer Pluronic F-68
PNIAA	Poly -N (isopropylacrylamide)
PS	Particle size
PVA	Poly vinyl alcohol
PVP	Poly vinyl pyrrolidine
r	Correlation coefficient
r^2	Regression coefficient
RH	Relative humidity
rpm	Revolutions per minute
SD	Standard deviation
SEM	Scanning electron microscope
STF	Simulated tear fluid
$t_{1/2}$	Biological half life
$t_{10\%}$	Time taken for 10 % drug release in hours
$t_{20\%}$	Time taken for 20 % drug release in hours
$t_{50\%}$	Time taken for 50 % drug release in hours
$t_{90\%}$	Time taken for 90% drug release in hours
T_{90}	Time taken for drug concentration to reduce to 90% of its labeled claim (shelf life)
TDW	Triple distilled water
TEM	Transmission electron microscopy
TPP	Tripolyphosphate
t_{max}	Time taken for maximum IOP reduction
USP	United States Pharmacopeia
UV-Vis-NIR	Ultraviolet- visible- near infrared

List of Tables

List of Figures

ABSTRACT

The main objective of the present work was to design, develop novel ophthalmic drug delivery systems for better ocular delivery of brimonidine tartrate for its potential use in treating glaucoma. Brimonidine tartrate, a selective alpha-2 agonist is used in the treatment of open angle glaucoma as ocular hypotensive agent. It is used as monotherapy or in combination with other antiglaucoma drugs. Recently it has also been reported to have neuroprotective function in glaucoma, thus making it an important member of the class of antiglaucoma agents. The currently available formulations of brimonidine tartrate (eye drops) have poor ocular bioavailability, poor ocular contact and require frequent dosing and thus result in patient noncompliance.

In order to improve the drawbacks of conventional formulations, novel formulations were proposed, which can improve the delivery of brimonidine tartrate by increasing ocular residence time along with controlled release of drug for a longer period of time.

Novel formulations such as in situ gels, ocular inserts and nanoparticles were prepared for brimonidine tartrate employing various techniques and polymeric combinations.

In situ gels were prepared using ion activated (gellan gum) and temperature activated, poly-(N-isopropyl acrylamide) in situ gelling polymer. The prepared in situ gels were evaluated for their physicochemical properties, gelation temperature, rheology, mucoadhesive strength and in vitro drug release. The results showed that the in situ gels were of good physicochemical properties, gelation temperature was found to be close to the temperature of topical eye. All the formulations were pseudoplastic in nature and mucoadhesive. The drug release from the optimized formulations were controlled and prolonged for a longer period of up to 16 h, depending on the polymer proportion in the formulations.

Ocular inserts were prepared by using hydrophilic/ swellable/ erodible and hydrophobic/ inert/ zwitterionoic polymers, either alone or in combination. The effect of polymer type and proportion on the physicochemical properties, mucoadhesive strength, erosion and in vitro drug release was extensively investigated. The prepared ocular inserts had acceptable physicochemical properties with good mucoadhesive strength which depended on the proportion of hydrophilic polymer proportion in the matrix. The in vitro drug release was modified by the addition of hydrophobic/ inert/ zwitterionoic polymer to the formulations. The optimized formulations showed a prolonged controlled release for up to 24 h with sufficiently high mucoadhesive strength.

Long acting nanoparticles formulations of brimonidine tartrate were prepared using combination of Eudragit RL 100 & Eudragit RS 100 and chitosan by multiple-emulsion solvent evaporation and ionic gelation method respectively. The effect of various formulation and process variables on the characteristics of nanoparticle (average particle size, drug loading and encapsulation efficiency) were investigated. The results showed that the characteristics of nanoparticles depended on the formulation and process variables. The in vitro drug release from the nanoparticles varied depending on the proportion of polymer in the formulation. The drug release was extended and controlled for a prolonged period with optimized formulations showing drug release up to 48-72 h.

The stability studies performed as per ICH guidelines at various storage conditions suggested that the selected optimized formulations were stable with reasonable predicted shelf life.

Based on in vitro results, few formulations were selected for in vivo ocular irritation and pharmacodynamic efficacy studies on rabbits. Glaucoma was induced by single posterior injection of alpha-chymotrypsin. The ocular irritation studies revealed the absence of any dosage form related irritation in the eye. All the formulations were well tolerated. In vivo IOP reduction efficacy studies showed that the selected formulations have a greater ability to reduce elevated IOP compared to conventional eye drop preparations. The area under the decrease in ΔIOP vs. time curve ($AUC_{(\Delta IOP\ vs.\ t)}$) showed that the extent and duration of IOP reduction was more prominent and prolonged. The AUC_{Rel} values were found to be in the range of 4-7 folds, thus suggesting improvement in clinical efficacy with the designed formulations.

It can be concluded that the novel formulations prepared (in situ gels, ocular inserts and long acting nanoparticles) have potential to improve the delivery of brimonidine tartrate, for more efficacious treatment of glaucoma.

TABLE OF CONTENTS

CHAPTER ONE

INTRODUCTION

1. INTRODUCTION

The 'eye' is considered as most specialised sensory organ that is relatively secluded and inaccessible from other organs of the body. Because of its anatomical isolation and the presence of various barriers surrounding the eye, the designing of drug delivery systems that meets the desired clinical attributes is a challenging task to the formulation scientist. Understanding of drug disposition ocular kinetics is limited due to non-availability of human eye tissues and most of the information is based on empirical animal models. Also the precorneal fluid dynamics that acts to wash off topically applied formulations contributes in rapid drainage of drug out of eye. All these result in a net absorption of less than 10 % of topically administered dose from the drug delivery system into the eyes. The low bioavailability from topical drops require frequent administration in order to maintain a therapeutically effective concentration in the eye at the site of action. Also the nasolacrymal drainage system tends to facilitate the systemic entry of the drugs and resulting in undesirable systemic side effects (Gibaldi and Perrier, 1982).

An ideal topical ocular drug delivery system should be the one which can reside in the precorneal space of the eye for a longer period of time, without causing any visual disturbances or ocular irritation, releases the drug slowly over a period of time with minimum or no systemic entry of the drug. All these requirements and specialized design attributes makes ocular drug delivery systems different from any other dosage forms both in terms of design and performance.

This chapter mainly reviews the; (i) anatomical and physiological considerations of eye pertaining to the ocular delivery and disposition, (ii) diseases affecting the eye, with an emphasis on glaucoma and its management, (iii) factors affecting the bioavailability of the administered drug in terms of pharmacokinetics and physicochemical properties of the drug, (iv) formulation approaches for better ocular drug delivery. In the end, objectives of the proposed research work to design novel ophthalmic drug delivery systems of Brimonidine tartrate has been discussed.

1.1. Anatomical and physiological considerations

The understanding of anatomical and physiological aspects of eye is necessary for developing a therapeutically effective and elegant dosage form for topical ocular applications. Also because of the numerous protective barriers surrounding the eye, the drug needs to pass through before reaching the site of action; it is impervative to understand the mechanisms and routes of permeation of drug.

Human eye has as circumference of 75 mm, volume of 6.5 ml and combined weight of 6.7 to 7.5 g (Dukes-Elder, 1961). The anatomy of eye and the routes of drug delivery pertaining to eye are shown in the Fig 1.1 and Fig 1.2 respectively. The various parts of eye pertaining to topical ocular drug delivery are described in the following sections.

1.1.1. Extra ocular structures

The extraocular structures of eye consist of orbit, eye brows, eye lids and extraocular muscles.

(a) Orbit: It is the bony cavity of the skull located on either side of the nose where eyes are rested. The globe occupies about 20% of the cavity on nearer to the upper and lateral sides (Riordan-Eva and Tabbara, 1992). The connective and adipose tissues and six extra ocular muscles help the eye in the vision.

(b) Conjunctiva: The conjunctiva is a thin vascular mucous membrane consisting of two or more layers of epithelia cells. The conjunctiva is a thin and vascular mucous membrane consisting of two to three layers of epithelial cells overlying a loose, highly vascular connective tissue. The tight junctions on the apical surface of the epithelium act as the main barrier for drug penetration (molecules > 20,000 D) across the tissue, although they are not as tight as the corneal epithelium, which is impermeable to molecules larger than 5000 D (Huang et al, 1989). The conjunctiva covers the anterior surface of the globe (bulbar conjunctiva) with the exception of the cornea, and is folded at the fornix (fornix conjunctiva) to form the palpebral conjunctiva, which lines the inner surface of the eyelids. The cul de sac occurs between the reflction of bulbar conjunctiva and palpebral conjunctiva. The bulbar conjunctiva represents the first barrier for permeation of topically applied drugs via the non-corneal route (Ahmed and Patton, 1985).

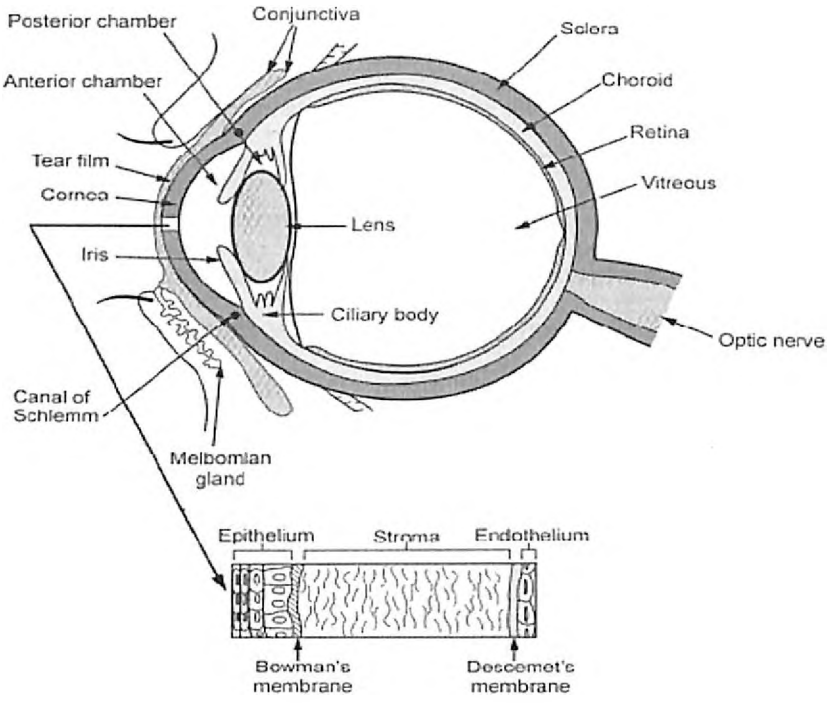

Fig 1.1: Schematic cross section of human eye and cornea (Riordan-Eva and Tabbara, 1992).

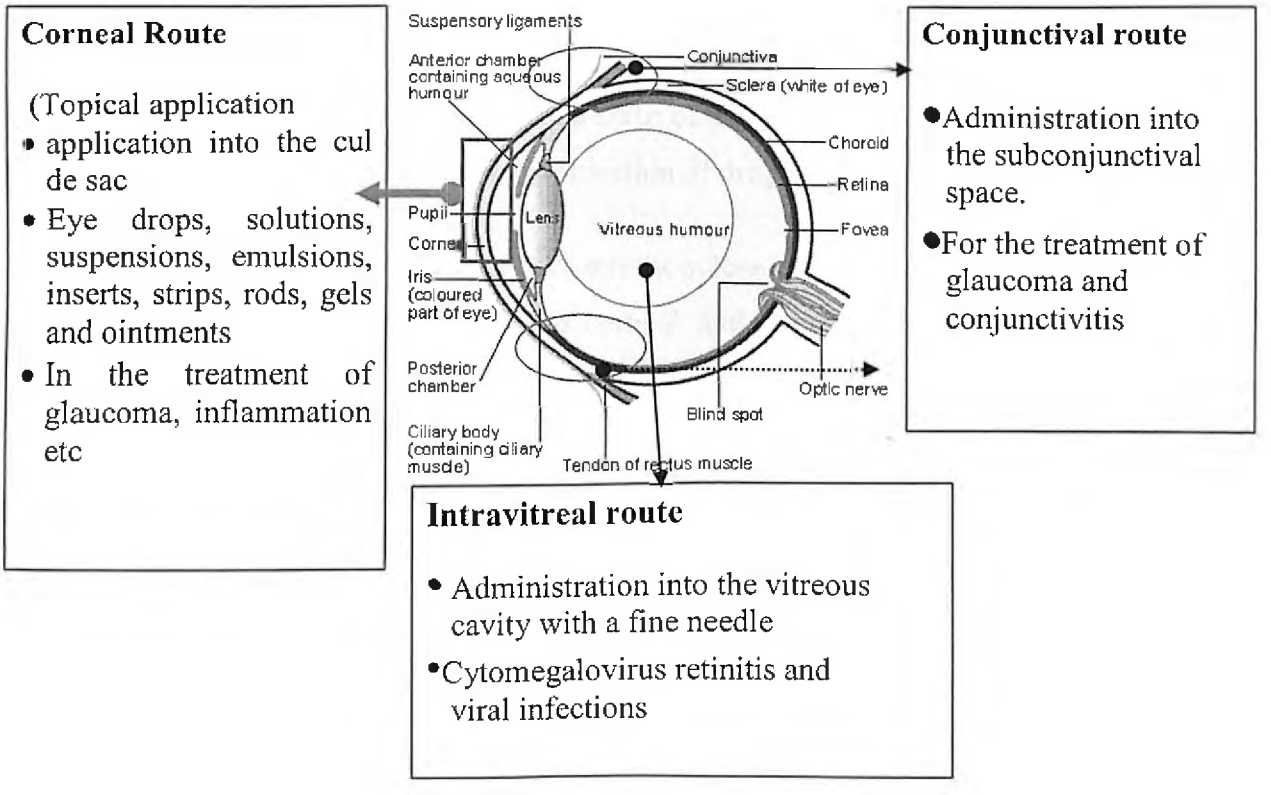

Fig 1.2: Anatomy of eye pertaining to various routes of ocular drug delivery.

(c) Eyebrows and eyelids: Eyebrows are positioned transversely above eyes along the superior orbital ridges of the skull. Owing to their position and curvature, they prevent perspiration or particles from running into the eyes and thus aids in the protection of the eye. Eyelids are two movable folds, upper and lower, which form the anterior protection for the eye. These mobile folds along with their dense sensory innervations and eyelashes protect the eye from mechanical or chemical injury, provide a barrier against excessive light, aid in blinking, and retard evaporation from the surface of the eye. Blinking, a coordinated movement of the orbicularis oculi, levator palpebrae, and Muller's muscle, serves to assist in spreading of the secreted tear film over the cornea and conjunctiva (Martola and Baum, 1968)

1.1.2. Anterior segment

The major parts of anterior segment are cornea, limbus, trabecuar meshwork and schlemm's canal, anterior uvea (iris, pupil and ciliary body) and lens (Duke-Elder, 1961).

(a) Cornea: The cornea is made of stroma (up to 90 % of its thickness), bounded externally by epithelium and Browman's membrane and internally by Descemet's membrane and the epithelium (Table 1.1). Cornea has a diameter of 11.5 mm and anterior corneal radius of curvature of about 7.8 mm. the endothelium is in contact with the aqueous humor of the anterior chamber and is about 200 times more permeable than the epithelium. Though cornea covers only one sixth of the total surface area of the eye, it is considered as the main pathway for the permeation of drugs into intraocular tissues.

(b) Limbus: It is the transitional zone between the sclera and conjunctiva and is about 1-2 mm in width. The limbic structures are corneal and anterior conjunctival epithelium (externally) and trabecular mesh work and schlemm's canal internally. The trabecular meshwork and schlemm's canal are located just above the apex of the peripheral anterior chamber angle between cornea and iris root. The trabecular meshwork and schlemm's canal forms routes for the outflow of aqueous humor from anterior segment of the eye.

Table 1.1: Various cell layers of the corneal membrane (Martola and Baum, 1968).

Layer	Thickness	Composition	Functions
Epithelium	50-60 μm	5-6 layers of epithelial cells, highly hydrophobic in nature	Outer most layer of the cornea and thus, barrier to invasion by foreign substances; holds tear to anterior surface of the eye
Bowman's membrane	8-14 μm	Homogenous acellular sheet consisting of fine fibrils and lacks elastin	Connective tissue between the basement membrane and stroma
Stroma	400-500 μm	200-250 alternating lamellae of collagenous tissue, highly hydrophilic in nature	Gives physical strength and optical transparency
Descemet's membrane	10-15 μm	Modified basement membrane of the epithelial cells	Imparts elasticity and resistance to proteolytic enzymes
Endothelium	5-6 μm	Lowest layer of the cornea with single layer of flattened epithelial cells with substantial intercellular space.	Active fluid transport through mitochondria, vesicles and ion pumps

(c) Anterior uvea: It consists of ciliary body, iris and pupil. The ciliary body comprises of ciliary muscles and ciliary processes. The secretion of aqueous humor takes place here and the ciliary body nourishes eye and helps in accommodation.

The iris is a thin disc suspended in aqueous humor between cornea and lens. The pupil, the central circular aperture of iris, composed of pigmented epithelial cell layer, the iridial sphincter, radial dilator muscle and the stroma.

(d) Lens: A biconvex, transparent epithelial body located behind the pupil between iris and vitreous body. It has a diameter of 10 mm. the lens consists of fibres derived from the proliferating lens epithelial cells.

1.1.3. Posterior segment

The main components of posterior segment are sclera, choroid, retina and optic nerve.

(a) Sclera: Sclera is the outermost film coat of the eye that is about 0.6-1 mm in thickness and 22 mm in diameter (Hogan et al, 1971). Sclera serves as a protective barrier for the eye. It is composed of collagen fibres as corneal stroma which is opaque (Hogan et al, 1971).

(b) Choroid: It is a vascularised tissue between retina and sclera consists of vessel layer and choriocapillary layer Bruch's membrane.

(c) Retina: It is a thin transparent tightly organised structure of neurons, glial cells and blood vessels. Retina consists of 9 layers and the thickness is approximately 0.11-0.18 mm. The layers of retina are, internal limiting membrane, nerve fibre layer, ganglionic cell layer, inner plexiform layer, inner nuclear layer, outer plexiform layer, outer nuclear layer, external limiting membrane and inner and outer segments of rods and cones.

(d) Optic nerves: Optic nerves are the means through which the retinal output travels to the optic chiasm (Anderson and Hoyt, 1969). It consists of myelinated fibres and has intraocular portion, intaorbital portion, intracanalicular portion and intecranial portion. The optic nerve is sheathed by the meninges, which is continuous with those of brain and it is the ophthalmic artery which is the primary source of all arterial branches to the optic nerve.

1.1.4. Eye fluids

Various fluids in the eye include the lachrymal system (including tear, secretory and drainage mechanism), aqueous humor and vitreous humor (Moroi and Lichter, 2001).

(a) Lachrymal system: It has glandular secretory elements and excretory ductal elements as collection portion (Moroi and Lichter, 2001). The tear is composed of salts, proteins, lipids, phospholipids, and enzymes in a water base. It moistens, lubricates and flushes the anterior surface of the eye. The tear is a trilaminar film with each layer having different composition. The anterior layer is made of lipid along with small amount of mucin and proteins. The middle layer, that comprises 98 % of the tear film, is predominantly aqueous in nature containing electrolytes, water and various proteins. The cul-de-sac normally holds 10 µl of tears and up to 25 % of the tear fluid is lost due to evaporation. Various physical properties of human tear are tabulated in Table 1.2. The tear drainage system starts through small puncta located on the medial aspects of both the upper and lower eyelids. Tears enter the puncta with each blinking and from the puncta move into the nose through canaliculi, lachrymal sac and nasolacrymal duct.

Table.1.2: Physical properties of human tear (Berman ER, 1991).

Physical property	Values
Osmotic pressure	311-350 mOsm/l
pH	7.4 (7.3-7.7)
Refractive index	1.357
Volume	7.0-30.0 µl
Oxygen tension (precorneal tear film)	140-160 mm Hg
Flow rate	0.5-2.2 µl/min
Buffer capacity	3.6×10^{-5}

(b) Aqueous humor: Aqueous humor is a clear colourless fluid with a chemical composition similar to that of blood plasma, but with low protein content. It is secreted by non-pigmented epithelial cells of the ciliary body, specifically by ciliary processes into the posterior chamber of the anterior segment of the eye. The approximate volume of aqueous humor held in posterior chamber is about 250 µl, with a turnover rate of approximately 1%. It flows through the narrow cleft between the front of the lens and the back of the iris to escape through the pupil into anterior chamber and finally gets drained off out of the eye via trabecular meshwork. The two enzymes involved here are sodium- potassium activated adenosine triphosphatase and carbonic anhydrase. These enzymes serve to transport sodium, chloride and bicarbonate ions into the enfolding of the non-pigmented epithelial cells, because of which an osmotic pressure gradient is created, that subsequently attracts water (Berman ER, 1991).

The aqueous humor contains mainly bicarbonate, chloride, sodium, calcium, potassium and phosphate ions. Proteins present are albumin, beta-globulins. It also contains ascorbates, glucose, lactates, amino acids etc.

The production of aqueous humor takes place by two processes

1. Filtration: As the blood flows into the ciliary body's capillaries, it gets filtered by endothelial cells of the capillaries, the resulting plasma then gets refiltered by pigmented and non-pigmented ciliary epithelial cells and subsequently poured into the posterior chamber of the eye as aqueous humor.

2. Active transport: It is also called Diamond-Bosset model, where in non-pigmented ciliary epithelial cells induces some osmotic pressure gradients in between the cells. This occurs due to the higher concentration of solutes in the proximal part of the intracellular

space, generates a flow of water. As it passes proximal part to the distal part, the concentration diminishes, the liquid ultimately releases as aqueous humor. The pathway of aqueous humor production in the eye is presented in Fig 1.3 (Ooteghem, 1993).

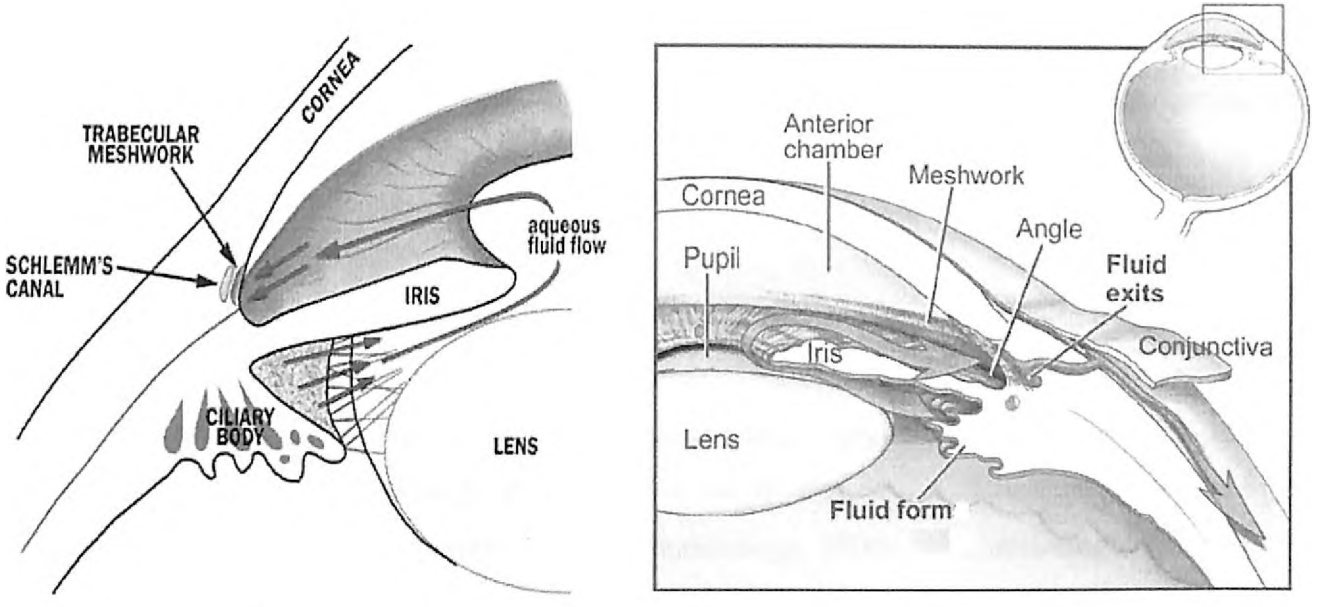

(a) (b)

Fig 1.3: Diagram showing the pathway of aqueous humor production in the eye. Arrow marks indicate the direction of aqueous humor outflow.

(c) Vitreous humor: Approximately 80 % of the eye's volume is a clear hydrogel medium. It contains water bound with collagen type II (99 %), hyaluronic acid, and proteoglycans. It also contains glucose, ascorbic acid, amino acids, and a number of inorganic salts. It acts as a metabolic pathway for the nutrients of the lens and the retina (Berman ER, 1991).

1.2. Diseases affecting eye

There are several diseases affecting the eye or its tissues, namely conjunctivitis, bacterial and viral infections, mycotic infections, uveitis, keratitis, age related macular degenerative diseases and glaucoma. The primary objective of this work was to design better ocular drug delivery system for the treatment of glaucoma. The following section describes etiology and glaucoma and its management.

1.2.1. Glaucoma

Glaucoma, a disease characterised by rise in intra ocular pressure (IOP), is a group of progressive optic neuropathies that have in common a slow progressive degeneration of retinal ganglion cells and their axons, resulting in visual loss. No particular risk factor for mediation of this pathology has been identified, yet intraocular pressure is the only proven treatable risk factor. Without adequate treatment, glaucoma can progress to visual disability and eventual blindness. Usually the resistance to aqueous humour outflow through the trabecular meshwork is the main causative factor associated with high intraocular pressure (Fechtner and Winreb, 1994).

Primary open-angle glaucoma (POAG) is a chronic, slowly progressive, multifactorial, and usually bilateral, though not necessarily symmetrical, optic neuropathy. It is characterized by atrophy and cupping of the optic nerve head, resulting in a distinctive pattern of visual field defects, with or without elevated intraocular pressure (IOP), in the presence of a widely open angle and in the absence of other causes of damage to the nerve fiber bundles (American Academy of Ophthalmology, 2000). The open-angle form of glaucoma is a chronic condition and is the most prevalent form of the glaucoma and is associated with an elevation of IOP. In this disease the primary therapeutic approach has been in lowering the IOP; however, new approaches are directed toward protecting the neuron from degeneration. The risk factors for open angle glaucoma include age (over 40 years), elevated IOP, family history of glaucoma, ocular trauma, a topical or systemic administration of endogenous corticosteroids, myopia, diabetes mellitus, hypertension, carotid vascular disease, anaemia and migraine headaches. The open angle glaucoma remains mostly asymptomatic, but the common diagnostic symptoms include prolonged ocular pain, vision blurriness etc

The closed-angle form is associated with a shallow anterior chamber, in which a dilated iris can occlude the outflow drainage pathway at the angle between the cornea and the ciliary body. This form is associated with acute and painful increase of intra ocular pressure, which must be controlled on an emergency basis with drugs or prevented by surgical removal of part of the iris (iridectomy) (American Academy of Ophthalmology, 2000).

(a) Treatment of glaucoma

Intraocular pressure is a function of the balance between fluid input and drainage out of the globe. The primary strategies for the treatment of glaucoma falls into two categories namely, (a) reduction of aqueous humor secretion and

1.2.1. Glaucoma

Glaucoma, a disease characterised by rise in intra ocular pressure (IOP), is a group of progressive optic neuropathies that have in common a slow progressive degeneration of retinal ganglion cells and their axons, resulting in visual loss. No particular risk factor for mediation of this pathology has been identified, yet intraocular pressure is the only proven treatable risk factor. Without adequate treatment, glaucoma can progress to visual disability and eventual blindness. Usually the resistance to aqueous humour outflow through the trabecular meshwork is the main causative factor associated with high intraocular pressure (Fechtner and Winreb, 1994).

Primary open-angle glaucoma (POAG) is a chronic, slowly progressive, multifactorial, and usually bilateral, though not necessarily symmetrical, optic neuropathy. It is characterized by atrophy and cupping of the optic nerve head, resulting in a distinctive pattern of visual field defects, with or without elevated intraocular pressure (IOP), in the presence of a widely open angle and in the absence of other causes of damage to the nerve fiber bundles (American Academy of Ophthalmology, 2000). The open-angle form of glaucoma is a chronic condition and is the most prevalent form of the glaucoma and is associated with an elevation of IOP. In this disease the primary therapeutic approach has been in lowering the IOP; however, new approaches are directed toward protecting the neuron from degeneration. The risk factors for open angle glaucoma include age (over 40 years), elevated IOP, family history of glaucoma, ocular trauma, a topical or systemic administration of endogenous corticosteroids, myopia, diabetes mellitus, hypertension, carotid vascular disease, anaemia and migraine headaches. The open angle glaucoma remains mostly asymptomatic, but the common diagnostic symptoms include prolonged ocular pain, vision blurriness etc

The closed-angle form is associated with a shallow anterior chamber, in which a dilated iris can occlude the outflow drainage pathway at the angle between the cornea and the ciliary body. This form is associated with acute and painful increase of intra ocular pressure, which must be controlled on an emergency basis with drugs or prevented by surgical removal of part of the iris (iridectomy) (American Academy of Ophthalmology, 2000).

(a) Treatment of glaucoma

Intraocular pressure is a function of the balance between fluid input and drainage out of the globe. The primary strategies for the treatment of glaucoma falls into two categories namely, (a) reduction of aqueous humor secretion and

(b) enhancement of aqueous outflow.

The loss of aqueous humour occurs be two pathways,

1. Drainage through the trabecular meshwork and canal of schlemm and into systemic circulation
2. Drainage through uveoscleral tissue

The drugs used in the management of glaucoma, broadly work by one of these two pathways. The major therapeutic drugs employed are parasympathomimetics, sympathomimetics, carbonic anhydrase inhibitors and prostaglandin analogues.

(i) Parasympathomimetics

This category of drugs stimulates the sphincter papillae, which stimulates ciliary body and opens the trabecular meshwork. The main parasympathomometic employed in the treatment of glaucoma is pilocarpine. Pilocarpine, the principal miotic is a direct acting cholinergic agonist with action at both, central and peripheral muscarinic receptors. As ophthalmological agent applied topically, the cholinomimetic action on smooth muscle cells leads to muscle contraction (Grierson et al, 1978). It causes cilllary constriction, spasm of accommodation and lowering of IOP through its activity at muscarinic receptor sites on iris sphincter and ciliary muscle (Krill and Newell, 1964).

(ii) Sympathomimetics

Non-selective and selective beta antagonists are used to treat glaucoma. Beta-receptor antagonists reduce IOP by decreasing aqueous fluid formation through inhibition of cyclic adenosine monophosphate (cAMP) production in ciliary epithelium in the ciliary body (Zimmermann and Kaufman, 1977). The drugs used include timolol, carteolol (all non-selective antagosists) and betaxolol (a selective beta-1 antagonist).

Alpha-2 agonists are also powerful inhibitors of aqueous humor production. The first available alpha agonist used was clonidine. Though it had a powerful IOP lowering effect, it suffered from systemic hypotensive side effect. Apraclonidine, which does not cross blood brain barrier effectively lowers IOP in short term. But it has been associated with an allergy like reactions and also tachyphylaxis (Hodapp et al, 1981). Brimonidine is a highly selective alpha 2 agonist. It is used as monotherapy as well as in combination with beta blockers (timolol). It causes a decrease in IOP by reducing the uveoscleral outflow and also decreasing the production of aqueous humor. It also increases the blood flow to the uvea (Burke, 1996).

(iii) Carbonic anhydrase inhibitors

Carbonic anhydrase (CA) is the enzyme which catalyzes the reversible hydratation of carbon dioxide and the dehydratation of carbonic acid. It is ubiquitous in the body and affects fluid transport across membranes within several organs including the kidney, red blood cells and choroid plexus in the central nervous system. Ciliary body, corneal endothelium and retinal pigment epithelium in the eye contain CA enzyme and inhibition of carbonic anhydrase isoenzyme II (CA II) in the ciliary body results in a reduction in ocular aqueous humour formation by decreasing bicarbonate secretion into the posterior chamber by the ciliary epithelial cells (Brechue and Maren, 1993). The drugs fall into the category of carbonic anhydrase inhibitor are acetazolamide, dorzolamide and brinzolamide. Dorzolamide was approved as the first topical carbonic anhydrase inhibitor. In some clinical trials, it was shown to be equally efficacious to betaxolol with high affinity for the CA-II isoenzyme (Lippa et al, 1991; Strahlman et al, 1995). Brinzolamide has high affinity for CA-II isoenzyme due to its high lipophilicity and lower aqueous solubility than dorzolamide at physiological pH. It forms a suspension at pH 7.4 which is more comfortable for the eye than the acidic pH of dorzolamide solution (pH 5.6).

(iv) Prostaglandins

They are relatively new class of ocular hypotensive agents. Four different prostaglandins have been approved for clinical use namely latanoprost, unoprostone, travoprost and bimatoprost. They reduce intra-ocular pressure by enhancing uveoscleral outflow and may also have some effect on the trabecular meshwork (Yamamoto et al, 1997; Camras et al, 2003). The prostaglandins are enjoying the reputation of being the systemically safest drugs in glaucoma treatment and show even more pronounced hypotensive effective than timolol (Sagara et al, 1999).

1.3. Factors affecting ocular bioavailability

1.3.1. Precorneal fluid dynamics

One of the most critical precorneal factors influencing bioavailability is the dynamics of fluid in the precorneal spaces. All forms of topical liquid dosage forms (aqueous solutions, oily solutions, suspensions and liposomes) are rapidly drained into the nasolachrymal passage with residence time varying from 4-23 mins (Lee and Robinson, 1979). The irritancy of the formulation contributes to the increase in the drainage rate and thus decrease in the residence time.

1.3.2. Pharmacokinetic considerations

Once the drug is applied topically into the lower cul de sac as eye drops, it mixes instantly with the tear fluid present in the eye as well as that secreted as a result of reflex action resulting in rapid spreading of drug solution all over the surface of the eye. Various anatomical as well as physiological factors such as drainage of the instilled volume, tear turnover, nasolacrymal drainage, non corneal absorption, metabolism and enzymatic degradation of drug on the corneal surface makes the drug less available at the site of action (Loftssona and Jarvinen, 1999). Various reports suggests less than 10 % of the instilled dose is delivered to intra ocular tissues, while remaining is either drained off the eye or absorbed systemically resulting in systemic side effects (Jarvinen et al, 1995; Loftssona and Jarvinen, 1999; Kaur et al, 2004). The various ocular drug absorption pathways are shown in the Fig 1.4.

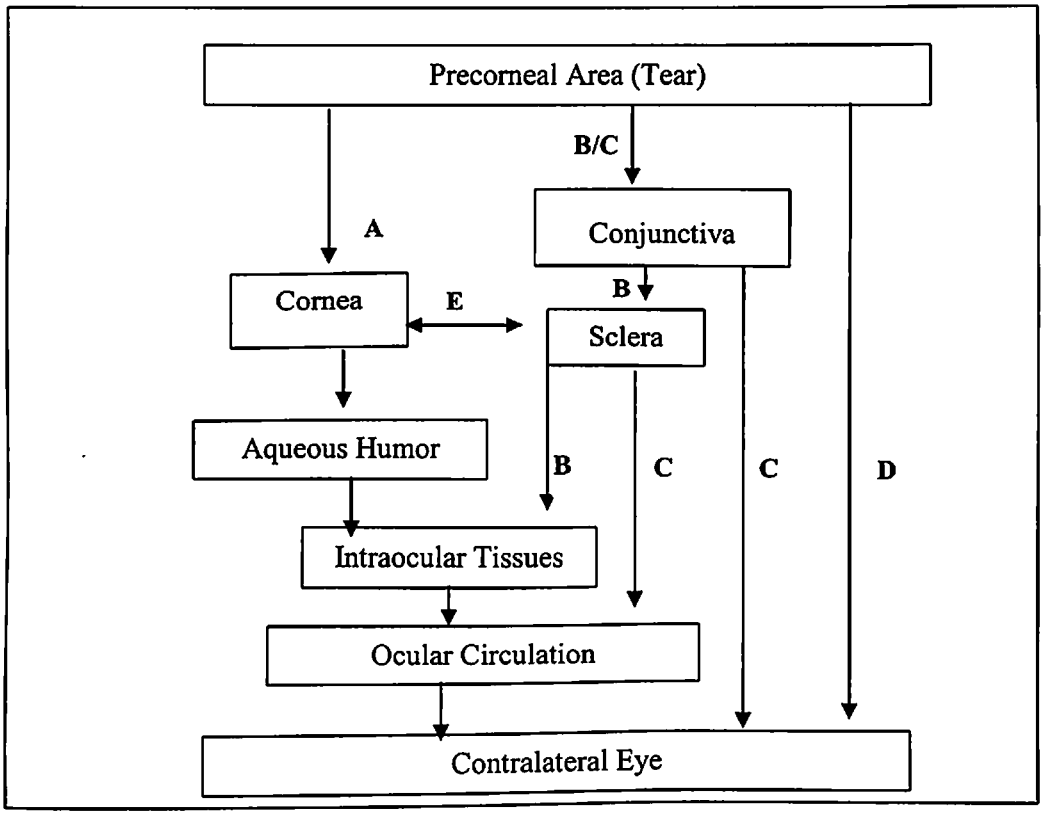

Fig 1.4: Various routes for drug penetration from topical ophthalmic applications (A = Corneal route, B = Non-corneal route, C = Systemic, D = Naso-lachrymal absorption route, E = Lateral diffusion) (Loftssona and Jarvinen, 1999; Lee and Robinson, 1979).

Corneal route is the major route of penetration for topically applied drugs. There are two major mechanisms of corneal drug absorption- transcellular and paracellular (Lee and Li, 1989). The paracellular transport involves delusive and convective transport occurring

through intercellular spaces and tight junctions, while transcellular pathway involves the cell/tissue partitioning and/or diffusion, channel diffusion and also carrier mediated transport.

General mechanism of passage of drug through corneal route are

a) At organ level: Corneal epithelium acts as a barrier for the penetration of drugs. For lipophilic drugs, the two top layers of epithelium acts as a rate limiting barriers.

b) At the cellular level: Small molecules like water, methanol, and ethanol readily traverse the cornea through aqueous pores, whose permeability constants are very high. The permeability coefficients are in the order of 0.1-4.0 x 10^{-5} cm/sec. Water soluble compounds such as peptides, ions and other charged compounds travel across the cornea via paracellular route (Huang et al, 1989).

1.3.3. Physicochemical properties of drug

The physicochemical properties of the drug like molecular weight, partition coefficient, pKa and solubility play an important role in the effective absorption of the drug through the corneal route.

The optimum lipophilicity for corneal absorption was found to be between 10-100 as determined with n-octanol/water system (Kaur and Smitha, 2002). For drugs with low partition coefficient, the lipophilic epithelium of the eye, while for highly lipophilic drugs hydrophilic stroma forms the rate limiting barrier for the absorption (Jarvinen et al, 1995; Le Bourlais et al, 1998; Loftssona and Jarvinen, 1999).

The drug permeation depends on the ionisation of the drug in the eye environment. The Unionised molecules penetrate lipid membranes more readily than ionised ones.

The charge of the molecule also affects the penetration of drug through the eye. Cationic drugs permeate cornea more readily than anionic drugs (Jarvinen et al, 1995; Le Bourlais et al, 1998; Loftssona and Jarvinen, 1999). The tight junction proteins contain negatively charged carboxylic groups, which can also decrease the permeation of positively charged drug applied topically.

(d) Molecular size of the drug that is easily permeable through the cornea is up to 5000 D, while conjunctiva can be permeated by drugs up to 20,000 D (Huang et al, 1989; Greaves et al, 1993). Corneal epithelium and stroma exert resistance to penetration with varying degree depending on the nature of the drug as shown in Table 1.3 (Schoenwald and Huang, 1983).

Table 1.3: Degree of corneal epithelial and stromal resistance to drug penetration for various types of drugs

Nature of the drug	Percent contribution of the corneal resistance	
	Corneal epithelial layer	Stromal layer
Hydrophilic (log P < 0)	90	5
Moderately lipophilic (log P = 0.1-1.6)	50	30
Lipophilic (log P = 1.6-2.5)	10	50

1.4. Formulation approaches in ocular delivery

The conventional dosage which are currently available in the market, such as solutions, suspensions and ointments constitute about 90 % of the total available ocular formulations (Lang, 1995; Le Bourlais et al, 1998). Because of their inability to reach the target site at therapeutic concentrations, the bioavailability always remained an issue of concern. The various routes of drug loss from the eye from a conventional ocular formulations have been shown in the Fig 1.5. Hence, the objective of any ocular formulation to be successful is to reduce the drug loss from the eye, either by retaining the formulation in the eye for a longer time, or by improving the precorneal absorption and permeation.

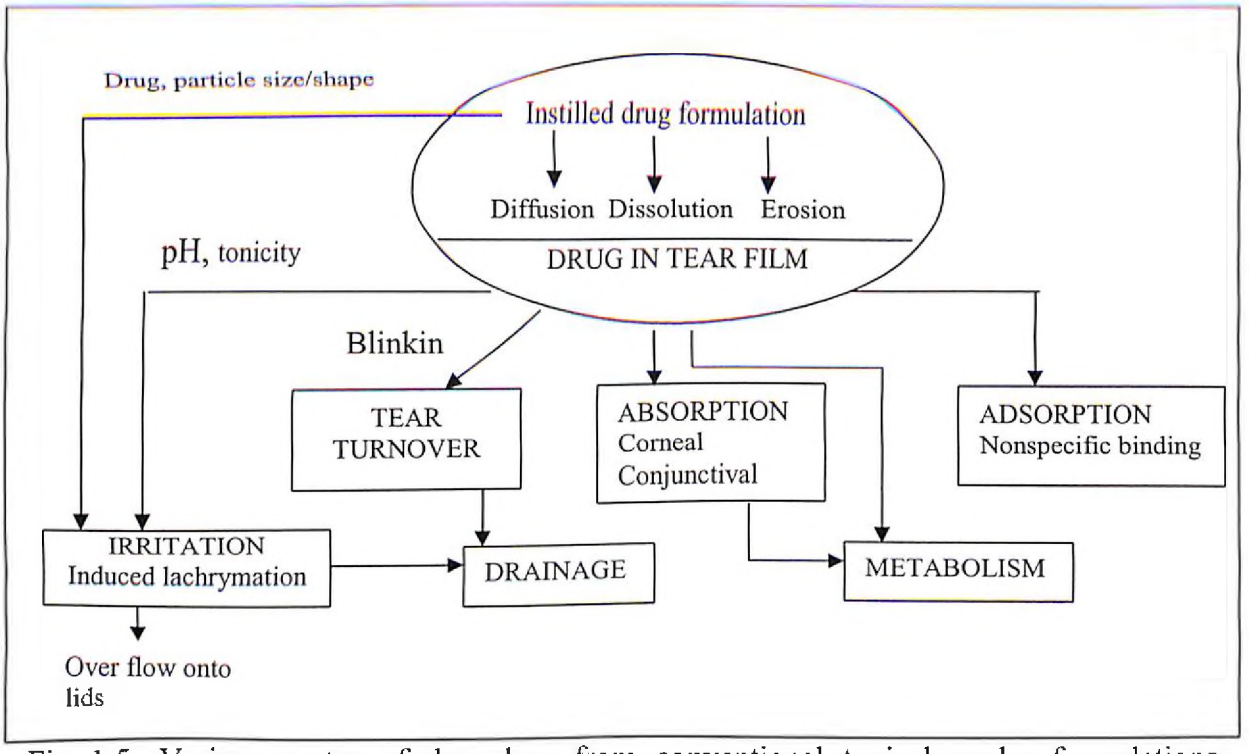

Fig 1.5: Various routes of drug loss from conventional topical ocular formulations (Olejnik, 1993)

1.4.1. Formulation additives in topical ophthalmic formulations

The most commonly employed formulation additives in the preparation of topical ophthalmic formulations are described below (Lang, 1995).

(a) Viscosity enhancers: Viscosity enhancers can be useful in the improving the ocular delivery as they can significantly reduce the surface tension and increase viscosity, thus increase ocular contact time, decrease the drainage rate, and increase drug bioavailability. But the main disadvantage of these polymers is their tendency to dry to a film on the eyelids. Polymers mainly used for this purpose include poly vinyl alcohol (PVA), methyl cellulose (MC), hydroxypropylmethylcellulose (HPMC), dextran-70, ethyl cellulose (EC) and polyvinyl pyrrolidone (PVP).

(b) Tonicity modifiers: An ophthalmic solution need to be isotonic to tear fluid, which is approximately equal to 0.9 % w/v NaCl (with a tolerance range equivalent to 0.5 % to 1.8 % w/v NaCl).

(c) Buffers: All ophthalmic drops are usually buffered at pH 7.4, the physiological pH of the eye. Buffering at either extreme acidic or basic pH would lead to increased lachrymation, blinking and corneal damage. Sometimes drug solutions or suspensions are formulated at pH very different from 7.4 due to stability and/or solubility consideration of the drug. Phosphate buffers are most commonly used in topical ophthalmic preparations.

(d) Stabilizers: Anti-oxidants like, sodium bisulphite or metabisulphite are used at concentration less than 0.3 % w/v to prevent the degradation of the active ingredient. Sometimes, ethylene diamine tetra acetic acid (EDTA), thiourea, and sodium thiosulphate are also used.

(e) Surface active agents: Non-ionic surfactants are used in extremely low concentrations to aid dispersing of steroidal or other drugs in suspension and to achieve solution clarity. The surfactants mainly used for this purpose are polysorbate 20 and 80 and polyoxyl 40 stearate.

(f) Vehicles: Purified water obtained by distillation, deionization or reverse osmosis is the universal vehicle for most of the ophthalmic solutions and suspensions. Vegetable oils of highest purity are sometimes used for certain drugs, to be formulated as ophthalmic drops, which are extremely sensitive to moisture. Vegetable oils commonly used are olive oil, castor oil, peanut oil, and sesame oil.

(g) Preservatives: Commonly used preservatives are benzalkonium chloride (0.004-0.02 % w/v), methyl paraben (0.1- 0.2 % w/v) and propylparaben. EDTA (chelating agent) is sometimes used to increase anti-pseudomonas activity along with benzalkonium chloride.

Semisolid preparation mainly used in ophthalmology is an anhydrous ointment in petrolatum base. The ointment vehicle is a mixture of mineral oil and white petrolatum. Ointments offer the advantage of longer contact time and better drug bioavailability. The major disadvantage is its greasy nature and blurring of vision.

1.4.2. Conventional topical ophthalmic preparations

Solutions are the most commonly employed dosage forms because of the simplicity of formulation development commercial production and high patient acceptance (Fitzgerald and Wilson, 1994). They suffer from major drawbacks such as rapid precorneal loss and uncontrolled systemic absorption via nasolacrymal passage or conjunctival duct causing severe systemic side effects. In order to compensate for the loss and maintain therapeutic levels in the eye, they need to be administered multiple times, thus resulting in patient incompliance.

Suspensions are dispersions of micronized drug (particle size less than 10-90 μm in a suitable vehicle. These are prepared with the assumption that the drug particle remain in the conjunctival sac for a longer time and can have better therapeutic value (Kupferman et al, 1974). For the moderate increase in bioavailability using suspension type preparations, there is substantial increase in production and handling costs (Davies et al, 1997). Also the particle size and shape of the drug remains a matter of concern. Higher particle size with needle shape or rough morphology causing discomfort and subsequent reflex tearing and loss of drug.

1.4.3. Viscous drug solutions

In order to improve the precorneal residence time and minimise the loss of drug, a simple approach is to incorporate viscosity enhancing polymers to the aqueous solutions. The increased viscosity can minimise the rapid drainage of the dosage form from the precorneal space of the eye and can thereby minimise the systemic absorption while enhancing the penetration of drug into the anterior chamber.

The most commonly used viscosifying agents include PVA and cellulose derivatives (MC and HPMC). Use of MC as viscosity enhancing agent has shown to minimize the drainage rate from the rabbit's eye (Chrai and Robinson, 1974). In a study by Kaur and Smita,

(2002), acetazolamide was formulated in carboxymethylcellulose (CMC) and the resulting viscous solution was compared with the saline solution of the drug in patients with unilateral open-angle glaucoma. The results showed that the longer duration of action was achieved. With use of PVA as viscosity enhancer, the corneal permeability of acetazolamide was improved (Kaur et al, 2004). The ocular shear rate, ranging from 0.03 per sec during inter-blinking to 4250 – 28500 during blinking (Tiffany, 1991) has a great influence on the rheological properties of the viscous dosage forms and can improve the bioavailability of drugs (Ooteghem, 1993). Newtonian systems do not show any significant enhancement in the bioavailability of incorporated drugs below a certain viscosity. At higher viscosities, blinking becomes painful and rapid reflex tearing draws of the administered solution (Ludwig et al, 1992). However viscosity cannot be the sole criteria to prolong the residence time. The mucoadhesive nature of the polymers and subsequent adherence of the dosage form to the eye tissues can improve the bioavailability more significantly than the viscosity enhancers alone. Mucoadhesion is the attachment of drug molecule or the dosage form to a specific biological tissue, organ more specifically to the surface of the tissue covered by mucin film by means of interfacial forces. Mucoadhesive polymers have been investigated for the purpose of improving the ocular delivery. They are macromolecular hydrocolloids with numerous hydrophilic functional groups and possess the correct charge to density ratio (Robinson and Miynek, 1995). For a polymer to be called as mucoadhesive, it should possess strong hydrogen bonding group, strong anionic charge, high molecular weight chain flexibility and surface energy properties for spreading on to the mucus (Park and Robinson, 1987). Various mucoadhesive polymers investigated are polyacrylic acids with carboxyl, hydroxyl, amide and sulphate groups (Robinson and Miynek, 1995).

1.4.4. In situ gelling systems

In situ gelling systems are viscous hydrogel polymer based systems, that exhibit sol-to-gel phase transition upon exposure to the physiological conditions due to change in the physico-chemical stimuli (ionic strength, temperature or pH) in the surrounding environment. These dosage forms offer advantage that it will be in solution form during shelf life and therefore provide ease of application. However they undergo rapid gelling upon instillation in the eye and therefore prolong the residence time of the formulation in the eye (Krauland et al, 2003).

Numerous polymers exhibiting the reversible phase transition have been investigated for ocular applications. The phase transition is triggered by numerous stimuli, such as pH of

the tears (eg. carbopol, cellulose acetate phthalate) (Gurny et al, 1985; Srividya et al, 2001; Sultana et al, 2006; Wu et al, 2006), temperature (eg. Xyloglucan, poloxamer 407, poly N-isopropylacrylamide, methyl cellulose) (Miyazaki et al, 2001; Wei et al, 2002), ionic strength; monovalent and divalent cations (eg. alginic acid, sodium alginate, gellan gum) (El-Kamel et al, 2002; Balasubramaniam et al, 2003). A summary of reported literature on in situ gel based systems are presented in Table 1.4.

Gellan gum is an anionic polysaccharide, undergoes phase transition from sol-to-gel upon contact with monovalent and divalent cations. The gel strength depends on the concentration of ions in the tear fluid. Several studies have been reported on gellan gum as carrier for ocular delivery as in situ gels (discussed in detail in Chapter V).

Poloxamers are another category of temperature sensitive in situ gelling polymer. It is a co-block co-polymer consisting of poly (oxyethylene) and poly (oxypropylene) units. The gelation temperature of poloxamer is around 32° C. Cellulose acetate phthalate (CAP) is free flowing solution at pH 4.4 and undergoes rapid transition when the pH is raised to 7.4.

1.4.5. Ocular inserts

Ocular inserts are defined as sterile devices with a thin, multilayered, drug impregnated, solid or semisolid consistency placed into cul-de-sac or conjuctival sac. They are more effective, require less frequent administration, do not require much of the formulation excipients and the release of the drug can be manipulated easily. Also accurate dosing is possible with the use of ocular inserts in ophthalmic applications. They are composed of polymeric support either as matrix or as reservoir containing drug which serves to prolong the contact time of the dosage form with the ocular tissues which in turn could improve bioavailability of the drug. The drawbacks associated with ocular inserts are interference with vision, foreign body sensation with poor tolerance and chances of moving off the eye.

The ocular inserts can be classified into three categories namely, insoluble, soluble and bioerodible ocular inserts. The insoluble ocular inserts are the one where the polymeric support remains insoluble throughout the release of the incorporated drug and the delivery system has to be removed from the site of application. Examples of such systems include diffusional systems, osmotic systems and contact lenses.

Table 1.4: Summary of applications of in situ gelling polymers for ocular delivery of drugs.

Drug	Polymer/bases	Reference
Carteolol	Alginic acid	Sechoy et al, 2000
	Gellan gum	El-Kamal et al, 2006
Ciprofloxacin	Mono amine-terminated poloxamer (MATP) and hyaluronic acid (HA) coupled graft copolymers	Cho et al, 2003
	Carbopol. Hydroxypropylmethyl-cellulose (HPMC), dodecylmaltoside	Ke et al, 2001
Dorzolamide HCl	Combination of poloxamer 407 and poloxamer F188.	Ammar et al, 2010
Doxorubicin	Chitosan/glycerophosphate	Wu et al, 2006
Forskolin	Poloxamer 407	Gupta and Samanta, 2010
Gatifloxacin and ^{99m}Technitium	Alginate/Hydroxypropyl methylcellulose	Liu et al, 2006
Human epithelial growth factor	hydroxy propyl beta cyclodextrine inclusion complex in Poloxamer F127, Poloxamer F68	Kim et al, 2002.
Indomethacin	Gellan gum	Balasubramaniam et al, 2003
Moxifloxacin HCl	Poloxamer	Shastri et al, 2010
Ofloxacin	Carbopol 940/ Hydroxypropyl-methylcellulose	Srividya et al, 2001
Perfloxacin mesylate	Gellan gum	Sultana et al, 2006
Pilocarpine	Carbopol 934 and Poloxamer F127 Xyloglucon and Poloxamer F127 Alginates Poloxamer F127, methyl cellulose Hydroxypropylmethylcellulose	Lin and Sung, 2000. Miyazaki et al, 2001 Cohen et al, 1997 Desai and Blanchard, 1998.
Placebo gels to study mechanical properties	Poloxamer F127/chitosan	Gratieri et al, 2010

Table 1.4 (contd.)

Gel to study ocular contact time	Gellan gum	Carlfors et al, 1998
Puerarin	Carbopol 980, hydroxypropylmethylcellulsoe (HPMC E4M), hydroxypropyl beta cyclodextrine (HP beta-CD)	Wu et al, 2007.
Timolol	Gellan gum Poloxamer F127, Carboxymethyl acrylate (CMA), hydroxypropyl-methylcellulsoe (HPMC)	Lindell and Engstrom, 1993; Rozier et al, 1989; Shibuya et al, 2003. El-Kamel, 2002
Vitamin B_{12}	Pluronic-g-poly acrylic acid copolymers using Pluronic F127 and Acrylic acid	Wen-di Ma et al, 2008

Soluble ocular inserts as well as bioerodable ocular inserts on the other hand are soluble at site of application and are not to be removed from the site of application. A wide variety of polymers have been used in the formulation of ocular inserts, they are natural, semi-synthetic and synthetic. Polymers include collagen and its derivatives, chitosan and its derivatives, sodium alginate, pectin, hydroxypropylmethylcellulose (HPMC), HPC (hydroxypropylcellulose), CMC (carboxymethylcellulose), PVP (poly vinyl pyrrolidine), polyacylic and poly methcrylic acid derivatives, poly ethylene oxides, polyester derivatives, poly orthoesters, poly (carboxylic acid) and its derivatives (Gurtler et al, 1995). Some of the recent advances in ocular inserts have been reviewed in the Table 1.5.

Table 1.5: Summary of applications of ocular inserts for ocular delivery of drugs.

Drug	Polymer/bases	Reference
Chloramphenicol, Atropine, Norfloxacin,Pilocarpine	Acrylic acid-functionalized chitosan reacted with either N-N isopropyl acrylamide or 2-hydroxyethyl methacrylate monomers	Verestiue et al, 2006
Ciprofloxacin	Sodium alginate, Eudragit RS and RL 100.	Charoo et al, 2003
	Drug dried waxy maize starch and CP 974P	Weyenberg et al, 2003
Cyclosporine A	Hydroxyethylmethacrylate (HEMA)	Gupta and Chauhan, 2010
Dexamethasone and tobramycin	N-methylchitosan based microspheres prepared into inserts with different grades of PEO	Zambito et al, 2006
Dexamethosone and gentamicin sulphate	Hydroxy propyl cellulose (HPC), hydroxypropylmethylcellulsoe (HPMC), ethyl cellulose (EC), carbopol (CP 974P) Cellulose acetate phthalate (CAP)	Baeyans et al, 2002.
Epidermal Growth Factor	Different types of alginates	Koelwel et al, 2008
Fluocinolone acetonide	Intravitreal inserts	Campochiaro et al, 2010
Gentamicin sulphate	Cellulose acetate phthalate (CAP), Carbopol, hydroxypropylmethylcellulsoe (HPMC), Hydroxy propyl cellulose (HPC), ethyl cellulose (EC),	Baeyens et al, 2002 Gurtler and Gurny, 1995b
Indomethacin	Cellulose derivatives (water soluble) and poly vinyl alcohol	Karatas and Baykara, 2000

Table 1.5 (Cond...)

Mitomycin C	Collagen implants	Zimmermann et al, 2004
Pilocarpine	Hydroxy propyl cellulose (HPC), Poly acrylic acid (PAA)	Harwood and Schwartz, 1982 Saettone et al, 1984
Ofloxacin	Poly ethylene oxide (PEO 200, 400,900, 2000) PEO 400, Eudragit L 100	Di colo et al, 2001a Di colo et al, 2001b
Oxytetracycline HCl	Silicone elastomers (polyacrylic acid or polymethacrylic acid grafted on polydimethylsiloxane)	Chetoni et al, 1998
Piroxicam	Poly vinyl pyrrolidine (PVP), hydroxypropylmethylcellulsoe (HPMC), carboxymethylcellulose (CMC), and carbopol	Gilhotra et al, 2009
Pradofloxacin	Hydrogel coating on thin metallic wire.	Pijls et al, 2005
Sodium fluorescein	Drum dried waxy maize starch and Carbopol 974P	Weyenberg et al, 2003.
Tisolol	Hydroxypropyl methacrylate	Sasaki et al, 1993
Tilisolol and prodrugs	Poly (2-hydroxy propyl metha-crylate) and O-butyryl and O-palmitoyl ester prodrug of tilisolol.	Kawakami et al, 2001.

1.4.6. Nanoparticulate systems

Nanoparticulate systems have been amongst the most widely studied particulate drug delivery systems in the past three decades. Nanoparticles are sub-micron sized polymeric colloidal particles with a diameter of 10 to 1000 nm in which drug can be either dissolved, entrapped, encapsulated or adsorbed (Kreuter, 1990). Nanoparticulate system consists of various polymers ranging from biodegradable, natural synthetic, lipids, phospholipids and even metals.

In order to achieve a better therapeutic efficacy, nanoparticulate drug delivery system must be retained in the cul de sac of the eye, and the entrapped drug must be released from the particles at a rate defined by the therapeutic need.

The first nanoparticulate drug delivery system studied was Piloplex® consisting of pilocarpine ionically bound to poly (methyl) methacrylate-acrylic acid copolymer. The formulation was designed for twice daily dosing in glaucoma patients, which bettered the multiple dosing drawbacks of pilocarpine eye drops (Klein et al, 1985). This formulation was not marketed due to non-biodegradability, local toxicity and the issues in preparing sterile formulations. The most commonly used polymers in the formulation are biodegradable polymers such as poly-lactic-co-glycolic-acid copolymers, polycaprolactone and poly alkylcyano acrylates.

Several reports are available in the literature on the polymers employed in the formulation of nanoparticles, methods of preparation and their characterization. Studies have shown that albumin nanoparticles can improve the therapy in cyto megalo virus (CMV) retinitis due to the biodegradable, non-toxic and non-antigenic properties of albumin (Irache et al, 2005). Pilocarpine was formulated as nanoparticulate form by using poly cyanoacrylates (Zimmer et al, 1994a), polylactic acid (Vidmar et al, 1985). Various drugs have been formulated as nanoparticles by the use of PLGA as polymer like betaxolol (Heussler et al, 1992), acyclovir (Giannavola et al, 2003, Sancho et al, 2003), 5-fluorouracil (Yeh et al, 2001), celecoxib (Ayalasomayajula et al, 2005), sparfloxacin (Gupta et al, 2009).

Various polymer systems employed for drugs of multiparticulate systems for ophthalmic application are summarized in Table 1.6.

1.4.7. Prodrugs

Prodrugs are pharmacologically inert molecules, which require a chemical or enzymatic transformation to get converted into the active form which would exert biological activity. Ocular prodrugs should have sufficient lipophilicity to cross the corneal barriers, and hydrophilicity to permeate through aqueous barriers. It should be stable in the ocular environments (Ding, 1998). While formulating into prodrug, the pathway and mechanism of drug penetration, functional groups of the drugs feasible for the prodrug formation and the activator, either enzyme or chemical environment present in the eye should be considered (Lee and Li, 1989). Esterases, a class of enzymes that cleave ester bond of the drug, have been paid a large attention while targeting a prodrug to the eye (Kupferman et al, 1974).

Table 1.6: Summary of various multiparticulate drug delivery systems reported for ocular drug delivery.

Polymer	Drug	Ocular administration route	Reference
Poly lactide-co-glycolic acid	Betaxolol	Topical	Heussler et al, 1990 & 1992
	Acyclovir	Topical	Giannavola et al 2003, Sancho et al, 2003
	Pilocarpine	Topical	Yoncheva et al, 2003
	Anti transforming growth factor beta 2	Subconjunctival	Santos et al, 2006
	5-Fluorouracil	Subconjunctival	Yeh et al, 2001
	Celecoxib	Subconjunctival	Ayalasomayajula et al, 2005
	Retinoic acid	Topical	Cirpanli et al, 2005
	rhGDNF	Intravitreal	Soler et al, 2005
	Recombinant vascular endothelial growth factor	Intravitreal	Cleland et al, 2001
	Anti vascular endothelial growth factor Aptamer	Transcleral	Carrasquillo et al, 2003
	Sparfloxacin	Topical	Gupta et al, 2009.
Polyalkylcyano acrylates	Pilocarpine	Topical	Zimmer et a, 1991a & b
	Betaxolol	Topical	Heussler et al, 1990 & 1992.
	Cyclophosphamide	Topical	Salgueiro et al, 2004
Methyl methacrylate copolymer and sulphomethyl methacrylate copolymer	Arecaidine propargyl ester & acelidine	Topical	Langer et al, 1997

Table 1.6 (Contd...)

Poly (epsilon) caprolactone	Indomethacin	Topical	Masson et al, 1992
	Flurbiprofen	Topical	Lacoulonche et al, 1999
	Cyclosporine	Topical	Aberturas et al, 2002
	Betaxolol	Topical	Heussler et al, 1990 & 1992.
Chitosan	Cyclosporine	Topical	Campos et al, 2001
Chitosan and sodium alginate	Gatifloxacin	Topical	Motwani et al, 2008.
Eudragits	Flurbiprofen	Topical	Pignatello et al, 2002
	Cloricromene	Topical	Pignatello et al, 2006
Albumin	Ganciclovir	Intravitreal	Merodioa et al, 2002
	Hydrocortisone	Intravitreal	Zimmer et al, 1994b
Polyacrylic acid	Brimonidine tartrate	Topical	De et al, 2003 & 2004
Polylactic acid	Pilocarpine	Topical	Vidmar et al, 1985
	Chloramphenicol	Topical	Shell et al, 1977.
	Budesonide	Subconjunctival	Kompella et al, 2003
Homolipid from goat and phospholipid	Diclofenac sodium	Topical	Attama et al, 2008.

Steroids are the first class of compounds to be formed as prodrugs. Dipivefrin, an epinephrine prodrug was introduced in 1970s. In a study it was found that dipivefrin was equally efficacious in reducing the IOP, but with lowered systemic side effects (Sasaki et al, 1976).

1.4.8. Use of penetration enhancers

The absorption of the drugs administered topically to the eye is dependent on the permeability of the corneal epithelium. In order to improve the permeation of drugs whose penetration is inherently low, agents known as permeation enhancers are added to improve the drug penetration by loosening the tight junctions between the epithelial cells. Various permeation enhancers employed are surfactants, bile salts, calcium chelators, preservatives, fatty acids and saponins. Surfactants in low concentrations change the physical properties of the membrane by chelating itself with the lipid bilayer and causing alteration in membrane integrity.

Bile salts also enhance the membrane permeation of the various biological pathways. They are ampiphilic molecules that can associate into micelles in the aqueous solutions. They change the rheological properties of the lipid bilayer, thus enabling the permeation of poorly absorbed drug (Sasaki et al, 1995).

Calcium chelators such as ethylene diamine tetra acetic acid (EDTA), acts as permeation enhancers by depleting calcium ions in the cells, which leads to global change within the cell and resulting in loosening of tight junctions between superficial epithelial cells. The permeation induced by calcium chelators is a paracellular transport (Hochman and Artusson, 1994). EDTA at a concentration of 0.5 % w/v can enhance the permeation of poorly permeable molecules. Benzalkonium chloride, a cationic surfactant and widely used preservative in ophthalmic preparations, is widely used now a days in improving the permeation of drugs.

1.5. Ideal ocular delivery system

The drug delivery systems employed for the treatment of ocular aliments suffer from many drawbacks, which consequently lead to decreased bioavailability, precorneal absorption and systemic side effects. The therapy becomes inconsistent especially for drug that require an optimum therapeutic concentration in the eye. The ideal delivery system for topical ocular delivery is the one which has prolonged contact with precorneal space, releases the drug as per the needs of the therapy, with enhanced bioavailability and no or minimum systemic absorption related systemic side effects. Also the dosage form should be well tolerated, causing no discomfort to the patient in term of vision or irritation should have minimum frequency of administration.

1.6. Objectives of the current research work

Brimonidine tartrate a selective alpha-2 agonist is used in the treatment of open angle glaucoma as ocular hypotensive agent. Its neuroprotective action along with antiglaucoma activity makes this a commonly prescribed drug in the treatment of glaucoma. It is recommended as monotherapy and in combination with other antiglaucoma agents in the effective management of glaucoma.

Currently brimonidine tartrate is available as topical eye drops (0.1 %, 0.15 % and 2.0 % w/v) alone and in combination with timolol. The eye drops suffer from variety of drawbacks. The idea was to achieve the desired therapeutic effect with lesser dosing and fewer or no side effects. The decrease in dosing frequency greatly improves patient compliance and assures round the clock medication.

Therefore, present research work was aimed at design and development of novel ophthalmic delivery systems for brimonidine tartrate in order to improve the precorneal residence time, prolonged ocular contact and prolonged release of drug to decrease the dosing frequency.

The Formulation strategies employed to achieve the above objective include,

(i) In situ gels: In situ gels were formulated by employing ion activated in situ gelling polymer or temperature activated in situ gelling systems. The effect of formulation variables on the viscosity, rheology, mucoadhesion, in vitro release and in vivo effects were extensively investigated.

(ii) Ocular inserts: Ophthalmic inserts were prepared by using varying combinations of hydrophilic, swellable/ erodible with hydrophobic/ inert/ zwitterionoic polymers alone and in combinations. The effect of polymer type, proportion and combination on mucoadhesion, in vitro release and in vivo effect was studied.

(iii) Long acting nanoparticles: Nanoparticles were prepared by using Eudragit or chitosan as carriers by multiple emulsion-solvent evaporation and ionic gelation method respectively. The effect of formulation and process variables on the particle size, drug loading and loading efficiency, in vitro drug release and in vivo effect were investigated.

To support the above listed formulation design and development work, suitable spectrophotometric analytical method was developed and validated. Various preformulation parameters of the drug like solubility, apparent partition coefficient, pKa, stability (solution state) and drug excipient compatibility studies were carried out. The optimized formulations were subjected to various stability studies.

Various in vivo performance studies carried out on best formulations include,

(i) Ocular irritation and toxicity studies using Draize test protocol.

(ii) Pharmacodynamic efficacy studies: Selected formulations, showing desired in vitro attributes were subjected for in vivo pharmacodynamic efficacy studies on rabbits after induction glaucoma by posterior injection of alpha-chymotrypsin. The ability of formulations to decrease the elevated intra ocular pressure was compared with that of marketed eye drop preparations. All the animal experiments were carried out with the approval of Institutional Animal Ethics Committee of BITS, Pilani.

1.7. REFERENCES

Aberturas MR, Molpeceres J, Guzman M, Garcia F. 2002. Development of a new cyclosporine formulation based on poly (caprolactone) microspheres. J. Microencapsul, 9; 61-72.

Ahmed I, Patton TF. 1985. Disposition of timolol and inulin in the rabbit eye following corneal versus non-corneal absorption. Int. J. Pharm. 38; 9-21.

American Academy of Ophthalmology: Preferred Practice Patterns TM: Open-angle Glaucoma. 2000; 38.

Ammar HO, Salama HA, Ghorab M, Mahmoud AA. 2010. Development of dorzolamide hydrochloride in situ gel nanoemulsion for ocular delivery. Drug Dev. Ind. Pharm, Jun 14. [Epub ahead of print].

Anderson DR, Hoyt WF. 1969. Ultrastructure of Intraorbital Portion of Human and onkey Optic Nerve. Arch. Ophthalmol, 82; 506-530.

Attama AA, Reichl S, Müller CC. 2008. Diclofenac sodium delivery to the eye: In vitro evaluation of novel solid lipid nanoparticle formulation using human cornea construct. Int. J. Pharm, 355; 307-313.

Ayalasomayajula SP, Kompella UB. 2005. Subconjunctivally administered celecoxib-PLGA microparticles sustain retinal drug levels and alleviate diabetes-induced oxidative stress in a rat model. Eur. J. Pharmacol, 511; 191-198.

Baeyens V, Kaltsatos V, Boisrame B, Varesio E, Veuthey JL, Fathi M, Balant LP, Gex-Fabry M, Gurny R. 1998. Optimized release of dexamethasone and gentamicin from a soluble ocular insert for the treatment of external ophthalmic infections. J. Control. Release, 52; 215-220.

Baeyens V, Felt-Baeyens O, Rougier S, Pheulpin S, Boisrame B, Gurny R. 2002. Clinical evaluation of bioadhesive ophthalmic drug inserts (BODI)$^{(R)}$ for the treatment of external ocular infections in dogs. J. Control. Release, 85; 163-168.

Balasubramaniam J, Kant S and Pandit JK. 2003. In vitro and in vivo evaluation of the Gelrite gellan gum-based ocular delivery system for indomethacin. Acta Pharmaceutica, 534; 251-261.

Berman ER. 1991. Biochemistry of eye. Perspectives in vision research. Series editor Colin Blakemore. Plenum Press, New York.

Brechue WF, Maren TH. 1993. Carbonic anhydrase inhibitory activity and ocular pharmacology of organic sulfamates. J. Pharmacol. Exp. Ther, 264: 670-675.

Burke J, Schwartz M. 1996. Preclinical evaluation of brimonidine. Surv. Ophthalmol, 41, (suppl 1); S9-S18.

Campochiaro PA, Hafiz G, Shah SM, Bloom S, Brown DM, Busquets M, Ciulla T, Feiner L, Sabates N, Billman K, Kapik B, Green K, Kane F; (Famous Study Group). 2010.

Sustained ocular delivery of fluocinolone acetonide by an intravitreal insert. Ophthalmology, 17; 1393-1399.

Campos AMD, Sanchez A, Alonso MJ. 2001. Chitosan nanoparticles: a new vehicles for the improvement of the delivery of drugs to the ocular surface. Application to Cyclosporine A. Int. J. Pharm, 224; 159-168.

Camras CB, Hedman K, US Latanoprost Study Group. 2003. Rate of response to latanoprost or timolol in patients with ocular hypertension or glaucoma. J. Glaucoma, 12; 466-469.

Carlfors J, Edsman K, Petersson R, Jornving K. 1998. Rheological evaluation of Gelrite® in situ gels for ophthalmic use. Eur. J. Pharm. Sci, 6; 113-119.

Charoo NA, Kohli K, Ali A, Anwer A. 2003. Ophthalmic delivery of ciprofloxacin hydrochloride from different polymer formulations: in vitro and in vivo studies. Drug Devel. Ind. Pharm, 29; 215-221.

Carrasquillo KG, Ricker JA, Rigas IK, Miller JW, Gragoudas ES, Adamis AP. 2003. Controlled delivery of the anti- VEGF aptamer EYE001 with poly (lactic-*co*-glycolic) acid microspheres. Invest. Ophthalmol. Vis. Sci, 44; 290-299.

Chetoni P, Di Colo G, Grandi M, Morelli M, Saettone MF, Darougar S. 1998. Silicone rubber/hydrogel composite ophthalmic inserts: preparation and preliminary in vitro/in vivo evaluation. Eur. J. Clin. Pharmacol, 46; 125-132.

Cho KY, Chung TW, Kim BC, Kim MK, Lee JH, Wee WR, Cho CS. 2003. Release of ciprofloxacin from poloxamer-graft-hyaluronic acid hydrogels in vitro. Int. J. Pharm, 260; 83-91.

Chrai SS, Robinson JR. 1974. Ocular evaluation of methylcellulose vehicle in albino rabbits. J. Pharm. Sci, 63; 1218-1223.

Cirpanli Y, Unlu N, Calis S, Hincal AA. 2005. Formulation and in-vitro characterization of retinoic loaded poly (lactic-co-glycolic acid) microspheres. J. Microencapsul, 22; 877-889.

Cleland JL, Duenas ET, Park A, Daugherty A, Kahn J, Kowalski J, Cuthbertson A. 2001. Development of poly-(D,L-lactide–coglycolide) microsphere formulations containing recombinant human vascular endothelial growth factor to promote local angiogenesis. J. Control. Release, 72; 13-24.

Cohen S, Lobel E, Trevgoda A, Peled Y. 1997. A novel in situ-forming ophthalmic drug delivery system from alginates undergoing gelation in the eye. J. Control. Release, 44; 201-208.

Davies NM, Wang G, Tucker IG. 1997. Evaluation of a hydrocortisone/ hydroxypropyl-[beta]-cyclodextrin solution for ocular drug delivery. Int. J. Pharm, 156; 201-209.

De TK, Rodman DJ, Holm BA, Prasad PN, Bergey EJ. 2003. Brimonidine formulation in polyacrylic acid nanoparticles for ophthalmic delivery. J. Microencapsul, 20; 361-374.

De TK, Bergey EJ, Chung SJ, Rodman DJ, Bharali DJ, Prasad PN. 2004. Polycarboxylic acid nanoparticles for ophthalmic drug delivery: an ex vivo evaluation with human cornea. J. Microencapsul, 21; 841-855.

Desai SD, Blanchard J. 1998. Evaluation of pluronic F127-based sustained release ocular delivery systems for pilocarpine using the albino rabbit eye model. J. Pharm. Sci, 87; 1190-1195.

Di Colo G, Zambito Y. 2001a. A study of release mechanisms of different ophthalmic drugs from erodible ocular inserts based on poly (ethylene oxide). Eur. J. Pharm. Biopharm, 54; 193-199.

Di Colo G, Burgalassi S, Chetoni P, Fiaschi MP, Zambito Y, Saettone MF. 2001b. Relevance of polymer molecular weight to the in vitro/in vivo performances of ocular inserts based on poly (ethylene oxide). Int. J. Pharm, 220; 169-177.

Ding S. 1998. Recent developments in ophthalmic drug delivery. PSTT, 1; 328-335.

Duke-Elder S, Wybar KC. 1961. The anatomy of the visual system. In, System of Ophthalmology, Vol. 2, Ed. Duke-Elder, S; Mosby, St. Lousis; 81.

El-Kamel AH. 2002. In vitro and in vivo evaluation of Pluronic F127-based ocular delivery system for timolol maleate. Int. J. Pharm, 241; 47-55.

El-Kamel A, Al-Dosari H, Al-Jenoobi F. 2006. Environmentally responsive ophthalmic gel formulation of carteolol hydrochloride. Drug Deliv, 13; 55-59.

Fechtner RD, Weinreb RN. 1994. Mechanisms of optic nerve damage in primary open angle glaucoma. Surv. Ophthalmol, 39; 23-42.

Fitzgerald P, Wilson CG. 1994. Polymeric systems for ophthalmic drug delivery. In S. Dimitriuitra (Ed.), Polymeric Biomaterials, New York: Marcel Dekker; 373-398.

Giannavola C, Bucolo C, Maltese A, Paolino D, Vandelli AM, Puglisi G, Vincent HLL, Fresta M. 2003. Influence of Preparation Conditions on Acyclovir-Loaded Poly-d,l-Lactic Acid Nanospheres and Effect of PEG Coating on Ocular Drug Bioavailability. Pharm. Res, 20; 584-590.

Gibaldi M, Perrier D. 1982. In, Pharmacokinetics. 2nd edn, Marcel Dekker, New York; 145.

Gilhotra RM, Gilhotra N, Mishra DN. 2009. Piroxicam bioadhesive ocular inserts: physicochemical characterization and evaluation in prostaglandin-induced inflammation. Curr. Eye Res, 34; 1065-1073.

Gratieri T, Gelfuso GM, Rocha EM, Sarmento VH, de Freitas O, Lopez RF. 2010. A poloxamer/chitosan in situ forming gel with prolonged retention time for ocular delivery. Eur. J. Pharm. Biopharm. 75; 186-193 [Epub 2010 Feb 25].

Greaves JL, Wilson CG, Birmingham AT. 1993. Assessment of the precorneal residence of an ophthalmic ointment in healthy subjects. Bri. J. Clin. Pharmacol, 35; 188-192.

Grierson I, Lee W, Abraham S. 1978. Effects of pilocarpine on the morphology of the human outflow apparatus. Br. J. Ophthalmol, 62; 302-313.

Gupta C, Chauhan A. 2010. Drug transport in HEMA conjunctival inserts containing precipitated drug particles. J. Colloid. Interface Sci, 347; 31-42.

Gupta H, Aqil M, Khar RK, Ali A, Bhatnagar A, Mittal G. 2009. Sparfloxacin-loaded PLGA nanoparticles for sustained ocular drug delivery. Nanomedicine. Oct 23. [Epub ahead of print].

Gupta S, Samanta MK. 2010. Design and evaluation of thermoreversible in situ gelling system of forskolin for the treatment of glaucoma. Pharm. Dev. Technol, 15; 386-393.

Gurny R, Boye T, Ibrahim H. 1985. Ocular therapy with nanoparticulate systems for controlled drug delivery. J. Control. Release, 2; 353-361.

Gurtler F, Gurny R. 1995. Patent literature review of ophthalmic inserts. Drug Dev. Ind. Pharm, 21; 1-18.

Gurtler F, Kaltsatos V, Boisrane B, Gurny R. 1995. Long acting soluble bioadhesive ophthalmic drug insert (BODI) containing gentamicin for veterinary use: optimisation and clinical investigation. J. Control. Release, 33; 231-236.

Harwood RJ, Schwartz JB. 1982. Drug release from compression molded films: preliminary studies with pilocarpine. Drug Dev. Ind. Pharm, 8; 663-682.

Heussler ML, Fessi H, Devissaguet JP, Hoffman M, Maincent P. 1992. Colloidal drug delivery systems for the eye: A comparison of the efficacy of three different polymers: Polyisobutyl cyanoacrylate, polylactic-co-glycolic acid, polyepsilon-caprolacton, STP. Pharma. Sci, 2; 98-104.

Heussler ML, Maincent P, Hoffman M, Spittler J, Couvreur P. 1990. Antiglaucomatousactivity of betaxolol chlorhydrate sorbed onto different isobutylcyanoacrylate nanoparticle preparations. Int. J. Pharm, 58; 115-122.

Hogan MJ, Alvarado JA, Weddell JE. 1971. The sclera. In, Histology of the human eye, Saunders, Philadelphia, Chap 5.

Hochman J, Artursson P. 1994. Mechanisms of absorption enhancement and tight junction regulation. J. Control. Release, 29; 253-267.

Hodapp E, Kolker AE, Kass MA. 1981. The effect of topical clonidine on intraocular pressure. Arch. Ophthalmol, 99; 1208-1211.

Huang AJ, Tseng SC, Kenyon KR. 1989. Paracellular permeability of corneal and conjunctival epithelia. Invest. Ophthalmol. Vis. Sci, 3; 684-689.

Irache JM. 2005. Albumin nanoparticles for the intravitreal delivery of anticytomegaloviral drugs. Mini. Rev. Med. Chem. 5; 293-305.

Jarvinen K, Jarvinen T, Urtti A. 1995. Ocular absorption following topical delivery. Adv. Drug Deliv. Rev, 16; 3-19.

Karatas A, Baykara T. 2000. Studies of indomethacin inserts prepared using water soluble polymers; I. Effect of preparation method and polymers on the drug release. S.T.P. Pharma. Sci, 10; 187-193.

Kaur IP, Smitha R. 2002. Penetration enhancers and ocular bioadhesives: two new avenues for ophthalmic drug delivery. Drug Dev. Ind. Pharm, 28; 353-369.

Kaur IP, Kapil M, Smitha R, Aggarwal D. 2004, Development of topically effective formulations of acetazolamide using HP-BETA-CD co-complexes. Curr. Drug Deliv, 1; 65-72.

Kawakami S, Nishida K, Mukai T, Yamamura K, Nakamura J, Sakaeda T, nakshima M, Sasaki H. 2001. Controlled release and ocular absorption of tilisolol utilizing ophthalmic insert incorporated lipophilic prodrugs. J. Control. Release, 76; 255-263.

Ke TL, Cagle G, Schlech B, Lorenzetti OJ, Mattern JJ. 2001. Ocular bioavailability of ciprofloxacin in sustained release formulations. Ocul. Pharmacol. Ther, 17; 555-563.

Kim EY, Gao ZG, Park JS, Li H, Han K. 2002. rhEGF/HP-beta-CD complex in poloxamer gel for ophthalmic delivery. Int. J. Pharm, 233; 159-167.

Klein HZ, Lugo M, Shields MB, Leon J, Duzman E. 1985. A dose-response study of piloplex for duration of action. Am. J. Ophthalmol, 99; 23-26.

Koelwel C, Rothschenk S, Fuchs-Koelwel B, Gabler B, Lohmann C, Gopferich A. 2008. Alginate inserts loaded with epidermal growth factor for the treatment of keratoconjunctivitis sicca. Pharm. Dev. Technol, 13; 221-231.

Kompella UB, Bandi N, Ayalasomayajula SP. 2003. Subconjunctival nano- and microparticles sustain retinal delivery of budesonide, a corticosteroid capable of inhibiting VEGF expression. Invest. Ophtholmol. Vis. Sci, 44; 1192-1200.

Krauland AH, Leitner VM, Bernkop-Schnurch A. 2003. Improvement in the in situ gelling properties of deacetylated gellan gum by the immobilization of thiol groups. J. Pharm. Sci, 92; 1234-1241.

Kreuter J. 1990. Nanoparticles as bioadhesive ocular drug delivery systems. In V.Lenaerts & R. Gurny (Eds.), Bioadhesive Drug Delivery Systems, Boca Raton: CRC Press; 203-212.

Krill AE, Newell FW. 1964. Effects of pilocarpine on ocular tension dynamics. Am. J. Ophthalmol, 57; 34-41.

Kupferman A, Pratt MV, Suckewer K, Leibowitz HM. 1974. Topically applied steroids in corneal disease. 3. The role of drug derivative in stromal absorption of dexamethasone. Arch. Ophthalmol, 91; 373-376.

Lacoulonche F, Gamisans F, Chauvet A, Garcıa ML, Espina M, Egea MA. 1999. Stability and in vitro drug release of flurbiprofen-loaded poly-epsilon-caprolactone nanospheres. Drug Dev. Ind. Pharm, 25; 983-993.

Lang JC. 1995. Ocular drug delivery conventional ocular formulations. Adv. Drug Deliv. Rev, 16; 39-43.

Langer K, Mutschler E, Lambrecht G, Mayer D, Troschau G, Stieneker F, Kreuter 1997. Methylmethacrylate sulfopropylmethacrylate copolymer nanoparticles for drug delivery Part II: Evaluation as drug delivery system for ophthalmic applications. Int. J. Pharm, 158; 219-231.

Lee VHL, Robinson JR. 1979. Mechanistic and quantitative evaluation of precorneal pilocarpine disposition in albino rabbits, J. Pharm. Sci, 68; 673-684.

Le Bourlais C, Acar L, Zia H, Sado PA, Needham T, Leverge R. 1998. Ophthalmic drug delivery systems - Recent advances. Progress in Retinal and Eye Research, 17; 33-58.

Lee VHL, Li VHK .1989. Prodrugs for improved ocular drug delivery. Adv. Drug Deliv. Rev, 3; 1-38.

Lin HR, Sung KC. 2000. Carbopol/pluronic phase change solutions for ophthalmic drug delivery. J. Control. Release, 69; 379-388.

Lindell, K, Engstrom S. 1993. In vitro release of timolol maleate from an in situ gelling polymer system. Int. J. Pharm, 95; 219-228.

Lippa EA, Schuman JS, Higginbotham EJ, Kass MA, Weinreb RN, Skuta GL, Epstein DL, Shaw B, Holder DJ, Deasy DA. 1991. MK-507 versus sezolamide. Comparative efficacy of two topically active carbonic anhydrase inhibitors. Ophthalmology, 98; 308-312.

Liu Z, Li J, Nie S, Liu H, Ding P, Pan W. 2006. Study of an alginate/HPMC based in situ gelling ophthalmic delivery system for gatifloxacin. Int. J. Pharm, 315; 12-17.

Loftssona T, Jarvinen T. 1999. Cyclodextrins in ophthalmic drug delivery. Adv. Drug Deliv. Rev, 36; 59-79.

Ludwig A, Van-Haeringen NJ, Bodelier VM, Ooteghem VM. 1992. Relationship between precorneal retention of viscous eye drops and tear fluid composition. Int. Ophthalmol, 16; 23-26.

Masson V, Billardon P, Fessi H, Devissagaut JP, Puisieux F. 1992. Tolerance studies and pharmacokinetic evaluation of indomethacin-loaded nanocapsules in rabbit eyes. Proc. Int. Symp. Control. Rel. Bioact. Mater, 19; 423.

Miyazaki S, Suzuki S, Kawasaki N, Endo K, Takahasli A, Attwood D. 2001. In situ gelling xyloglucan formulations for sustained ocular delivery of pilocarpine hydrochloride. Int. J. Pharm, 229; 29-36.

Moroi SE, Lichter PR. 2001 Ocular pharmacology. In, Goodman & Gilman's The Pharmacological Basis of Therapeutics. 10th edn, Eds. Hardman, JG, limbird, LL, Gilman, AG; McGraw Hill Medical Publishing Division, NewYork; 1819.

Martola EL, Baum JL. 1968. Central and Peripheral Corneal Thickness: A Clinical Study, Arch. Ophthalmol, 79; 28-30.

Merodioa M, Irachea JM, Valamaneshb F, Mirshahib M. 2002. Ocular disposition and tolerance of ganciclovir-loaded albumin nanoparticles after intravitreal injection in rats. Biomaterials, 23; 1587-1594.

Motwani SK, Chopra S, Talegaonkar S, Kohli K, Ahmad FJ, Khar RK. 2008. Chitosan-sodium alginate nanoparticles as submicroscopic reservoirs for ocular delivery: formulation, optimisation and in vitro characterisation. Eur. J. Pharm. Biopharm, 68; 513-525.

Olejnik, O. 1993 Conventional systems in ophthalmic drug delivery. In, Ophthalmic Drug Delivery Systems. Vol 58, Ed. Mitra, A. K, Marcel Dekker, New York; 177.

Ooteghem, MM. 1993. In: Edman, P. (Ed.), Biopharmaceutics of Ocular Drug Delivery. CRC Press, Boca Raton; 27-41.

Park H, Robinson JR. 1987. Mechanisms of mucoadhesion of poly (acrylic acid) hydrogels. Pharm. Res, 4; 457-464.

Pignatello R, Bucolo C, Spedalieri G, Maltese A, Puglisi G. 2002. Flurbiprofen-loaded acrylate polymer nanosuspensions for ophthalmic application. Biomaterials, 23; 3247-3255.

Pignatello R, Ricupero N, Bucolo C, Maugeri F, Maltese A, Puglisi G. 2006. Preparation and Characterization of Eudragit Retard Nanosuspensions for the Ocular Delivery of Cloricromene. AAPS PharmSciTech, 7; Article 27.

Pijls RT, Sonderkamp T, Daube GW, Krebber R, Hanssen HHL, Nuijts RMMA. 2005. Studies on a new device for drug delivery to the eye. Eur. J. Pharm. Biopharm, 59, 283-288.

Riordan-Eva P, Tabbara KF. 1992. Anatomy and embryology of the eye. In, General Opthalmology, 13th edn, Eds. Vaughan, D, Asbury T, Riordan-Eva P; Appleton and Lange, Norwalk, Chap. 8.

Robinson JR, Milynek GM. 1995. Bioadhesive and phase-change polymers for ocular drug delivery. Adv. Drug Deliv. Rev, 16; 45-50.

Rozier A, Mazuel C, Grove J, Plazonnet B. 1989. Gelrite®: A novel, ion-activated, in-situ gelling polymer for ophthalmic vehicles. Effect on bioavailability of timolol. Int. J. Pharm, 57; 163-168.

Sasaki H, Igarashi Y, Nagano T, Nishida K, Nakamura J. 1995. Different effects of absorption promoters on corneal and conjunctival penetration of ophthalmic beta-blockers. Pharm. Res, 12; 1146-1150.

Sasaki H, Tei C, Nishida K, Nakamura J. 1993. Drug release from an ophthalmic insert of a beta-blocker as an ocular drug delivery system. J. Control. Release, 27; 127-137.

Saettone MF, Giannaccini B, Chetoni P, Galli G, Chiellini E. 1984. Vehicle effects in ophthalmic bioavailability: an evaluation of polymeric inserts containing pilocarpine. J. Pharm. Pharmacol, 36; 229-234.

Sagara T, Gaton DD, Lindsey JD, Gabelt BT, Kaufman PL, Weinreb RN. 1999. Topical prostaglandin F2alpha treatment reduces collagen types I, III, and IV in the monkey uveoscleral outflow pathway. Arch. Ophthalmol, 117; 794-801.

Salgueiro A, Egea MA, Espina M, Valls O, Garcia ML. 2004. Stability and ocular tolerance of cyclophosphamide-loaded nanospheres. J. Microencapsul, 21; 213-223.

Sancho CM, Vanrell RH, Negro S. 2003. Poly (D,L-lactide-co-glycolide) microspheres for long term intravitreal delivery of acyclovir: influence of fatty and non fatty additives. J. Microencapsul, 20; 799-810.

Santos ALG, Bochot A, Doyle A, Tsapis N, Siepmann J, Siepmann F, Schmaler J, Besnard M, Francine BC, Fattal E. 2006. Sustained release of nanosized complexes of poly ethylenimine and anti-TGF-β2 oligonucleotide improves the outcome of glaucoma surgery. J. Control. Release, 112; 369-381.

Schoenwald RD, Huang H S. 1983. Corneal penetration behavior of beta-blocking agents I: Physicochemical factors, J. Pharm. Sci, 72; 1266-1272.

Sechoy O, Tissie G, Sebastian C, Maurin, F, Driot JY, Trinquand C. 2000. A new long acting ophthalmic formulation of Carteolol containing alginic acid. Int. J. Pharm, 207; 109-116.

Shastri DH, Prajapati ST, Patel LD. 2010. Studies on poloxamer based mucoadhesive in situ ophthalmic hydrogel of moxifloxacin HCl Curr. Drug Deliv, 17 [Epub ahead of print].

Shell JW. 1977. Ophthalmological bioerodible drug dispensing formulation. U.S. Patent 4,001, 388.

Shibuya T, Kashiwagi K, Tsukahara S. 2003. Comparison of efficacy and tolerability between two gel-forming timolol maleate ophthalmic solutions in patients with glaucoma or ocular hypertension. Ophthalmlogica, 217; 31-38.

Soler AC, Pouessel AA, Doat M, Picaud S, Halhal M, Simonutti M, Julienne MCV, Benoit, Francine JP, Cohen B. 2005. Intravitreous injection of PLGA microspheres encapsulating GDNF promotes the survival of photoreceptors in the rd1/rd1 mouse. Mol. Vision, 11; 1002-1011.

Srividya B, Cardoza RM, Amin PD. 2001. Sustained ophthalmic delivery of ofloxacin from a pH-triggered in situ gelling system. J. Control. Release, 73; 205-211.

Strahlman E, Tipping R, Vogel R. 1995. A doublemasked, randomized 1-year study comparing dorzolamide (Trusopt),timolol, and betaxolol. International Dorzolamide Study Group. Arch. Ophthalmol, 113: 1009-1016.

Sultana Y, Aqil M, Ali A. 2006. Ion-activated, Gelrite-based in situ ophthalmic gels of pefloxacin mesylate: comparison with conventional eye drops. Drug Deliv, 13; 215-219.

Tiffany JM. 1991. The viscosity of human tears. Int. Ophthalmol. 156; 371-376.

Verestiue L, Natasescu O, Brbu E, Sarvaiy I, Green KL, TsiboklisJ. 2006. Functionalised chitosan/NIPAM(HEMA) hybrid polymer networks as inserts for ocular drug delivery: synethsis, in vitro assesment and in vivo evaluation. J. Biomed. Mater. Res, 77; 726-735.

Vidmar V, Pepeljnjak S, Jalseniak J. 1985. The in vivo evaluation of poly (lactic acid) microcapsules of pilocarpine hydrochloride. J. Microencapsul, 2; 289-292.

Wei G, Xu H, Ding PT, Li SM. 2002. Thermosetting gels with modulated gelation temperature for ophthalmic use: The rheological and gamma scintigraphic studies. J. Control. Release, 83; 65-74.

Wen-di Ma, Xu H, Nie S, Pan W. 2008. Temperature-responsive, pluronic-g-poly(acrylic acid) copolymers in situ gels for ophthalmic drug delivery: rheology, in vitro drug release, and in vivo resident property. Drug Dev. Ind. Pharm, 34: 258-266.

Weyenberg W, Vermeirw A, Haese ED, Vanhaelewyn G, Kestelyn P, Callens F, Nelis HJ, Remon JP, Ludwing A. 2004. Effect of different strerilization methods on the properties of bioadhesive powders and ocular minitablets and clinical evaluation. Eur. J. Pharm. Sci, 23; 77-87.

Weyenberg W, Vermeire A, Remon, JP, Ludig A. 2003. Characterisation and in vivo evaluation of ocular bioadhesive minitablets compressed at differerent forces. J. Control. Release, 89; 329-340.

Wu J, Su ZG, Ma GH. 2006. A thermo- and pH-sensitive hydrogel composed of quaternized chitosan/glycerophosphate. Int. J. Pharm, 315; 1-11.

Wu C, Qi H, Chen W, Hiang C, Su C, Li W, Hou S. 2007. prepararation and evaluation of a Carbopol/HPMC based in situ gelling ophthalmic system for puerarin. Yakugaku Zassi, 127; 183-191.

Yamamoto T, Kitazawa Y, Azuma I, Masuda K. 1997. Clinical evaluation of UF-021 (Rescula; isopropyl unoprostone). Surv. Ophthalmol, 41; (Suppl 2); 99-103.

Yeh MK, Tung SM, Lu DW, Chen JL. 2001. Chiang C H. Formulation factors for preparing ocular biodegradable delivery system of 5-fluorouracil microspheres. J. Microencapsul, 18; 507-519.

Yoncheva K, Vandervoort J, Ludwig A. 2003. Influence of process parameters of high-pressure emulsification method on the properties of pilocarpine loaded nanoparticles. J. Microencapsul, 20; 449-458.

Zambito Y, Zaino C, Di Colo G. 2006. Effects of N-trimethylchitosan on transcellular and paracellular transcorneal drug transport. Eur. J. Pharm. Biopharm, 64; 721-724.

Zimmer AK, Mutschler, Lambrecht G, Mayer D, Kreuter J. 1994a. Pharmacokinetic and Pharmaco dynamic aspects of an ophthalmic pilocarpine nanoparticles delivery system. Pharm. Res, 11; 1435-1441.

Zimmer AK, Maincent P, Thouvenot P, Kreuter J. 1994b. Hydrocortisone delivery to healthy and inflamed eyes using a micellar polysorbate 80 solution or albumin nanoparticles. Int. J. Pharm, 110; 211-222.

Zimmer A, Kreuter J, Robinson JR. 1991. Studies on the transport pathway of PBCA nanoparticles in ocular tissues, J. Microencapsul, 8; 497-504.

Zimmermann TJ, Kaufman HE. 1977. Timolol, dose response and duration of action. Arch. Ophthalmol, 95; 605-607.

Zimmermann C, Drewe J, Flammer J, Shaarawy T. 2004. In vitro release of mitomycin C from collagen implants. Cur. Eye Res, 28; 1-4.

CHAPTER TWO

DRUG PROFILE

2. Brimonidine tartrate

2.1. Description

Brimonidine tartrate, (BRT) [5-bromo-6-(2-imidazolidinylideneamino) quinoxaline L-tartrate] (Fig 2.1) is a relatively selective alpha-2 adrenergic receptor agonist for ophthalmic application, an ocular hypotensive agent, used in the treatment of open angle glaucoma.

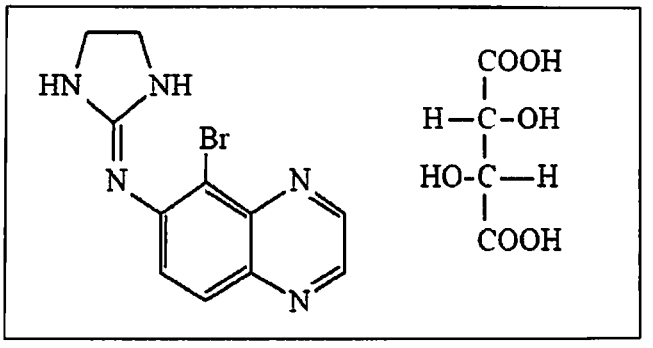

Fig 2.1: Structure of brimonidine tartrate

2.2. Physicochemical properties

BRT is off-white to pale yellow powder. It has a molecular weight of 442.24 as the tartrate salt. It has good water solubility, which is pH dependent. Its pKa is 7.5, as determined by potentiometric method (Chien et al, 1990), while it was found to be 7.2 by UV spectrophotometric method. The apparent partition coefficient is found to be 1.78 (n-octanol/water) (Bhagav et al, 2010)

2.3. Analytical methods

Since the drug is not official in any of the pharmacopoeias, there is no official method of analysis. The reported methods of analysis are discussed in the Chapter III (Analytical method development).

2.4. General Pharmacology

2.4.1. Mechanism of action

BRT is a potent alpha-2 adrenoreceptor agonist, is more selective for alpha-2 receptors than alpha-1. The selectivity is up to 1780 folds for alpha-2 receptors over alpha-1 (Wilensky, 1996; Cantor, 2000; Cantor, 2006). Since its introduction as an antiglaucoma agent, BRT has become one among the first line of drug in the treatment for open angle glaucoma, due to its neuroprotective action along with promising IOP reduction ability (Wilensky, 1996).

BRT has ocular hypotensive effect on both ocular hypertensive as well as normotensive eyes. It decreases the IOP by decreasing the production of aqueous humor and increasing the outflow of it by uveoscleral pathways (Toris et al, 1999). By these two mechanisms, BRT causes a decrease in the IOP. Tracers experiments in rabbits using BRT has showed an enhancement of uveoscleral outflow up to 57% with 0.1% w/v BRT solution (Lee et al, 1992; Serle, 1996). Also numerous reports revealed that BRT at higher concentration level decreases the production of aqueous humor in animal models like monkeys (Serle, 1991; Gabeh et al, 1994), suggesting that BRT acts on both aqueous humor production and uveoscleral outflow.

BRT is less lipophilic analogue of clonidine; the first drug of this series. The IOP lowering effect of clonidine was significant, but that was accompanied by a dramatic drop in the blood pressure upon systemic absorption. Hence the use of clonidine was very much limited. Subsequent introduction of alpraclonidine (0.5 % w/v and 1% w/v), effectively lowered IOP and its non entry into brain via blood brain barrier, made this drug an attractive alternative to clonidine. But because of its high incidence of allergy like reactions and tachyphylaxis (Hodapp et al, 1981) and poor alpha-2 receptor affinity, prompted the design of a new selective drug, brimonidine tartrate. The presence of quinoxaline ring in the structure resulted in higher alpha-2 selectivity for BRT (Burke, 1996).

2.4.2. Neuroprotection

BRT is reported to be neuroprotective on retinal ganglionic cells (RCG) in glaucoma induced animal models (Ahmed et al, 2001). Neuroprotective mechanisms of brimonidine are mediated via stimulation of alpha-2 adrenergic receptors. Alpha-2 adrenergic receptor stimulation may inhibit pro-apoptotic mitochondrial signalling (Wheeler et al, 2001). Further, alpha-2 adrenergic receptor stimulation can activate the anti-apoptotic phosphatidyl inositol-3-(PI-3) kinase and protein kinase/ Akt pathways. These are major pathways in the promotion of cell survival that block apoptosis by phosphorylation-dependent inhibition of pro-apoptotic signaling molecules, including BAD (BCL-2 associated death promoter), caspase-9 and activation of anti-apoptotic molecules such as NF-kappa B (Wheeler et al, 2001; Wheeler et al, 2003). Alpha-2 adrenergic stimulation also leads to activation of extracellular signal-regulated kinase (ERK) and increased synthesis of survival factors, such as bFGF and BCL-2 (Ballif et al, 2001; Xia et al, 1995). Brimonidine has been shown to protect cultured neuronal cells from apoptosis induced by serum or potassium withdrawal and this neuroprotection was mediated by the PI3-kinase-

activated Akt pathway (Tatton et al, 2001a). Furthermore, brimonidine has been shown to activate ERK and Akt pathways in vivo. Intraperitoneal administration of brimonidine 1 mg/kg to rats led to an up-regulation of bFGF, BCL-2, and BCL-X L synthesis (Lai et al, 2002). Also it was found that the mRNA and protein levels of bFGF, BCL-2 and BCL-X L remained high even 24 hours after brimonidine administration and thus the neuroprotective action of BRT could last longer than the presence of drug (Tatton et al, 2001b).

Apoptosis is genetically and biochemically controlled process that propagates slowly, in a step by step manner, in comparison to necrosis where the cell death occurs prematurely (Tatton, 1999). Cytochrome C, an intermediate in apoptosis, released from mitochondria activates a caspase cascade resulting in proteolytic degradation of the cell leading to apoptosis. Members of the B cell lymphoma-2 (BCL-2) family play a crucial role in regulating mitochondrial membrane permeability and cytochrome C release.

BCL-XL and BCL-2 are present in the retina and are anti-apoptotic because they prevent cytochrome C release; BAD and BAX (BCL-2 associated X protein) are pro-apoptotic because they increase mitochondrial membrane permeability and cytochrome C release (Tatton et al, 2001b). They do this by forming a dimer with either BCL-2 or BCL-XL and inactivating them. Phosphorylation of BAD prevents its dimerization with BCL-2 or BCL-XL and prevents apoptosis (Zha et al, 1997). Anti-apoptotic signals, like growth factors, promote RGC survival; pro-apoptotic signals, including elevated IOP and ischemia, induce RGC death. The survival of RGCs is dependent on a delicate balance between these cell survival and cell death signals (Meyer-Franke et al, 1995) and apoptosis is triggered when the balance is tilted in favour of cell death.

2.4.3. Pharmacokinetics of topical brimonidine

Ocular distribution studies in rabbits and monkeys has shown that upon topical instillation, BRT readily penetrates the eye and reaches pharmacologically active concentrations into the aqueous humor and ciliary body (Acheampong et al, 1995; Acheampong et al, 2002) with corneal route being the primary absorption pathway (Cantor, 2000 & 2006). In humans, upon topical administration, BRT entered systemic circulation, has a biological half life of 2 h (Cantor, 2000 & 2006). Because of the rapid metabolism of systemically absorbed BRT, the chances of systemic adverse effects are low.

In humans, the systemic metabolism of BRT is extensive. It is metabolized primarily by liver. BRT and it metabolites are excreted majorly by urinary excretion. Approximately 87

% of the orally administered radioactive dose was eliminated within 120 hrs, with 74 % excreted in urine. Monoamine inhibitors decrease the IOP lowering effect of BRT.

2.4.4. Therapeutic uses

Brimonidine tartrate is indicated in the treatment of primary open angle glaucoma or ocular hypertension for lowering the intra ocular pressure.

Brimonidine is a potential first line agent in the effective treatment of primary open angle glaucoma, with therapeutic efficacy comparable to that of timolol. The cardiovascular adverse effects of timolol are not seen in case of BRT. It is devoid of other effects of currently used antiglaucoma agents such as pilocarpine (night blindness), dorzalamide (sulphonamide related adverse effects), dipivefrine (ocular irritation) and the cardiovascular effects of timolol and betaxolol.

Also because of its neuroprotective action, the injury caused by prolonged elevated IOP can be treated effectively with BRT along with controlling IOP. The neuroprotective effect of BRT is independent of IOP lowering effect, as the systemically available BRT does not reduce IOP but act as neuroprotective agent (Yoles et al, 1999).

2.4.5. Adverse effects and tolerability

BRT is comparatively safer and tolerable than most of the antiglaucoma agents. It is not contraindicated in cardiopulmonary cases, where most of the currently used antiglaucoma agents are contraindicated (Schuman et al, 2000). The common adverse event in case of prostaglandins like eyelash growth and increased pigmentation of the iris or eyelid is not observed in BRT. Adverse events rare and are usually ocular in nature. Ocular adverse events of BRT occurring in about 10-20% subjects receiving eye drops include allergic conjunctivitis, conjunctival hyperemia, pruritis of eye, burning sensation, conjunctival folliculosis, hypertension, oral dryness, and visual disturbances (Allergan Inc. 2008: Alphagan® P product monograph).

Adverse events observed in about 1-4% of the subjects under study/monitoring are allergic reaction, asthenia, blepharitis, blepharoconjunctivitis, blurred vision, bronchitis, cataract, conjunctival edema, conjunctival hemorrhage, conjunctivitis, cough, dizziness, dyspepsia, dyspnea, epiphora, eye discharge, eye dryness, eye irritation, eye pain, eyelid edema, eyelid erythema, fatigue, flu syndrome, follicular conjunctivitis, foreign body sensation, gastrointestinal disorder, headache, hypercholesterolemia, hypotension, infection, insomnia, keratitis, lid disorder, pharyngitis, photophobia, rash, rhinitis, sinus infection, sinusitis, somnolence, stinging, superficial punctate keratopathy, tearing, visual field

defect, vitreous detachment, vitreous disorder, vitreous floaters, and worsened visual acuity. The events like corneal erosion, hordeolum, nasal dryness, and taste perversion were reported in less than 1 % of the subjects (Allergan Inc. 2008: Alphagan® P product monograph).

Post-marketing reported adverse effect include bradycardia, depression, iritis, keratoconjunctivitis sicca, miosis, nausea, skin reactions (including erythema, eyelid pruritus, rash, and vasodilation) and tachycardia, apnea, hypotension, hypothermia, hypotonia, and somnolence.

The first BRT formulation Alphagan® had a pH of 6.4 and had benzalkonium chloride as preservative. Due to the reported toxicity of benzalkonium chloride on repeated use, the BRT was reformulated with an aim of improving tolerability while maintaining ocular bioavailability. The new formulations Alphagan® P with BRT conc of 0.15 % w/v, used Purite® (0.005 % w/v) as preservative. Purite® is a oxychloro complex and a oxidative preservative that can easily gets converted into natural tear components (sodium and chloride ions, oxygen and water) upon exposure to light (Katz, 2002). This formulation showed comparable IOP lowering efficacy to that of one with 0.2% w/v drug and showed better ocular tolerability (Katz, 2002). This could be due to that fact that the latter formulation had a pH of 7.4, which favours the drug to be in unionised form at that pH, hence more amount of drug can penetrate the cornea (Dong et al, 2004).

2.4.6. Contraindications

BRT formulations are contraindicated in patients with hypersensitivity to brimonidine tartrate or any component of this medication. It is also contraindicated in patients receiving monoamine oxidase inhibitor therapy.

2.4.7. Precautions

Although BRT ophthalmic solution had minimal effect on the blood pressure of patients in various clinical studies, caution should be exercised in treating patients with severe cardiovascular disease. BRT formulations should be used with caution in patients with depression, cerebral or coronary insufficiency, Raynaud's phenomenon, orthostatic hypotension, or thromboangiitis obliterans. BRT may cause fatigue and /or drowsiness in some patients. Patients who engage in hazardous activities should be cautioned of the potential for a decrease in mental alertness (Allergan Inc. 2008: Alphagan® P product monograph).

2.4.8. Drug Interactions

Though extensive and specific drug interactions studies have not been carried out, there is possibility of an additive or potentiating effect with CNS depressants (alcohol, barbiturates, opiates, sedatives, or anesthetics). Alpha-agonists, as a class, may reduce pulse and blood pressure, therefore concomitant use of anti-hypertensives and/or cardiac glycosides, requires careful monitoring (Allergan Inc. 2008: Alphagan® P product monograph).

2.4.9. Pediatric use

The safety and effectiveness of brimonidine tartrate ophthalmic solution have not been studied in pediatric patients below the age of 2 years. Brimonidine tartrate ophthalmic solution is not recommended for use in pediatric patients under the age of 2 years. In a well-controlled clinical study conducted in pediatric glaucoma patients (ages 2 to 7 years) the most commonly observed adverse events with brimonidine tartrate ophthalmic solution 0.2 % w/v dosed three times daily were somnolence (50% - 83% in patients ages 2 to 6 years) and decreased alertness. In pediatric patients 7 years of age or older (>20kg), somnolence appears to occur less frequently (25%). Approximately 16% of patients on brimonidine tartrate ophthalmic solution discontinued from the study due to somnolence (Allergan Inc. 2008: Alphagan® P product monograph).

2.4.10. Dosage and administration

BRT is currently available as eye drop solutions in varying strength (0. 1 % w/v, 0.15 % w/v and 0.2 % w/v) and in combination with timolol (BRT 0.2% w/v and timolol 0.5 % w/v). The recommended dose is one to two drops in three times a day depending on the severity of glaucoma (Allergan Inc. 2008: Alphagan® P product monograph).

2.5. Currently available dosage forms

The following are the description of the three ophthalmic formulations of BRT manufactured by Allergen Inc, Irvine, USA.

- **ALPHAGAN® P** (brimonidine tartrate ophthalmic solution) has a clear, greenish yellow colour. It has an osmolality of 250-350 mOsmol/kg and a pH of 7.4-8.0 (0.1 % w/v) or 6.6-7.4 (0.15 % w/v).

  Each ml of **ALPHAGAN® P** contains brimonidine tartrate 0.1% w/v (1.0 mg/ml) or 0.15 % w/v (1.5 mg/ml).

2.4.8. Drug Interactions

Though extensive and specific drug interactions studies have not been carried out, there is possibility of an additive or potentiating effect with CNS depressants (alcohol, barbiturates, opiates, sedatives, or anesthetics). Alpha-agonists, as a class, may reduce pulse and blood pressure, therefore concomitant use of anti-hypertensives and/or cardiac glycosides, requires careful monitoring (Allergan Inc. 2008: Alphagan® P product monograph).

2.4.9. Pediatric use

The safety and effectiveness of brimonidine tartrate ophthalmic solution have not been studied in pediatric patients below the age of 2 years. Brimonidine tartrate ophthalmic solution is not recommended for use in pediatric patients under the age of 2 years. In a well-controlled clinical study conducted in pediatric glaucoma patients (ages 2 to 7 years) the most commonly observed adverse events with brimonidine tartrate ophthalmic solution 0.2 % w/v dosed three times daily were somnolence (50% - 83% in patients ages 2 to 6 years) and decreased alertness. In pediatric patients 7 years of age or older (>20kg), somnolence appears to occur less frequently (25%). Approximately 16% of patients on brimonidine tartrate ophthalmic solution discontinued from the study due to somnolence (Allergan Inc. 2008: Alphagan® P product monograph).

2.4.10. Dosage and administration

BRT is currently available as eye drop solutions in varying strength (0. 1 % w/v, 0.15 % w/v and 0.2 % w/v) and in combination with timolol (BRT 0.2% w/v and timolol 0.5 % w/v). The recommended dose is one to two drops in three times a day depending on the severity of glaucoma (Allergan Inc. 2008: Alphagan® P product monograph).

2.5. Currently available dosage forms

The following are the description of the three ophthalmic formulations of BRT manufactured by Allergen Inc, Irvine, USA.

- **ALPHAGAN® P** (brimonidine tartrate ophthalmic solution) has a clear, greenish yellow colour. It has an osmolality of 250-350 mOsmol/kg and a pH of 7.4-8.0 (0.1 % w/v) or 6.6-7.4 (0.15 % w/v).

  Each ml of **ALPHAGAN® P** contains brimonidine tartrate 0.1% w/v (1.0 mg/ml) or 0.15 % w/v (1.5 mg/ml).

Inactives: sodium carboxymethylcellulose, sodium borate, boric acid, sodium chloride, potassium chloride, calcium chloride, magnesium chloride, Purite® 0.005% w/v (0.05 mg/ml) as a preservative, purified water, with hydrochloric acid and/or sodium hydroxide to adjust pH.

- **ALPHAGAN®** (brimonidine tartrate ophthalmic solution) 0.5 % w/v has a clear, greenish yellow colour. It has a pH of 5.6 - 6.6.

  Each ml of **ALPHAGAN®** contains brimonidine tartrate 0.5 % w/v (5 mg/ml).

  Inactives: citric acid, polyvinyl alcohol, sodium chloride, sodium citrate, purified water, benzalkonium chloride (0.05 mg), hydrochloric acid and/or sodium hydroxide may be added to adjust pH.

- **COMBIGAN® eye drops** (brimonidine tartrate and timolol maleate eye drops)

  Clear, greenish-yellow sterile solution.

  Each ml contains brimonidine tartrate 2.0 mg/ml and timolol as maleate 5.0 mg/ml

  Inactive ingredients: Dibasic sodium phosphate heptahydrate, monobasic sodium phosphate monohydrate, benzalkonium chloride, hydrochloric acid, sodium hydroxide, purified water.

2.6. REFERENCES

Acheampong AA, Shackleton M, John B, Burke J, Wheeler L, Tang-Liu D. 2002. Distribution of brimonidine into anterior and posterior tissues of monkey, rabbit and rat eyes. Drug Metab. Dispos, 30; 421-429.

Acheampong AA, Shackleton M, Tang-Liu DD. 1995. Comparative ocular pharmacokinetics of brimonidine after a single dose application to the eyes of albino and pigmented rabbits. Drug Metab. Dispos, 23; 708-712.

Ahmed FA, Hegazy K, Chaudhary P, Sharma SC. 2001. Neuroprotective effect of alpha-2 agonist (brimonidine) on adult rat retinal ganglion cells after increased intraocular pressure. Brain Res, 913; 133-139.

Allergan Inc. 2008. Product monograph for brimonidine tartrate eye drops: Alphagan ® P. Revised: 08/2008, Allergan, Inc. Irvine, CA 92612, U.S.A.

Ballif BA, Blenis J. 2001. Molecular mechanisms mediating mammalian mitogen-activated protein kinase (MAPK) kinase (MEK)-MAPK cell survival signals. Cell Growth Differ, 12; 397-408.

Bhagav P, Deshpande P, Pandey S, Chandran S. Development and validation of stability indicating UV spectrophotometric method for the estimation of brimonidine tartrate in pure form, formulations and preformulation Studies. Der Pharmacia Lettre, 2010; 2(3): 106-122.

Burke J, Schwartz M. 1996. Preclinical evaluation of brimonidine. Surv. Ophthalmol, 41, (suppl 1); S9-S18.

Cantor LB. 2000. The evolving pharmacotherapeutic profile of brimonidine, an alpha 2-adrenergic agonist, after four years of continuous use. Expert Opin. Pharmacother, 1; 815-834.

Cantor LB. 2006. Brimonidine in the treatment of glaucoma and ocular hypertension. Ther. Clin. Risk Manag, 2; 337-346.

Chien DS, Homsy JJ, Gluchowski C, Tang-Liu DD. 1990. Corneal and Conjunctival/Scleral penetration of p-aminoclonidine, AGN 190342 and clonidine in rabbit eyes. Cur. Eye Res, 9; 1051-1059.

Dong JQ, Babusis DM, Welty DF, Acheampong AA, Tang-Liu D, Whitcup SM. 2004. Effects of the preservative purite on the bioavailability of brimonidine in the aqueous humor of rabbits. J. Ocul. Pharmacol. Ther, 20; 285-292.

Gabeh BT, Robinson JC, Hubbard WC. 1994. Apraclonidine and brimonidine effects on anterior ocular and cardiovascular physiology on normal and sympathectomized monkeys. Exp. Eye Res, 59; 633-644.

Hodapp E, Kolker AE, Kass MA. 1981. The effect of topical clonidine on intraocular pressure. Arch. Ophthalmol, 99; 1208-1211.

Katz LJ. 2002. Twelve-month evaluation of brimonidine-purite versus brimonidine in patients with glaucoma or ocular hypertension. J. Glaucoma, 11; 119-126.

Lai R, Chun T, Hasson D, Lee S, Mehrbod F, Wheeler L. 2002. Alpha-2 adrenoceptor agonist protects retinal function after acute retinal ischemic injury in the rat. Vis. Neurosci, 19; 175-185.

Lee PY, Serle JB, Podos SM. 1992. Time course of the effect of UK 14304-18 (brimonidine tartrate) on rabbit uveoscleral outflow (abstract). Invest. Ophthalmol. Vis. Sci, 33; 1118.

Meyer-Franke A, Kaplan MR, Pfrieger FW, Barres BA. 1995. Characterization of the signaling interactions that promote the survival and growth of developing retinal ganglion cells in culture. Neuron, 15; 805-819.

Schuman JS. 2000. Effects of systemic beta-blocker therapy on the efficacy and safety of topical brimonidine and timolol. Brimonidine study groups 1 and 2. Ophthalmology, 107; 1171-1177.

Serle JB. 1996. A comparison of the safety and efficacy of twice daily brimonidine 0.2% versus betaxolol 0.25% in subjects with elevated intraocular pressure. Surv. Ophthalmol, 41 (Suppl 1); S39-S46.

Serle JB, Steidl S, Wang RE. 1991. Selective %-adrenergic agonists B-HT 920 and UK14, 304-18: Effects on aqueous humor in monkeys. Arch. Ophthalmol, 109; 1158-1162.

Tatton WG. 1999. Apoptotic mechanisms in neurodegeneration: possible relevance to glaucoma. Eur. J. Ophthalmol, 9 (Suppl 1); S22-S29.

Tatton NA, Tezel G, Insolia SA, Nandor SA, Edward PD, Wax MB. 2001a. In situ detection of apoptosis in normal pressure glaucoma. A preliminary examination. Surv. Ophthalmol, 45 (Suppl 3); S268-S272.

Tatton WG, Chalmers-Redman RM, Sud A, Podos SM, Mittag TW. 2001b. Maintaining mitochondrial membrane impermeability. an opportunity for new therapy in glaucoma? Surv. Ophthalmol, 45 (Suppl 3); S277-S283.

Torris CB, Camras CB, Yablonski ME. 1999. Acute versus chronic effects of brimonidine on aqueous humor dynamics in ocular hypertensive patients. Am. J. Ophthalmol, 128; 8-14.

Wheeler LA, Tatton M, Elstner M, Chalmers-Redman RME, Tatton WG. 2001. Alpha-2 adrenergic receptor activation by brimonidine reduces neuronal apoptosis through Akt (protein kinase B) dependent new synthesis of bcl-2. Invest. Ophthalmol. Vis. Sci, 42; S441.

Wheeler L, WoldeMussie E. Lai R. 2003. Role of alpha-2 agonists in neuroprotection. Surv. Ophthalmol, 48 (Suppl 1); S47-S51.

Wilensky JT. 1996. The role of brimonidine in the treatment of open angle glaucoma. Surv. Ophthalmol, 41, Supp 1; S3-S7.

Xia Z, Dickens M, Raingeaud J, Davis RJ, Greenberg ME. 1995. Opposing effects of ERK and JNK-p38 MAP kinases on apoptosis. Science, 270; 1326-1331.

Yoles E, Wheeler LA, Schwartz M. 1999. Alpha2-adrenoreceptor agonists are neuroprotective in a rat model of optic nerve degeneration. Invest. Ophthalmol. Vis. Sci, 40; 65-73.

Zha J, Harada H, Osipov K, Jockel J, Waksman G, Korsmeyer SJ. 1997. BH3 Domain of BAD is required for heterodimerization with BCL-X L and pro-apoptotic activity. J. Biol. Chem, 272; 24101-24104.

CHAPTER THREE

ANALYTICAL METHOD DEVELOPMENT

3.1. INTRODUCTION

Accurate and precise analytical method is an essential tool in the development of formulations. The design attributes of the developed formulations can be accurately measured by a developed and validated analytical method. The analytical method development is the first step in the rational development of formulations.

An extensive survey of literature did not reveal any validated UV-spectrophotometric method for the estimation of BRT in pure form and in pharmaceutical ophthalmic dosage forms. An UV- spectrophotometric method for the quantitation of the drug at 319 nm in phosphate buffer saline (pH 7.4) has been reported as part of formulation design and evaluation procedure (De et al, 2003). However, validation data was not presented in the report. Few liquid chromatographic (LC) methods have been reported for the analysis of BRT in eye drops (Shirke and Pai, 2002), pharmaceutical formulations and in biological samples (Chien et al, 1990). Some LC methods have also been reported for the estimation of BRT in plasma, serum and in aqueous humor (Acheampong and Tau-Liu, 1995; Karamanos et al, 1999) and in ocular tissues (Chien et al, 1990; Acheampong et al, 2002). An on-line H/D exchange LC-MS/MS and 3-isotope tracer methods has been reported for the estimation of metabolites of BRT (Ni et al, 2007). Recently a liquid chromatographic method has been reported for the analysis of three potential impurities in BRT (Madhavi et al, 2009). A stability indicating assay of BRT ophthalmic solution and stress testing using hydrophilic interaction liquid chromatography has also been reported for the estimation of BRT (Ali et al, 2009). A rapid and sensitive LC/MS/MS analytical method has been reported for the quantification of BRT in ocular fluids and tissues (Jiang et al, 2009). The reported chromatographic and other techniques employ sophisticated instrumentation, are time consuming, require costly solvents and other chemicals and cannot be used for routine laboratory analysis. A simple, sensitive, accurate and cost effective UV- spectrophotometric method is required for the routine analysis of drug in bulk, in pharmaceutical formulations and also samples obtained from in vitro dissolution and stability studies.

Hence, in the present study a rapid, simple, sensitive, accurate and reproducible analytical method with better detection range for estimation of BRT in pure form and in its pharmaceutical dosage forms was developed and validated. Based on forced degradation studies, the method was also tested for its stability indication ability (no attempt was made to quantify or characterize impurities). This method would at best indicate any change in the UV absorbance profile of the drug due to change in chromophoric groups present in

the drug. The results of the analysis were validated by applying suitable statistical methods (USP 2009; ICH 1996 guidelines; Chandran and Singh, 2007) and by recovery studies (Bolton and Bon, 2004).

3.2. MATERIALS AND INSTRUMENTS

3.2.1. Materials

BRT was obtained as gift sample from FDC Ltd. Mumbai, India. Potassium dihydrogen orthophosphate, sodium hydroxide and isopropyl alcohol were purchased from S.D. Fine Chemicals, Mumbai, India. Excipients used in the preparation of the designed ophthalmic formulations were of pharmaceutical or spectroscopy grades. High quality pure water was prepared using Millipore purification system (Millipore, Model Elix SA 67120, Molsheim, France). The formulations used for recovery studies were developed in-house. BRT ophthalmic solution (0.2 % w/v) was prepared in laboratory using phosphate buffer saline (pH 7.4) under aseptic conditions. The inactive ingredients present in the ocular inserts include HPMC, EC, MCC, magnesium stearate, poly vinyl pyrrolidone K-30, while ocular gels contained HPMC, carbopol, benzalkonium chloride, benzyl alcohol and buffers. In situ gel formulations composed of gellan gum, benzalkonium chloride and other additives. Nanoparticle formulations contained Eudragit RL 100 and Eudragit RS 100, lecithin and pluronic F68. All other chemicals and solvents used were of pharmaceutical/analytical grade.

3.2.2. Instruments

A scanning UV-VIS NIR spectrophotometer (Jasco, Tokyo, Japan, Model V-570) connected to computer loaded with spectra manager® software, with automatic wavelength accuracy of 0.1 nm, a 10 mm matched quartz cells was used for all the absorbance measurement.

3.3. METHODS

3.3.1. Method development

To develop a sensitive UV-spectrophotometric method, various solvent systems were investigated in order to optimize the method parameters. Parameters like sensitivity, interference from the matrix, ease of preparation, need for pH adjustment, tolerance for pH variation, suitability for drug content estimation and stability, analysis time and cost factors were taken into consideration while selecting the solvent.

3.3.2. Preparation of standard calibration curve

Three different stock solutions of BRT were prepared by dissolving 5 mg of drug in 100 ml of phosphate buffer [(pH 7.4; 0.05M KH_2PO_4 (79.1 parts) and 0.045M NaOH (20.9 parts)] to get a final concentration of 50 µg/ml. Suitable dilutions of the stocks were prepared in series of 10 ml calibrated volumetric flasks using the same media. Various concentrations were prepared in the range of 3-18 µg/ml. By scanning a suitable standard solution in the UV-VIS spectrophotometer in the wavelength range of 200-400 nm with the scanning speed of 400 nm per min, the λ_{max} of the drug in the above media was determined as shown in Fig 3.1. Absorbance values for standard dilutions were measured at λ_{det} 248 nm. The results are listed in Table 3.1 and the statistical regression data and validation parameters are shown in the Table 3.2.

3.3.3. Analytical method validation

Following procedure was employed for validating the developed method.

Linearity of the proposed method was determined by measuring the absorbance of the standard solutions in the concentration range of 3-18 µg/ml and performing least square regression analysis.

(i) Accuracy

To determine the accuracy, three concentration levels of the standard drug solutions (3, 9 & 18 µg/ml) were prepared in triplicates (n=9) and were analyzed. Accuracy was determined in terms of the mean percent recovery along with standard deviation. The results are shown in the Table 3.3. One way ANOVA results for test of linearity of the BRT solutions is presented in Table 3.4. In addition, the accuracy of the proposed method was checked using standard addition method. To each of the pre-analyzed standard calibration and formulation samples, a known amount of drug sample was added and the total concentration was determined by measuring absorbance of the resultant solution by using the proposed method. The percent analytical recovery was calculated by comparing the concentration resulted with the addition of spiked samples with actual expected theoretical increase in concentration (Table 3.5).

(ii) Precision

Precision was determined using different levels of the drug concentrations (same as that of accuracy determination) prepared from the independent stock solutions and analyzed. Intra-day precision was determined by carrying out the analysis at three different time

points for three concentrations in a day. Similarly inter-day precision was determined by doing analysis on three consecutive days. The results are shown in Table 3.3.

(iii) LOD and LOQ

LOD and LOQ of the proposed methods were calculated on the basis of standard deviation of response and slope of the regression equation. LOD and LOQ were calculated as LOD = 3.3 σ / S and LOQ = 10 σ/ S, where 'σ' is the standard deviation of Y- intercept of regression equation and 'S' is the slope of the calibration curve. The results are shown in Table 3.3.

(iv) Specificity

Specificity of the proposed method was determined by preparing drug and placebo solutions using some commonly used excipients like hydroxypropylmethylcellulose (HPMC), ethyl cellulose (EC), lactose, starch, methyl cellulose, microcrystalline cellulose, sodium chloride, dextrose, talc, magnesium chloride, benzalkonium chloride and benzyl alcohol separately in the solvent (phosphate buffer pH 7.4) as per the proposed method. The samples were then checked for the absorbance at the wavelength of 200-400 nm. The overlayed absorption spectrum of drug with some of the formulation excipients is shown in Fig 3.2.

(v) Robustness

Robustness of the method was determined by changing the pH of the medium (phosphate buffer of pH from 6.9 to 7.9) and measuring the absorbance of standard solutions. Effect of change of analyst was also investigated on the robustness of the method.

(vi) Recovery studies

The method employed for the estimation of drug from the formulations is as follows:

Ophthalmic solutions: An aliquot of ophthalmic solution of BRT equivalent to 2 mg was taken and suitably diluted with the medium under study and analyzed by the proposed method. From the absorbance values of five replicates, the drug content/ml was calculated on average concentration basis.

Ocular inserts: Ten ocular inserts were accurately weighed and finely powdered. An aliquot of the triturate equivalent to 1.0 mg of BRT was accurately weighed, dissolved in phosphate buffer (pH 7.4) and sonicated for 30 mins. The resulting solution was filtered through Whatman filter paper No # 40, suitably diluted and analyzed using the proposed

method. From the absorbance values of five replicates, the drug content/ml was calculated on average weight basis.

Ocular gel: Aliquots of gel equivalent to 2 mg of drug was taken and dissolved in phosphate buffer (pH 7.4) by sonication. The resultant solution was filtered using Whatmann filter paper No # 40, suitably diluted and analyzed by the proposed method. The drug content/gram was calculated from the absorbance values of five replicates, on average concentration basis.

In situ gel: A known amount of in situ gel formulation equivalent to 2 mg of drug was weighed accurately and dispersed in phosphate buffer pH 7.4, stirred well, sonicated for 15 mins in order to extract the drug. The resulting solution was filtered through Whatmann Filter paper No1, suitably diluted with phosphate buffer pH 7.4 and analyzed. The result was calculated on average concentration basis.

Nanoparticles: For Eudragit based nanoparticles, the drug content estimation was carried out by dispersing accurately weighed freeze-dried formulations in selected organic solvent (methylene chloride, ethyl acetate) in a calibrated tube under ultrasonication for 10 mins at room temperature. The drug was the extracted from it by adding phosphate buffer (pH 7.4) and shaking for 10 mins at room temperature. The aqueous layer was separated out and diluted suitably and analyzed as five replicates, on average concentration basis.

The results of recovery studies are shown in Table 3.5 and the Two-Way ANOVA test results for variation in recovery between and within the formulations are shown in the Table 3.6.

(vii) Bench top stability studies

The bench top stability studies of the drug solution was carried out by storing the standard solution of concentration 12 µg/ml in phosphate buffer (pH 7.4) at controlled room temperature (25° C ± 2° C). At different time intervals up to 24 h, samples were withdrawn and diluted suitably with phosphate buffer (pH 7.4) and analyzed for the amount of drug. The overlayed UV absorption spectra of BRT stored at controlled room temperature is shown in Fig 3.3.

(viii) Forced degradation studies

Forced degradation studies provide an idea of specificity and stability indicating nature of the developed analytical method. This study was carried out by subjecting the drug to stress conditions like acid and alkali treatment and temperature stress conditions. However

no attempts were made to isolate the degradation products from the drug. The details of the procedure are as follows:

For acid degradation studies, in a calibrated volumetric flask (taken in triplicate), 4.5 ml of 50 µg/ml solution of drug in phosphate buffer (pH 7.4), 8.0 ml of 0.1N hydrochloric acid was added and volume was made up to 25 ml with phosphate buffer (pH 7.4). The solution was allowed to stand for 9 h at 50° C. At an interval of 3, 6, 9 h samples were withdrawn and UV- spectrum of the samples were recorded at 200-400 nm. Similar procedure was employed for alkali degradation studies wherein 0.1N hydrochloric acid was replaced with 0.1N sodium hydroxide in the procedure.

To study temperature stress effect, a 10 mg drug sample wrapped in aluminium foil was maintained at 50°C for 9 h on a heating plate. At an interval of 3, 6, 9 h samples were withdrawn and UV- spectrum of the samples were recorded at 200-400 nm after suitable dilution with the medium under study. The overlayed UV absorption spectra for forced degradation studies are shown in Fig 3.4(a) (acidic), 3.4(b) (alkali) and 3.4(c) (temperature).

3.4. RESULTS AND DISCUSSION

3.4.1. Method development

In the present work, a UV-spectrophotometric method was developed and validated for the estimation of BRT in pure form and in formulations. The various solvents such as water, buffers such as phosphate (pH 5.6-8.0), acetate (pH 3.5-5.6) and citrate (pH 3.0-7.0) and organic solvents like methanol, acetonitrile alone or in combinations of different proportions were investigated. The selection of phosphate buffer (pH 7.4) was based on the sensitivity, pH tolerance, ease of preparation and applicability in routine analysis, stability of the drug in the solvent and cost. The λ_{det} of BRT in phosphate buffer (pH 7.4) was found to be 248 nm and the UV- absorption spectra of 9 µg/ml standard solution of BRT in phosphate buffer (pH 7.4) is shown in the Fig 3.1(a). The absorbance values of BRT standard solutions in the concentration range of 3-18 µg/ml is shown in the Table 3.1 and the overlay spectra is presented in the Fig 3.1(b).

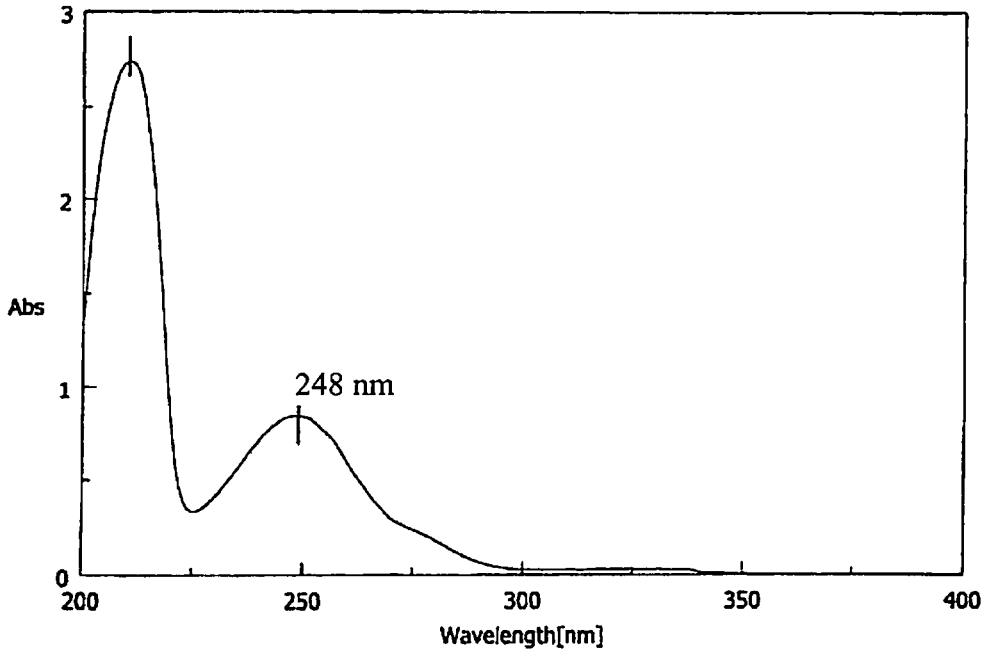

Fig 3.1(a):UV-absorption spectrum of 12µg/ml standard solution of brimonidine tartrate in phosphate buffer (pH 7.4) at λ_{det} of 248 nm.

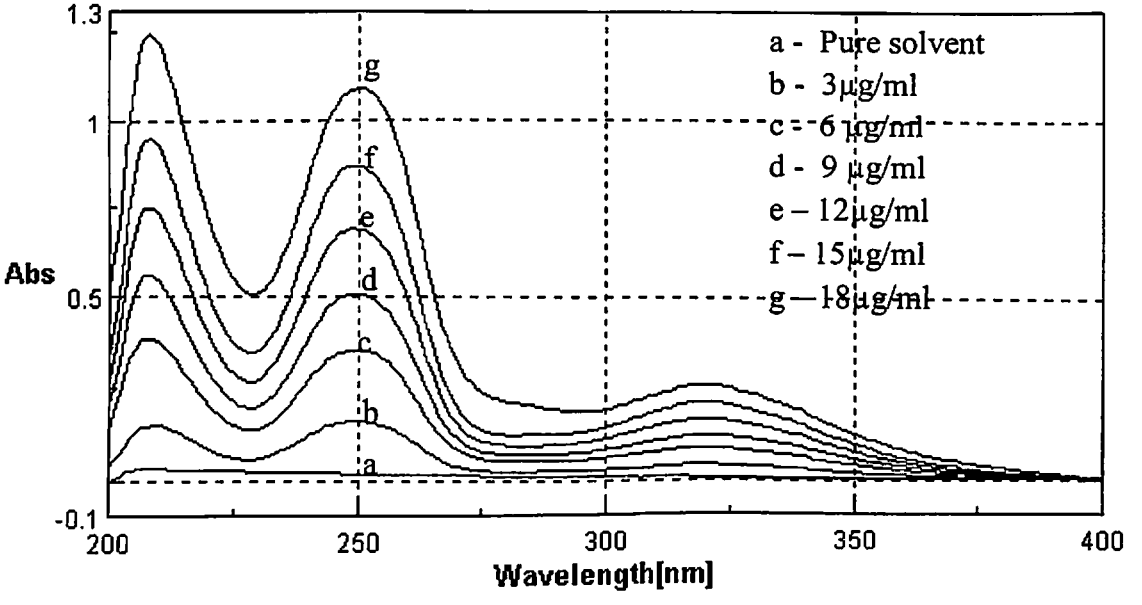

Fig 3.1(b): Overlay spectrum of brimonidine tartrate standard solutions (3-18 µg/ml) in phosphate buffer (pH 7.4).

Table 3.1: Calibration data of the proposed UV method for the estimation of brimonidine tartrate at 248 nm in phosphate buffer (pH 7.4).

Concentration (µg/ml)	Absorbance (± S.D)[a]	% RSD
3	0.1938 ± 0.0033	1.69
6	0.3825 ± 0.0018	0.48
9	0.5807 ± 0.0010	0.18
12	0.7613 ± 0.0013	0.17
15	0.9510 ± 0.0020	0.21
18	1.1423 ± 0.0028	0.24

[a] mean ± standard deviation of nine separate determinations; RSD: Relative standard deviation.

3.4.2. Calibration curve development

The linear regression equation of drug in phosphate buffer (pH 7.4) was found to be Y = 0.0630 X + 0.0050, where Y is the absorbance (µV) and X is the concentration (µg/ml), with a regression coefficient of 0.9999. The statistical regression data and validation parameters of the developed method are represented in the Table 3.2. The linearity of the regression equation was demonstrated by excellent regression coefficient with a negligible scatter of points around the regression line. The slope value without intercept on the ordinate fell within the 95% confidence interval limits of reported slope which indicated that the calibration line did not deviate much from the origin. The standard error of slope, intercept and estimate was found to be 3.047×10^{-4}, 3.560×10^{-3} and 3.811×10^{-3} respectively further confirming the precision of the proposed method.

Table 3.2: Statistical regression data and validation parameters for brimonidine tartrate at 248 nm in phosphate buffer (pH 7.4)

Statistical parameters	**Values**
Regression equation	Y = 0.0630. X + 0.0050
Regression coefficient (R^2)	R^2 = 0.9999
Standard error of slope	3.047×10^{-4}
Standard error of intercept on ordinate	3.560×10^{-3}
Standard error of estimate	3.811×10^{-3}
95% confidence interval of intercept	- 0.0041 to 0.0156
95% confidence interval of slope	0.0622 to 0.0639
Slope without intercept	0.0635

Table 3.3: Validation report for the determination of brimonidine tartrate in standard solutions

Analytical parameter	**Results**		
Accuracy	% Recovery = 99.92 ± 0.94		
Precision (% RSD)	Conc. (µg/ml)	Intra-day	Inter-day
	3	1.391	1.366
	9	0.195	0.038
	18	0.223	0.077
	Mean % RSD ± SD	0.60 ± 0.67	0.49 ± 0.76
Linearity	3-18 µg/ml		
Specificity	A 9 µg/ml solution of drug in phosphate buffer (pH 7.4) buffer pH 7.4 at λ_{det} of 248 nm will show an absorbance of 0.5807 ± 0.18.		
LOD[a]	0.15 µg/ml		
LOQ[a]	0.45 µg/ml		
Robustness	A change in solvent pH by ± 0.5 and change in analyst resulted in % RSD not more than 1.23		

[a] Based on S.D. of the response and the slope of the regression curve

3.4.3. Analytical method validation

The developed method was validated as per ICH Q2B guidelines (ICH, 1996) and statistical methods (Bolton and Bon, 2004). The validation summary for the proposed method is presented in the Table 3.3.

The linearity of the method was determined by linear regression and residual analysis of the results of calibration standard solutions of BRT. The linearity range of the method was found to be 3-18 µg/ml at λ_{det} of 248 nm. As the slope without intercept was well within the 95 % confidence interval limits, the proposed method can be considered as linear over the range of 0-18 µg/ml. A one-way ANOVA test of linearity was performed on absorbance values obtained for calibration standards. The calculated F value was found to be very less compared to the tabulated value at 5% level of significance indicating that the method is linear in the proposed range (Table 3.4).

Table 3.4: One-way ANOVA test for linearity of pure brimonidine tartrate solution by the proposed method

Source of Variation	**Sum of squares**	**Degree of freedom**	**Mean sum of squares**	**F_{Calc}**	**F_{crit} [a]**
Between Groups	2.211×10^{-5}	8	2.76×10^{-6}	2.2×10^{-5}	2.153
Within Groups	5.650	45	1.26×10^{-1}		
Total	5.650	53			

[a] Theoretical value of F (8,45) for one-way ANOVA at 5% level of significance

(i) Accuracy

The accuracy of the proposed method (expressed as mean % recovery) was found to be 99.92 ± 0.94 in the selected solvent (Table 3.3).

(ii) Precision

The precision of the developed method was studied by determining the repeatability and intermediate precision. The repeatability or intra assay and intermediate precision values expressed as % RSD were found to be 0.60 ± 0.67 and 0.49 ± 0.76 respectively. The low values of % RSD indicated the excellent precision of the developed method (Table 3.3).

(iii) LOD and LOQ

The LOD of analytical method is the lowest absolute concentration of the analyte which can be detected but not necessarily be quantified under the given experimental conditions. Similarly LOQ is the lowest concentration of an analyte which can be quantified with acceptable precision and accuracy. LOD of the proposed method was found to be 0.15 µg/ml and the LOQ was found to be 0.45 µg/ml respectively. Low LOD and LOQ values indicated high sensitivity of the developed method (Table 3.3).

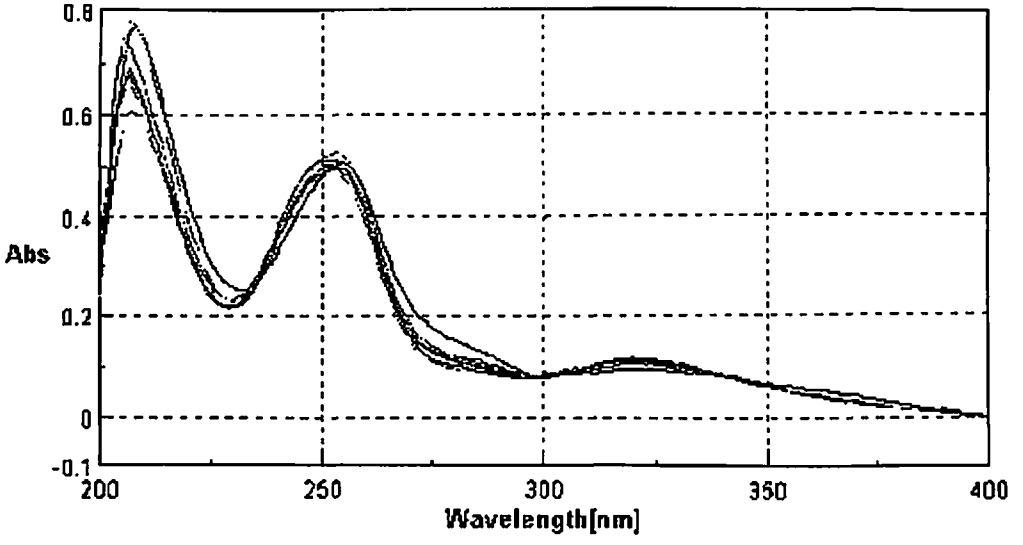

Fig 3.2: Overlayed UV- absorption spectra of 9 µg/ml standard solution of brimonidine tartrate spiked with common formulation excipients.

(iv) Specificity

The proposed method was found to be specific for BRT, as UV- spectrum of the drug remained unchanged in the presence of common excipients added in the study (Fig 3.2). A drug solution of 12 µg/ml in phosphate buffer (pH 7.4) at λ_{det} 248 nm shows specifically an absorbance of 0.7613 ± 0.0013 (Table 3.3).

(v) Robustness

No significant change in the absorbance was observed with change in the pH of the media by ± 0.5. Also there is no significant change in the absorbance due to change in the instrument and analyst with % RSD value was found to be 1.23 (Table 3.3).

(vi) Recovery studies

Drug content estimation from formulations and analytical recovery studies

The developed method was further validated by estimating the drug content from prepared formulations. Results are shown in the Table 3 5. The estimated drug content values for different formulations were obtained as 1.97 ± 0.02 mg/ml for ophthalmic solution; 0.98 ± 0.02 mg/12 mg ocular insert for ocular insert; and 1.97 ± 0.01 mg/g for ocular gel; 1.98 ± 0.01 mg/ml for in situ gel formulation and 1.99 ± 0.01 mg/41.7 mg of the formulation in case on nanoparticles. The % RSD in all the cases was less than 1%.

Table 3.5: Results of recovery studies of brimonidine tartrate from its formulation matrix by the proposed method

Formulation	**Label claim**	**Recovery** [a]		**% Analytical recovery (Mean ± SD)**
		Mean ± SD	**% RSD**	
Ophthalmic solutions	2.0 mg/ml	1.9674 ± 0.018	0.925	98.37 ± 0.91
Ocular inserts	1.0 mg/12 mg ocular insert	0.9746 ± 0.016	0.828	97.30 ± 0.80
Ocular gels	2.0 mg/g	1.9721 ± 0.007	0.363	98.60 ± 0.35
In situ gels	2.0 mg/g	1.9832 ± 0.009	0.763	98.56 ± 0.51
Nanoparticles	2 mg/41.7 mg[#].	1.9899 ± 0.009	0.985	99.46 ± 0.34

[a] Mean ± SD and % RSD for three samples analyzed in triplicate; # based on the loading efficiency of nanoparticle formulation BNP-1:1(150).

A two-way ANOVA test at 5% level for drug content estimation from these formulations indicated low $F_{Calculated}$ value when compared to tabulated value (Table 3.6) suggesting non- interference from the varied formulation matrix in the estimation of drug. Analytical recovery values ranged from 96.49 to 99.28%, further indicating specificity of the proposed method.

Table 3.6: Two-way ANOVA test (without replication) for estimation of brimonidine tartrate in various ophthalmic formulations by the proposed method

Source of Variation	Sum of square	Degree of freedom	Mean sum of squares	F_{calc}	F_{crit} [a]
Between formulations	5.1221	4	1.280	2.1911	3.006
Within formulation	1.1331	4	0.332	0.5696	3.006
Residual	9.350	16	0.584		
Total	15.804	24			

[a] Theoretical value of F (4,16) for two-way ANOVA at 5 % level of significance.

(vii) Bench top stability studies

The bench top stability at controlled room temperature (25° C ± 2° C), showed that there was no significant change in drug's absorption spectra upto 24 hrs, as shown in the Fig 3.3. This suggests that the method can be applied in the routine analysis of pure drug and its formulations in quality control testing without any fear of sample degradation.

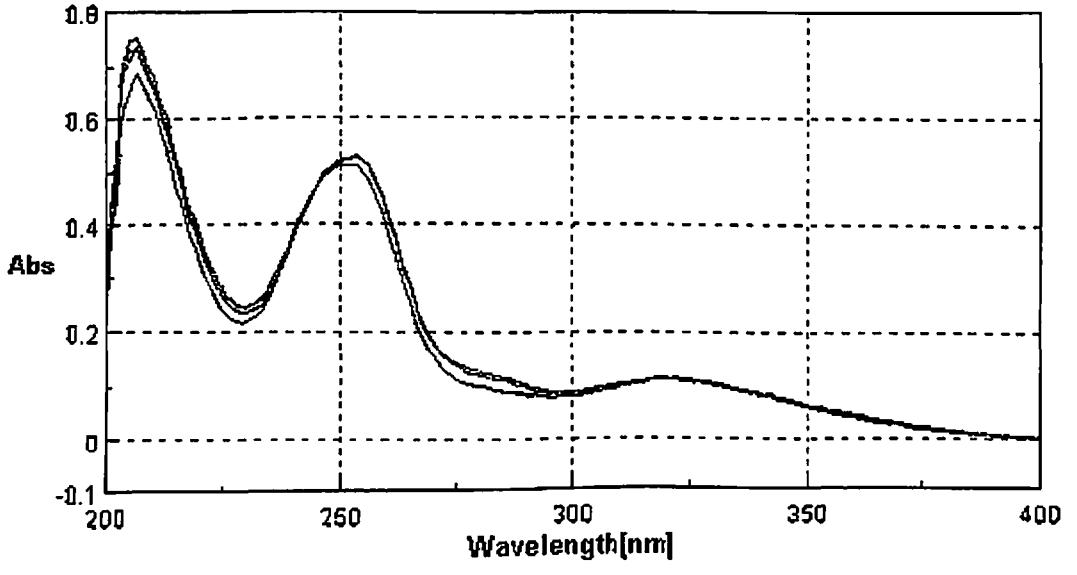

Fig 3.3: Overlayed UV-absorption spectra of BRT (12 µg/ml) at controlled room temperature at different time intervals.

(viii) Forced degradation studies

The forced degradation studies were performed to study the stability indicating attribute of the proposed method. The ability of the method to trace out the degradation of the drug, as evident by the shift in the UV- absorption spectra of the drug is an indicator for the method's specificity for the drug in the given experimental conditions and also provides information on its stability indicating property. The UV spectrum (200-400 nm) of BRT after exposure to acidic, alkaline and heat treatments showed a significant deviation from the zero time control. The typical UV- absorption spectra for acid, alkaline and heat exposure studies are shown in Fig 3.4(a), Fig 3.4(b) and Fig 3.4(c) respectively.

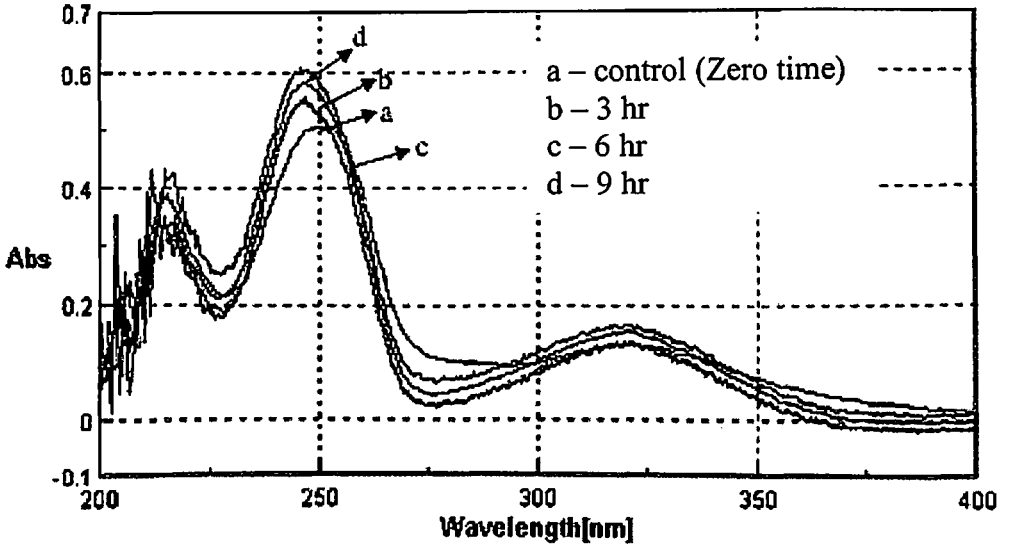

Fig 3.4(a): Overlayed UV absorption spectrum of 9 µg/ml concentration of BRT in 0.1N HCl at 0, 3, 6, 9 h kept at 50°C.

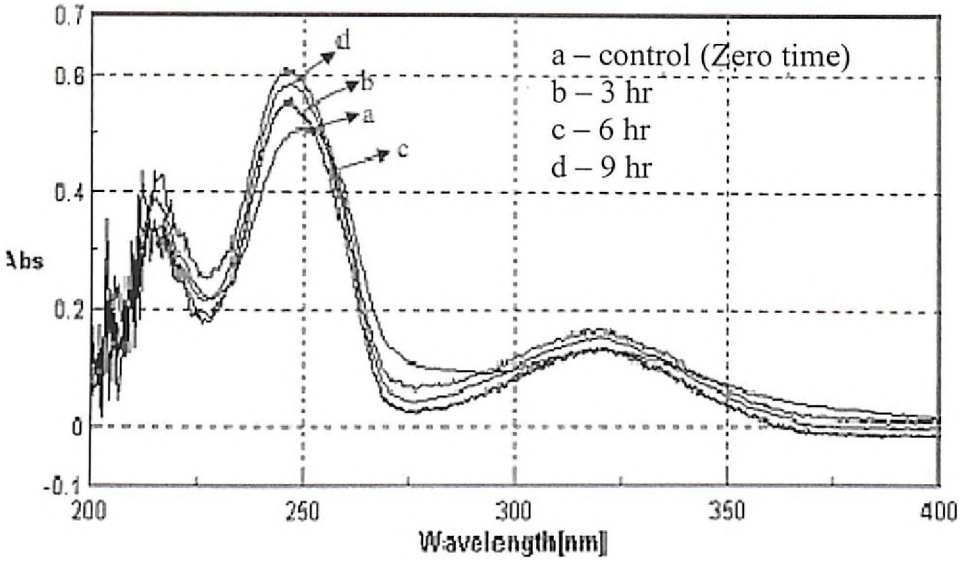

Fig 3.4(b): Overlayed UV-absorption spectrum of 9µg/ml concentration of BRT in 0.1N NaOH at 0, 3, 6, 9 h kept at 50°C.

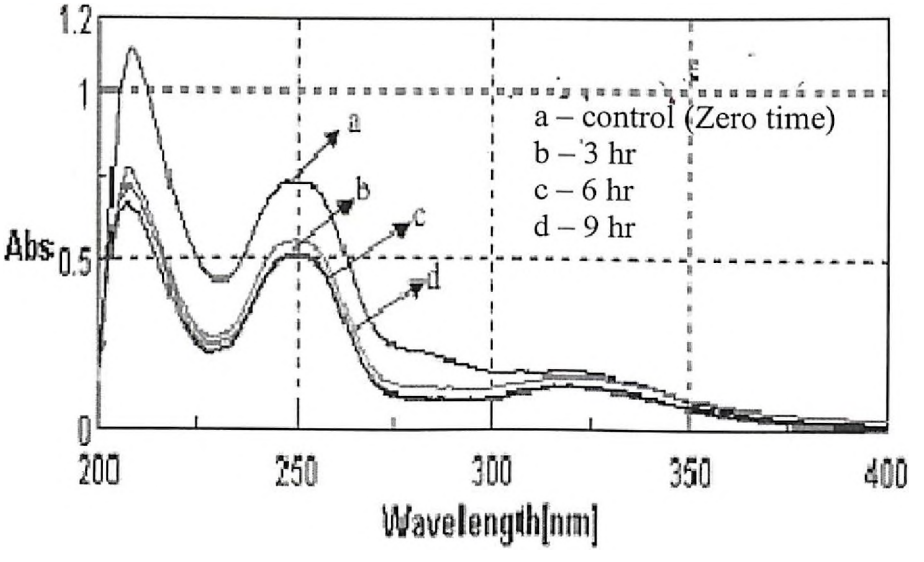

Fig 3.4(c): Overlayed UV-absorption spectrum of 9 µg/ml concentration of BRT under temperature stress condition at 0, 3, 6, 9 h.

In acidic and basic environment, the drug showed degradation, as can be visualized by a shift in the UV spectra of BRT with changes in shape of the spectrum. Solid drug sample when exposed to heat at 50° C caused a decrease in the absorption values without alteration in the shape of the spectra. The method is thus specific to the detection of BRT in phosphate buffer (pH 7.4) and any occurrence of slight degradation is observed by shift in the UV absorption profile.

3.5. CONCLUSIONS

From the present studies it can be concluded that, the developed and validated method for the estimation of BRT in pure form and its ophthalmic formulations is simple, accurate, rapid, precise and cost effective. The method is very sensitive with LOD and LOQ of 0.15 µg/ml and 0.45 µg/ml. The proposed method does not utilize special extraction procedures in recovering the drug from the formulation excipients matrices, hence it is fast and has low probability of sample preparation error. The drug content estimation values in different formulations and analytical recovery values were in agreement with the theoretical claims indicating the specificity of the proposed method and non- interference of formulation additives. Hence the method can be a good tool in estimating pure drug, drug content in designed dosage form, and in vitro dissolution studies and in stability studies. The developed and validated method was successfully employed for drug content estimation, analysis of in vitro release samples and stability studies for the prepared in situ gels, ocular inserts and nanoparticle formulations as a part of this research work. Further the method can be used as stability indicating method due to the high stability of the analyte in the solvent system used and detection of any degradation at the selected wavelength of the analysis.

3.6. REFERENCES

Acheampong A, Tang-Liu DD. 1995. Measurement of brimonidine concentrations in human plasma by a highly sensitive gas chromatography/mass spectrometric assay. J. Pharm. Biomed. Anal, 13; 995-1002.

Acheampong AA, Shackleton M, John B, Burke J, Wheeler L, Tang-Liu D. 2002. Distribution of brimonidine into anterior and posterior tissues of monkey, rabbit, and rat eyes. Drug Metab. Dispos, 30; 421-429.

Ali MS, Khatri AR, Munir MI, Ghori M. 2009. A stability-indicating assay of brimonidine tartrate ophthalmic solution and stress testing using HILIC. Chromatographia, 70; 539-544.

Bolton S and Bon C. 2004. Pharmaceutical statistics: practical and clinical applications, 4th ed. Marcel Dekker Inc, New York.

Chien DS, Homsy JJ, Gluchowski C, Tang-Liu DD. 1990. Corneal and conjunctival/scleral penetration of p-aminoclonidine, AGN 190342, and clonidine in rabbit eyes. Cur. Eye Res, 9; 1051-1059.

De TK, Rodman DJ, Holm BA, Prasad PN, Bergey EJ. 2003. Brimonidine formulation in polyacrylic acid nanoparticles for ophthalmic delivery. J. Microencapsul, 20; 361-374.

International Conference on Harmonisation (ICH), 1996. Technical requirements for Registration of Pharmaceuticals for Human Use: Harmonised Tripartite Guideline on Validation of Analytical Procedures: text and methodology, Q2 (R1), Step 4 version, incorporated Nov 2005 (parent guideline Oct 1995, complementary guideline on methodology Nov 1996).

Jiang S, Chappa AK, Proksch JW. 2009. A rapid and sensitive LC/MS/MS assay for the quantitation of brimonidine in ocular fluids and tissues. J. Chromatography B, 877; 107-114.

Karamanos NK, Lamari F, Katsimpris J, Gartaganis S. 1999. Development of an HPLC method for determining the alpha2-adrenergic receptor agonist brimonidine in blood serum and aqueous humor of the eye. Biomed. Chromatogr, 13; 86-88.

Madhavi A, Naidu A, Rao DVS, Srinivasu P. 2009. Development and validation of a new LC method for analysis of brimonidine tartrate and related compounds. Chromatographia, 69; 1413-1419.

Ni J, Rowe J, Heidelbaugh T, Sinha S, Acheampong A. 2007. Characterization of benzimidazole and other oxidative and conjugative metabolites of brimonidine in vitro and in rats in vivo using on-line H/D exchange LC-MS/MS and stable-isotope tracer techniques. Xenobiotica, 37; 205-220.

Shirke RR, Pai N. 2002. RP-HPLC determination of brimonidine tartrate in brimonidine tartrate eye drops. Indian drugs, 39; 484-486.

Chandran S and Singh RSP. 2007. Comparison of various international guidelines for analytical method validation. Pharmazie, 62; 4-14.

United States Pharmacopeia (USP), XXXII, 2009.Validation of compendial methods, 32nd edn; Rockvile, MD; United States Pharmacopeial Convention Inc; 2439-2442.

CHAPTER FOUR

PREFORMULATION STUDIES

4.1. INTRODUCTION

Preformulation studies are necessary and an important step between drug discovery and clinical development in the drug development process. Preformulation studies are aimed at understanding the drug's physicochemical and other related properties including its possible interaction with excipients. They are mainly useful in profiling the active drug substance and drug excipient compatibility studies. The dosage form in its final primary and secondary packing can undergo variety of interactions and transformations - physical and chemical - and these interactions can lead to severe dosage form related problems such as production of undefined impurities, organoleptic, physical and chemical changes in the drug molecule. Hence a thorough understanding of drug's physicochemical properties such as solubility in aqueous and non-aqueous solvents, crystallinity and polymorphism, partition coefficient and ionisation pattern, solution and solid state stability and drug excipient interaction pattern are extremely important prior to dosage form design.

An extensive study of solubility of drug in varying pH, buffer strength and in different organic solvents will lead to understanding of drug aqueous solubility and ionisation pattern. The pKa and ionisation constant of the drug helps in understanding the degree of ionisation and pKa-pH partition profiles are helpful in predicting drug stability profile and in vivo transcorneal permeation profile upon ocular administration. The ionisation pattern also helps in selecting suitable pH and solvent combinations in formulation design, drug analysis and extraction for analyte from in vitro and also from biological matrices. Partition coefficient of drug plays a crucial role in understanding the drug behaviour in vivo like precorneal disposition, metabolism and bioavailability in the ocular target site and also in selecting suitable excipients. The selection of suitable form of polymorph/ hydrates also plays a vital role as different polymorphs and hydrates will have varying physicochemical and also varying in vivo characteristics. Polymorph specific stability also important in selection of packaging material for the final dosage form. The most critical part of preformulation studies is the selection of suitable excipients for the drug in developing an elegant and stable dosage form from the pool of different functional categories of excipients.

Various analytical tools like Fourier Transform Infrared spectroscopy (FT-IR), Differential Scanning Calorimetry (DSC), Nuclear Magnetic Resonance Spectroscopy, Diffusional reflectance spectroscopy along with methods of drug quantification such as UV, HPLC are employed for preformulation studies.

The objective of this work was to determine the preformulation parameters of BRT such as solubility in aqueous media, apparent partition coefficient, pKa, solution state stability and drug excipient compatibility studies in order to develop suitable, elegant and stable formulations for ocular delivery.

4.2. MATERIALS, EQUIPMENTS & INSTRUMENTS

4.2.1. Materials

Brimonidine tartrate was obtained as a gift sample from FDC Ltd, Mumbai (India), Sodium hydrogen phosphate, dihydrogen potassium orthophosphate, sodium hydroxide and phosphoric acid were purchased from CDH Chemicals, Mumbai, India. High quality pure water was prepared using Millipore purification system (Millipore, Molsheim, France, Model Elix SA 67120). All other excipients, chemicals or solvents used were either of pharmaceutical or analytical grade.

4.2.2. Equipments & Instruments

An incubator shaker (MAC Instruments, India) was used for solubility studies and partition coefficient determination studies. For all the analytical studies, including preformulation, UV-Visible spectrophotometer (Jasco, Tokyo, Japan, Model V-570) connected to computer loaded with spectra manager® software, with automatic wavelength accuracy of 0.1 nm, with 10 mm matched quartz cells was used. Humidity chambers (Newtronics, India) was used to maintain ambient (25° C ± 2° C/60 ± 5% RH) and ATC (40° C ± 2° C/75 ± 5% RH) conditions. Hot air oven (MAC instruments, India) was used for drying purpose. A pH meter (Eutech, pH Tutor) fitted with glass electrode, filled with potassium chloride solution was used for all the pH measurements. Thermal studies were carried out using Differential scanning calorimeter (Shimadzu Japan, model: DSC-60, integrator-TA-60WS thermal analyser, integrating software- TA-60WS collection monitor version 1.51, analysis software-TA60, principle-heat flux type, temperature range of -150 to 600 °C, heat flow range ± 40 mW, temperature program rate- 0 to 99 °C per min, atmosphere- inert nitrogen at 30 ml per min). Infrared analysis was done using Fourier Transform Infrared (FT-IR) spectrophotometer (Shimadzu, Japan, model IRPrestige-21) connected to IRSolutions, version 1.10 software.

4.3. METHODS

4.3.1. Determination of solubility profile

The solubility profile of BRT was determined using modified shake flask method in buffered solutions. An excess of BRT was added to each of the 2 ml of the buffers taken in micro-centrifuge tubes maintained on a mechanical orbital shaker at 37 ± 0.5° C. An excess of undissolved drug was always maintained in each of the tubes for the entire duration of the study. The tubes were shaken on mechanical orbital shaker for 24 hours. Samples from the tubes were collected, suitably diluted and analyzed by developed UV spectrophotometric method (Chapter III – Analytical method development).

Different buffered media employed were, phosphate buffers of pH ranging from 5 to 8.0 (pH 4.0, 4.5, 5.0, 5.5, 6.0, 6.5, 7.0, 7.4, 8.0) as per the procedures enlisted in Indian Pharmacopoeia (2007). NaCl was added in sufficient amount to adjust the ionic strength 0.3M. The results of solubility determination studies are shown in the Table 4.1 and illustrated in the Fig 4.1.

4.3.2. Determination of apparent partition coefficient

The apparent partition coefficient (P_{App}) of BRT was determined by traditional shake flask method (Walter et al, 1985) at 37° C ± 0.5° C using n-octanol or chloroform as organic phase and water or phosphate buffer (pH ranging from 5.5 to 8.5, pH adjusted with 0.1N NaOH or 0.1N HCl) as aqueous phase. The organic and aqueous phases were equilibrated with each other by shaking them together for about 12 h and then separating at 37° C ± 0.5° C. The ionic strength of the buffers was adjusted to 0.15 M with NaCl. The aqueous phase was centrifuged after equilibration in order to remove small n-octanol droplets befouling it as a result of the emulsion formation during shaking. To a known volume (2 ml) of aqueous phase containing drug dissolved in it, 2 ml of organic phase was added into a 5 ml tube and allowed to stir for 24 h on an orbital shaker at a temperature of 37.0 ± 0.5 °C, in triplicates. Samples were withdrawn at 12 and 24 h, centrifuged (4000 rpm, 15 mins), suitably diluted with phosphate buffer (pH 7.4) and analyzed spectrophotometrically at 248 nm. The concentration of drug in aqueous phase at time zero (C_0) and the concentration at time t (C_t) were determined. Each logP value is calculated as average of three determinations. The results are shown in the Table 4.2 and represented as pH-partition profile in Fig 4.2. The apparent partition coefficient was calculated using the equation,

$$P_{App} = [C_{0\,(Aqueous)} - C_{t\,(Aqueous)}] / C_{t\,(Aqueous)}]$$

4.3.3. Determination of dissociation constant (pKa)

If the criterion of different UV absorbance profile for ionised and unionised species is met, an accurate and precise measurement of dissociation constant is possible by spectrophotometric method (Albert, 1962; Barbosa et al, 2001; Beltran et al, 2003). The method followed was as below (Roman et al, 1998; Singh et al, 1999).

Buffers of varying pH in the range of 1.2-13 were prepared using 0.2 M NaH_2PO_4, 0.2 M K_2HPO_4 and 0.2 M NaCl to give a final buffer molarity of 0.01M and ionic strength of 0.02M. The pH of these solutions were adjusted with 0.1N NaOH (pH 12.5) or 0.1 N HCl (pH 1.2). The primary stock solution of BRT (1000 µg/ml) was prepared in triple distilled water (TDW) and an aliquot volume was transferred into individual calibrated volumetric flasks and diluted with media of varying pH to give a concentration of 10 µg/ml. The resulting solutions were immediately scanned in the range of UV wavelength of 200-400 nm at a scanning speed of 200 nm/sec and UV absorbance spectras were recorded. The obtained spectras were then overlapped to determine the wavelength where maximum change in the absorbance amongst the absorbing species at different pH was seen. The absorbance values at the wavelength was plotted against pH. A first derivative absorbance spectrum was plotted by taking ΔAbs/ΔpH vs. pH and the pKa was obtained directly as the point of inflection in ΔAbs/ΔpH vs. pH curve (graphical method) as shown in Fig 4.4. Subsequently pKa was also calculated using the following equation.

$$pKa = pH + \log (A_i - A / A - A_u)$$

where A_i is the absorbance of the ionized species (absorbance of BRT in 0.1 N HCl, pH 1.2), A_u is the absorbance of neutral species (absorbance of BRT in 0.1 N NaOH, pH 12.4) and A is the absorbance of test solution. The pKa values obtained is an average of three determinations for each set of pH.

4.3.4. Stability studies

As a part of preformulation studies, both solution state and solid state stability studies (drug excipient compatibility studies) were performed. The solution state stability studies were performed in buffered pH solutions stored at ambient and accelerated storage conditions. Solid state stability studies were carried out in the presence of different excipients and polymers which are proposed to be used in the formulation development of

BRT in the current study. The results were fitted into various mathematical models to assess the nature of degradation kinetics and to express in terms of degradation rate constant, regression coefficient and shelf life.

(i) Solution state stability studies

In order to study the pH - stability profile of BRT (degradation rate constant vs.pH), different pH media were prepared as per IP (Indian Pharmacopeia, 2007) and USP (US Pharmacopeia, USP-32/NF-27, 2009). Sodium chloride was added in sufficient concentration to maintain the ionic strength in all the pH media. The pH solutions were prepared in the pH range of 2 - 12.5. The drug solutions of 50 μM, 500 μM and 2000 μM were prepared in different pH media. The prepared solutions were filled and sealed into ampoules and stored at ambient (25° C ± 2° C/60 ± 5% RH) and ATC (40° C ± 2° C/75 ± 5% RH). At predetermined time intervals, samples were withdrawn and analysed after suitable dilution by UV- spectrophotometric method to estimate the drug content. The degradation rate constants (K_{deg}) T_{90} and R^2 were determined at different storage conditions in various pH solutions.

(ii) Drug- excipient compatibility studies

Drug-excipient compatibility studies (solid state stability studies) were performed for BRT in the presence various polymers and excipients in order to asses the presence of any instability (incompatibility) amongst the set of excipients with the drug.

Drug and various excipients such as HPMC (K4M, K15M, K100M), PEO (100 kDa and 400 kDa, Eudragits (ERS 100, ERL 100), ethyl cellulose (EC-50), pluronic PF-68, chitosan were weighed separately, geometrically mixed, thoroughly blended and the resulting mix was passed through sieve no # 100 to ensure a uniform blending. The drug alone (as control) and in combination (drug to excipient ratio of 1:1) with above mentioned excipients were stored in tightly capped screw cap vials at ambient (25° C ± 2° C/60 ± 5 % RH) and in ATC (40° C ± 2° C/75 ± 5% RH). Samples were withdrawn at predetermined time intervals and analysed for the drug content after suitable dilution by spectrophotometric analytical method (Chapter III-Analytical method development). The results are shown in Table 4.5.

Differential scanning calorimetric study was carried out for both pure drug and individual excipients and for the combination of drug and excipients. After suitably processing the samples, about 4 mg of the sample was accurately weighed and was sealed in standard aluminium pans with lid by crimping. The hold temperature was set to 300° C (range: 30 -

300° C) and the heating rate was set to 10° C per min. The sample heating environment was kept under nitrogen gas at a flow rate of 50 ml/min.

Exothermic peaks were recorded in the thermograms for all the samples. The thermograms of pure drug and pure excipient were overlayed with the thermograms of drug-excipient mixture in order to determine the presence of any incompatibility in the mixture, which could be visible by a shift or masking of drug melting peak at the melting point region of the drug. The representative thermograms of drug with various excipients are shown in the Fig 4.6 and Fig 4.7.

4.4. RESULTS AND DISCUSSION

4.4.1. Determination of solubility profile

The solubility results of BRT at varying pH are shown in the Table 4.1 and graphically represented in Fig 4.1. The solubility of BRT was found be pH dependent, with higher solubility in acidic side and lower solubility at basic pH. From the pKa results, it was evident that drug is weakly basic in nature. It exists predominately in ionized form at lower pH, hence a higher solubility of free base. As the pH is increased, solubility was found to decrease. The solubility in TDW was found to be 29.9 mg/ml.

Table 4.1: pH-solubility profile of BRT in aqueous buffer solutions.

pH of aqueous buffer media	Solubility (mg/ml)
4.0	639.9 ± 3.1
4.5	325.7 ± 3.3
5.0	224.8 ± 4.2
5.5	158.5 ± 2.3
6.0	99.5 ± 1.2
6.5	69.0 ± 2.3
7.0	37.9 ± 2.2
7.4	23.2 ± 1.3
8.0	6.8 ± 0.6
Water (TDW)	29.9 ± 1.3

Each data represents the average of three independent determinations with standard deviation

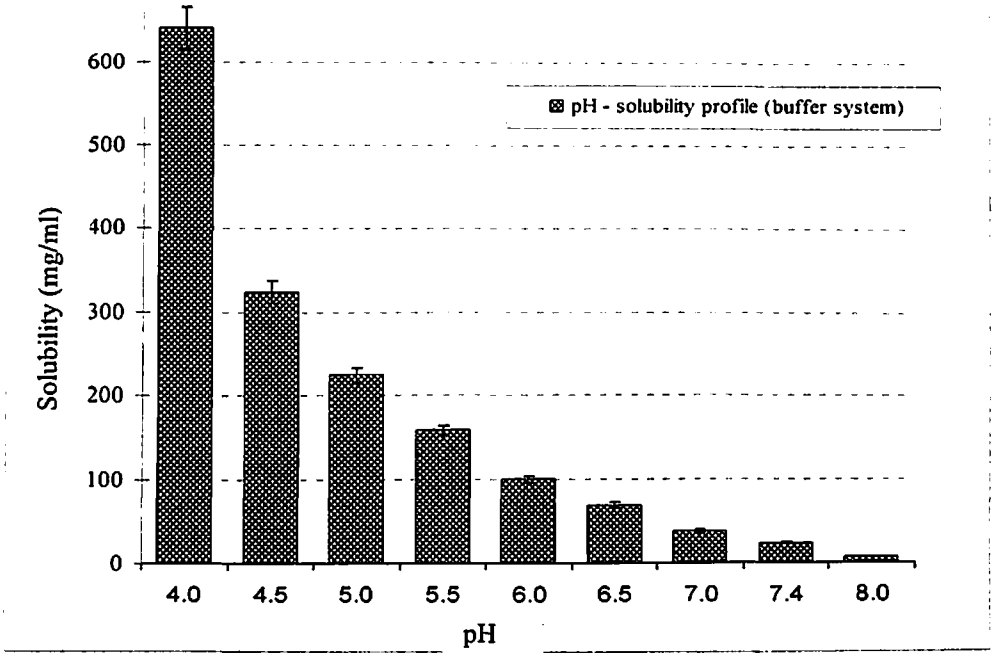

Fig 4.1: pH-solubility profile of brimonidine tartrate in aqueous buffer systems. Each data point represents the average of three independent determinations with standard deviation

4.4.2. Determination of apparent partition coefficient

The apparent partition coefficient of BRT between organic phases (chloroform and octanol) and aqueous media (buffers of varying pH and water) are presented in Table 4.2. The time needed to reach equilibrium was found to be approximately 3 hours.

Table 4.2: Apparent partition coefficient data of BRT at different pH media

Chloroform / Aq. media			**n-octanol / Aq. media**		
Composition of aq. media	**P_{App} (Mean ± SD)**	**Log P_{App} (Mean ± SD)**	**Composition of aq. media**	**P_{App} (Mean ± SD)**	**Log P_{App} (Mean ± SD)**
pH 5.5 buffer	1.80 ± 0.01	0.25 ± 0.01	pH 5.5 buffer	0.14 ± 0.01	-0.86 ± 0.02
pH 6.0 buffer	1.93 ± 0.03	0.28 ± 0.04	pH 6.0 buffer	0.16 ± 0.01	-0.78 ± 0.03
pH 6.5 buffer	2.01 ± 0.02	0.30 ± 0.02	pH 6.5 buffer	0.26 ± 0.01	-0.58 ± 0.03
pH 7.0 buffer	2.10 ± 0.03	0.32 ± 0.03	pH 7.0 buffer	0.42 ± 0.01	-0.37 ± 0.02
pH 7.4 buffer	2.19 ± 0.02	0.34 ± 0.02	pH 7.4 buffer	0.78 ± 0.01	-0.11 ± 0.01
pH 8.0 buffer	2.32 ± 0.01	0.37 ± 0.01	pH 8.0 buffer	1.80 ± 0.02	0.25 ± 0.03
pH 8.5 buffer	2.33 ± 0.01	0.37 ± 0.03	pH 8.5 buffer	1.70 ± 0.01	0.23 ± 0.02

Each data represents the average of three independent determinations with standard deviation

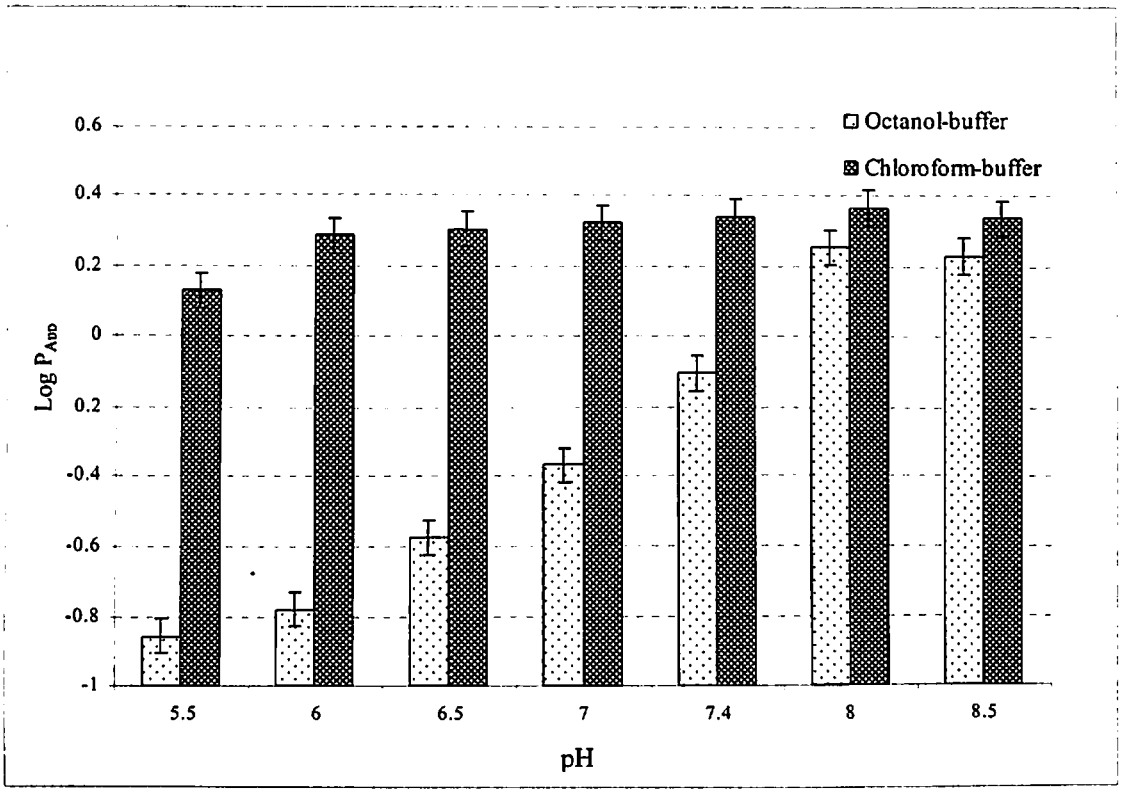

Fig 4.2: pH-partition profile of brimonidine tartrate across the pH range. Each data represents the average of three independent determinations with standard deviation.

The partition coefficient of BRT between n-octanol/water and chloroform/water system was found to be 0.25 ± 0.04 and 0.25 ± 0.03 respectively.

From the Table 4.2 and Fig 4.2, it was evident that, the P_{App} values in n-octanol/buffer system was highly pH dependent. The P_{App} values were less at pH 5.5 and increased gradually with an increase in the pH of the buffer media. From the pKa determination studies, BRT was found to be weakly basic (pKa of 7.22). At acidic pH, a relatively low P_{App} was due to the ionisation of drug below its pKa, due to the presence of basic functional groups in the drug molecule and at neutral pH range drug might exists as zwitterion form. The degree of ionisation of drug majorly governs its partition across the organic and aqueous phases. As the pH is increased, P_{App} values increased due to fact that pH was approaching pKa of the drug and the degree of ionisation was relatively lesser (De et al, 2003). A very high P_{App} was obtained at pH 7.4 and 8.0, as drug predominately existed in unionised form.

In the case of chloroform/aqueous media system, a relatively higher value of P_{App} was obtained in comparison to n-octanol/aqueous system, which could be due to the strong

acidic nature of chloroform, thereby partitioning of more drug into the organic phase compared to that of octanol phase.

4.4.3. Determination of Dissociation constant (pKa)

Based on spectrophotometric determination of pKa of BRT, (results are shown in the Table 4.3), the average pKa was found to be 7.22. The pKa of BRT determined by potentiometric method was 7.5 (Chien et al, 1990).

The UV absorbance spectras of various absorbing species at different pH were recorded in the range of 200-400 nm (Fig 4.3). They are overlayed in order to determine the wavelength for pKa determination. The wavelengths selected for the determination of absorbance of BRT in ionised and neutral forms, was the point where the maximum difference existed between various species (ionised, neutral) of the BRT at varying pH solutions. For the accurate determination of pKa, a range of wavelength from 234-250 were selected and absorbance of BRT in varying pH buffers were noted down. A first derivative spectra of ΔAbs/ΔpH Vs pH plotted (Fig 4.4), showed the pKa to be in the range of 6-8, with a sharp change in absorbance with respect to change in pH (ΔAbs/ΔpH) against pH. Graphically pKa was found be 7.3, as determined from the peak of first derivative spectra. The results of pKa determination using Henderson Hesslebatch equation is shown in the Table 4.3. The pKa by this method was found to be 7.22 ± 0.18. The pKa values were found to be almost same at the entire wavelength selected. The ionisation at lower pH was due to the protonation of amino groups of BRT, which decreases as the pH is increased. At pH = pKa, an equal amount of ionised (protonated) and unionised (non- protonated) species were formed.

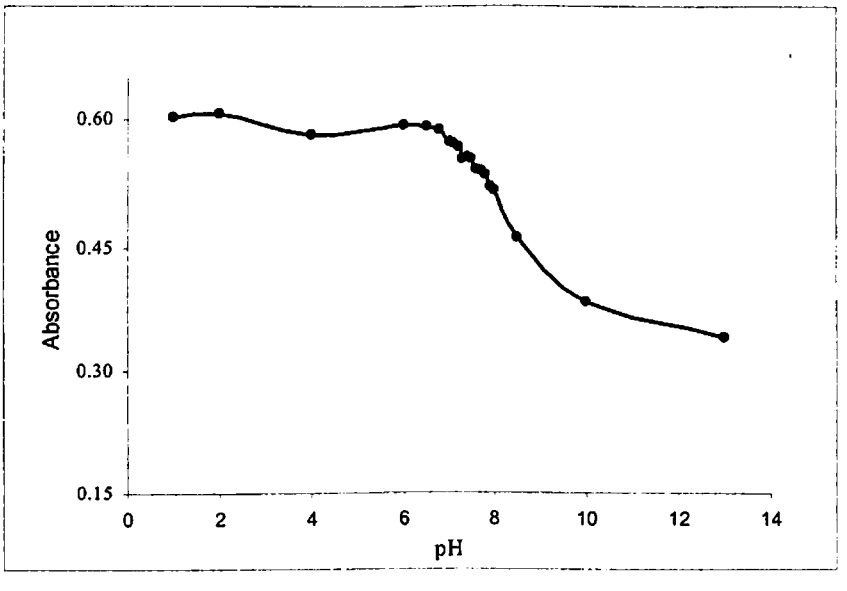

Fig 4.3: pH absorbance profile of brimonidine tartrate across the pH range.

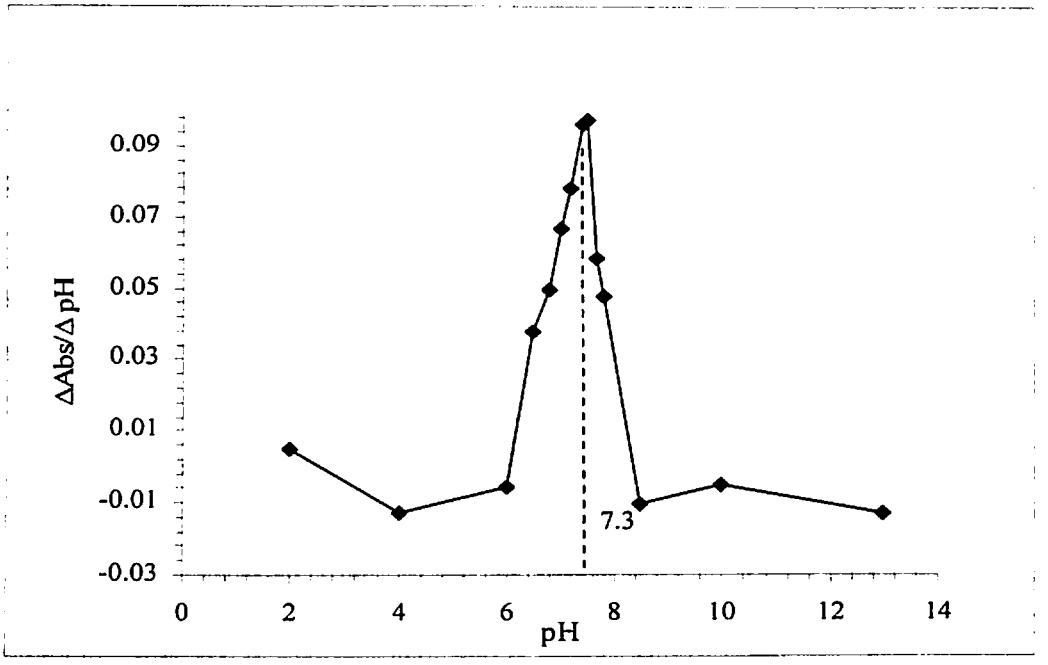

Fig 4.4: First derivative absorbance spectra of brimonidine tartrate with respect to pH.

Table 4.3: pKa of brimonidine tartrate in multiple wavelengths and multiple pH range.

pH	pKa at Wavelength (nm)								
	234	**236**	**238**	**240**	**242**	**244**	**246**	**248**	**250**
6.50	7.33	7.13	7.03	6.98	7.42	7.33	7.09	7.32	7.10
6.81	7.03	6.91	6.88	6.8	7.02	6.99	6.90	7.31	7.39
7.01	7.09	6.97	7.11	7.06	7.10	7.01	7.15	7.08	7.18
7.10	7.34	7.20	7.28	7.14	7.20	7.08	7.12	7.16	7.27
7.22	7.43	7.29	7.28	7.24	7.36	7.19	7.22	7.26	7.36
7.31	7.29	7.38	7.47	7.42	7.22	7.35	7.25	7.43	7.53
7.51	7.02	7.51	7.41	7.04	7.33	7.30	7.12	7.22	7.90
7.67	6.92	7.22	7.32	7.31	7.41	7.08	7.21	7.21	7.45
7.82	6.96	6.92	7.42	7.45	7.32	7.22	7.32	7.16	7.28
7.99	7.42	7.43	7.38	7.21	7.04	7.10	7.40	7.21	7.23
Average pKa = 7.22 ± 0.18									

Each data represents the average of three independent determinations.

4.4.4. Stability studies

(i) Solution state stability studies

The solution state stability studies were carried out in varying pH of the aqueous buffer solutions at ambient and ATC conditions. The log percent remaining to be degraded was plotted against time and was found to be linear suggesting that degradation rate was of first order. The degradation rate constant (K_{deg}) was determined from the slope of the respective curves of different buffers of varying pH. The results are shown in the Table 4.4. The studies carried out at three different concentrations suggested that the degradation kinetics of BRT was pH dependent, with minimum degradation at neutral pH. The K_{deg} was found to be in the range of 3.81 x 10^{-3} $days^{-1}$ (pH 2) to 1.02 x 10^{-3} $days^{-1}$ (pH 7) at 50 µM concentration level at ambient conditions, while at ATC, it was found to be 5.62 x 10^{-3} $days^{-1}$ (pH 12) to 2.21 x 10^{-3} $days^{-1}$ (pH 7.4). Similarly for 500 µM concentration, the K_{deg} was found to be 4.01 x 10^{-3} $days^{-1}$ (pH 2) to 1.12 x 10^{-3} $days^{-1}$ (pH 7.4) at ambient conditions and 5.91 x 10^{-3} $days^{-1}$ to 2.42 x 10^{-3} $days^{-1}$ at ATC respectively. At 2000 µM concentration, the K_{deg} was found to be in the range of 4.91 x 10^{-3} $days^{-1}$ (pH 12.5) to 1.32 x 10^{-3} $days^{-1}$ (pH 7 and 7.4) under ambient conditions and 5.22 x 10^{-3} $days^{-1}$ (pH 12.5) to 2.63 x 10^{-3} $days^{-1}$ (pH 7.4) at ATC. The extreme pH had a drastic effect on the degradation of drug, as the K_{deg} was found be higher compared to other pH. The pH-degradation profile curve (Fig 4.5), showed that the degradation was minimal in the pH range of 6.0 to 8.0, while at extremes the degradation was found to be high. The pH-degradation profile of BRT at three concentration levels (50 µM, 500 µM and 2000 µM is shown in Fig 4.5.

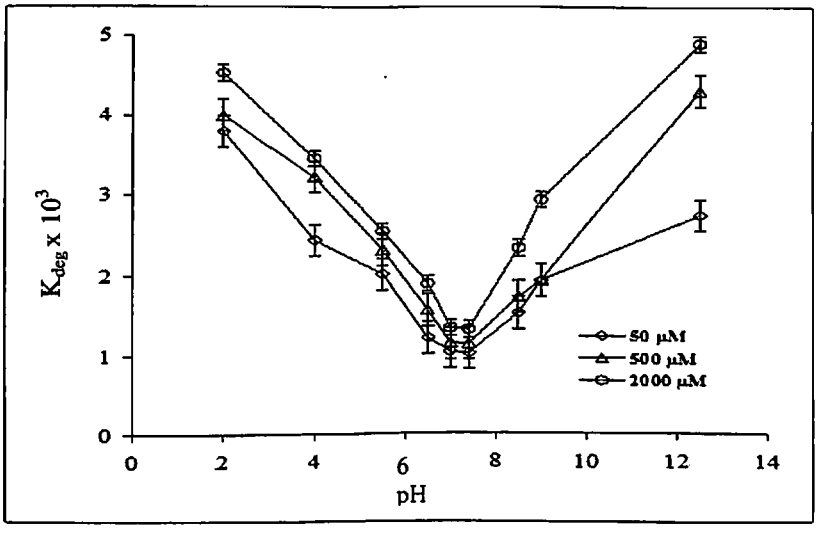

Fig 4.5: pH-degradation profile of brimonidine tartrate at ambient conditions. Each data represents the average of three independent determinations with SD.

Table 4.4: Solution state pH dependent stability kinetics of brimonidine tartrate in different aqueous buffered systems

Conc. (µM)	pH	Ambient (25 ± 2° C/ 60 ± 5 %RH)			ATC (40 ± 2° C/ 75 ± 5% RH)		
		K_{deg} (x 10^3) (day^{-1}) *	R^2	T_{90} (Days)	K_{deg} (x 10^3) (day^{-1}) *	R^2	T_{90} (Days)
0	2.0	3.81 ± 0.21	0.9333	40.0	4.21 ± 0.22	0.8733	36.2
	4.0	2.43 ± 0.23	0.9210	62.5	3.60 ± 0.12	0.8964	42.2
	5.5	2.02 ± 0.21	0.9455	76.0	3.31 ± 0.11	0.9322	46.1
	6.5	1.29 ± 0.29	0.9302	126.7	2.51 ± 0.09	0.9012	60.8
	7.0	1.02 ± 0.09	0.9431	149.0	2.42 ± 0.10	0.9122	63.3
	7.4	1.21 ± 0.10	0.9342	152.0	2.21 ± 0.13	0.9011	69.1
	8.5	1.51 ± 0.12	0.9243	101.3	3.90 ± 0.07	0.7822	39.0
	9.0	1.91 ± 0.12	0.964	80.0	4.61 ± 0.07	0.8911	33.0
	12.5	2.71 ± 0.21	0.9433	35.3	5.62 ± 0.11	0.9011	27.1
500	2.0	4.01 ± 0.12	0.8722	38.0	4.92 ± 0.18	0.8933	31.0
	4.0	3.22 ± 0.11	0.9322	47.2	3.64 ± 0.12	0.8102	42.2
	5.5	2.31 ± 0.09	0.9322	66.1	3.53 ± 0.21	0.9011	43.4
	6.5	1.54 ± 0.10	0.9102	98.4	2.81 ± 0.13	0.8211	54.3
	7.0	1.13 ± 0.21	0.8922	134.5	2.51 ± 0.07	0.7822	60.8
	7.4	1.12 ± 0.11	0.9210	135.7	2.42 ± 0.09	0.7022	63.3
	8.5	1.71 ± 0.09	0.9072	89.4	3.98 ± 0.13	0.9622	38.2
	9.0	1.91 ± 0.07	0.9472	80.0	4.83 ± 0.11	0.8922	31.7
	12.5	4.33 ± 0.19	0.9293	50.8	5.91 ± 0.21	0.7822	25.8
2000	2.0	4.53 ± 0.11	0.9433	33.5	5.20 ± 0.22	0.822	29.2
	4.0	3.45 ± 0.12	0.9846	43.9	4.21 ± 0.20	0.7277	36.2
	5.5	2.53 ± 0.05	0.8933	60.0	3.94 ± 0.21	0.9022	39.0
	6.5	1.87 ± 0.05	0.8433	81.3	3.21 ± 0.17	0.9102	47.5
	7.0	1.32 ± 0.12	0.9322	115.2	2.83 ± 0.12	0.8922	54.3
	7.4	1.32 ± 0.10	0.9312	116.9	2.63 ± 0.13	0.8322	58.5
	8.5	2.32 ± 0.11	0.9032	66.1	4.32 ± 0.09	0.8422	35.3
	9.0	2.91 ± 0.09	0.8922	52.4	4.91 ± 0.21	0.8022	31.0
	12.5	4.91 ± 0.14	0.8321	31.0	5.22 ± 0.22	0.7822	29.2

* Mean ± S.D, ATC- Accelerated test conditions, K_{deg}- degradation rate constant (in $days^{-1}$), R^2- regression coefficient, T_{90}- shelf life (in days). Each data represents the average of three independent determinations.

It was observed that drug degradation followed first order reaction kinetics. The degradation rate constant was found to be high at extremes pH (both at extreme acidic and extreme alkaline), and was less in neutral pH (6-8) for all the three levels of drug concentrations investigated. This could be due to the fact that, at extreme acidic conditions, due to the protonation of amino group, the charge cloud over the aromatic ring increases, hence subsequently leading to ionisation and degradation. At extreme alkaline conditions it could be due to the drastic effects of OH^- ions, the degradation was again high. The concentration of drug solution in the buffer media also found to be affecting K_{deg}, as at lower concentration (50 μM), the K_{deg} was lesser compared to higher concentration (500 μM and 2000 μM). The K_{deg} values were found to be drastically increased in ATC in a similar manner to that of ambient conditions, showing that temperature also plays a role in degradation of BRT.

(ii) Drug excipient compatibility studies

The thermograms of BRT excipeints, and physical mixture with different excipients stored at ambient and ATC are shown in Fig 4.6 and Fig 4.7.

The melting endotherms of BRT were well preserved in all the cases. BRT showed a melting peak endotherm at 207 - 209° C (Fig 4.6). The degradation kinetics followed first order kinetics. Table 4.5 represents the degradation rate constants and shelf life of drug-excipient compositions. The K_{deg} of pure BRT was found to be 0.78 $x10^{-3}$ and 3.22 $x10^{-3}$ $month^{-1}$ when stored at ambient and ATC respectively. The corresponding T_{90} was found to be 194.8 and 47.2 months respectively.

As shown in the Fig 4.6(a) and 4.6(b), in the case of BRT: Eudragit physical admixture, the melting peaks of drug were distinctly seen and the enthalpy remained unchanged. Similarly in cases of PEO (PEO 100 kDa and PEO 400 kDa) [Fig 4.6(c) and 4.6(d)] respectively, the endothermic peak of BRT was broadened and but no change in the shape of the endotherm and enthalpy was observed. The observations suggested the absence of incompatibility. In cases of drug HPMC (HPMC K4M, K15M, K100M) mixture [Fig 4.7(a), 4.7(b) and 4.7(c)] respectively, the endothermic peak of BRT remained unchanged and no change in peak shape or enthalpy was observed, thus the mixtures were considered to be compatible. Similar results were obtained in case of drug and EC-50 mixture [Fig 4.7(d)] (Table 4.5).

The K_{deg} values ranged from 0.41 $x10^{-3}$ $month^{-1}$ to 0.78 $x10^{-3}$ $month^{-1}$ for all the combinations when stored at ambient conditions.

When stored at ATC, there was significant degradation, with K_{deg} ranging from 2.78 $x10^{-3}$ $month^{-1}$ to 3.22 $x10^{-3}$ $month^{-1}$. The K_{deg} was lowest for the drug combination with PF-68. Thus this study gives information regarding the stability of BRT with selected excipients at various storage conditions while deciding the formulation excipeints.

Table 4.5: Degradation kinetics of brimonidine tartrate in solid admixtures with different excipients.

BRT: Excipient admixture	Ambient			ATC		
	K_{deg} x 10^3 (month $^{-1}$)	T_{90} (month)	R^2	K_{deg} x 10^3 (month $^{-1}$)	T_{90} (month)	R^2
BRT	0.78 ± 0.02	194.8	0.9212	3.22 ± 0.02	47.2	0.8933
BRT:ERL 100	0.61 ± 0.02	208.2	0.9321	3.11 ± 0.02	49.0	0.9122
BRT:ERS 100	0.61 ± 0.03	211.1	0.9322	3.10 ± 0.03	50.3	0.8933
BRT: PEO 100 kD	0.51 ± 0.01	230.3	0.9102	2.82 ± 0.02	53.9	0.8933
BRT: PEO 100 kD	0.50 ± 0.02	240.5	0.9011	2.79 ± 0.01	55.0	0.9210
BRT:HPMC K4M	0.55 ± 0.02	245.1	0.8211	3.02 ± 0.01	50.3	0.9211
BRT:HPMC K15M	0.56 ± 0.03	241.2	0.9033	3.08 ± 0.03	49.3	0.8933
BRT:HPMC K100M	0.54 ± 0.02	230.3	0.8322	3.12 ± 0.01	48.7	0.9012
BRT:EC	0.58 ± 0.02	214.0	0.8922	2.89 ± 0.04	52.5	0.8862
BRT: chitosan	0.61 ± 0.03	237.5	0.7822	3.19 ± 0.03	47.6	0.8729
BRT: PF-68	0.41 ± 0.02	257.6	0.8732	2.78 ± 0.03	54.6	0.8622

BRT- Brimonidine tartrate, Ambient - (25° C ± 2° C/ 60 ± 5 %RH), ATC- Accelerated test conditions (40° C ± 2° C/ 75 ± 5 %RH), K_{deg}:- First order degradation rate constant ($month^{-1}$), T_{90}- shelf life (months), R^2- Regression coefficient. Each data represents the average of three independent determinations with standard deviation.

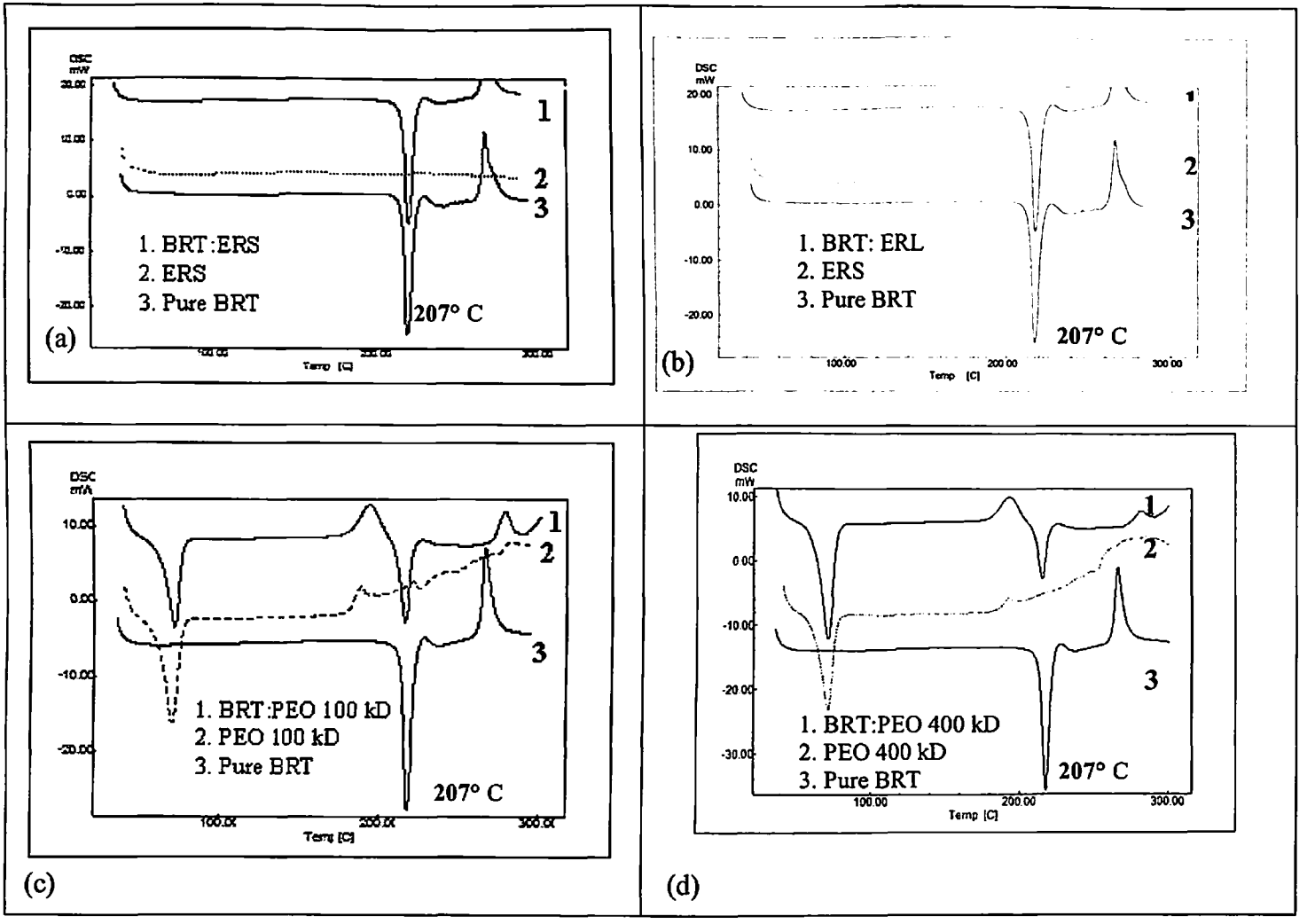

Fig 4.6 : Representative thermograms of brimonidine tartrate with (a) ERS 100, (b) ERL 100, (c) PEO 100 kD and (d) PEO 400 kD

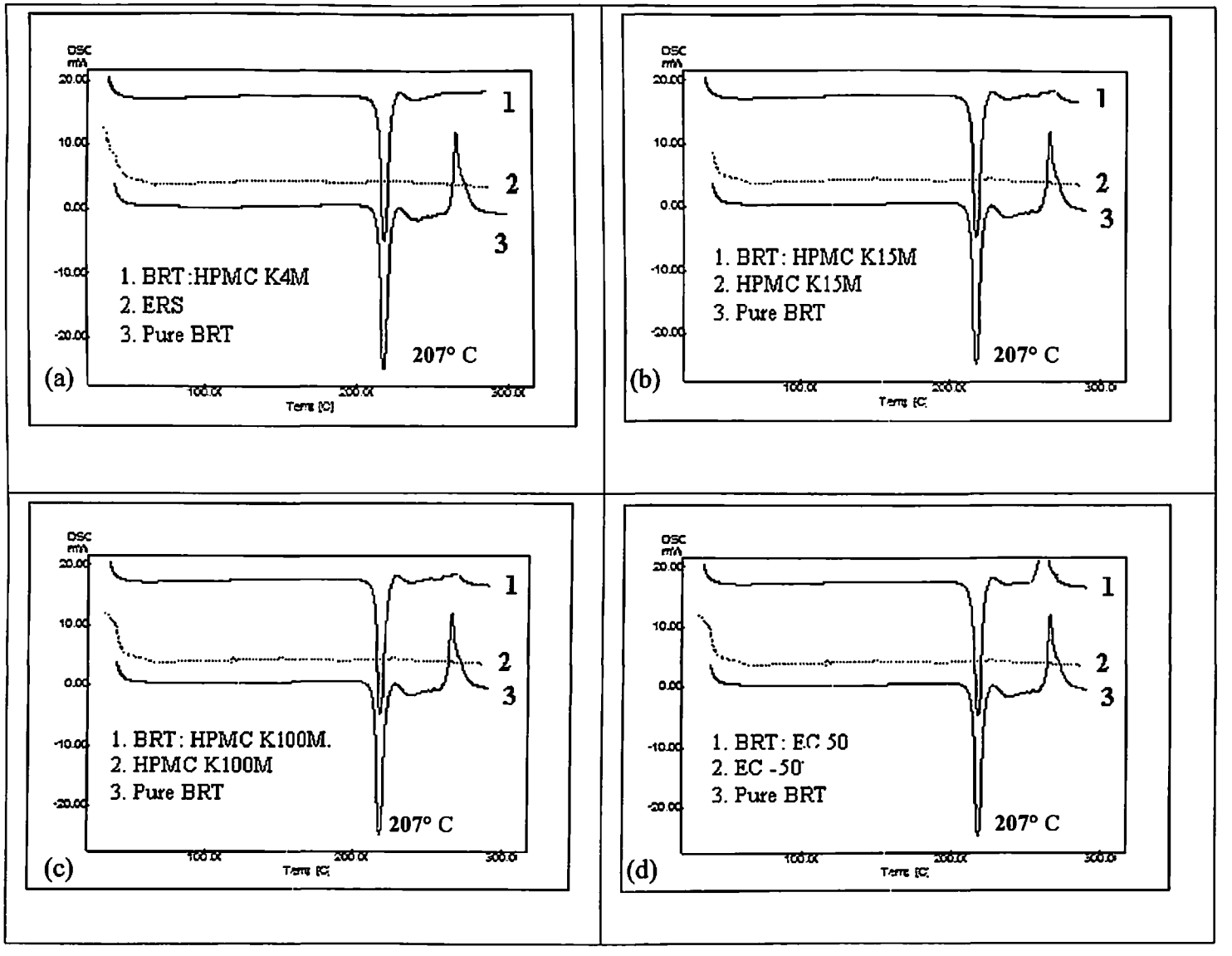

Fig 4.7: Representative thermograms of brimonidine tartrate with (a) HPMC K4M, (b) HPMC K15, (c) HPMC K100M and (d) EC-50

4.5. CONCLUSIONS

The preformulation studies were performed for brimonidine tartrate to determine some of physicochemical parameters (solubility, apparent partition coefficient, dissociation constant) which are helpful in developing appropriate formulations and to detect any drug-excipient incompatibility amongst the selected excipients in the development of formulations. The solubility of BRT was found to be pH dependent, higher solubility at lower pH was observed. The log P_{app} was found to be 0.25 in n-octanol/water system. The P_{app} was found to be highly pH dependent. The pKa was found to be 7.22 ± 0.18.

The solution state stability studies performed at three levels of concentration in buffered conditions followed first order degradation kinetics. The degradation rate constant was found to be dependent on concentration of drug, pH of the buffer and temperature. At neutral pH (6.5-7.5), drug was more stable than at acidic or alkaline conditions. Solid state stability studies performed with admixtures of drug and different excipients showed that the selected excipients for the development of ocular inserts and nanoparticle formulations were compatible with the drug with no signs of major incompatibility.

4.6. REFERENCES

Albert A, Serjeant EP. 1962. Ionisation constants of acids and bases a laboratory manual. Methuen, Wiley, London.

Barbosa J, Barron DJ, Cano J, Jimenez-Lozano E, Sanz-Nebot V, Toro I. 2001. Evaluation of electrophoretic method versus chromatographic, potentiometric and absorptiometric methodologies for determing p*K*a values of quinolones in hydroorganic mixtures. J. Pharm. Biomed. Anal, 24; 1087-1098.

Beltran JL, Sanli N, Fonrodona G, Barron D, Ozkan G, Barbosa J. 2003. Spectrophotometric, potentiometric and chromatographic pKa values of polyphenolic acids in water and acetonitrile–water media. Analytica Chimica Acta, 484; 253-264.

Chien DS, Homsy JJ, Gluchowski C, Tang-Liu DD. 1990. Corneal and conjunctival/scleral penetration of p-aminoclonidine, AGN 190342, and clonidine in rabbit eyes. Cur. Eye Res, 9; 1051-1059.

De TK, Rodman DJ, Holm BA, Prasad PN, Bergey EJ. 2003. Brimonidine formulation in polyacrylic acid nanoparticles for ophthalmic delivery. J. Microencapsul, 20; 361-374.

Indian Pharmacopeia, 2007. Indian Pharmacopeial forum.

Roman L, Mirel S, Florean E, Oprean R. 1998. The potentiometric and spectrophotometric determination of dissociation constants for same 2-mercapto-5-*R*-amino-1,3,4-thiadiazole derivatives. J. Pharm. Biomed. Anal, 18; 137-144.

Singh S, Sharda N, Mahajan L. 1999. Spectrophotometric determination of pKa of nimesulide. Int. J. Pharm, 176; 261-264.

US Pharmacopeia. 32, 2009. US Pharmcopeial convention, Rockville, MD, 1434-1435.

Walter H. Brooks DE, Fisher D. 1985. Partitioning in aqueous two phase systems, Academic Press, London.

CHAPTER FIVE

IN SITU GEL FORMULATIONS

5.1. INTRODUCTION

In situ gels are ocular drug delivery systems that are conveniently instilled into the eye as a liquid, where they undergo a transition into a gel phase when they come in contact with the trigger in the cul-de sac of the eye. The eye drop preparations have an advantage of ease of application, but are not retained in the eye for a longer period of time. On the other hand, viscous gels can be retained in the ocular tissues for a prolonged period of time, but there is difficulty of application due to their viscosity (Peppas et al, 2000). These problems can be overcome by polymers or systems called in situ gel forming or phase transition systems. In situ gelling systems are in solution form in formulation container, but upon instillation, due to a trigger undergo phase transition to form a gel. The sol-gel transitions are triggered by physiological factors such as temperature, pH, ionic content etc. These triggers causes the formation of a stiff gel form which if sufficiently strong enough in terms of gel strength, can be retained in the eye for a longer period of time and can sustain/extend the release of therapeutic agent for a longer period of time.

These 'stimuli-responsive' polymeric systems are the one in which polymer conformation in solution is dictated by both the polymer-solvent and polymer-polymer interactions (Soppimath et al, 2002). When in contact with a good solvent, polymer-solvent interactions dominate and the polymer chains are relaxed due to minimal inter-segmental interactions. When in contact with a poor solvent, the polymer will aggregate due to a restricted chain movement because of increased polymer-polymer interaction. Such a phase change leads to varying physical properties of the polymer solution. It is thus possible to alter the polymer-solvent interaction by changing the pH, temperature, and ionic strength of the solution. This new concept of producing gel in situ was suggested for the first time in the early 1980s (Hui and Robinson, 1985; Friteyre and Mazuel, 1987).

Upon instillation in the eye, these stimuli responsive vehicles undergo a viscosity increase due to change in temperature, pH, or electrolyte composition and thus leading to increased precorneal retention (Hui and Robinson 1985; Friteyre and Mazuel, 1987; Meseguer et al, 1993).

The two in situ gel forming systems investigated in this part of the research work include,

(a) Ion activated in situ gel system (gellan gum)

(b) Temperature activated in situ gel system [poly (N-isopropylacrylamide)].

5.1.1. Ion-activated in situ gelling systems

These systems undergo a sol-gel transition upon contact with physiological ions in the site of application or site of action. Many of the polysaccharides fall into the class of ion sensitive gel forming agents (Guo et al, 1998; Bhardwaj et al 2000). They are capable of gelation in the presence of monovalent or divalent ions such as calcium, sodium, potassium, magnesium etc. Various polymers that gel in the presence of monovalent and/or divalent cations include gellan gum (Gelrite®), pectins with low methoxy values, alginic acid, sodium alginate, and carrageenan.

In the present work, gellan gum was investigated for its ability to form gel upon contact with the monovalent/ divalent cations of the eye. Gellan gum is a linear, anionic hetero polysaccharide secreted by the microbe *Sphingomonas elodea* (formerly known as *Pseudomonas elodea*). The polysaccharide can be produced by aerobic fermentation and isolated from the fermentation broth by alcohol precipitation. The polymer backbone of gellan gum (Fig 5.1) consists of glucose, glucuronic acid, and rhamnose in the molar ratio 2:1:1 (Jansson and Landberg, 1983). These are linked together to give a tetrasaccharide repeat unit. The native polysaccharide is partially esterified with L-glycerate and acetate (Kuo et al, 1986) but the commercially available gellan gum; Gelrite® is completely de-esterified by alkali treatment.

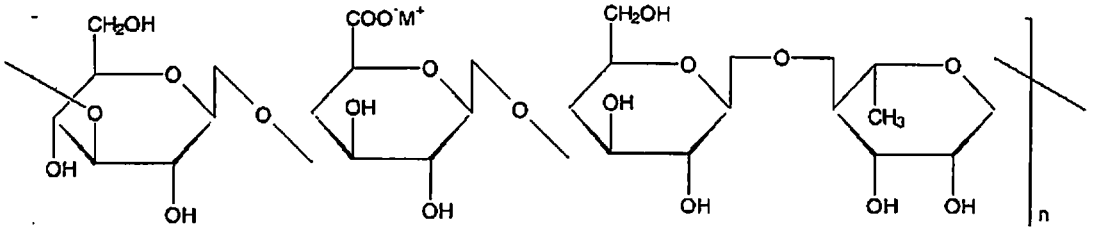

Fig 5.1: Chemical structure of gellan gum

Gellan gum has an unique property as its dispersion in water in low concentrations (up to 1 % w/v) forming a slightly viscous solution with the viscosity subsequently increasing markedly in the presence of a physiological level of cations such as divalent (calcium, magnesium), monovalent ions (sodium, potassium).

Recently gellan gum has been approved as a pharmaceutical excipient in the development of ocular dosage forms, and is currently has been utilised in the formulations of a controlled-release glaucoma formulation Timoptic-XE® (timolol maleate in situ gel;

Merck Inc). Gellan gum has been paid increasingly high attention as drug delivery carrier for ophthalmic drug delivery purpose.

Rozier et al (1989) studied the application of gellan gum for the ocular delivery of timolol. The results showed that the polymer is safe, non toxic and improved the ocular bioavailability of the drug compared to the control. Gellan gum in situ gel formulations showed better corneal penetration and improved ocular concentrations in cornea and in aqueous humor than HEC gels as control.

Paulsson et al (1999) studied the rheological properties of gellan gum (Gelrite®). Thermal scans were used to investigate the gel formation and other changes in the structure of the samples when the macromolecular and ionic contents were altered. The effect of different ions in tear fluid (Na^+, K^+, Ca^{++}) on the gel strength and the consequences of dilution due to the ocular protective mechanisms were investigated. Sodium ions were found to be the most important gel-promoting ion in situ. It was also found that gels are formed in tear fluid even when the concentration of Gelrite® is only 0.1 % w/v. Samples with concentrations of Gelrite® of 0.5-1 % w/v do not require more than 10–25% of the ions those in tear fluid to form gels.

The mechanism of gelation of gellan gum upon contact with ions has been explained by many models (Robinson et al, 1991; Morris, 1990). In the sol form, in ion free environment, the viscosity of the solution is very less and gellan gum forms double helices at room temperature. These helices are closely associated, but with weaker forces of attraction (Van der Waals forces). At this state, the viscosity of sol is like the viscosity of water. As soon as the environment changes due to the introduction ions (monovalent and/or divalent), the cross linking of the polymer takes place while some of the helices associate into aggregates. In this state the viscosity of the system will be more and this is what is responsible for the gel formation from sol. Also changes in the ionic strength lead to the change in the concentration of ions inside the gel, causing changes in swelling behaviour of the polymeric system (Fig 5.2).

Effect of temperature on the gellan gum helices is also well known. On heating the gellan gum solution in an ion free environment, the polymer becomes a disordered coil. Heating the solution in an ionic environment, causes melting of non-aggregated helices followed by aggregated helices (gel state) while the latter occurs at a higher temperature and in second transition.

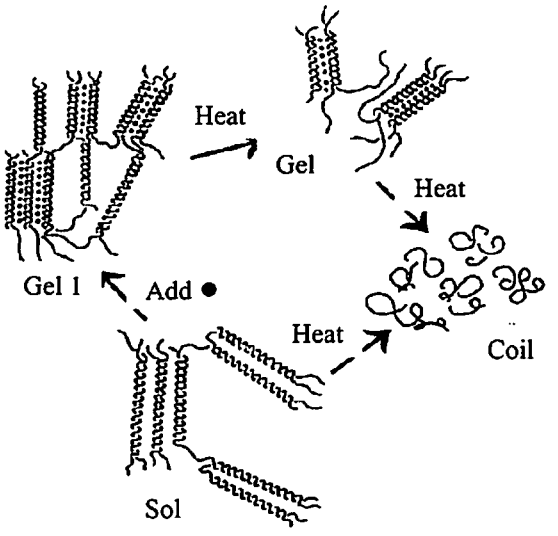

Fig 5.2: Model for the formation of Gelrite® gels on addition of cations (●). (Robinson et al, 1991).

5.1.2. Temperature activated in situ gelling system

The temperature sensitive hydrogels have been investigated in the design of variety of drug delivery systems including ocular route. They have the ability to swell or de-swell as a result of change in surrounding environment temperature.

They are classified into following three categories.

(a) Negative temperature sensitive hydrogels are those which have lower critical solution temperature (LCST). These polymers swell below LCST and contract upon heating above the LCST. The polymers like poly-(N-isopropylacrylamide) (PNIAA) show decrease in their water solubility as the temperature rises. Its shows an on-off type of drug release with drug release at low temperature and no drug release at higher temperature, thus showing a pulsatile type drug release (Fig 5.3). The hydrogels with LCST are used in controlled release of drugs, proteins and also in liposomes (Soppimath et al, 2002; Kono et al, 2001).

(b) Positive temperature sensitive hydrogels have upper critical solution temperature (UCST) and contracts upon decreasing the temperature below UCST. Examples of these kinds of hydrogels include poly (acrylic acid) and polyacrylamide (Qiu and Park, 2001).

(c) Thermo reversible gels are the one which are free flowing liquids at ambient temperature but gels as the temperature is raised. Pluronics, which are tri-block polymers prepared from poly (ethylene oxide)-poly (propylene oxide)-poly (ethylene oxide) and tri-block copolymers of poly (ethylene glycol)-poly-(dl-lactic acid-co-glycolic acid)-poly

(ethylene glycol) (PEG-PLGA-PEG) (Jeong et al, 1999) or PLGS-PEG-PLGA fall in this category (Kim et al, 2001).

Poly-(N-isopropylacrylamide) (PNIPAA) is the most widely used temperature sensitive hydrogel and is unique in the sense that it undergoes phase transition at narrow temperature range of approximately 32° C (Schild et al, 1992; Boutris et al, 1997; Costa et al, 2002; Eeckman et al, 2004a; Eeckman et al, 2004b; Liu et al 2004). Many efforts have been made to modify the LCST of PNIAA to near body temperature so that rapid and instant gelation can be obtained at body temperature (Cao et al, 2007; Liu et al, 2004; Malonne et al, 2005).

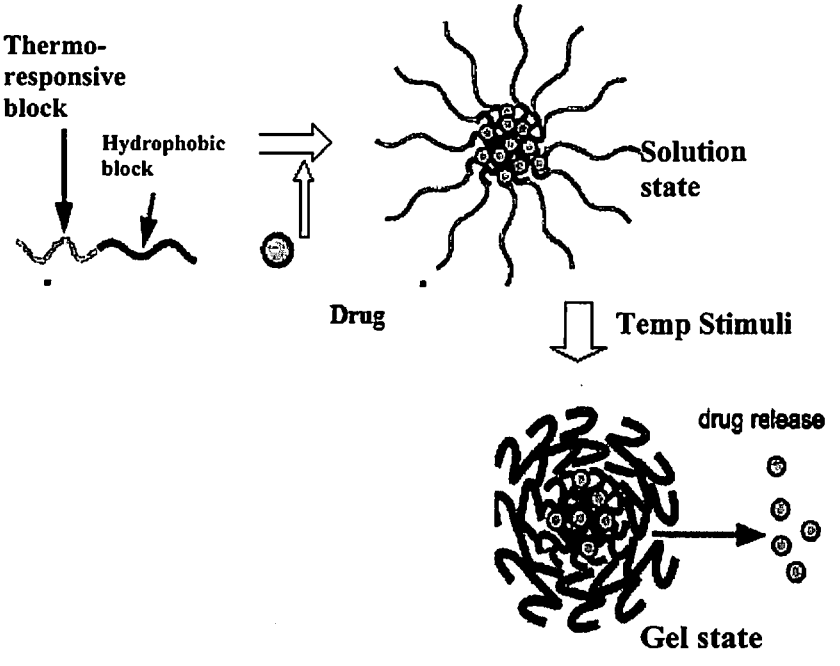

Fig 5.3: Schematic representation of drug release from thermo-sensitive polymer micelle upon temperature increase (Nakayama et al, 2006).

The objective of this part of work was to investigate the suitability of ion activated in situ gelling polymer (gellan gum) and temperature activated in situ gelling polymer, (poly-N-isopropylacrylamide), in formulating in situ gels of BRT and to study the effect of polymer concentration, presence of tonicity modifiers and other additives on the characteristics of developed in situ gels such as gelation temperature, rheology, mucoadhesion, in vitro drug release profile and stability.

5.2. MATERIALS AND EQUIPMENTS

5.2.1. Materials

BRT was obtained as a gift sample from FDC Ltd, Mumbai, India. Deacetylated gellan gum (Gelrite®), poly (N-isopropylacrylamide), benzalkonium chloride, benzyl alcohol

were purchased from Sigma Aldrich, Bangalore, India. All other chemicals and reagents used were of pharmaceutical/ analytical grade.

5.2.2. Equipments

Magnetic shaker with heater (MAC Instruments, India) was used for the preparation of in situ gels. For all the analytical studies, including preformulation, UV-Visible spectrophotometer (Jasco, Tokyo, Japan, Model V-570) connected to computer loaded with spectra manager® software, with automatic wavelength accuracy of 0.1 nm, a 10 mm matched quartz cells was used. Humidity chambers (Newtronics, India) were used to maintain ambient (25° C ± 2° C/60 ± 5% RH) and ATC (40° C ± 2° C/75 ± 5% RH) conditions. High quality pure water was prepared using Millipore purification system (Millipore, Model Elix SA 67120, Molsheim, France). Hot air oven (MAC instruments, India) was used for drying purposes. A pH meter (Eutech, pH Tutor) fitted with glass electrode, filled with potassium chloride solution was used for all the pH measurements. In vitro release studies were carried out using USP Type I dissolution apparatus (basket type, Electrolab TDT-08L, Mumbai, India). The rheological studies were performed using Brookfield (RVDV-II + pro) viscometer (Brookfield Engineering lab Inc Middleboro, USA). Data was acquired using a computer with software Brookfield wingather V 2.4. The apparatus consisted of a water jacketed small sample adaptor with a co-axial cylindrical spindle and a chamber (SC4-21/13R).

5.3 METHODS

5.3.1. Preparation of in situ gel formulations

(i) Preparation of ion activated in situ gel

The in situ gels were prepared on the weight basis. The formulation composition is shown in the Table 5.1. Weighed quantities of gellan gum (Gelrite®) was dispersed in ultrapure water containing benzalkonium chloride (0.02 % w/w). Solutions of gellan gum at different concentrations (0.2-1.4 % w/w) were prepared by heating the dispersions to 90° C for 20 mins with continuous stirring on a magnetic stirrer. The resulting clear solution was allowed to cool to room temperature, while on stirring. Finally weighed amount of BRT was dissolved in small amount of water and added to the above solutions and the weight was made up to the mark with ultrapure water. To mimic the situation wherein in situ gel upon ocular administration is diluted with the tear fluid in the eye, some formulations (prepared in ultrapure water) were diluted with Simulated tear fluid (STF) in different proportions of in situ gel to STF (1:0.25,1:0.5,1:0.75,1:1,1:1.5,1:2) with

continuous mixing to get homogenous solutions. In order to study the effect of osmolarity on the rate of gel formation, few formulations were prepared consisting of glycerol as osmogen (2 % w/w) and a few were also prepared in phosphate buffer saline pH 7.4. The composition of gellan gum based ion activated in situ gels of BRT are presented in Table 5.1.

The composition of STF (per 100g) is as follows, sodium chloride - 0.67 g, sodium bicarbonate - 0.20 g, calcium chloride dihydrate - 0.008 g, purified water to 100 g (Ooteghem et al, 1993). All the formulations were filtered, and packed into screw capped vials followed by autoclaving at 121° C for 20 mins and stored at refrigerated conditions.

Table 5.1: Formulation composition for gellan gum based brimonidine tartrate in situ gel formulations.

Formulation	BRT (% w/w)	Gellan gum (% w/w)	Benzalkonium chloride (% w/w)	Glycerol (% w/w)	Vehicle
BGG02	0.2	0.2	0.02	-	Water
BGG04	0.2	0.4	0.02	-	Water
BGG06	0.2	0.6	0.02	-	Water
BGG08	0.2	0.8	0.02	-	Water
BGG10	0.2	1.0	0.02	-	Water
BGG12	0.2	1.2	0.02	-	Water
BGG14	0.2	1.4	0.02	-	Water
BGG06G	0.2	0.6	0.02	2.0	Water
BGG08G	0.2	0.8	0.02	2.0	Water
BGG10G	0.2	1.0	0.02	2.0	Water
BGG06STF	0.2	0.6	0.02	-	STF
BGG08STF	0.2	0.8	0.02	-	STF
BGG10STF	0.2	1.0	0.02	-	STF
BGG06P	0.2	0.6	0.02	-	PBS
BGG08P	0.2	0.8	0.02	-	PBS
BGG10P	0.2	1.0	0.02	-	PBS
BGG06WD	-	0.6	0.02	-	Water
BGG08WD	-	0.8	0.02		Water
BGG10WD	-	1.0	0.02		Water

BRT- Brimonidine tartrate, STF: Simulated tear fluid, PBS: phosphate buffer saline pH 7.4, Water used was of Milli Q grade.

(ii) Preparation of temperature activated in situ gels

The gels of PNIPAA were prepared on weight basis. The composition of different in situ gel preparations are shown in Table 5.2. Weighed amount of polymer was dissolved in phosphate buffer saline by stirring on a magnetic stirrer. Drug was dissolved in small amount of purified water and added to the polymer solution slowly with stirring.

Benzalkonium chloride (0.02 % w/w) was added to the above in situ gels preparations as preservative. Isotonicity of the in situ gels was adjusted with sodium chloride. Finally the weight of the formulation was made up with purified water. All the formulations were filtered, packed into screw capped vials and stored at refrigerator.

The effect of proportion of PNIPAA on the characteristics and performance of prepared in situ gels were investigated. In order to investigate the effect of addition of hydrophilic, gel forming polymers on the gelling temperature, rheology and in vitro release profile, HPMC K4M was added to some of the formulations. HPMC based PNIPAA in situ gels were prepared by hydrating the HPMC in water for 6 hours followed by the addition of PNIAA and drug solution to it and finally the preservative was added under continuous stirring. In all the cases the temperature of the system was maintained at 5° C. The effect of various formulations vehicles such as water and phosphate buffer saline (pH 7.4) was also investigated.

Table 5.2: Formulation composition of PNIPAA based brimonidine tartrate in situ gel formulations.

Formulation code	BRT (% w/w)	PNIAA (% w/w)	HPMC K4M (% w/w)	Benzalkonium chloride (%w/w)	Vehicle
BPNIA01	0.2	0.1	-	0.02	PBS
BPNIA02	0.2	0.2	-	0.02	PBS
BPNIA04	0.2	0.4	-	0.02	PBS
BPNIA06	0.2	0.6	-	0.02	PBS
BPNIA08	0.2	0.8	-	0.02	PBS
BPNIA10	0.2	1.0	-	0.02	PBS
BPNIA12	0.2	1.2	-	0.02	PBS
BPNIA14	0.2	1.4	-	0.02	PBS
BPNIA10H1	0.2	1.0	1.0	0.02	PBS
BPNIA12H1	0.2	1.2	1.0	0.02	PBS
BPNIA14H1	0.2	1.4	1.0	0.02	PBS
BPNIA10H2	0.2	1.0	2.0	0.02	PBS
BPNIA12H2	0.2	1.2	2.0	0.02	PBS
BPNIA14H2	0.2	1.4	2.0	0.02	PBS
BPNIA10H3	0.2	1.0	3.0	0.02	PBS
BPNIA12H3	0.2	1.2	3.0	0.02	PBS
BPNIA14H3	0.2	1.4	3.0	0.02	PBS
BPNIA10W	0.2	1.0	-	0.02	Water
BPNIA12W	0.2	1.2	-	0.02	Water
BPNIA14W	0.2	1.4	-	0.02	Water

BRT- Brimonidine tartrate, PNIAA- poly (N-isopropyl acrylamide), HPMC K4M- Hydroxypropyl methylcellulose (4000 cP), PBS- phosphate buffer saline (pH 7.4), isotonicity adjusted with sodium chloride. Water used was of Milli Q grade.

5.3.2. Evaluation of formulations

(i) Determination of drug content

A known amount of in situ gel formulation equivalent to 2 mg of the drug was weighed accurately and dispersed in phosphate buffer pH 7.4, stirred well and sonicated for 15 mins in order to extract the drug. The resulting solution was filtered through Whatmann Filter paper No 1, suitably diluted with phosphate buffer pH 7.4 and analysed spectrophotometrically at 248 nm (Chapter III- Analytical method development) to determine amount of drug present in the formulated in situ gel preparations.

(ii) Gelation studies

Gelation studies of the developed in situ gel formulations was performed by placing 100 µL of the solution in a vial containing 2 mL of STF pH 7.4 (freshly prepared and equilibrated at 37° C). The gelation was observed visually and the time taken for gel formation and time taken for the formed gel to dissolve was recorded. The results are shown in Table 5.3.

(iii) Determination of $T_{sol\text{-}gel}$ (temperature activated in situ gel)

The gelation temperature ($T_{sol\text{-}gel}$) determination was performed as per the previous reports (Ryu et al, 1999; Kim et al, 2002; Fawaz et al, 2004).

(a) Magnetic bar method

The prepared in situ gels were maintained on a heating magnetic stirrer with a water bath. The formulations were heated slowly at a rate of 1° C per min from 5° C to 50 ° C, with a constant stirring speed of 50 rpm. The temperature was measured using a precise calibrated thermometer. The temperature at which the revolving magnetic bar stopped was noted down as gelation temperature and designated as $T_{sol\text{-}gel}$.

(b) Rheological method

The gelation temperature $T_{sol\text{-}gel}$ was also determined by using Brookfield viscometer. The formulations were maintained in a water jacketed small sample adaptor with water circulating through the jacket. The water was heated gradually at 1° C per min and the shear rate was maintained at 0.47 sec^{-1}. This shear rate was selected after preliminary investigation at varying speeds. The heating rate was at 1° C per min from temperature of 5° C to 50° C. The $T_{sol\text{-}gel}$ was taken graphically as the inflection point of the plot of viscosity vs. temperature. The results are illustrated in Fig 5.7 and the gelation temperature of various formulations are presented in the Table 5.7.

(iv) Rheological studies

The rheological studies were performed using Brookfield (RVDV-II + pro) viscometer (Brookfield Engineering lab Inc Middleboro, USA). Data was acquired using a computer with software Brookfield wingather V 2.4. The apparatus consisted of a water jacketed small sample adaptor with a co-axial cylindrical spindle and a chamber (SC4-21/13R). Studies were carried out with formulations prepared in water, STF (pH 7.4) and phosphate buffer saline (pH 7.4) at a temperature of 37° C ± 0.5° C. The rpm was varied from 0.1-20 and the viscosity was noted down. Shear rates (G) in dynes-cm^2 vs. shear stress (F) in sec^{-1} were plotted to ascertain the nature of prepared formulations. Also rheological measurements were taken after diluting the formulations with different proportions of STF and the viscosity of samples were measured as described above. The results are shown in Fig 5.4.

(v) Mucoadhesive strength measurement

Mucoadhesive strength of designed in situ gels was determined using in-house modification of reported methods (Chandran, 2003). Mucoadhesion was determined by an experimental set up developed in-house using an accurate analytical balance. The left pan of the balance was replaced with Teflon block (6 cm x 6.2 mm) with a vertically perpendicular extension of 2 cm x 1.5 cm. Goat mucosal tissue was obtained from a local slaughter house at Pilani, India. The lower block was tied with a mucosal membrane and was maintained in STF at 37° C.

The formulations for mucoadhesion measurements were mounted on the lower surface of the upper block. The in situ gel formulations were maintained in contact with the mucosal membrane with some weight (40 g) on it for about 15 mins. After 15 mins, weights were removed and the experiment was initiated. The water was added drop wise using a micropipette to the other side of the pan slowly until the formulation gets detached from the membrane. The rate of addition of water was kept constant for all the mucoadhesive strength determination study (about 3 minutes). The preliminary studies were performed to optimise the rate of addition of water, contact time of formulation with the membrane before adding weights. The mucoadhesion was calculated as the force (in terms of weight) required for the detachment and expressed as force per unit contact surface area of the formulations. The results are presented in Table 5.4.

(vi) In vitro release studies

The in vitro release of BRT from in situ gel formulations were studied using a suitable treated dialysis membrane (cut off 12-14 kD, Sigma Aldrich, India). Freshly prepared STF (pH 7.4) was used as a media. The surface area of the membrane was 2.71 cm^2 and the temperature was maintained at 37° C ± 0.5° C. Accurately weighed 1g of in situ gel formulations were placed inside the diffusion cell, which was placed in a in a modified USP type I (basket) containing 25 ml STF. Samples were withdrawn at different time intervals and replaced with an equal volume of pre-warmed medium. The samples were analysed by spectrophotometrically at 248 nm. The percent drug released at each time point was calculated and plotted as a function of time (Fig 5.5 and Fig 5.6). The drug release data was fitted into various release kinetics models such as zero order, first order, Higuchi's square root kinetics and Korsmeyer Peppas (KP) model to determine the mechanism of drug release from the formulations.

(vii) Stability studies

Stability studies were carried out on gel formulation according to ICH (International Conference on Harmonization) guidelines. A sufficient quantity of in situ gel in sealed glass vials was stored in stability chamber (Thermo labs, India) maintained at Ambient (25° C ± 2° C/60 ± 5 % RH) and ATC (40° C ± 2° C/75 ± 5 % RH). Samples were withdrawn at 0, 30, 60, 90, and 180 days. The physical stability of gel was observed periodically for the occurrence of turbidity or gelation. The drug content and the viscosity of formulation were measured at predetermined time interval. The degradation rate constant was calculated. The results are shown in Table 5.6.

5.4. RESULTS AND DISCUSSION

In order to improve the patient compliance by improving the mode of administration, with a prolonged residence time in the eye, a novel in situ gelling polymer- gellan gum (Geltite®), and temperature activated in situ gelling polymer- poly (N-isopropylacrylamide) were investigated for the suitability attributes. The formulations prepared were evaluated for drug content, gelation studies, rheological studies, mucoadhesion studies, in vitro drug release profile and stability.

5.4.1. Ion activated in situ gelling systems (Gellan gum)

(i) Physicochemical characterisation

The prepared in situ gels were found to have good physical characteristics in terms of appearance and texture. The formulations were clear transparent to translucent in appearance. The texture was found to be smooth and free from any gritty particles. The formulations prepared in water were free flowing and had excellent pourability up to a gellan gum concentration of 1.0 % w/w (BGG10). Further increase in polymer concentration resulted in formation of viscous formulations which had poor flow and pourability. The formulations prepared in phosphate buffer (pH 7.4) showed relatively higher viscosity than those in water and had relatively lesser pourability. The formulations prepared in STF as vehicle, had translucent appearance and were viscous.

(ii) Gelation studies

The rate of gelation was found to be critical in the successful development of in situ gelling systems for ocular delivery (Edsman et al, 1998), also the osmololarity of the formulation plays a crucial role in the rapid gel formation (Calrfors et al, 1998).

The rate and extent of gelation (in terms of time required for gel formation and its dissolution in the media) increased with increase in the concentration of gellan gum. The gel formation was rapid in formulations with higher concentrations of polymer (BGG10), while at lower concentrations, negligible or no gel formation was observed (Table 5.3). The three selected formulations based on the results of preliminary studies; BGG06, BGG08 and BGG10, were studied further to investigate the effect of presence of salts and osmolarity agent on the rate and extent of gelation. The selection of formulation was based on the viscosity and preliminary gelation studies. The formulations were prepared in water, phosphate buffer (pH 7.4) and also in STF pH 7.4 as vehicles.

The presence of glycerol (2 % w/w) in the formulations altered the salt uptake by the polymer and thereby relatively slower rate of gelation was observed. The time for the formation of gel from the solution, varied from 40 to 50 seconds. This could be explained by the fact that the rate of salt uptake and thereby gel formation is dependent primarily on the osmotic gradient between the gel and the surrounding environment. The presence of glycerol in the formulation increased the osmolarity of the formulation, thereby has decreased the rate of salt uptake by the gellan gum from the surrounding environment (STF), hence a relatively slower rate of gelation was observed (Carlfors et al, 1998). The lower extent of gelation in the formulations with glycerol could also be because of the washing off of the sol or prematurely formed gel before forming a stiff gel, due to slower

rate of gelation. The rate of gel formation in vivo, upon instillation of the in situ gel in solution form determines the contact time and residence time of the in situ formed gel in the eye. The rapid and reflux secretion of tear fluid, when any formulation is applied to eye can drain away the formulation if the gel formation is slower. Hence the presence of optimised concentration of in situ gelling polymer surrounded by an environment which supports the instant formation of gel is essential.

The formulations prepared in STF were preformed gels and no further gelation was observed. This could be due to the formation of gel by the gellan gum in the presence of monovalent and divalent cations present in the STF. These gels were stiff and the time taken for them to dissolve was more compared to respective formulations with similar concentration of gellan gum. In the case of formulation BGG10, the formulation lasted for more than 10 h.

In formulations prepared in phosphate buffer (pH 7.4), a relatively slower rate of gelation was observed compared to the formulations prepared in water as solvent. All the formulations prepared in phosphate buffer as vehicle showed a rate of gelation of 40-50 seconds, relatively slower than those formulations prepared with respective concentration of gellan gum. This could be because the presence of salts in phosphate buffer caused gelation to some extent due the presence of sodium ions and also due to decrease in the osmotic gradient between the formulation and the surrounding environment, thus decreasing the salt uptake and slowing down rate of gelation. The extent of gelation was slightly lesser than formulations with respective concentrations of gellan gum, prepared in water. The extent of gelation was also relatively lesser for formulation BGG10P with the time for dissolving the formed gel found to be about 7 h.

The formulations prepared without adding drug, to investigate the effect of presence of drug on the rate and extent of gelation, showed that the presence of drug has no effect on the rate and extent of gelation. Thus, when salt free solution of gellan gum prepared in water and without addition of glycerol is administered into the eye, the gel formation only depends on the electrolytes of the tear fluid.

Table 5.3: Results of rate and extent of gelation studies for gellan gum based brimonidine tartrate in situ gel formulations by visual observation method.

Formulation	Rate of gelation#	Extent of gelation*
BGG02	NG	NG
BGG04	30 sec	Less than 30 mins
BGG06	20-30 sec	3 h
BGG08	20-30 sec	6-7 h
BGG10	20-30 sec	10 h
BGG12	##	More than 10 h
BGG06G	40-50 sec	2 h
BGG08G	40-50 sec	4 h
BGG10G	40-50 sec	7 h
BGG06STF	NG	4 h
BGG08STF	NG	8h
BGG10STF	NG	More than 10 h
BGG06P	40-50sec	2 h
BGG08P	40-50 sec	4 h
BGG10P	40-50 sec	7 h
BGG06WD	20-30 sec	3 h
BGG08WD	20-30 sec	6 -7 h
BGG10WD	20-30 sec	10 h

#- rate of gelation as the time required to form a visible gel, * Extent of gelation as the time taken for the gel to dissolve, NG- No visible gel formation, ## - gelling could not be seen as the viscosity of the formulation before gelation was very high.

Carlfors et al (1998) reported the effect of osmolarity on the human eye contact time for gellan gum formulations incorporated with glycerol in various proportions. A glycerol concentration dependent decrease in ocular contact time was observed in the study. The formulation with no glycerol showed a precorneal contact time of 33 h (Gelrite®: 0.4 % w/v), while the same formulation with glycerol (1.5 % w/v) showed an ocular contact time of 4 to 5 h. The formulation with Gelrite® of 0.6 % w/v (with no glycerol) showed a contact time of approximately 22 h while that with glycerol (1.5 % w/v) showed a contact time of 5 to 7 h. Also the increase in glycerol proportion resulted in drastic decrease in ocular contact time, thus demonstrating the effect of osmolarity on the gel formation.

(iii) Rheological studies

Rheological experiments are used for investigating the stress response of the ion activated in situ gelling systems subjected to a varying strain, providing information on the viscoelastic hydrodynamic properties. The rheological studies of gellan gum based in situ gel formulations were performed to ascertain the flow behaviour of gels upon exposure to

the shear stimuli. Rheological studies were carried out on the formulations; BGG06, BGG08 and BGG10, by preparing in water and STF separately. The results are shown in Fig 5.4. Addition of STF showed an instantaneous gelation, however the nature and strength of gel formed depended critically on the concentration of the polymer in the formulation. The formulation with STF as vehicle showed higher viscosity compared to those with in situ addition of STF to the formulation. This situation is the ideal case and as occurs in the eye where there is no dilution of the formulation upon instillation, the electrolytes present in the tear fluid are further absorbed in gel formation.

All the formulations, prepared in STF as vehicle as well as those diluted with STF, were found to be shear thinning systems, with the viscosity decreased with increase in shearing stress. A pseudoplastic type of rheological behaviour is better preferred for ophthalmic drug delivery as irritation due to high viscosity can be minimised upon rapid blinking of eye. The ocular shear rate is very high ie, 0.035 sec^{-1} between inter-blinking periods and 4250-28500 sec^{-1} during blinking. Hence, the formulations that exhibit high viscosity under low stress rate and low viscosity under high shear rate conditions are mostly preferred for eye.

Formulations were diluted with varying proportions of STF (25-200%), in most of the cases a stiff gel was formed upon contact with STF. The rheological behaviour was studied for these STF diluted formulations by changing the shear stress and noting down the viscosity. The above formulations were also prepared in STF as solvent. The rapid gel formation was observed with the addition of STF to the formulation prepared in water as vehicle. But a low viscosity was observed compared to formulation prepared in STF, due to limited electrolytes in the added STF (in varying proportions). As the proportion of STF was increased, though the more availability of electrolytes in the added STF, a decrease in the viscosity was seen. This could be due to the dilution of formulation by the STF. The increase in viscosity due to electrolytes of STF was nullified by the dilution of formulations and decrease in the concentration of gellan gum due to water in the STF.

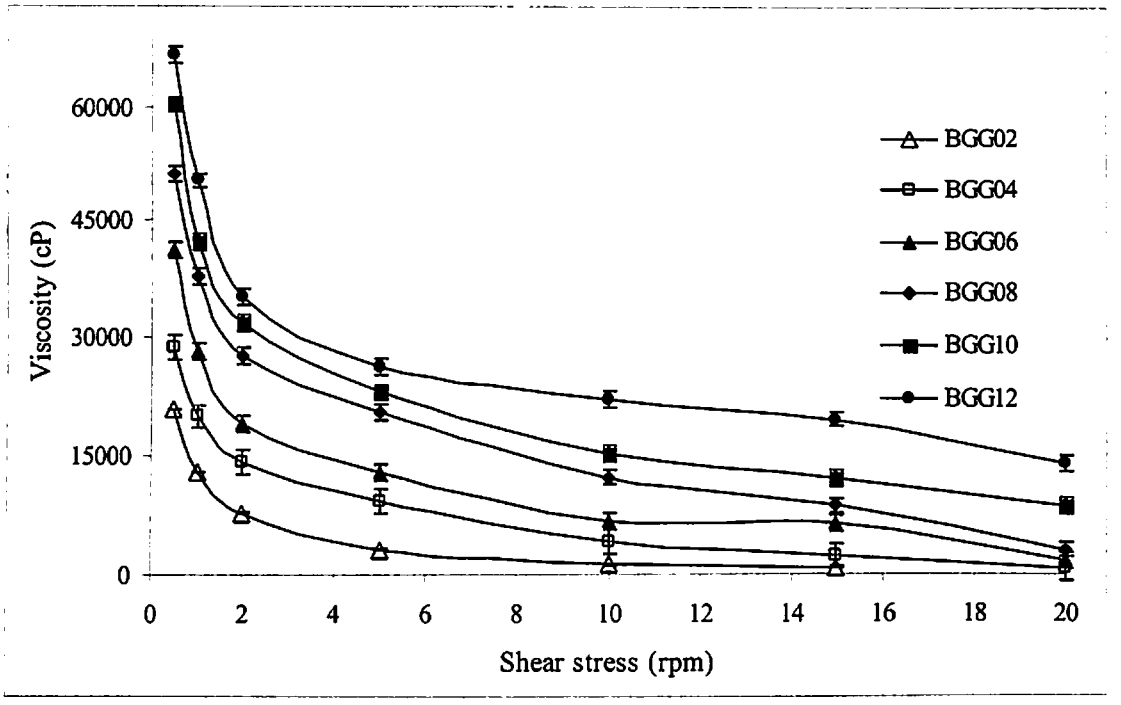

Fig 5.4: Rheological behaviour of gellan gum based brimonidine tartrate in situ gel formulations prepared in simulated tear fluid as vehicle. Each data point represents the average of two batches in triplicate with standard deviation.

In the formulations; BGG06, BGG08 and BGG10, no concentration dependent rheology was observed, all the three formulations showed pseudoplastic type of rheological behaviour. The drainage of formulations from the eye is rapid for formulations with low elasticity. Further dilution with STF facilitating further decrease in concentration and elasticity.

(iv) Mucoadhesive strength determination

The mucoadhesive strength determination studies on goat mucosal membrane showed that all the formulations were mucoadhesive with good force of detachment. Results are presented in the Table 5.4. The mucoadhesive strength is very essential for the ocular formulations to be retained in the eye for a longer period of time and also to prevent the movement or spreading of the formulation which can cause blurring of vision and discomfort to the patient.

Gellan gum concentration dependent mucoadhesive strength was observed for formulations with varying proportions of gellan gum. As the proportion of gellan gum in the in situ gel formulation was increased a proportional increase in the mucoadhesive strength was observed.

The presence of glycerol as osmolarity modifier showed no effect on the mucoadhesive strength of the formulations. The formulations prepared with STF as vehicle showed

higher mucoadhesive strength compared to those prepared in water as vehicle. This could be the absolute mucoadhesive strength that can be obtained for a given gellan gum proportion as the situation mimics the availability of highest amount of electrolytes for the gelling. The presence of phosphate buffer as vehicle and the presence of drug in the formulations did not show much effect on the mucoadhesive strength.

Table 5.4: Results of mucoadhesive strength determination studies of gellan gum based brimonidine tartrate in situ gel formulations.

Formulation	Force of detachment (N/cm^2)
(a) Effect of polymer proportion	
BGG02	0.017 ± 0.002
BGG04	0.025 ± 0.003
BGG06	0.078 ± 0.002
BGG08	0.097 ± 0.004
BGG10	0.101 ± 0.003
BGG12	0.125 ± 0.007
(b) Effect of glycerol	
BGG06G	0.081 ± 0.006
BGG08G	0.101 ± 0.010
BGG10G	0.111 ± 0.011
(c) Effect of STF as vehicle	
BGG06STF	0.098 ± 0.012
BGG08STF	0.101 ± 0.013
BGG10STF	0.112 ± 0.012
(d) Effect of phosphate buffer saline vehicle	
BGG06P	0.079 ± 0.014
BGG08P	0.098 ± 0.012
BGG10P	0.100 ± 0.013
(e) Effect of drug	
BGG06WD	0.080 ± 0.018
BGG08WD	0.096 ± 0.019
BGG10WD	0.102 ± 0.012

Each data point represents the average of two batches done in triplicate with standard deviation.

(v) In vitro drug release studies

The drug release profile of the developed ion activated in situ gelling formulations using gellan gum is presented in Fig 5.5. The drug release pattern was primarily influenced by the proportion of gellan gum present in the formulation. The formulations with higher proportion of gellan gum, formed stiff gel upon contact with STF and the formed gel prolonged the release of the incorporated drug.

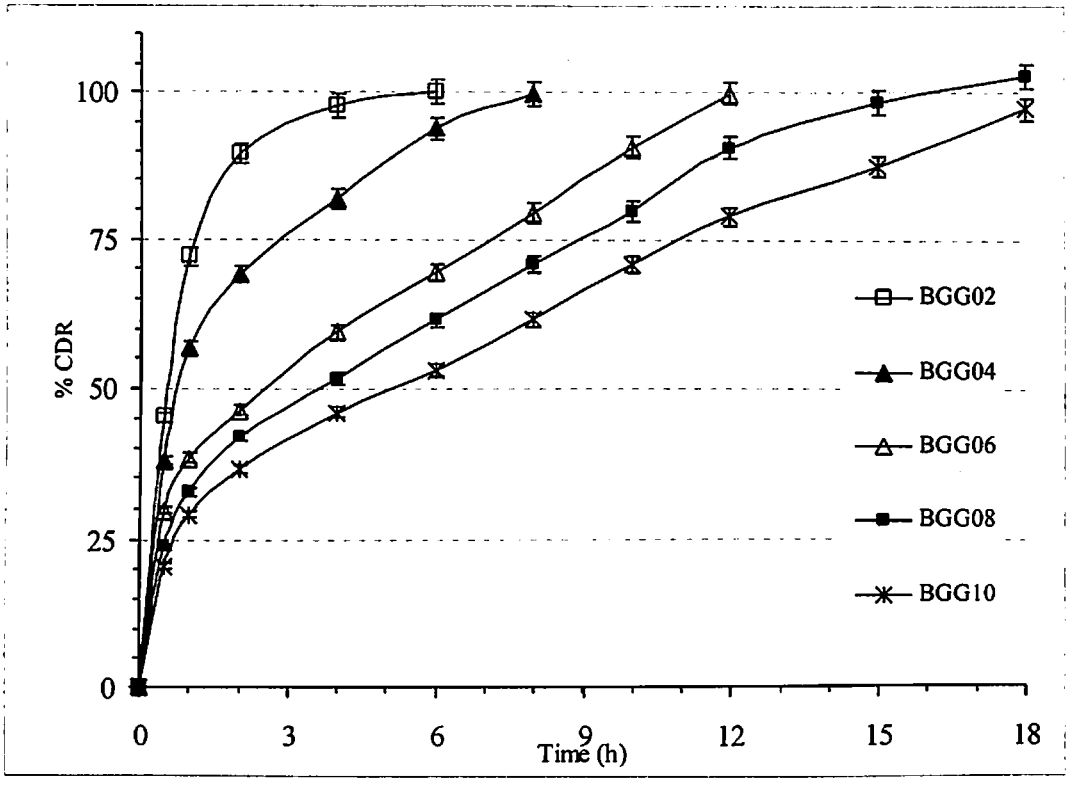

Fig 5.5: In vitro drug release profile of gellan gum based brimonidine tartrate in situ gel formulations prepared with varying proportions of gellan gum. Each data point represents the average of two batches in triplicate with standard deviation.

The drug release from formulation BGG02 containing 0.2 % w/w gellan gum was much faster with a release rate constant of 0.59 $h^{-0.51}$ and the duration of drug release lasted for only 4 h ($t_{90\%}$: 3 h). This could be due to formation of gel with low strength. Increase in the gellan gum concentration to 0.4 % w/w (BGG04), the release was extended to 6-7 h ($t_{90\%}$: 5.2 h) and release rate was found to be 0.54 $h^{-0.52}$. Further increase in gellan concentration to 0.6 % w/w resulted in further retardation of drug release with release rate of 0.45 $h^{-0.49}$ and $t_{90\%}$ of 10.7 h. Increase in the gellan gum proportion to 0.8 % w/w (BGG08), resulted further prolongation of drug release for 13.3 h ($t_{90\%}$). With the formulation BGG10 (gellan gum concentration of 1.0 % w/w) the drug release duration was extended with $t_{90\%}$ of 17.2 h and drug release rate was 0.36 $h^{-0.49}$.

All the formulation showed high initial burst release. The initial release (within 1 h) for formulations with lower proportions of gellan gum in the formulations can be correlated with the results of rate of gelation. The rapidity with which gel was formed significantly affects the initial release and subsequently the extent of prolongation of drug release. A gellan gum concentration dependent decrease in the initial burst release was observed. At higher concentration of gellan gum, rate of gelation was rapid and hence a lower initial burst release compared to the formulations with lower polymer concentration. The high

burst release could be due to the fact that the gels were prepared by complete solubilisation of drug and proper hydration of the polymer. The drug release pattern for the formulated gellan gum in situ gel is characteristic of hydrophilic matrix. The drug release declines with time after an initial burst release. But the polymer hydration and water penetration does not play a role in drug release. As the drug was readily available in dissolved state in the pre-hydrated and water saturated polymer matrix. The rate of erosion and subsequent dissolution of polymer gel in a time dependent manner was responsible for further prolongation of drug release. The drug release data was fitted into different release kinetics models like, zero order, first order, Higuchi square root kinetics and Korsmeyer-Peppas (KP model) models. The release exponent, 'n' value in the KP model was used to ascertain the drug release mechanism. The 'K', 'R^2' values for each of the model is given in the Table 5.5. The value of release exponent varied from 0.49 to 0.57 indicating that the drug release from the gellan gum in situ gel formulations was by Fickian diffusion kinetics transport mechanism. The Higuchi's square root kinetics also confirmed the diffusion controlled release behaviour of the polymer.

Formulations containing glycerol showed a more rapid initial drug release compared to formulations with no glycerol as shown in Fig 5.6. This could be due to, as discussed earlier, slower rate of gelation of formulations upon contact with STF due to the reduced osmotic gradient across the formulation and the surrounding environment. But the drug release profile remained significantly unaltered. The drug release from the formulations prepared in phosphate buffer as vehicle showed similar pattern of release to that prepared with glycerol. The high initial release was also observed and the drug release prolonged for longer time similar the formulations with glycerol.

Table 5.5: Results of drug release kinetics studies for gellan gum based brimonidine tartrate in situ gel formulations fitted into various kinetic models.

Batch code	Zero order		First order		Higuchi model	KP model			$t_{10\%}$ (h)	$t_{50\%}$ (h)	$t_{90\%}$ (h)
	K*	$R^{2¥}$	K*	$R^{2¥}$	$R^{2¥}$	K*	$R^{2¥}$	n #			
BGG02	13.2	0.6906	0.93	0.9863	0.9917	0.59	0.9725	0.51	0.02	0.4	3.0
BGG04	10.3	0.8910	0.42	0.9702	0.9922	0.54	0.9908	0.52	0.07	0.9	5.2
BGG06	6.8	0.9862	0.20	0.9862	0.9892	0.45	0.9892	0.49	0.09	2.2	10.7
BGG08	5.1	0.9613	0.17	0.9419	0.9758	0.40	0.9768	0.48	0.11	3.1	13.3
BGG10	4.2	0.9701	0.14	0.9201	0.9743	0.36	0.9852	0.49	0.22	4.2	17.2

* K- release rate constant, ¥ R^2- regression coefficient, # n- release exponent, $t_{10\%}$, $t_{50\%}$ and $t_{90\%}$- time taken (in h) for 10, 50 and 90 percent drug release respectively.

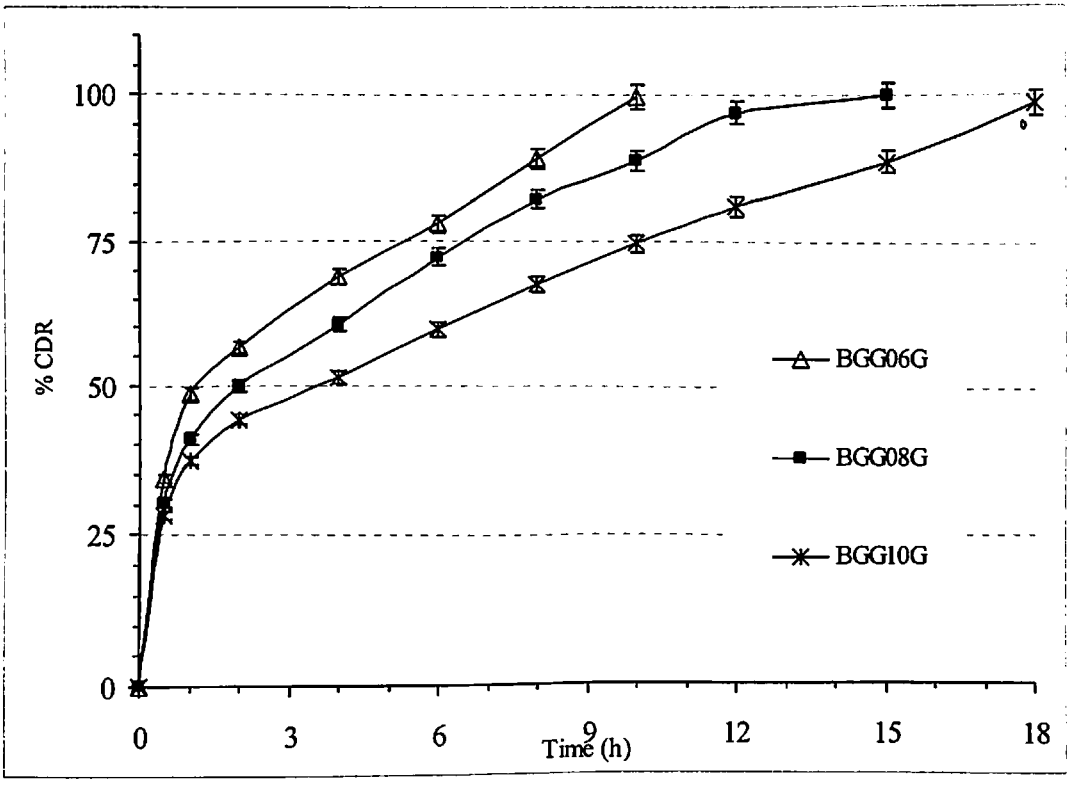

Fig 5.6: In vitro drug release profile of gellan gum based brimonidine tartrate in situ gel formulations with glycerol. Each data point represents the average of two batches in triplicate with standard deviation.

(vi) Stability studies

The stability studies of the selected formulation carried out as per ICH guidelines at both ambient and accelerated conditions showed that the selected in situ gel formulations were stable at both the storage conditions with a no significant degradation observed at accelerated condition (Table 5.6). The organoleptic parameters like colour, appearance, texture, and viscosity remained unaltered for the entire duration of the studies. The drug release profile was also found minimally altered.

Table 5.6: Stability study results of selected gellan gum based brimonidine tartrate in situ gel formulations stored at various conditions.

Formulation Code	Storage condition	Drug content		K_{deg} x 10^3 (month $^{-1}$) (Mean ± SD)	T_{90} (months)
		Initial	After 6 M		
BGG06	Ambient	99.02 ± 2.01	97.02 ± 2.11	0.58 ± 0.03	47.3
	ATC	99.02 ± 2.3	92.11 ± 1.21	3.21 ± 0.04	
BGG08	Ambient	100.45 ± 2.4	96.67 ± 1.02	0.71 ± 0.02	48.25
	ATC	98.45 ± 2.2	94.23 ± 1.42	3.15 ± 0.05	
BGG10	Ambient	101.22 ± 1.0	99.63 ± 1.75	0.51 ± 0.07	25.76
	ATC	100.22 ± 1.1	95.03 ± 2.12	5.90 ± 0.06	

K_{deg}: degradation rate constant, ATC: Accelerated temperature condition. T_{90}: shelf life in months. Each data point represents the average of two batches in triplicate with standard deviation.

5.4.2. Temperature activated in situ gelling system (PNIAA)

(i) Physicochemical characteristics of in situ gels

The prepared temperature sensitive PNIAA in situ gels were found to have good physicochemical properties such as appearance, colour and texture. The assay values were found to be within acceptable limits. The results are shown in the Table 5.7.

The in situ gel formulations prepared using varying amounts of PNIAA was found to be colourless and transparent below $T_{sol\text{-}gel}$, and formed a translucent to turbid gels at $T_{sol\text{-}gel}$. This could be explained by the mechanism of gelation where in the solubility of the polymer decreases with increase in the temperature above $T_{sol\text{-}gel}$ resulting in gel formation. The in situ gels prepared with HPMC as viscosifying agent were transparent to translucent in appearance below $T_{sol\text{-}gel}$ while formed a translucent to turbid gels at $T_{sol\text{-}gel}$. The presence of water as vehicle showed no effect on the appearance of the in situ gels.

All the prepared in situ gel formulations showed excellent pourability below $T_{sol\text{-}gel}$ while the viscosity increased at $T_{sol\text{-}gel}$. The presence of HPMC in the formulation increased viscosity, but the formulations were pourable below $T_{sol\text{-}gel}$ while at $T_{sol\text{-}gel}$ the formulations were viscous and were non flowable at $T_{sol\text{-}gel}$. All the prepared formulations showed drug content in the range of 98.34 to 102.02 % w/w which is within the acceptable limits.

(ii) Gelation temperature determination

The PNIAA based in situ gel formulations formed gel upon increasing the temperature to gelation temperature ($T_{sol\text{-}gel}$). The $T_{sol\text{-}gel}$ of prepared gels varied from 30° C to 34° C depending on the composition of in situ gel formulations as shown in Fig 5.7. The two methods employed in gelation temperature determination, gave similar and reproducible results. The $T_{sol\text{-}gel}$ of various formulations was shown in the Table 5.7 and Fig 5.7. The formulations with polymer alone at various concentration levels showed varying $T_{sol\text{-}gel}$ values of 33.2° C to 30.6° C. At lower concentration, 0.1 % w/w (BPNIA01) and 0.2 % w/w (BPNIA02), the gelation was not observed. In these cases, the appearance of turbidity was seen, but both the methods of gelation determination were unable to determine the $T_{sol\text{-}gel}$ due to low viscosity of the resulting gels. Further increase in polymer proportion to 0.4 % w/w (BPNIA04) the gelation was seen at 33.2° C. An increase in the polymer proportion resulted in slight decrease in gelation temperature. At highest level of polymer, 1.4 % w/w (BPNIA14), the gelation temperature shifted to 30.6° C.

The mechanism of thermo-gelation in aqueous solutions is the decrease in solubility attributed to changes in the overall hydrophilicity of the polymer chains upon temperature change. When a polymer is dissolved in water, three types of interactions take place; between polymer molecules, between polymer and water molecules and also between water molecules. For polymers exhibiting an lower critical solution temperature, (eg: PNIAA), an increase in temperature results in a negative free energy of the system which makes water-polymer association unfavourable, facilitating the other two types of interactions to predominate (Schmaljohann, 2006). Polymer micelle packing and coil to helix transition causing network formation are examples of the conformational changes that take place at the critical solution temperature. The result is a reversible physical linking of the polymer chains, and gels can therefore return to solution after the thermal stimulus is removed.

Table 5.7: Physicochemical characteristics of PNIAA based brimonidine tartrate in situ gel formulations.

Formulation code	Appearance	Assay (%)	$T_{sol-gel}$ (° C)	Flow behaviour	Force of detachment (N/cm^2)
BPNIA01	Colourless and transparent	98.4 ± 2.1	NG	Newtonian	0.017 ± 0.002
BPNIA02	Colourless and transparent	100.0 ± 0.9	NG	Newtonian	0.025 ± 0.003
BPNIA04	Colourless and transparent	99.02 ± 2.1	33.2 ± 0.3	Non-Newtonian	0.078 ± 0.002
BPNIA06	Colourless and transparent	99.2 ± 1.2	33.1 ± 0.4	Non-Newtonian	0.097 ± 0.004
BPNIA08	Colourless and transparent	100.2 ± 1.3	32.2 ± 0.3	Non-Newtonian	0.101 ± 0.003
BPNIA10	Colourless and transparent	99.4 ± 1.9	31.6 ± 0.2	Non-Newtonian	0.125 ± 0.007
BPNIA12	Colourless and transparent	100.0 ± 3.4	31.2 ± 0.2	Non-Newtonian	0.148 ± 0.006
BPNIA14	Colourless and transparent	99.7 ± 3.3	30.6 ± 0.3	Non-Newtonian	0.174 ± 0.010
BPNIA10H1	Colourless and translucent	99.9 ± 3.4	31.4 ± 0.2	Non-Newtonian	0.155 ± 0.011
BPNIA12H1	Colourless and translucent	99.9 ± 1.3	31.0 ± 0.2	Non-Newtonian	0.178 ± 0.012
BPNIA14H1	Colourless and translucent	102.0 ± 1.2	30.2 ± 0.3	Non-Newtonian	0.194 ± 0.013
BPNIA10H2	Colourless and translucent	99.2 ± 2.1	31.2 ± 0.2	Non-Newtonian	0.185 ± 0.012
BPNIA12H2	Colourless and translucent	99.5 ± 3.2	31.2 ± 0.2	Non-Newtonian	0.203 ± 0.014
BPNIA14H2	Colourless and translucent	98.3 ± 0.5	30.5 ± 0.3	Non-Newtonian	0.214 ± 0.012
BPNIA10H3	Colourless and translucent	98.7 ± 1.1	31.3 ± 0.2	Non-Newtonian	0.233 ± 0.013
BPNIA12H3	Colourless and translucent	99.3 ± 1.3	31.0 ± 0.2	Non-Newtonian	0.273 ± 0.018
BPNIA14H3	Colourless and translucent	99.3 ± 2.4	30.2 ± 0.3	Non-Newtonian	0.289 ± 0.019
BPNIA10W	Colourless and transparent	98.5 ± 2.2	31.6 ± 0.2	Non-Newtonian	0.125 ± 0.012
BPNIA12W	Colourless and transparent	100.3 ± 1.2	31.2 ± 0.2	Non-Newtonian	0.148 ± 0.021
BPNIA14W	Colourless and transparent	98.7 ± 1.2	30.6 ± 0.3	Non-Newtonian	0.174 ± 0.022

$T_{sol-gle}$: Gelation temperature. Each data point represents the average of two batches in triplicate with standard deviation,

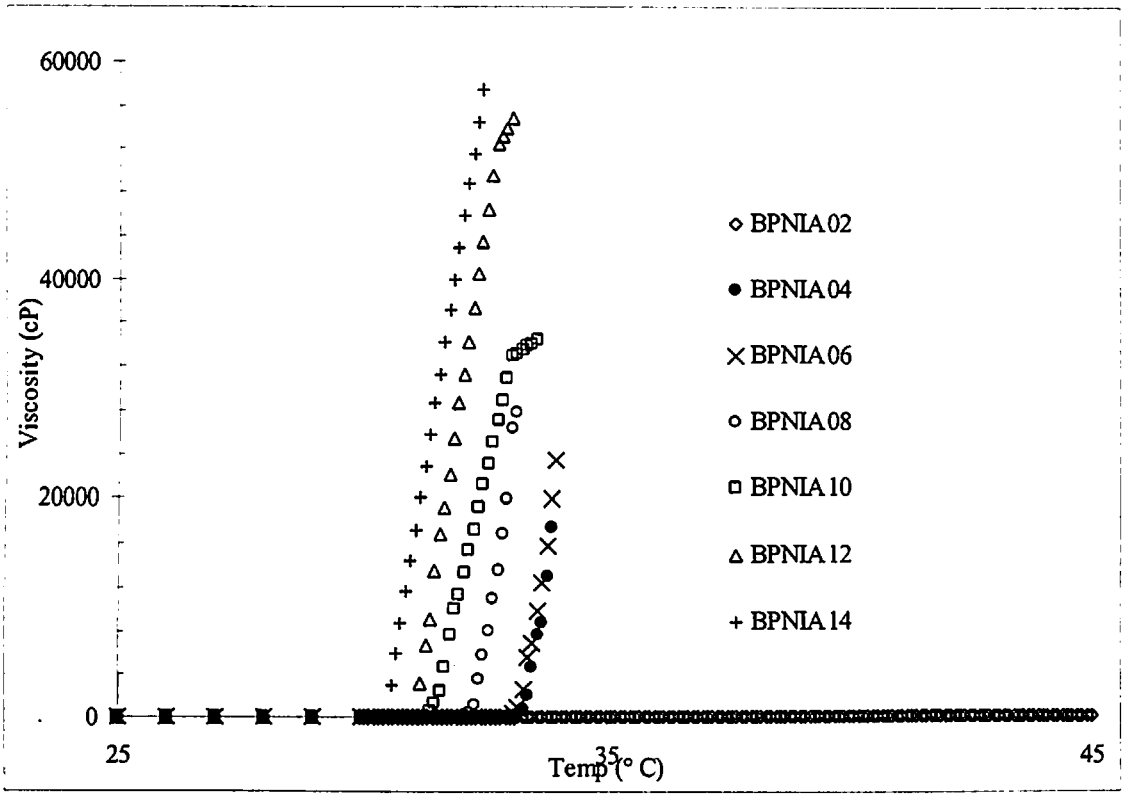

Fig 5.7: Plot showing the gelation temperature of PNIAA based brimonidine tartrate in situ gel formulation with varying PNIAA proportions (Inflection point was considered as gelation temperature). Each data point represents the average of two batches in triplicate.

(iii) Effect of addition of HPMC on gelation temperature

The PNIAA polymer in aqueous solution upon increase in temperature forms a stiff and rigid gels in higher proportions. In order to overcome that and to form a smooth and rigid gel, viscosifying agent such as HPMC K4M was incorporated into the in situ gel formulations in different proportions (1 %, 2 % and 3% w/w). The effect of HPMC on the gelation temperature was investigated. The addition of HPMC to the in situ gel formulations did not cause any change in the $T_{sol\text{-}gel}$ of in situ gels at all the three proportions investigated. The results are illustrated in Fig 5.8.

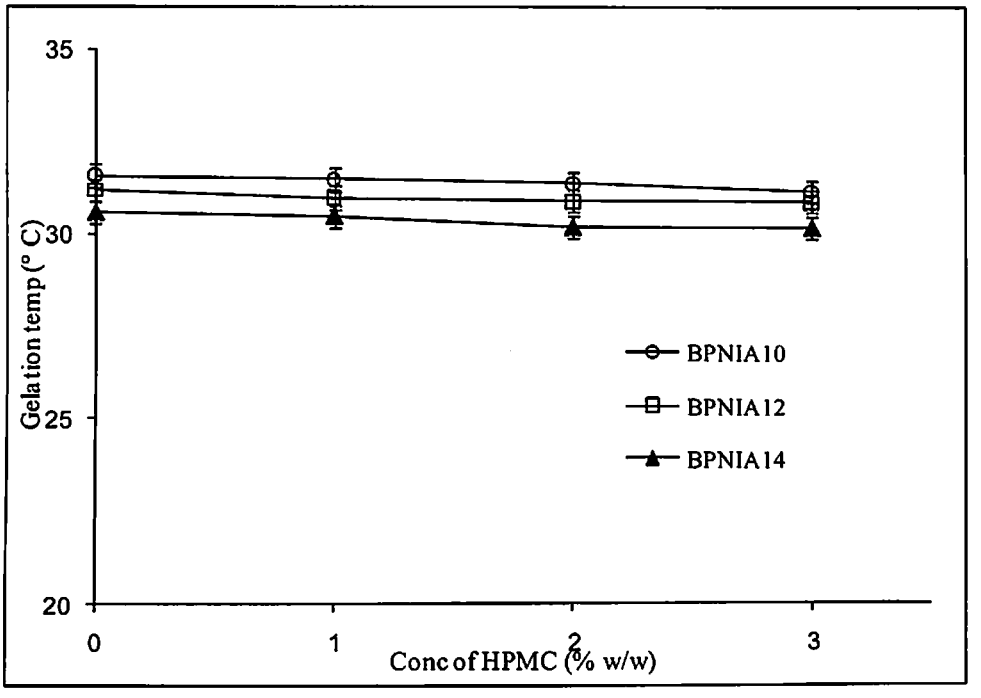

Fig 5.8: Effect of concentration of HPMC on the gelation temperature of PNIAA based brimonidine tartrate in situ gel formulations. Each data point represents the average of two batches in triplicate with standard deviation.

(iv) In vitro release studies

The drug release profile from PNIAA based in situ gels are shown in the Fig 5.9, Fig 5.10 and Fig 5.11. The drug release profile for PNIAA based in situ gel formulations prepared using varying proportions of PNIAA (Fig 5.9), showed high initial release followed by a slow and controlled release of drug over a period of time. The release from the gelled system was found to be more prolonged and found to be dependent on the proportion of the polymer. In lower proportions of polymer the formation of softer gels resulted in faster drug release compared to formulations with higher polymer proportions. In case of formulations with 0.2-0.4 % w/w PNIAA, the drug release was more rapid and lasted for 2-3 h.

As the proportion of polymer was increased to 0.6 % w/w (BPNIA06), the release rate constant was found to be 0.54 $h^{-0.53}$ with a $t_{10\%}$ of 0.02 h and $t_{90\%}$ of 5.2 h. Further increase in polymer proportion resulted in more prolonged release over a period of time. Formulation with 0.8 % w/w PNIAA (BPNIA08), the release rate was found to be 0.50 $h^{-0.57}$, with $t_{10\%}$ of 0.04 h and $t_{90\%}$ of 6.2 h. Higher proportion of PNIAA further retarded the release of drug. With the increase in the PNIAA proportion to 1.0 % w/w, the release rate was reduced to 0.46 $h^{-0.48}$ and with further increase in PNIAA proportion to 1.2 % w/w, the release rate constant was found to 0.40 $h^{-0.48}$, with $t_{90\%}$ of 8.8 h. Formulation with

PNIAA proportion of 1.4 % w/w, showed a tremendous decrease in release rate of 0.37 $h^{-0.49}$ and the release of entrapped drug was extended for a longer period of time with $t_{90\%}$ of 14.9 h.

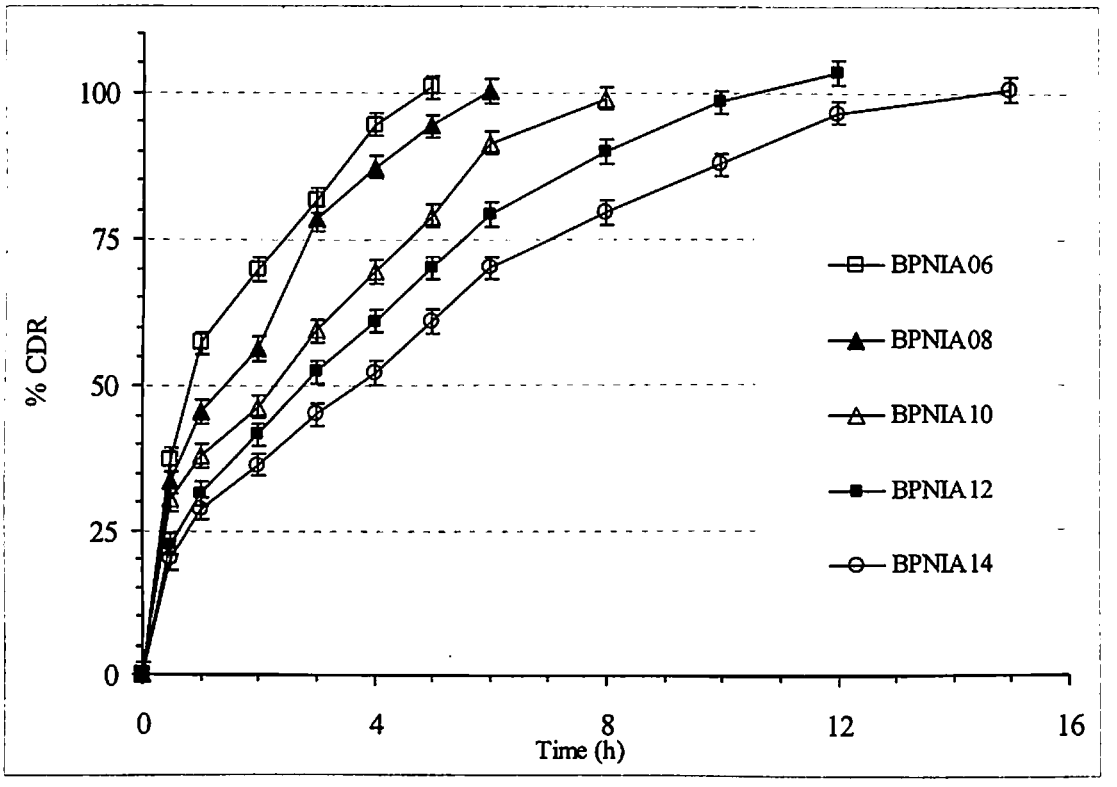

Fig 5.9: In vitro release profile of PNIAA based brimonidine tartrate in situ gel formulations prepared with varying proportions of polymer. Each data point represents the average of two batches in triplicate with standard deviation.

The drug release from PNIAA based in situ gels followed non-Fickian anamolous at lower concentrations of PNIAA (up to 0.8 % w/w), but shifted to Fickian diffusion based release mechanism at higher concentrations (Table 5.8).

With the addition of HPMC K4M (1 % w/w) to the in situ gel formulations, the drug release was found be retarded further in comparison to formulations without HPMC. Increase in the HPMC proportion to 2 % w/w further resulted in the prolongation of as The mechanism of drug release was by diffusion controlled mechanism as indicated by the value of 'n' (Table 5.8). Further increase in HPMC K4M proportion prolonged the drug release, but resulted in drastic increase in viscosity of the formulations making them nonpourable at normal conditions of temperature. The dissolution data for the 3 % w/w HPMC based formulations are not presented.

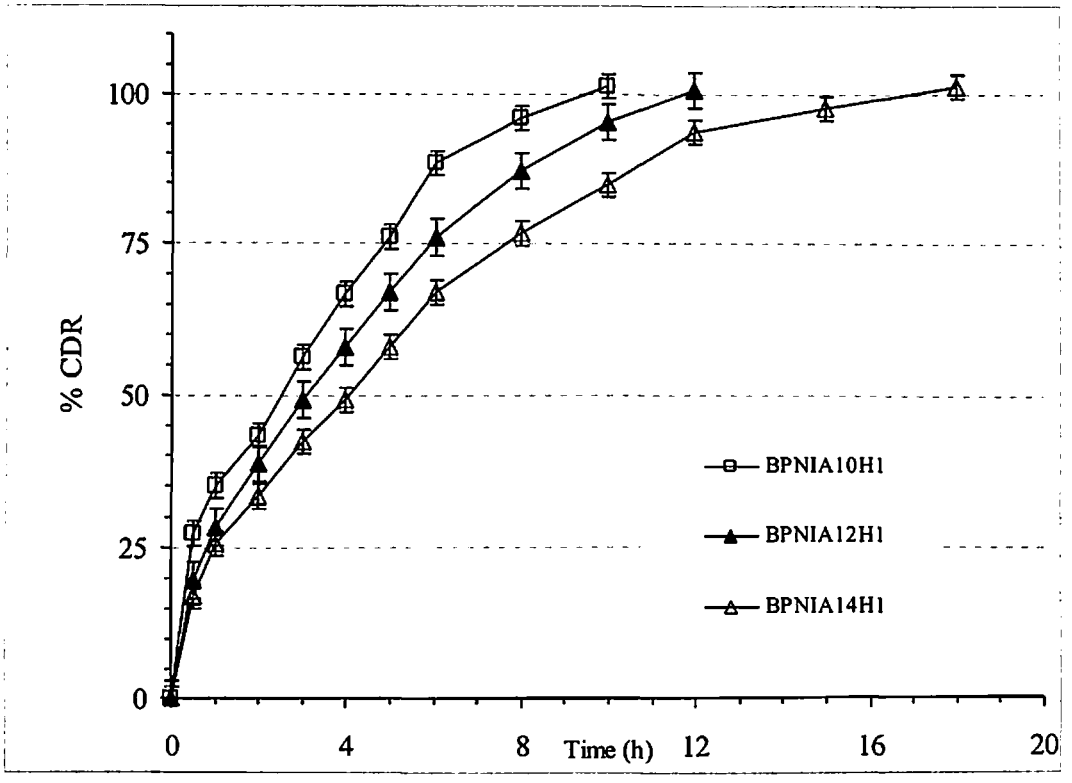

Fig 5.10: In vitro drug release profile of PNIAA based brimonidine tartrate in situ gel formulations prepared with HPMC K4M (1.0 % w/w). Each data point represents the average of two batches done in triplicate with standard deviation.

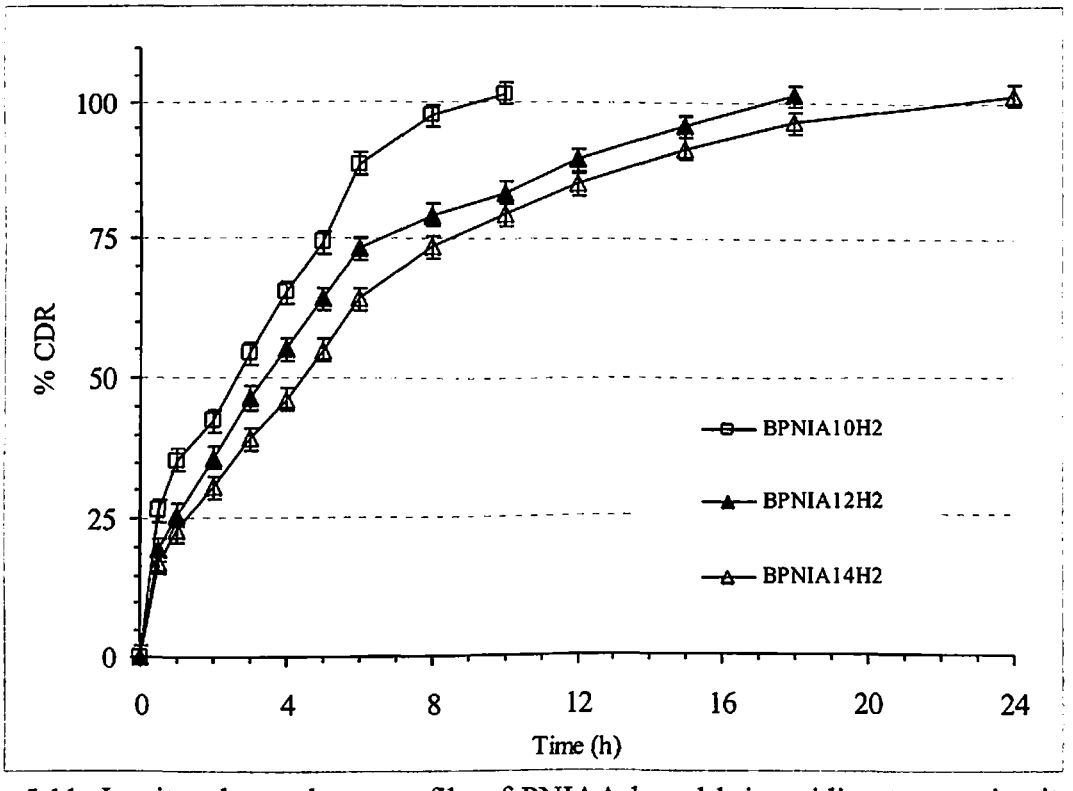

Fig 5.11: In vitro drug release profile of PNIAA based brimonidine tartrate in situ gel formulations prepared with HPMC K4M (2.0 % w/w). Each data point represents the average of two batches done in triplicate with standard deviation.

Table 5.8: Results of drug release kinetics studies for PNIAA based brimonidine tartrate in situ gel formulations fitted into various kinetic models.

Batch code	Zero order		First order		Higuchi model	KP model			$t_{10\%}$ (h)	$t_{50\%}$ (h)	$t_{90\%}$ (h)
	K*	$R^{2¥}$	K*	$R^{2¥}$	$R^{2¥}$	K*	$R^{2¥}$	n #			
BPNIA06	9.2	0.8882	0.52	0.9602	0.99212	0.54	0.9918	0.53	0.02	0.8	5.2
BPNIA08	7.8	0.9677	0.30	0.9862	0.9811	0.50	0.9812	0.57	0.04	2.1	6.2
BPNIA10	6.4	0.9813	0.28	0.9419	0.9721	0.46	0.9722	0.48	0.05	3.3	7.9
BPNIA12	4.3	0.9710	0.20	0.9982	0.9771	0.40	0.9852	0.48	0.10	3.9	8.8
BPNIA14	2.2	0.9822	0.14	0.9921	0.9322	0.37	0.9722	0.49	0.13	4.2	14.8
BPNIA10H1	5.5	0.9813	0.23	0.9419	0.9521	0.40	0.9722	0.48	0.04	6.3	6.4
BPNIA12H1	4.0	0.9715	0.18	0.9982	0.9271	0.30	0.9852	0.53	0.05	7.7	10.1
BPNIA14H1	1.9	0.9522	0.12	0.9921	0.9422	0.26	0.9722	0.49	0.55	8.7	14.0
BPNIA10H2	4.4	0.9613	0.19	0.9419	0.9672	0.40	0.9722	0.54	0.04	6.3	7.9
BPNIA12H2	3.8	0.9371	0.11	0.9982	0.9820	0.30	0.9852	0.53	0.05	7.7	12.9
BPNIA14H2	1.2	0.9822	0.08	0.9921	0.9352	0.26	0.9722	0.52	0.55	8.7	17.8

* K- release rate constant, ¥ R^2- regression coefficient, # n- release exponent, $t_{10\%}$, $t_{50\%}$ and $t_{90\%}$- time taken (in h)for 10, 50 and 90 percent drug release respectively. KP- Korsmeyer Peppas model

(v) Stability studies

The stability studies of the selected formulation carried out as per ICH guidelines at both ambient and accelerated conditions showed all the selected in situ gel formulations are stable at both the storage conditions, with all the parameters remained within the acceptable limits (Table 5.9). The organoleptic parameters like colour, appearance, texture, and viscosity remained unaltered for the entire duration of the studies. The drug release was also found minimally altered.

Table 5.9: Stability study results of selected PNIAA based brimonidine tartrate in situ gel formulations stored at various conditions.

Formulation Code	Storage condition	Drug content		K_{deg} x 10^3 (month $^{-1}$) (Mean ± SD)	T_{90} (months)
		Initial	After 6 M		
BPNIA10	Ambient	99.4 ± 1.9	97.42 ± 2.31	0.44 ± 0.03	47.20
	ATC	100.0 ± 3.4	93.01 ± 1.81	3.22 ± 0.06	
BPNIA12	Ambient	99.7 ± 3.3	95.77 ± 1.22	0.36 ± 0.02	47.94
	ATC	99.4 ± 1.9	93.33 ± 1.92	3.17 ± 0.05	
BPNIA14	Ambient	100.0 ± 3.4	97.33 ± 1.45	0.39 ± 0.07	35.93
	ATC	99.7 ± 3.3	94.53 ± 2.32	4.23 ± 0.06	
BPNIA10H2	Ambient	99.2 ± 2.1	95.83 ± 1.83	0.44 ± 0.03	50.33
	ATC	99.5 ± 3.2	92.93 ± 2.44	3.02 ± 0.04	
BPNIA12H2	Ambient	98.3 ± 0.5	96.22 ± 1.56	0.46 ± 0.02	35.59
	ATC	99.2 ± 2.1	93.22 ± 1.36	4.27 ± 0.05	
BPNIA14H2	Ambient	99.5 ± 3.2	98.07 ± 2.44	0.59 ± 0.07	36.71
	ATC	98.3 ± 0.5	93.33 ± 1.64	4.14 ± 0.03	

K_{deg}: degradation rate constant, ATC: Accelerated test condition. T_{90}: shelf life in months. Each data point represents the average of two batches done in triplicate with standard deviation.

5.5. CONCLUSIONS

With the aim of developing a suitable ocular delivery system for brimonidine tartrate for better management of glaucoma, ease of administration and prolonged residence time and enhanced ocular bioavailability, two novel in situ gel forming polymers were investigated. One was based on ion sensitive gelling polymer (gellan gum) while the other was using temperature activated in situ gelling polymer, [poly- N (isopropyl acrylamide)]. In situ gels were prepared and effect of various formulation variables were investigated to study their effect on gel forming characteristics. Gellan gum based in situ gels showed rapid gelation upon contact with cations of the tear fluid, while PNIAA based formulation gelated upon increase in temperature. The rheological behaviour was found to be pseudoplastic shear thinning systems, which is optimal for ocular applications. In vitro release studies showed prolonged release for a 15-18 h of time. Stability studies showed that the selected formulations were stable during the 6 months of storage. The best formulations from each series (gellan gum series: BGG06, BGG08, BGG10 and PNIAA series: BPNIA10, BPNIA12H2 and BPNIA14H2) were selected for in vivo pharmacodynamic efficacy studies in glaucomatous rabbits to ascertain and compare the IOP lowering efficacy to that of marketed formulation (Details are presented in chapter VIII). Hence, it can be concluded that the both selected in situ gelling polymers were ideally suited for the development of improved drug delivery systems for BRT in treating glaucoma. These formulations and have the potential to improve the therapeutic outcome and reduce the frequency of administration.

5.6. REFERENCES

Bhardwaj TR, Kanwar M, Lal R, Gupta A. 2000. Natural gums and modified natural gums as sustained-release carriers. Drug Dev. Ind. Pharm. 26; 1025-1038.

Boutris C, Chatzi EG, Kiparissides C. 1997. Characterisation of the LCST behaviour of aqueous poly (N-isopropylacrylamide) solutions by thermal and cloud point techniques. Polymer, 38; 2567-2570.

Cao Y, Zhang C, Shen W, Cheng Zhihong, Yu LL Ping Q. 2007. Poly (N-isopropylacrylamide)-chitosan as thermosensitive in situ gel-forming system for ocular drug delivery. J. Control. Release. 120; 186-194.

Carlfors J, Edsman K, Petersson R, Jornving K. 1998. Rheological evaluation of Gelrite® in situ gels for ophthalmic use. Eur. J. Pharm. Sci, 6; 113-119.

Chandran S. 2003. Studies on novel approaches for better ocular delivery of flurbiprofen. Ph.D Thesis, Birla Institute of Technology and Science, Pilani; 1-383.

Costa ROR, Freitas RFS. 2002. Phase behaviour of poly (N-isopropylacrylamide) in binary aqueous solutions. Polymer, 43; 5879-5885.

Eeckman F, Moes AJ, Amighi. 2004a. Poly (N-isopropylacrylamide) copolymers for constant temperature controlled drug delivery. Int. J. Pharm, 273; 109-119.

Eeckman F, Moes AJ, Amighi K. 2004b. Synthesis and characterization of thermosensitive copolymers for oral controlled drug delivery, Eur. Polym, J, 40; 873-881.

Edsman K, Carlfors J, Petersson R. 1998. Rheological evaluation of poloxamer as an in situ gel for ophthalmic use. Eur. J. Pharm. Sci, 6; 105-112.

Fawaz F, Koffi A, Guyot M, Millet P. 2004. Comparative in vitro-in vivo study of two quinine rectal gel formulations. Int. J. Pharm, 280; 151-162.

Friteyre MC, Mazuel C. 1987. Pharmaceutical composition of the type which undergoes liquid-gel phase transition. Eur. Patent EP0227494 A1.

Guo JH, Skinner GW, Harcum WW, Barnum PE. 1998. Pharmaceutical applications of naturally occurring water-soluble polymers. PSTT, 1; 254-261.

Hui HW, Robinson, JR. 1985. Ocular delivery of progesterone using a bioadhesive polymer. Int. J. Pharm, 26; 203-213.

Jansson PE, Lindberg B. 1983. Structural studies of gellan gum, an extracellular polysaccharide elaborated by *Pseuomonas elodea*. Carbohydr. Res, 124; 135-139.

Jeong B, Choi YK, Bae YH, Zentner G, Kim SW. 1999. New biodegradable polymers for injectable drug delivery systems. J. Control. Release, 62; 109-114.

Kuo MS, Mort AJ, Dell A. 1986. Identification and location of L-glycerate, an unusual acyl substituent in gellan gum. Carbohydr. Res, 156; 173-187.

Kim YJ, Choi S, Koh JJ, Lee M, Ko KS, Kim SW. 2001. Controlled release of insulin from injectable biodegradable triblock copolymer. Pharm. Res, 18; 548-550.

Kim EY, Gao ZG, Park JS, Li H, Han K. 2002. rhEGF/HP- beta –CD complex in poloxamer gel for ophthalmic delivery. Int. J. Pharm, 233; 159-167.

Kono K. 2001. Thermosensitive polymer-modified liposomes. Adv. Drug Deliv. Rev, 53; 307-319.

Liu W, Zhang B, Lu WW, Li X, Zhu D, De YK, Wang Q, Zhao C, Wang C. 2004. A rapid temperature-responsive sol–gel reversible poly (N-isopropylacrylamide)-g-methylcellulose copolymer hydrogel. Biomaterials, 25; 3005-3012.

Malonne H, Eeckman F, Fontaine D, Otto A, Vos LD, Moes A, Fontaine J, Amighi K. 2005. Preparation of poly (N-isopropylacrylamide) copolymers and preliminary assessment of their acute and subacute toxicity in mice. Eur. J. Pharm. Biopharm, 61; 188-194.

Meseguer G, Gurny R, Buri, P, Rozier A, Plazonnet B. 1993. Gamma scintigraphic study of precorneal drainage and assessment of miotic response in rabbits of various ophthalmic formulations containing pilocarpine. Int. J. Pharm, 95; 229-234.

Morris VJ. 1990. Biotechnically produced carbohydrates with functional properties for use in food systems. Food Biotechnol, 4; 45-57.

Nakayama M, Okano T, Miyazaki T, Kohori F, Sakai K, Yokoyama M. 2006. Molecular design of biodegradable polymeric micelles for temperature-responsive drug release, J. Control. Release, 115; 46-56.

Ooteghem MV. 1993. In: Edman P. (Ed.), Biopharmaceutics of ocular drug Delivery. CRC Press, Boca Raton; 27-41.

Paulsson M, Hagerstrom H, Edsman K. 1999. Rheological studies of the gelation of deacetylated gellan gum (Gelrite®) in physiological conditions. Eur. J. Pharm. Sci, 9; 99-105.

Peppas NA, Bures P, Leobandung W, Ichikawa H. 2000. Hydrogels in pharmaceutical formulations. Eur. J. Pharm. Biopharm, 50; 27-46.

Qiu Y, Park K. 2001. Environment-sensitive hydrogels for drug delivery. Adv. Drug Deliv. Rev, 53; 321-339.

Robinson G, Manning CE, Morris ER. 1991. Conformation and physical properties of the bacterial polysaccharides gellan, welan and rhamsan, In Food polymers, gels, and colloids, Dickinson E (Ed), Royal Society Chemistry, London.

Rozier A, Mazuel C, Grove J, Plazonnet B 1989. Gelrite®: A novel, ion-activated, in-situ gelling polymer for ophthalmic vehicles. Effect on bioavailability of timolol. Int. J. Pharm, 57; 163-168.

Ryu JM, Chung SJ, Lee MH, Kim CK, Shim CK. 1999. Increased bioavailability of propranolol in rats by retaining thermally gelling liquid suppositories in the rectum. J. Control. Release, 59; 163-172.

Schild HG. 1992. Poly (N-isopropylacrylamide): experiment, theory and application, Prog. Polym. Sci, 17; 163-249.

Schmaljohann D. 2006. Thermo- and pH-responsive polymers in drug delivery. Adv. Drug Deliv. Rev, 58; 1655-1670.

Soppimath KS, Aminabhavi TM, Dave AM, Kumbar SG, Rudzinski WE. 2002. Stimulus-responsive "smart" hydrogels as novel drug delivery systems. Drug Dev. Ind. Pharm, 28; 957-974.

CHAPTER SIX

SOLID OCULAR INSERTS

6.1. INTRODUCTION

Solid ocular inserts offer many advantages over conventional formulations in terms of increased residence in the eye, prolonged release of incorporated drugs and more accurate dosing with a low risk of systemic adverse effects. And since they are in solid state, will have higher shelf life and presence of formulation additives like preservative is not required. Also once daily or weekly administration is possible. Due to the mucoadhesive property which can be easily incorporated in ocular inserts by addition of mucoadhesive polymer, help to overcome the ocular limitations and enhance the ocular bioavailability of drugs by improving the precorneal residence time of drugs and also decrease the non-productive drug loss related systemic toxicities (El-Shanawany, 1992; Weyenberg et al, 2006).

Ocular inserts can be designed as films, erodible & non-erodible inserts, rods and shields for drug delivery to the eye. These polymeric delivery systems are known to sustain and control drug release avoiding pulsed entry of the potent drugs (Worthen et al, 1974). Though they can deliver the dose precisely and more accurately, but are not well tolerated or accepted by patients due to difficulties in placement in lower cul de sac or as implants, psychological factors due to solid in nature, and possible interference with vision (Greaves et al, 1992; Gurtler et al, 1995).

Polymers used in ocular inserts can be of natural, synthetic or semi synthetic in nature. Further, they can be either water soluble polymers with linear chains or water insoluble polymers joined by cross linking agents. Most commonly employed polymers for ocular insert design are nonionic polymers such as hydroxypropylmethylcellulose (Paliwal et al, 2009; Gilhotra et al, 2009), polycationics such as chitosan (Di Colo et al 2002b; Verestiuc et al, 2006), polyanionics like polyacrylic acid derivatives e.g. carbopol (Weyenberg et al, 2004; Weyenberg et al, 2006; Bodzag et al, 2010), polycarbophils (Lee et al, 1994; Hornof et al, 2003), carboxymethylcellulose (Paliwal et al, 2009; Gilhotra et al, 2009), hydroxypropylcellulose and ethyl cellulose (Baeyens et al, 2002), Polyorthoesters (Einmahl et al, 1999), hydroxypropyl methacrylate (Sasaki et al, 1993; Sasaki et al, 2003), Gelfoam® device (Nadkarni and Yalkowsky 1993; Simamora et al, 1998; Lee and Yalkowsky, 1999). Other cellulosic polymers such as methylcellulose; hydroxylethyl-cellulose, hydroxypropylmethylcellulose, hydroxypropylcellulose were introduced as viscolizers into artificial tear preparations to retard canalicular drainage and improve contact time (Bourlais et al, 1998).

Poly ethylene oxide (PEO) is a hydrophilic gel-forming polymer with molecular weight dependent physicochemical properties like rate of swelling and erosion. The polymer has tendency of hydrating upon contact with water to form a superficial gel which eventually erodes slowly, releasing the incorporated drug at a sustained rate (Di Colo et al, 2001; Maggi et al, 2002). The drug release from PEO matrices are governed principally by polymer swelling and erosion and/or drug diffusion through the hydrated gel layer or all mechanisms together (Saettone et al, 1995). It possesses good mucoadhesion properties and excellent compressibility. But due to their rapid hydration, swelling and subsequent erosion property, designing a prolonged release formulation of drugs using PEO alone is a challenging task as the rate of release increases with time due to the rapid erosion of PEO matrices (Di Colo et al, 2001a & b).

Addition or combination of polymers with different properties could be an approach to improve the drug delivery applications of PEO. Eudragits, derivatives of acrylic acid and methyl methcrylates, could be another polymer that improves the duration of drug release while retaining the mucoadhesive properties. Eudragits are chemically inert polymers and are non-hydrating and non swellable, upon contact with water show little erosion. The bulk of drug release from Eudragit matrix occurs by diffusion, but Eudragit polymers are poorly mucoadhesive. Ocular inserts with insufficient level of mucoadhesive strength can slide on the ocular surfaces and can cause eye irritation.

An appropriate grade of PEO with Eudragit in suitable proportion can result in desired drug release profile while retaining optimum mucoadhesive strength throughout the duration of drug release.

The primary objectives of this section of the research work was to design and evaluate ocular inserts prepared using hydrophilic/ swellable/ erodible and hydrophobic/ inert/ zwitterionic polymers, either alone or in combination. The effect of type and proportion of polymers on the physicochemical properties, mucoadhesive strength, erosion and in vitro release profile were extensively investigated. The formulations showing desired in vitro release profile and adequate mucoadhesion were investigated for in vivo IOP lowering efficacy.

6.2. MATERIALS & EQUIPMENTS

6.2.1. Materials

BRT was obtained as a gift sample from FDC Ltd, Mumbai, India. Poly ethylene oxide (molecular weights 100 kD and 400 kD), HPMC (K4M, K15M and K100M) were purchased from Sigma Aldrich, Bangalore, India. Eudragit (RS 100 and RL 100) were

obtained as gift sample from Evonik Deggusa, Mumbai, India. Ethyl cellulose (22 cP and 50 cP) were obtained from Signet Chemicals, India. All other chemicals and reagents used were of pharmaceutical or analytical grade.

6.2.2. Equipments

A five digit analytical balance (Mettler Toledo AG135, Mettler, GMBH, Greifensee, Switzerland) was used for all weighing purposes. Tablet compression machine (Rimek, Mohali, India) was used in the compression of ocular inserts. Texture analyser (TA-XT2, Stable Microsystems, UK) was used for determining crushing strength. Friability was determined in a Campbell Electronic Friabilator (Campbell Electronics, Mumbai, India). Humidity chambers (Newtronics, India) were used to maintain ambient (25° C ± 2 °C/60 ± 5% RH) and ATC (40° C ± 2° C/75 ± 5% RH) conditions. High quality pure water was prepared using Millipore purification system (Model Elix SA 67120, Molsheim, France). In vitro release studies were carried out using USP Type I dissolution apparatus (basket type, Electrolab TDT-08L, Mumbai, India).

6.3. METHODS

6.3.1. Preparation of ocular inserts

Weighed amounts of drug and polymers were passed through sieve no # 100 and dried in vacuum. The dried drug and polymer were blended together and granulated using isopropyl alcohol as granulating fluid. The resulting granules were dried, passed through sieve no # 60 and lubricated with 0.5 % w/w magnesium stearate. The lubricated blend was compressed into ocular inserts using 4 mm die punches on tablet compression machine (Rimek, Mohali, India). The schematic representation of preparation procedure is shown in the Fig 6.1. The ocular inserts based formulations were designed to study the following:

(a) Effect of proportion and molecular weight of hydrophilic polymer (PEO 100 kD and PEO 400 kD) and HPMC (K4M, K15M and K100M),

(b) Effect of proportion and type of inert/ zwitterionic polymers (Eudragits RL 100 or Eudragit RS 100) and hydrophobic polymers (EC-22 cP and EC-50 cP),

(c) Effect of combination of hydrophilic polymers (PEO 100 kD or PEO 400 kD) with inert/ zwitterionic polymers (Eudragits RL 100 and Eudragit RS 100) with hydrophobic polymers (EC-22 cP and EC-50 cP) on the physicochemical properties, mucoadhesive strength, erosion pattern and in vitro drug release profile.

The components of designed ocular inserts are enlisted in the Table 6.1(a) and 6.1(b) for single polymer based ocular inserts and Table 6.2(a), 6.2(b), 6.2(c) and 6.2(d) for polymer combination based ocular inserts.

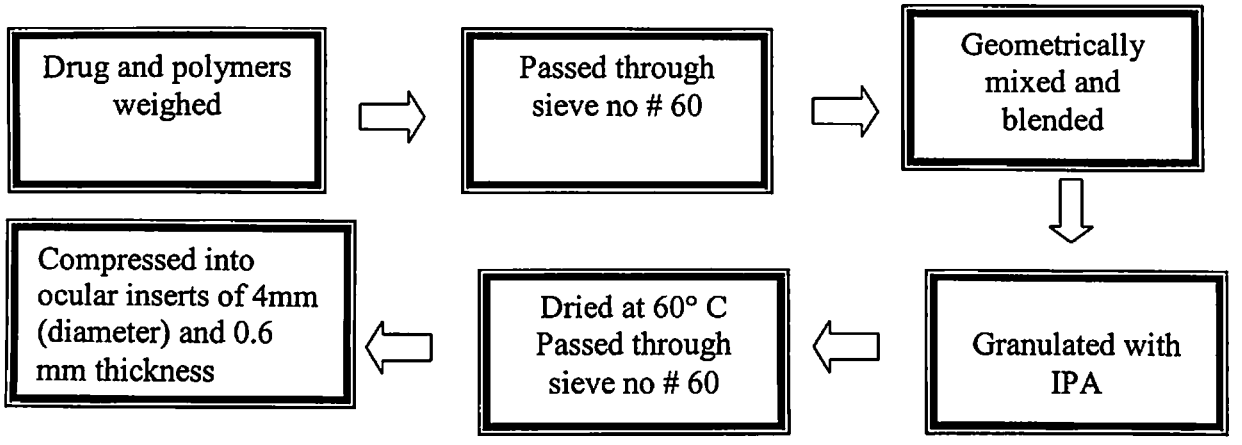

Fig 6.1: Schematic representation of brief preparative procedure for the ocular inserts formulations.

6.3.2. Evaluation of ocular inserts

The Designed ocular inserts were evaluated for various physicochemical properties, mucoadhesive strength, erosion pattern and in vitro drug release studies as presented below.

(i) Drug content estimation

For drug content estimation, twenty ocular inserts from 3 batches were accurately weighed and pulverised in mortar and pestle. An aliquot amount of triturate equivalent to 1 mg of BRT was taken and drug was extracted using phosphate buffer (pH 7.4) by sonication, filtered and suitably diluted and analysed spectrophotometrcally at 248 nm (Chapter III-analytical method development).

(ii) Crushing strength/ hardness

Crushing strength/hardness of the prepared ocular inserts was determined on three ocular inserts of each batch by texture profile analysis method using Texture analyser (TA-XT2, Stable Microsystems, UK) which was connected with a 30 kg weight load cell, using a 4 mm diameter analytical probe. The instrument had a force of resolution of 0.1g, measurement accuracy of 0.001% and distance resolution of 0.001 mm. The probe was programmed to penetrate the formulation at a speed of 0.1 mm per second and withdrawn at a speed of and distance of 1 mm. Crushing strength was calculated as the maximum force (in Newtons) from the force time curve.

Table 6.1(a): Formulation composition and physicochemical properties of single polymer (hydrophilic) based brimonidine tartrate ocular inserts.

Formulation code	Ingredients (in percentage)					Physicochemical parameters				
	PEO 100 kD	PEO 400 kD	HPMC K4M	HPMC K15M	HPMC 100KM	BRT Content (mg)	Weight # (mg)	Assay (%) ¥	Crushing strength/hardness (N)*	Friability (%) Ψ
(a) PEO 100 kD based formulations										
BP1100	100	-	-	-	-	1.0	12.09 ± 0.11	98.0 ± 2.1	28.2 ± 2.2	0.2
BP160	60	-	-	-	-	1.0	7.67 ± 0.22	100.1 ± 0.9	26.5 ± 2..8	0.3
BP120	20	-	-	-	-	1.0	3.22 ± 0.11	99.4 ± 2.1	25.2 ± 1.1	0.4
(b) PEO 400 kD based formulations										
BP4100	-	100	-	-	-	1.0	12.76 ± 0.30	98.4 ± 1.9	28.0 ± 2.1	0.2
BP460	-	60	-	-	-	1.0	6.42 ± 0.23	101.2 ± 1.3	26.2 ± 1.8	0.4
BP420	-	20		-	-	1.0	3.14 ± 0.13	100.2 ± 1.2	26.2 ± 2.1	0.5
(c) HPMC K4M based formulations										
BH4100	-	-	100	-	-	1.0	11.99 ± 0.43	99.3 ± 3.4	29.2 ± 1.1	0.2
BH460	-	-	60	-	-	1.0	6.53 ± 0.43	99.9 ± 3.3	26.9 ± 1.2	0.3
BH420	-	-	20	-	-	1.0	3.34 ± 0.44	101.0 ± 3.4	24.2 ± 0.2	0.5
(d) HPMC K15M based formulations										
BH15100	-	-	-	100	-	1.0	12.44 ± 0.29	99.3 ± 2.2	25.2 ± 1.0	0.3
BH1560	-	-	-	60	-	1.0	7.66 ± 0.23	102.1 ± 1.2	22.2 ± 2.1	0.4
BH1520	-	-	-	20	-	1.0	3.26 ± 0.24	98.8 ± 1.3	22.3 ± 2.0	0.6
(e) HPMC K100M based formulations										
BH10100	-	-	-	-	100	1.0	12.29 ± 0.11	98.6 ± 1.3	27.6 ± 1.7	0.3
BH1060	-	-	-	-	60	1.0	7.78 ± 0.23	98.3 ± 0.5	26.3 ± 1.8	0.4
BH1020	-	-	-	-	20	1.0	3.32 ± 0.21	99.5 ± 3.2	26.2 ± 1.1	0.3

PEO – Poly ethylene oxide (mol. wt: 100 kD and 400 kD), HPMC – hydroxypropylmethylcellulose (viscosity grades: K4M, K15M and K100M). Percentage of polymer refers to the % w/w calculated based on the polymer content in the ocular inserts out of total weight of ocular inserts, # mean of 20 ocular inserts from 3 batches; ¥ mean of 10 ocular inserts from 3 batches; * mean of 3 ocular inserts from 3 batches; Ψ based on 20 ocular inserts.

Table 6.1(b): Formulation composition and physicochemical properties of single polymer (Zwitterionic/hydrophobic) based brimonidine tartrate ocular inserts.

Formulation code	Ingredients (in percentage)				Physicochemical parameters				
	ERL 100	ERS 100	EC-22	EC-50	BRT Content (mg)	Weight [#] (mg)	Assay [¥] (%)	Crushing strength/Hardness (N) *	Friability (%) [Ψ]
(a) ERL 100 based formulations									
BERL100	100	-	-	-	1.0	12.11 ± 0.11	98.0± 2.1	25.2 ± 2.2	0.5
BERL60	60	-	-	-	1.0	7.69 ± 0.12	100.1± 0.9	24.5 ± 2..8	0.7
BERL20	20	-	-	-	1.0	3.34 ± 0.24	99.1± 1.1	23.2 ± 2.2	0.3
(b) ERS 100 based formulations									
BERS100	-	100	-	-	1.0	12.36 ± 0.40	98.1± 1.9	26.0 ± 2.1	0.3
BERS60	-	60	-	-	1.0	7.76 ± 0.23	100.7 ± 2.3	23.9 ± 1.8	0.7
BERS20	-	20	-	-	1.0	3.31 ± 0.13	101.2 ± 1.2	23.3 ± 2.1	0.4
(b) EC-50 based formulations									
BE5100	-	-	-	100	1.0	11.90 ± 0.33	99.1± 2.4	27.2 ± 2.1	0.5
BE560	-	-	-	60	1.0	7.61 ± 0.23	99.0 ± 1.3	26.9 ± 1.2	0.5
BE520	-	-	-	20	1.0	3.27 ± 0.44	100.2 ± 1.4	24.2 ± 0.2	0.5
(d) EC-22 based formulations									
BE2100	-	-	100	-	1.0	12.44 ± 0.29	98.3 ± 1.2	29.2 ± 1.0	0.3
BE260	-	-	60	-	1.0	7.69 ± 0.23	100.2 ± 1.2	27.2 ± 2.8	0.3
BE2200	-	-	20	-	1.0	3.31± 0.24	99.5 ± 2.2	25.3 ± 1.0	0.7

ERL 100 – Eudragit RS 100, ERS 100- Eudragit RS 100, EC-50 and EC-22- Ethyl cellulose (50 cP and 22 cP viscosity grades), Percentage of polymer refers to the % w/w calculated based on the polymer content in the ocular inserts out of total weight of ocular inserts, [#] mean of 20 ocular inserts from 3 batches; [¥] mean of 10 ocular inserts from 3 batches; * mean of 3 ocular inserts from 3 batches; [Ψ] based on 20 ocular inserts.

Table 6.2(a): Formulation composition and physicochemical properties of polymer combination (PEO with Eudragits) based brimonidine tartrate ocular inserts

Formulation code	Ingredients (%w/w)				Physicochemical parameters				
	PEO		Eudragit		BRT Content (mg)	Weight (mg) #	Assay (%) ¥	Crushing strength/ hardness (N) *	Friability (%) Ψ
	100 kD	400 kD	ERS 100	ERL 100					
(a) Combination of PEO 100 kD and Eudragit RL 100									
BP1100ERL00	100	-		0	1.0	12.44 ± 0.23	102.2 ± 1.2	29.2 ± 2.1	0.4
BP180ERL20	80	-	-	20	1.0	11.90 ± 0.33	98.4 ± 3.4	28.2 ± 2.1	0.7
BP160ERL40	60	-	-	40	1.0	12.53 ± 0.43	99.5 ± 3.3	29.9 ± 1.2	0.6
BP140ERL60	40	-	-	60	1.0	12.22 ± 0.44	101.2 ± 3.5	28.3 ± 0.2	0.5
BP120ERL80	20	-	-	80	1.0	12.44 ± 0.29	99.4 ± 2.2	29.2 ± 1.0	0.3
BP100ERL100	0	-	-	100	1.0	12.44 ± 0.23	102.2 ± 1.2	29.2 ± 2.1	0.4
(b) Combination of PEO 100 kD and Eudragit RS 100									
BP180ERS20	80	-	20	-	1.0	11.99 ± 0.22	101.1 ± 1.0	28.6 ± 2..8	0.6
BP140ERS60	40	-	60	-	1.0	12.36 ± 0.40	99.2 ± 2.0	28.0 ± 2.1	0.3
BP120ERS80	20	-	80	-	1.0	12.22 ± 0.23	100.2 ± 2.3	29.2 ± 1.8	0.7
BP100ERS100	0	-	100	-	1.0	12.44 ± 0.23	102.2 ± 1.2	29.2 ± 2.1	0.4
(c) Combination of PEO 400 kD and Eudragit RL 100									
BP4100ERL00	-	100		0	1.0	12.45 ± 0.24	99.9 ± 2.3	29.3 ± 2.0	0.6
BP480ERL20	-	80	-	20	1.0	11.89 ± 0.44	101.2 ± 3.2	29.8 ± 2.1	0.5
BP460ERL40	-	60	-	40	1.0	12.54 ± 0.29	100.2 ± 2.6	30.2 ± 1.2	0.3
BP440ERL60	-	40	-	60	1.0	12.44 ± 0.44	99.2 ± 1.2	28.9 ± 1.0	0.6
BP420ERL80	-	20	-	80	1.0	12.48 ± 0.48	99.0 ± 1.0	28.0 ± 1.0	0.2
(d) Combination of PEO 400 kD and Eudragit RL 100									
BP480ERS20	-	80	20	-	1.0	12.22 ± 0.41	100.7 ± 2.3	30.2 ± 1.6	0.3
BP460ERS40	-	60	40	-	1.0	12.21 ± 0.23	99.3 ± 0.6	28.2 ± 1.8	0.2
BP440ERS60	-	40	60	-	1.0	12.11 ± 0.51	99.0 ± 3.2	29.2 ± 2.1	0.3
BP420ERS80	-	20	80	-	1.0	11.94 ± 0.53	102.2 ± 1.2	27.2 ± 0.6	0.4

PEO – Poly ethylene oxide (mol. wt: 100 kD and 400 kD), HPMC percentage of polymer refers to the % w/w calculated based on the polymer content in the ocular inserts out of total weight of ocular inserts, # mean of 20 ocular inserts from 3 batches; ¥ mean of 10 ocular inserts from 3 batches; * mean of 3 ocular inserts from 3 batches; Ψ based on 20 ocular inserts.

Table 6.2(b): Formulation composition and physicochemical properties of polymer combination (PEO with EC) based brimonidine tartrate ocular inserts.

	PEO 100 kD	PEO 400 kD	EC- 22	EC- 50	BRT Content (mg)	Weight # (mg)	Assay ¥ (%)	Crushing strength/Hardness (N) *	Friability (%) Ψ
(a) Combination of PEO 100 kD and EC-22									
BP1-100	100	-	0	-	1.0	12.41 ± 0.23	102.2 ± 1.0	29.2 ± 2.1	0.4
BP180E220	80	-	20	-	1.0	11.53 ± 0.22	101.0 ± 0.9	23.5 ± 2..8	0.5
BP160E240	60	-	40	-	1.0	11.91 ± 0.24	100.3 ± 2.1	27.2 ± 1.1	0.6
BP140E260	40	-	60	-	1.0	12.21 ± 0.40	98.2 ± 1.8	28.0 ± 2.1	0.3
BP120E280	20	-	80	-	1.0	12.13 ± 0.23	101.2 ± 1.3	24.2 ± 1.8	0.7
BE2-100	0	-	100	-	1.0	12.34 ± 0.23	100.2 ± 2.2	29.2 ± 2.1	0.4
(b) Combination of PEO 100 kD and EC-50									
BP180E520	80	-	-	20	1.0	11.99 ± 0.23	99.3 ± 3.4	24.2 ± 2.1	0.5
BP160E540	60	-	-	40	1.0	12.23 ± 0.43	98.4 ± 1.3	29.9 ± 1.2	0.6
BP140E560	40	-	-	60	1.0	12.42 ± 0.44	100.2 ± 3.4	25.2 ± 0.2	0.5
BP120E580	20	-	-	80	1.0	12.44 ± 0.29	99.3± 2.2	29.2 ± 1.0	0.3
BE5-100	0	-	-	100	1.0	12.24 ± 0.33	102.2 ± 1.2	24.2 ± 2.1	0.4
(b) Combination of PEO 400 kD and EC-22									
BP4-100	-	100	0	-	1.0	12.35 ± 0.24	94.8 ± 2.3	29.3 ± 2.0	0.6
BP480E220	-	80	20	-	1.0	12.32 ± 0.41	100.6 ± 2.3	30.2 ± 1.6	0.3
BP460E240	-	60	40	-	1.0	12.11 ± 0.23	99.3 ± 0.5	28.3 ± 1.8	0.3
BP440E260	-	40	60	-	1.0	12.01 ± 0.51	98.0 ± 2.2	24.2 ± 2.1	0.3
BP420E280	-	20	80	-	1.0	11.95 ± 0.53	102.2 ±1.2	27.2 ± 0.6	0.3
(b) Combination of PEO 400 kD and EC-50									
BP480E520	-	80	-	20	1.0	11.79 ± 0.44	101.2 ± 3.2	29.8 ± 2.1	0.5
BP460E540	-	60	-	40	1.0	12.14 ± 0.29	101.2 ± 1.6	31.2 ± 1.2	0.5
BP440E560	-	40	-	60	1.0	12.54 ± 0.44	99.2 ± 1.2	23.9 ± 1.0	0.6
BP420E580	-	20	-	80	1.0	12.28 ± 0.48	98.0 ± 1.0	23.0 ± 1.0	0.5

PEO – Poly ethylene oxide (mol. wt: 100 kD and 400 kD), E2 and E5 represents Ethyl cellulose 22 cP and 50 cP respectively. Percentage of polymer refers to the % w/w calculated based on the polymer content in the ocular inserts out of total weight of ocular inserts, # mean of 20 ocular inserts from 3 batches; ¥ mean of 10 ocular inserts from 3 batches; * mean of 3 ocular inserts from 3 batches; Ψ based on 20 ocular inserts.

Table 6.2(c): Formulation composition and physicochemical properties of polymer combination (HPMC with Eudragits) based brimonidine tartrate ocular inserts.

Formulation code	Ingredients (in percentage)					Physicochemical parameters				
	HPMC K4M	HPMC K15M	HPMC K100M	ERS 100	ERL 100	BRT Content (mg)	Weight # (mg)	Assay ¥ (%)	Crushing strength/Hardness (N) *	Friability (%) Ψ
BH4-100	100	-	-	0	-	1.0	12.31 ± 0.10	99.9 ± 2.1	25.2 ± 2.2	0.5
BH480ERS20	80	-	-	20	-	1.0	11.59 ± 0.22	101.0 ± 0.9	23.5 ± 2.8	0.5
BH460ERS40	60	-	-	40	-	1.0	11.92 ± 0.24	100.3 ± 2.1	27.2 ± 1.1	0.6
BH440ERS60	40	-	-	60	-	1.0	12.26 ± 0.40	98.2 ± 1.8	28.0 ± 2.1	0.3
BH420ERS80	20	-	-	80	-	1.0	12.12 ± 0.23	101.2 ± 1.3	24.2 ± 1.8	0.7
BERS-100	0	-	-	100	-	1.0	12.34 ± 0.23	100.2 ± 2.2	29.2 ± 2.1	0.4
BH480ERL20	80	-	-	-	20	1.0	11.99 ± 0.23	99.3 ± 3.4	24.2 ± 2.1	0.5
BH460ERL40	60	-	-	-	40	1.0	12.23 ± 0.43	98.4 ± 1.3	29.9 ± 1.2	0.6
BH440ERL60	40	-	-	-	60	1.0	12.42 ± 0.44	100.2 ±3.4	25.2 ± 0.2	0.5
BH420ERL80	20	-	-	-	80	1.0	12.44 ± 0.29	99.3 ± 2.2	29.2 ± 1.0	0.3
BERL-100	0	-	-	-	100	1.0	12.24 ± 0.33	102.2 ± 1.2	24.2 ± 2.1	0.4
BH15-100	-	100	-	0	-	1.0	12.35 ± 0.24	94.8 ± 2.3	29.3 ± 2.0	0.6
BH1580ERS20	-	80	-	20	-	1.0	12.32 ± 0.41	100.6 ± 2.3	30.2 ± 1.6	0.3
BH1460ERS40	-	60	-	40	-	1.0	12.11 ± 0.23	99.3 ± 0.5	28.3 ± 1.8	0.3
BH1540ERS60	-	40	-	60	-	1.0	12.01 ± 0.51	98.0 ± 2.2	24.2 ± 2.1	0.3
BH1520ERS80	-	20	-	80	-	1.0	11.95 ± 0.53	102.2 ± 1.2	27.2 ± 0.6	0.3
BH1580ERL20	-	80	-	-	20	1.0	11.79 ± 0.44	101.2 ± 3.2	29.8 ± 2.1	0.5
BH1460ERL40	-	60	-	-	40	1.0	12.14 ± 0.29	101.2 ± 1.6	31.2 ± 1.2	0.5
BH1540ERL60	-	40	-	-	60	1.0	12.54 ± 0.44	99.2 ± 1.2	23.9± 1.0	0.6
BH1520ERL80	-	20	-	-	80	1.0	12.28 ± 0.48	98.0 ± 1.0	23.0 ± 1.0	0.5
BH10-100	-	-	100	0	-	1.0	12.35 ± 0.24	94.8 ± 2.3	29.3 ± 2.0	0.6
BH1080ERS20	-	-	80	20	-	1.0	12.32 ± 0.41	100.6 ± 2.3	30.2 ± 1.6	0.3
BH1060ERS40	-	-	60	40	-	1.0	12.11 ± 0.23	99.3 ± 0.5	28.3 ± 1.8	0.3
BH1040ERS60	-	-	40	60	-	1.0	12.01 ± 0.51	98.0 ± 2.2	24.2 ± 2.1	0.3
BH1020ERS80	-	-	20	80	-	1.0	11.95 ± 0.53	102.2 ± 1.2	27.2 ± 0.6	0.3
BH1080ERL20	-	-	80	-	20	1.0	11.79 ± 0.44	101.2 ± 3.2	29.8 ± 2.1	0,5
BH1060ERL40	-	-	60	-	40	1.0	12.14 ± 0.29	101.2 ± 1.6	31.2 ± 1.2	0.5
BH1040ERL60	-	-	40	-	60	1.0	12.54 ± 0.44	99.2 ± 1.2	23.9 ± 1.0	0.6
BH1020ERL80	-	-	20	-	80	1.0	12.28 ± 0.48	98.0 ± 1.0	23.0 ± 1.0	0.5

HPMC – hydroxypropylmethylcellulose (viscosity grades: K4M, K15M and K100M). ERL 100 - Eudragit RS 100, ERS 100- Eudragit RS 100Percentage of polymer refers to the % w/w calculated based on the polymer content in the ocular inserts out of total weight of ocular inserts, # mean of 20 ocular inserts from 3 batches; ¥ mean of 10 ocular inserts from 3 batches, * mean of 3 ocular inserts from 3 batches; Ψ based on 20 ocular inserts

Table 6.2(d): Formulation composition and physicochemical properties of polymer combination (HMPC with EC) based brimonidine tartrate ocular inserts

Formulation code	Ingredients (in percentage)					Physicochemical parameters				
	HPMC K4M	HPMC K15M	HPMC K100M	EC-22	EC-50	BRT Content (mg)	Weight # (mg)	Assay * (%)	Crushing strength/Hardness (N) *	Friability (%) Ψ
BH4-100	100	-	-	0	-	1.0	12.01 ± 0.12	98.9 ± 2.2	26.2 ± 2.2	0.6
BH480E220	80	-	-	20	-	1.0	11.20 ± 0.22	100.0 ± 0.9	24.5 ± 2.8	0.4
BH460E240	60	-	-	40	-	1.0	11.32 ± 0.24	101.2 ± 2.1	25.2 ± 1.1	0.3
BH440E260	40	-	-	60	-	1.0	12.16 ± 0.40	98.8 ± 1.8	27.0 ± 2.1	0.3
BH420E280	20	-	-	80	-	1.0	12.42 ± 0.23	102.2 ± 1.3	23.2 ± 1.8	0.7
BE2-100	0	-	-	100	-	1.0	12.34 ± 0.23	100.2 ± 2.2	24.2 ± 2.1	0.4
BH480E520	80	-	-	-	20	1.0	11.91 ± 0.23	99.4 ± 3.4	23.2 ± 2.1	0.5
BH460E540	60	-	-	-	40	1.0	11.23 ± 0.43	97.4 ± 1.3	28.9 ± 1.2	0.5
BH440E560	40	-	-	-	60	1.0	12.32 ± 0.44	101.2 ± 3.4	24.2 ± 0.2	0.5
BH420E580	20	-	-	-	80	1.0	12.14 ± 0.29	99.3 ± 2.2	23.2 ± 1.0	0.3
BE5-100	-	-	-	-	100	1.0	12.24 ± 0.33	102.2 ± 1.2	24.2 ± 2.1	0.4
BH15-100	-	100	-	0	-	1.0	11.35 ± 0.24	99.2 ± 2.3	27.3 ± 2.0	0.6
BH1580E220	-	80	-	20	-	1.0	11.32 ± 0.41	100.3 ± 2.3	32.2 ± 1.6	0.3
BH1460E240	-	60	-	40	-	1.0	12.31 ± 0.23	99.4 ± 0.5	28.3 ± 1.8	0.3
BH1540E260	-	40	-	60	-	1.0	12.21 ± 0.51	98.1± 2.2	24.2 ± 2.1	0.3
BH1520E280	-	20	-	80	-	1.0	11.85 ± 0.53	101.2 ± 1.2	27.2 ± 0.6	0.4
BH1580E520	-	80	-	-	20	1.0	11.99 ± 0.44	100.2 ± 3.2	29.8 ± 2.1	0.5
BH1460E540	-	60	-	-	40	1.0	11.14 ± 0.29	101.2 ± 1.6	31.2 ± 1.2	0.5
BH1540E560	-	40	-	-	60	1.0	12.34 ± 0.44	99.6 ± 1.2	22.9 ± 1.0	0.6
BH1520E580	-	20	-	-	80	1.0	12.24 ± 0.48	98.0 ± 1.0	23.0 ± 1.0	0.6
BH10-100	-	-	100	0	-	1.0	12.33 ± 0.24	97.8 ± 2.3	27.3 ± 2.0	0.6
BH1080E220	-	-	80	20	-	1.0	12.55 ± 0.41	101.6 ± 2.3	31.2 ± 1.6	0.2
BH1060E240	-	-	60	40	-	1.0	12.01 ± 0.23	99.5 ± 0.5	28.3 ± 1.8	0.3
BH1040E2S60	-	-	40	60	-	1.0	12.29 ± 0.51	98.2 ± 2.2	23.2 ± 2.1	0.3
BH1020E280	-	-	20	80	-	1.0	11.99 ± 0.53	102.4 ± 1.2	26.2 ± 0.6	0.3
BH1080E520	-	-	80	-	20	1.0	11.78 ± 0.44	100.8 ± 3.2	29.8 ± 2.1	0.5
BH1060E540	-	-	60	-	40	1.0	12.04 ± 0.29	101.9 ± 1.6	30.2 ± 1.2	0.5
BH1040E560	-	-	40	-	60	1.0	12.34 ± 0.44	99.8 ± 1.2	23.9 ± 1.0	0.6
BH1020E580	-	-	20	-	80	1.0	12.18 ± 0.48	98.5 ± 1.0	22.0 ± 1.0	0.5

HPMC – hydroxypropylmethylcellulose (viscosity grades: K4M, K15M and K100M). EC-22 and EC-50 ethyl cellulose, 100Percentage of polymer refers to the % w/w calculated based on the polym content in the ocular inserts out of total weight of ocular inserts, # mean of 20 ocular inserts from 3 batches; ¥ mean of 10 ocular inserts from 3 batches. * mean of 3 ocular inserts from 3 batches; Ψ based 20 ocular inserts

(ii) Friability studies

Friability of the formulated ocular inserts was determined for 20 ocular inserts using Roche's friabilator and falling shocks at 25 rpm, operated for 4 minutes. The weights were noted down before and after the experiment and the percent friability was calculated from the weights before and after the study.

The results of weight variation, drug content estimation, crushing strength/hardness and friability are presented in Table 6.1(a) & 6.1(b) for single polymer based ocular inserts and Table 6.2(a), 6.2(b), 6.2(c) & 6.2(d) for combination polymer based ocular inserts.

(iv) Mucoadhesive strength determination

Mucoadhesive strength of designed ocular inserts was determined based on in house modification of reported methods (Chandran, 2003). Mucoadhesive strength was determined by an experimental set up developed in-house using an accurate analytical balance. The left pan was replaced with Teflon block (6 cm x 6.2 mm) with a vertically down perpendicular extension of 2 cm x 1.5 cm. Goat mucosal tissue was obtained from a local slaughter house at Pilani, India. The lower block was tied with a mucosal membrane and was maintained in STF (pH 7.4) at 37° C ± 0.5° C. The ocular inserts for mucoadhesive strength measurements were attached to the lower surface of the upper block using glue. The ocular inserts were kept in contact with the mucosal membrane with some weight (40 g) on in for about 15 minutes. After 15 mins, weights were removed and the experiment was initiated. The water was added drop wise using a micropipette to the other side of the pan slowly until the ocular insert gets detached from the membrane. The rate of addition of water was kept constant for all the mucoadhesive strength determination study (about 3 minutes). The preliminary studies were performed to optimise the rate of addition of water, contact time of ocular inserts with the membrane before adding weights.

The mucoadhesion was calculated as the force in terms of weight required for the detachment, calculated as force per unit contact surface area of the ocular inserts, expressed in Newtons/cm^2.

(v) In vitro release studies

In vitro drug release studies were performed using modified USP type I (basket type) apparatus. Small glass cylinders of 50 ml capacity were fitted in place of dissolution media vessel. Weighed ocular inserts were placed in the containers, while maintaining the cylinder in dissolution apparatus containing 25 ml of STF (pH 7.4) at 37° C ± 0.5° C while the speed was maintained at 50 rpm. Samples were withdrawn at different intervals, diluted suitably

and analysed spectrophotometrically at 248nm. The percentage of drug released at each time interval was calculated as cumulative percent drug release.

The in vitro drug release data was analysed using Microsoft Excel 2003. In the case of polymer matrices that undergo swelling and subsequent erosion, Korsmeyer Peppas (KP model) (Peppas and Sahlin, 1989) is considered to be suitable, as there might be several processes like polymer chain relaxation, swelling and hence change in matrix geometry and subsequent erosion. All the above processes might ultimately results in altered matrix geometry. The KP model was applied to the release data up to 60% of the drug release.

The KP model is given by

$$M_t / M_\infty = K\, t^n$$

where 'K' is the release rate constant incorporating structural and geometric characteristics of the matrix, 'M_t' is the amount of drug released at time t and 'M_∞' is the amount of drug released at infinite time, 'n' is the release exponent indicative of release mechanism, as presented in Appendix-III.

The values of n, K and R^2 were used to determine the release rate mechanism and a best fit model. Based on the regression analysis of log % CDR vs. log time, data using Eq.6.1, the value of n, K and R^2 were determined and are presented in the Table 6.4, Table 6.5 and Table 6.6. Using n and K values, the $t_{10\%}$, $t_{50\%}$, and $t_{90\%}$ (time for 10%, 50% and 90% drug release respectively) were calculated. The results are presented in Table 6.3 (for hydrophilic polymer based ocular inserts), Table 6.4 (for inert/ zwitterionic and hydrophobic polymer based ocular inserts), Table 6.5 [combination of hydrophilic (PEO) and inert/zwitterionic (Eudragits) polymer based ocular inserts], Table 6.6 [combination of hydrophilic (PEO) with hydrophobic (EC) polymer based ocular inserts], Table 6.7 [combination of hydrophilic (HPMC) and inert/ zwitterionic (Eudragits) polymer based ocular inserts] and Table 6.8 [combination of hydrophilic (HPMC) and hydrophobic (EC) polymer based ocular inserts].

(vi) Erosion studies

In order to determine the exact mechanism of drug release and to investigate the role of matrix erosion on the drug release mechanism, erosion rate determination studies were carried out on ocular inserts formulations with single polymer systems. The method followed was as follows.

Weighed inserts (W_0) were placed in a closed plastic container with a mesh underneath in a medium of freshly prepared STF (pH 7.4) and equilibrated at 37° C ± 0.5° C in USP type I (basket type) apparatus at 100 rpm. At different time intervals, each container was taken out from the mesh. Excess of the media was blotted off and insert the weighed (W_1) on analytical balance (Metler Toledo, AG-135, GmbH, Switzerland).

The wet ocular inserts were then dried in an oven at 55° C till a constant weight was obtained (W_2). The experiment was performed in triplicates for each time point and fresh samples were used at each individual time points. The percentage erosion (ES) was calculated as

$$\% ES = W_0\text{-}W_2/W_0 * 100$$

The percent drug release was plotted against percent matrix erosion and the slope of the best fit line was considered to determine the role of erosion in drug release.

(vii) Batch reproducibility and stability studies

Two batches of each series of each of the formulation were prepared again separately and were evaluated as per the procedure mentioned above and the results were compared. Stability studies were carried out on the selected ocular inserts formulation according to ICH (International Conference on Harmonization) guidelines (ICH, 1996). A required quantity of ocular inserts were packed into small cellophane packets and were stored in a stability chambers (Thermo labs, Mumbai, India) maintained at ambient (25° C ± 2° C /60 ± 5% RH) and at ATC (40° C ± 2° C/75 ± 5% RH). Samples were withdrawn at 0, 1, 2, 3 and 6 month intervals and the physical parameters, drug content and in vitro release profile were evaluated.

6.4. RESULTS AND DISCUSSION

6.4.1. Physicochemical characteristics

The prepared formulations were slightly yellowish in color, flat surfaced, circular with 4 mm in diameter, thickness ranging from 0.3-0.6 mm. The thickness of ocular inserts prepared from single polymer system at 20% w/w polymer proportion was 0.3 mm while that with 100 % w/w polymer proportion was 0.6 mm. the weight varied with the amount of polymer in the system, from 3.2 ± 0.2 mg to 12 ± 0.5 mg. Drug content was found to be 1.0 ± 0.05 mg. The friability of designed formulations was within acceptable limits of NMT 1%. The

crushing strength of designed ocular inserts varied from 23 to 30 N [Table 6.1(a), and 6.1(b) and Table 6.2(a), 6.2(b), 6.2(c) and 6.2(d)].

6.4.2. Single polymer based ocular insert formulations

(i) Effect of hydrophilic polymer proportion (PEO)

The drug release from PEO matrices is elicited by instant water absorption into the matrix resulting in the formation of gel layer on the crystalline polymer. The water soluble drugs incorporated in the matrices, released primarily by diffusion after the drug dissolves in the hydrated polymer and diffuses out of the swollen matrix. Meanwhile with time, as erosion supersedes diffusion and gelled layer starts eroding, the polymer erosion is expected to play a major role in the drug release from the PEO matrices. The drug release kinetics after fitting the release data in P model in presented in Table 6.3.

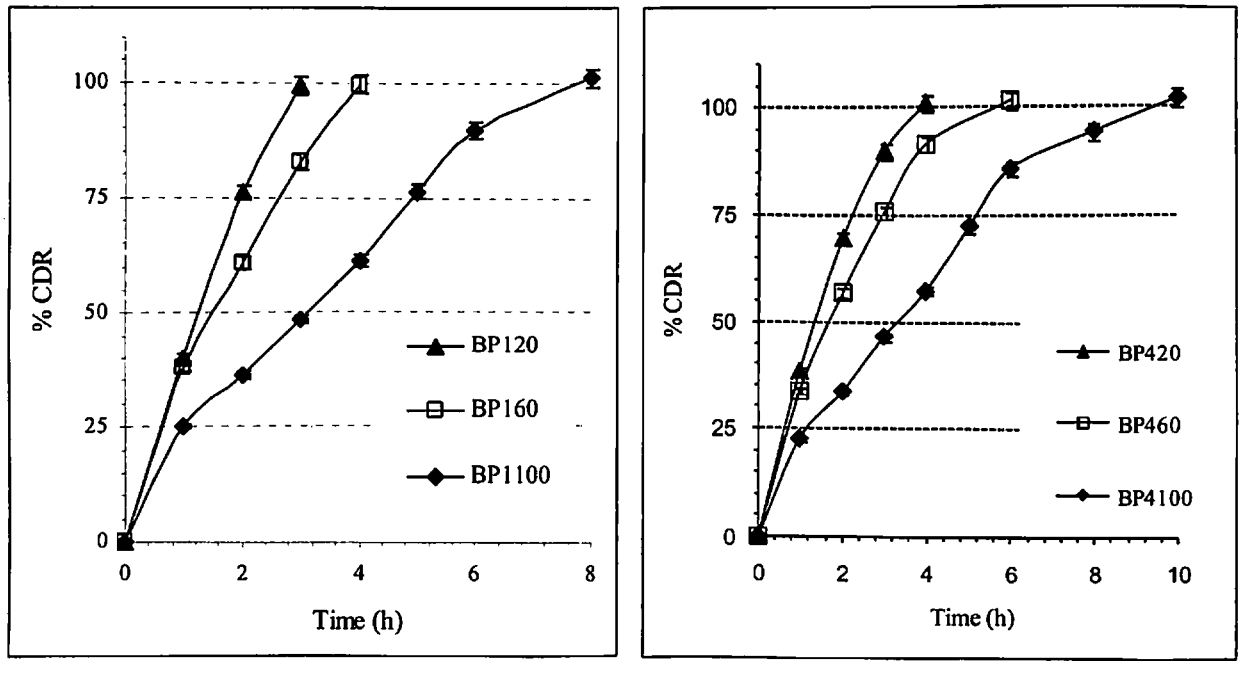

(a) (b)

Fig 6.2: In vitro drug release profile of PEO based brimonidine tartrate ocular insert formulations prepared with different proportion of (a) PEO 100 kD, (b) PEO 400 kD. Each data point represents the average of two batches in triplicate with standard deviation.

The drug release was found to be extended as the proportion of PEO 100 kD was increased in the ocular inserts matrix. The release rate, calculated using KP model, were found to be 0.48 $h^{-0.94}$, 0.46 $h^{-0.71}$ and 0.32 $h^{-0.71}$ for the formulations with 20 %, 60 % and 100 % w/w of PEO 100 kD respectively (Table 6.3). All the three formulations showed acceptable initial burst release with $t_{10\%}$ values of 0.2 to 0.3 h with the duration of the drug release prolonged with the increase in the percentage of PEO in the ocular inserts [Fig 6.2(a)]. The

corresponding $t_{90\%}$ values were obtained as 2.6, 3.4, 6.6 h respectively for 20 %, 60 % and 100 % w/w PEO 100 kD containing ocular inserts.

The rate of gel formation and surface erosion from the PEO matrix mainly depended on the molecular weight and hydrodynamics of the dissolution medium. In case of PEO 400 kD, the swelling and subsequent stronger gel formation together with slow erosion of the polymer contribute to more extended duration of release of the drug in comparison to that of PEO 100 kD [Fig 6.2(b)].

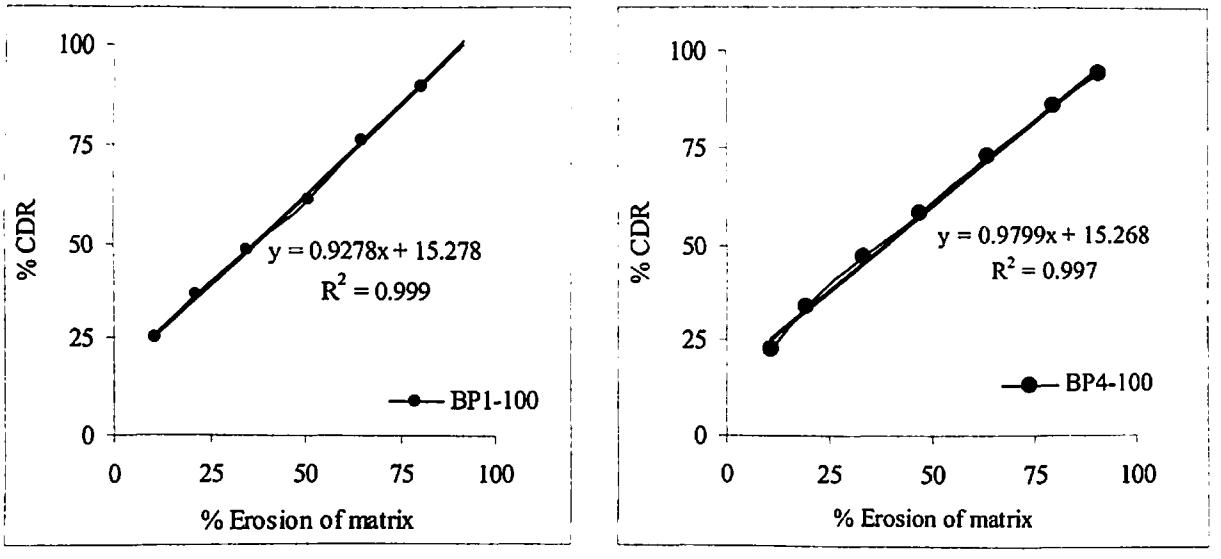

(a) (b)

Fig 6.3: Relationship between percent matrix erosion with percent drug released for PEO based brimonidine tartrate ocular insert formulations prepared with (a) PEO 100 kD and (b) PEO 400 kD at 100 % w/w proportion. Each data point represents the average of two batches in triplicate.

The release rate for the formulations prepared with PEO 400 kD alone were found to be 0.47 $h^{-0.81}$, 0.43 $h^{-0.70}$ and 0.29 $h^{-0.70}$ for 20 %, 60 %, 100 % w/w of PEO 400 kD respectively (Table 6.3). Acceptable initial release was observed in the case of ocular inserts prepared using PEO 400 kD alone, with $t_{10\%}$ values of 0.1, 0.2 and 0.3 h, while $t_{90\%}$, was found to be 3.1, 4.0 and 7.5 h respectively for 20 %, 60 % and 100 % w/w PEO 400 kD ocular inserts. The value of release exponent for both PEO 100 kD and PEO 400 kD based ocular inserts indicated non-Fickian anamolous drug transport. (Saettone et al, 1995; Di Colo et al, 2002; Di Colo et al, 2001). The drug release was expected to be governed by a combination of diffusion and polymer erosion. To further establish the mechanism of drug release, the percent released was plotted against percent erosion of matrix for formulations prepared using 100 % w/w of PEO 100 kD and PEO 400 kD alone. The results are depicted in the Fig

6.3(a) for BP1-100 (100 % w/w PEO 100 kD) and in Fig 6.6(b) for BP4-100 (100 % w/w of PEO 400 kD). In both the cases, the percent drug release was found to correlated with very high goodness of fit (slope value approaching unity) with percent erosion of matrix indicating that the drug release is predominately governed by erosion process (Pongjanyakul et al, 2007).

The drug release kinetics for the formulations, after fitting the in vitro release data into suitable models is shown in the Table 6.3.

(ii) Effect of hydrophilic swellable polymer (HPMC)

The various ocular inserts were prepared by varying the proportions of HPMC at three different levels, 100 % w/w, 60 % w/w and 20 % w/w of the ocular inserts matrix using three viscosity grades of HPMC, namely HPMC K4M, HPMC K15M and HPMC K100M. The result of in vitro drug release profile for HPMC based ocular inserts is shown in the Fig 6.4(a), 6.4(b) and 6.4(c).

HPMC undergoes rapid hydration and subsequent swelling upon contact with aqueous media, forming a diffusional barrier around the matrix in which it is incorporated. The drug incorporated in the matrix should, therefore has to dissolve in the solvent penetrated and pass through the diffusional layer.

In the case of ocular inserts formulations with HPMC K4M, at 20 % w/w level, the drug release was much faster ($t_{10\%}$ of 0.2 h and $t_{90\%}$ of 3.2 h) with a drug release rate of 0.45 $h^{-0.76}$. As the HPMC proportion was increased to 60 % w/w (BH1-60), the release was retarded compared with $t_{10\%}$ and $t_{90\%}$ were observed to be 0.2 h and 3.7 h respectively and the release rate was found to be 0.38 $h^{-0.88.}$ Further increase of HPMC K4M proportion to 100 % w/w resulted in extension of drug release up to 6 h, with a release rate of 0.29 $h^{-0.88}$ and the $t_{10\%}$ and $t_{90\%}$ were found to be 0.2 h and 5.1 h respectively. Similar results were observed in the case of ocular inserts formulations with HPMC K15M and HPMC K100M. As shown in the Table 6.3, the drug release rate decreases with increase in HPMC level (20 % w/w, 60 %w/w and 100 % w/w).

The drug release rate for formulations with HPMC K15M at 20 % w/w, 60 %w/w and 100 % w/w levels were found to be 0.41 $h^{-0.80}$, 0.37 $h^{-0.81}$ and 0.27 $h^{-0.81}$ respectively. The drug release was comparatively more retarded than that of ocular inserts formulations with HPMC K4M, with $t_{90\%}$ of 3.5 h, 4.8 and 6.3 h for the formulations with 20 % w/w, 60 % w/w and 100 % w/w of polymer proportion.

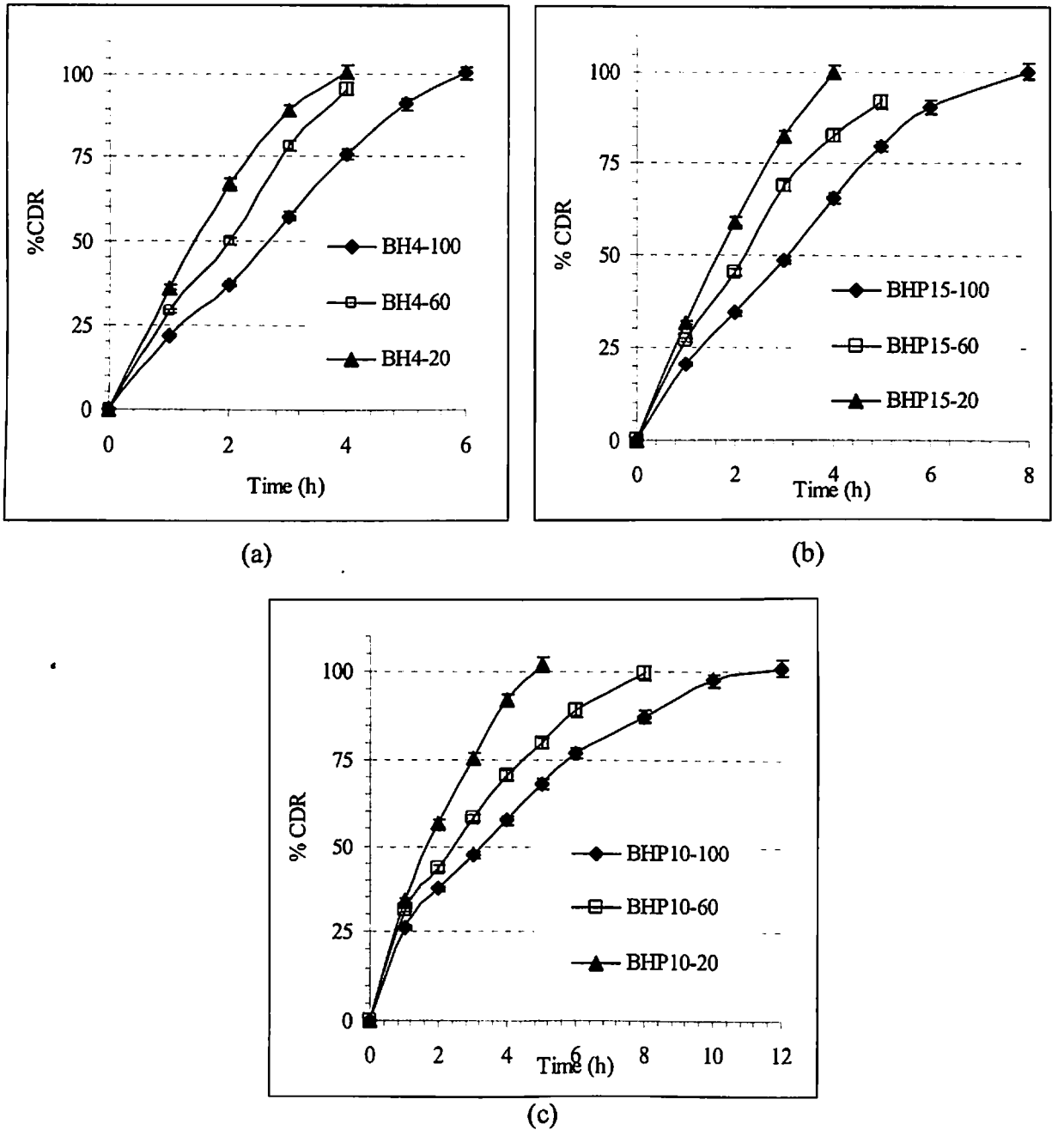

Fig 6.4: In vitro drug release profile of HPMC based brimonidine tartrate ocular insert formulations prepared with different proportion of (a) HPMC K4M, (b) HMPC K15M and (c) HPMC K100M. Each data point represents the average of two batches in triplicate with standard deviation.

In the case of ocular inserts formulations with HPMC K100M, the release rate was further decreased, the release rate constants were found to be 0.42 $h^{-0.70}$, 0.33 $h^{-0.71}$ and 0.27 $h^{-0.70}$ respectively for formulations with 20 % w/w, 60 %/w and 100 % w/w polymer proportions. The corresponding $t_{90\%}$ values for the formulations were found to be 4.0, 6.3 and 8.7 h respectively. The higher retardation of drug release at higher viscosity grades of HPMC was due to the formation of more profused diffusional layer of increased thickness and viscosity. The good initial release was due to release of surface bound drug, which dissolved

immediately upon contact with the dissolution fluid. But it was observed that in comparison to two lower viscosity grades (HPMC K4M and HPMC K15M), there was no significant difference in the drug release profile in terms of prolongation of drug release profiles for HPMC K100M. This could be due to the existence of 'limiting HPMC viscosity' beyond which no further significant retardation of drug release was observed.

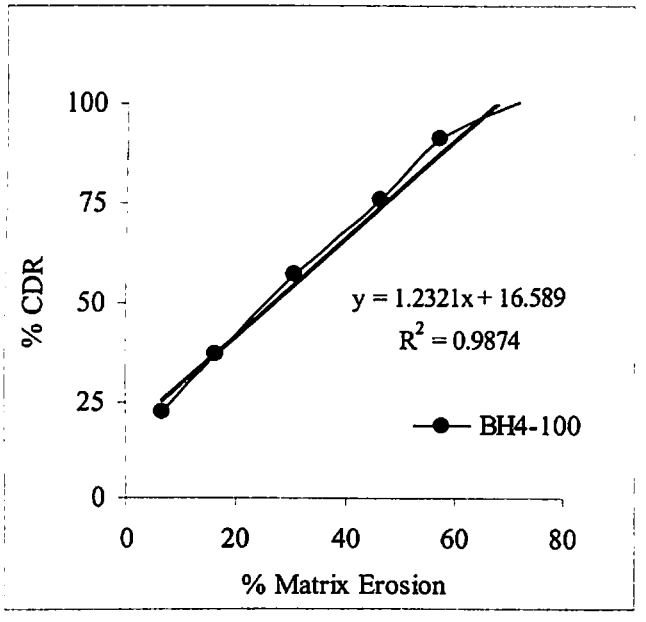

(a)

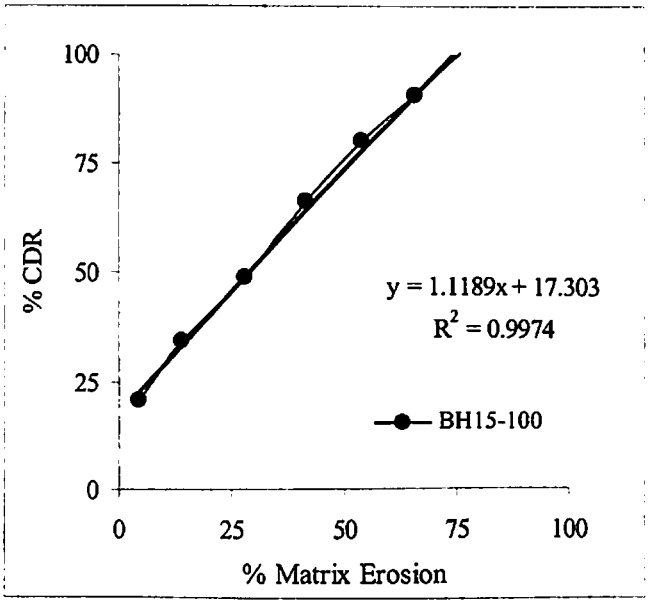

(b)

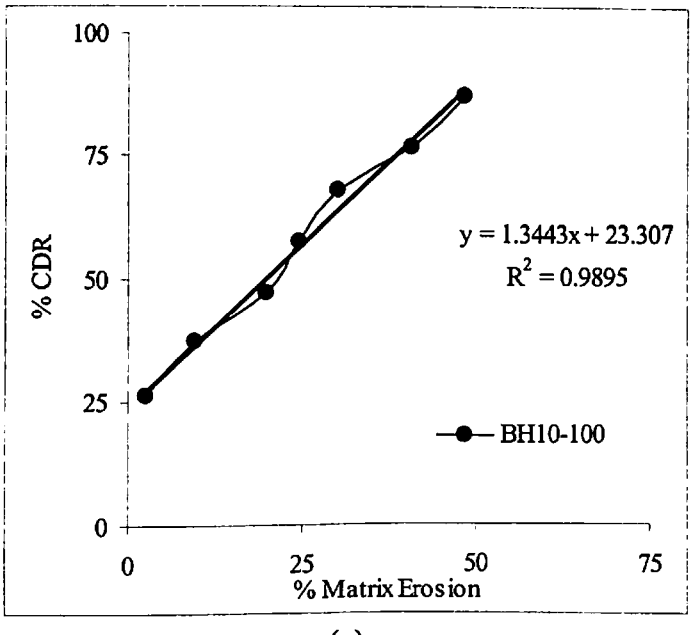

(c)

Fig 6.5: Relationship between percent matrix erosion with percent drug released for HPMC based brimonidine tartrate ocular insert formulations prepared with (a) HPMC K4M, (b) HMPC K15M and (c) HPMC K100M at 100 w/w proportion. Each data point represents the average of two batches in triplicate.

When the drug release data was fitted into KP model, the mechanism of drug release was found to be non-Fickian anamolous transport in all the three formulations of three viscosity grade HPMC in all the formulations (Table 6.3). The 'n' values ranged from 0.7 to 0.8 indicating drug release is based on combination of diffusion, swelling and erosion. To further confirm this, the percent drug released was plotted against percent matrix erosion for all the three formulations at 100 % w/w polymer proportion levels.

From the Fig 6.5 (a), (b) and (c), it is evident that a very high goodness of fit (slope value of best fit was just above unity) suggesting that the drug release was well correlated, but higher than percent matrix erosion. Hence it can be suggested that the erosion along with diffusion played a role in the release of drug.

(iii) Effect of inert/ zwitterionic polymer proportion (Eudragit RL 100 & RS 100)

Eudagits are methacrylic and methyl methacrylate copolymers which are known to form a hard, compact and non-erodible matrix. Since ERL 100 and ERS 100 exist in salt form (with low content of quaternary ammonium groups), they exhibit a pH independent permeability and release of incorporated drugs. In case of BRT ocular inserts formulated using ERS 100 and ERL 100 as the release retardant matrix base, the drug release was extended beyond 24 h. However the formulations prepared with ERL 100 showed comparatively faster rate of release as they are more permeable to water than ERS 100, thereby facilitating better penetration of dissolution media.

As shown in the release profiles Fig 6.6(a) and (b), the release rate constants, were found to be 0.34 $h^{-0.54}$, 0.27 $h^{-0.58}$, 0.14 $h^{-0.57}$ for the formulations with 20 %, 60 % and 100 % w/w of ERL 100 proportion and 0.33 $h^{-0.50}$, 0.29 $h^{-0.52}$ and 0.17 $h^{-0.52}$ for the formulations with 20 %, 60 % and 100 % w/w of ERS 100 (Table 6.4).

The initial release as indicated by $t_{10\%}$ value, varied from 0.2 h to 0.5 h (in case of ERL 100) and from 0.2 h to 0.4 h (in case of ERS 100). The duration of release ($t_{90\%}$) value varied from 9.9 h (20 % w/w) to 25.6 h (100 % w/w) for ERL 100 ocular inserts and from 10.3 h (20 % w/w) to 27.1 h (100 % w/w) for ERS 100 ocular inserts. The release exponent (n) was found to indicate non-Fickian anamolous drug transport (Table 6.4).

Table 6.3: Results of drug release kinetics studies for hydrophilic polymers (PEO 400 kD, PEO 400 kD, HPMC K4M, HPMC K15M, and HPMC K100M) based brimonidine tartrate ocular insert formulations fitted into Korsmeyer-Peppas model.

Batch code	KP model			$t_{10\%}$ (h)	$t_{50\%}$ (h)	$t_{90\%}$ (h)
	K (h^{-n})	$R^{2\,¥}$	n #			
BP1-100	0.32	0.9833	0.71	0.3	2.9	6.6
BP1-60	0.46	0.9933	0.71	0.2	1.5	3.4
BP1-20	0.48	0.9822	0.94	0.2	1.3	2.6
BP4-100	0.29	0.9868	0.70	0.3	3.2	7.5
BP4-60	0.43	0.9950	0.70	0.2	1.8	4.0
BP4-20	0.47	0.9814	0.81	0.1	1.4	3.1
BH4-100	0.29	0.9908	0.88	0.2	2.6	5.1
BH4-60	0.38	0.9892	0.88	0.2	1.9	3.7
BH4-20	0.45	0.9852	0.76	0.2	1.5	3.2
BH15-100	0.27	0.9932	0.81	0.2	3.0	6.3
BH15-60	0.37	0.9931	0.81	0.2	2.7	4.8
BH15-20	0.41	0.9725	0.80	0.1	1.7	3.5
BH10-100	0.27	0.9908	0.70	0.2	3.2	8.7
BH10-60	0.33	0.9892	0.71	0.2	3.0	6.3
BH10-20	0.42	0.9852	0.70	0.2	1.8	4.0

K- release rate constant (h^{-n}), R^2- regression coefficient, n- release exponent indicator of drug release mechanism, $t_{10\%}$, $t_{50\%}$, $t_{90\%}$- time taken (in h) for 10, 50 and 90 % drug release respectively.

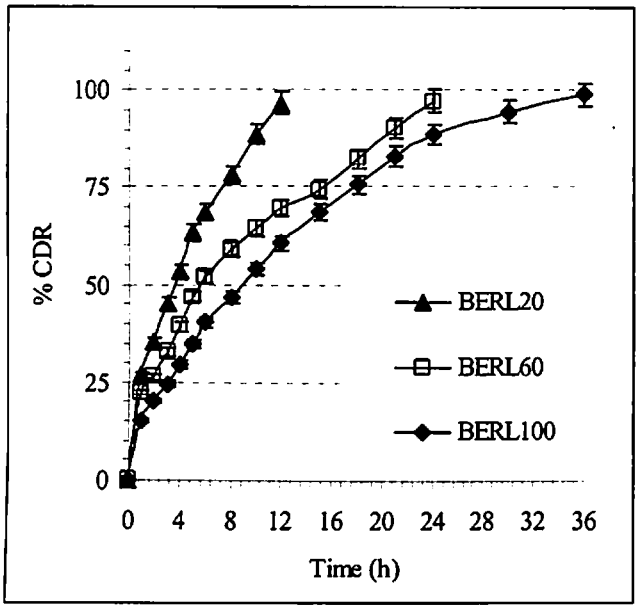

(a)

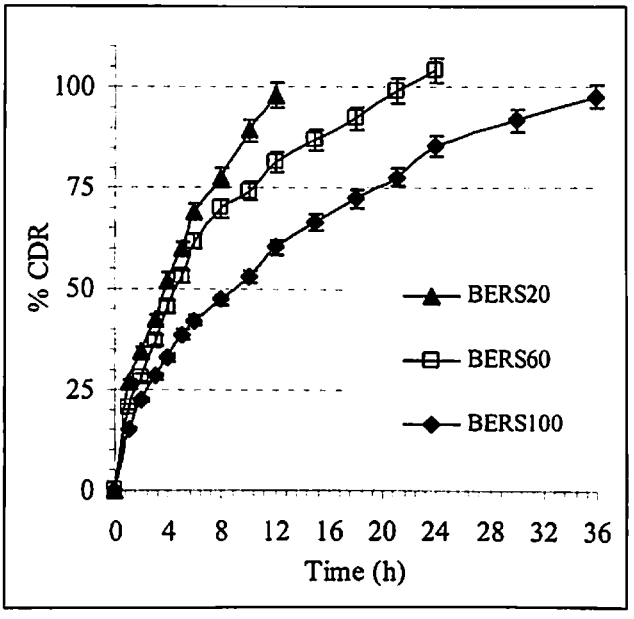

(b)

Fig 6.6: In vitro drug release profiles of Eudragit based brimonidine tartrate ocular insert formulations prepared with different proportions of (a) ERL 100, (b) ERS 100. Each data point represents the average of two batches in triplicate with standard deviation.

The relationship between percent drug released vs. percent erosion of the matrix showed that in case of 100 %`w/w of polymer for both ERL 100 [Fig 6.7(a)] and ERS 100 [Fig 6.7(b)], showed a considerably high percent drug release in comparison to percent erosion of matrix with the slope value of the best fit curve was found to be more than 2.0 in both the cases, thus suggested that the drug release to occur predominately by diffusion than erosion.

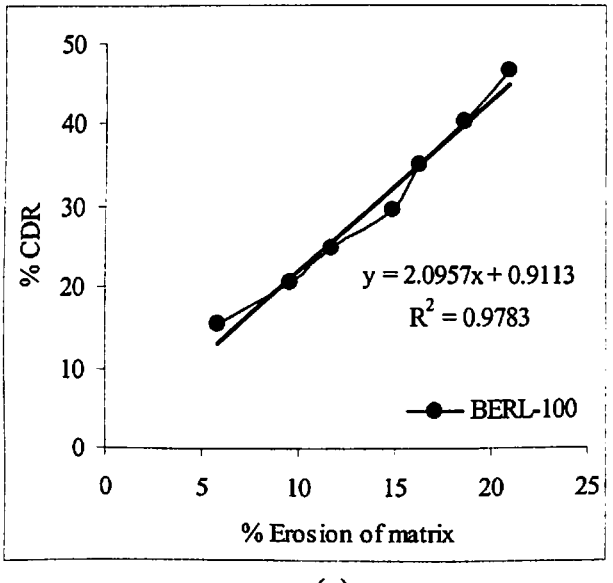

(a)

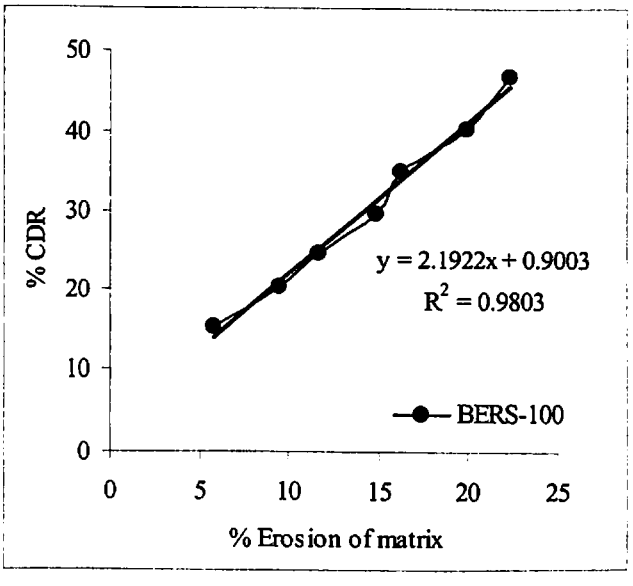

(b)

Fig 6.7: Relationship between percent matrix erosion with percent drug released for Eudragit based brimonidine tartrate ocular inert formulations prepared with (a) ERL 100 and (b) ERS 100 at 100 w/w proportion. Each data point represents the average of two batches in triplicate with standard deviation.

(iv) Effect of hydrophobic polymer proportion (Ethyl cellulose)

Ethyl cellulose, an inert, hydrophobic polymer was investigated as matrix former at three different levels (20 %, 60 % and 100 % w/w) to investigate the effect of polymer proportion on the drug release, erosion pattern and mucoadhesive strength. The drug release from EC matrix was more extended and release rate was much slower compared to HPMC matrix [Fig 6.8(a) and (b)].

In the ocular inserts formulations with 20 % w/w of EC-22, the drug release rate was 0.34 $h^{-0.56}$, while for 60 % w/w and 100 % w/w levels it was 0.29 $h^{-0.51}$ and 0.20 $h^{-0.55}$ respectively. The drug release was much delayed with $t_{90\%}$ of 9.7 h, 16.4 h and 21.2 h for 20 % w/w, 60 % w/w and 100 % w/w levels of EC-22 in the formulations.

Similar trend was also noticed in the case of formulations with EC-50 based ocular inserts formulations. The drug release was much more extended and delayed with $t_{90\%}$ of 12.4 h, 22.6 h and 31.2 h respectively for formulations with EC-50 at 20 % w/w, 60 % w/w and 100 % w/w levels.

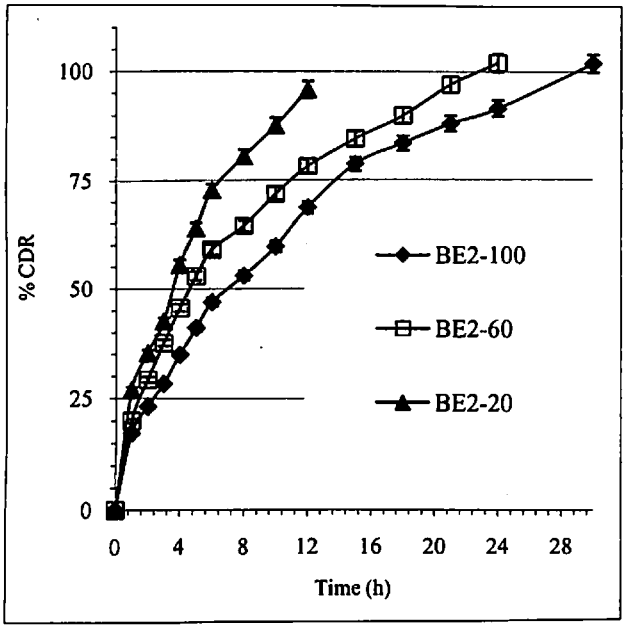

(a)

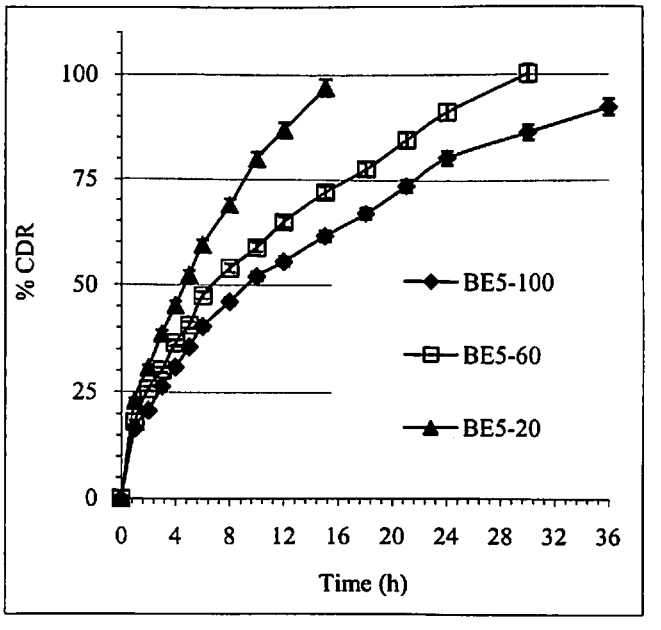

(b)

Fig 6.8: In vitro drug release profile of EC based brimonidine tartrate ocular insert formulations prepared with different proportions of (a) EC-22 and (b) EC-50. Each data point represents the average of two batches in triplicate with standard deviation.

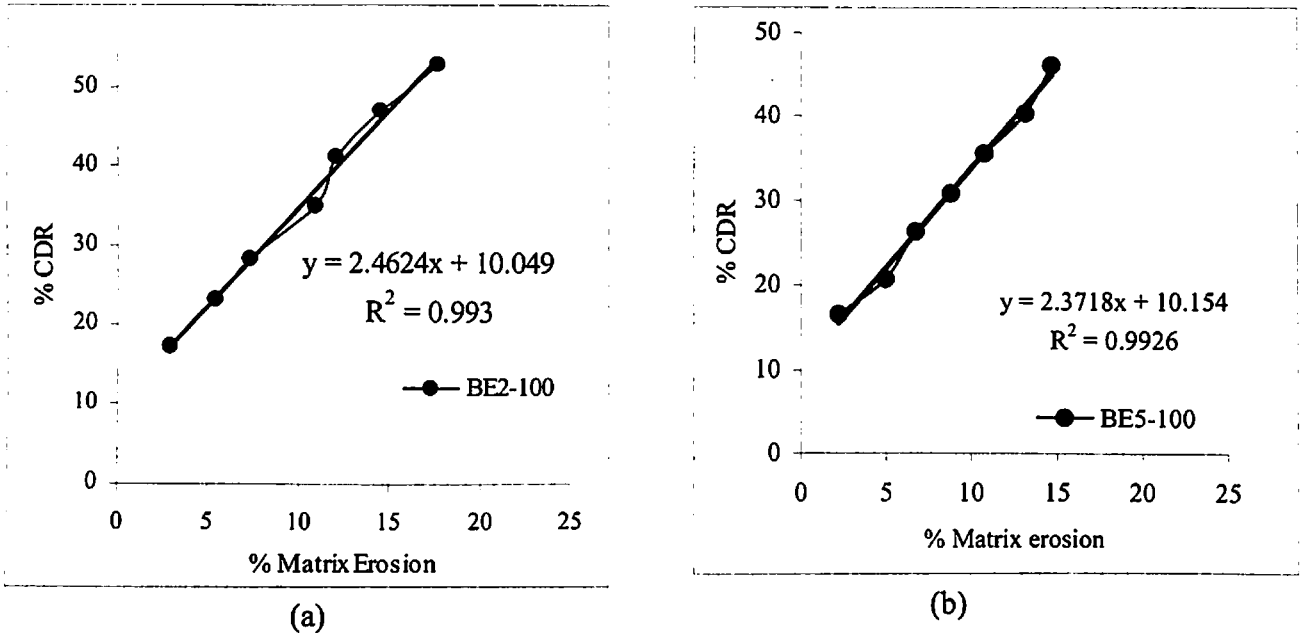

Fig 6.9: Relationship between percent matrix erosion with percent drug released for EC based brimonidine tartrate ocular insert formulations prepared with (a) EC-22 and (b) EC-50 at 100 % w/w proportion. Each data point represents the average of two batches in triplicate.

The drug release was found to be by Fickian diffusion mechanism with release exponent was approximately of 0.5. Since EC forms a compact non erodible and non swellable matrix, the drug release was bound to be diffusion based mechanism. A plot of percent drug released vs. percent matrix erosion [Fig.6.9 (a) and (b)] showed that the drug release was much faster than the percent erosion of the matrix. Slope of best fit line suggested that the drug release was predominately by diffusion mechanism rather than by erosion of the matrix.

6.4.3. Ocular inserts with combination of polymers

(i) Effect of combination of hydrophilic and hydrophobic zwitterionic polymers

(a) Combination of PEO 100 kD with Eudragit

The drug release from BRT ocular inserts designed using combination of PEO 100 kD and ERL 100 or ERS 100 was found to vary depending upon the relative proportion of PEO and Eudragit in the matrix. The results of in vitro release studies performed on the formulations with varying proportions of PEO 100 kD and ERL 100 is shown in the Fig 6.10. As the relative proportion of ERL 100 was decreased in the matrix from 100 % w/w to 0 with the corresponding increase in PEO 100 kD proportion, the rate of release was found to be increased.

Table 6.4: Results of drug release kinetics studies for inert/ zwitterionic (ERL 100 and ERS 100) and hydrophobic polymers (EC-22 and EC-50) based brimonidine tartrate ocular insert formulations fitted into Korsmeyer- Peppas model.

Batch code	KP model			$t_{10\%}$ (h)	$t_{50\%}$ (h)	$t_{90\%}$ (h)
	K (h^{-n})	$R^{2\ ¥}$	n #			
BERL-100	0.14	0.9825	0.57	0.5	9.1	25.6
BERL-60	0.27	0.9708	0.58	0.2	6.1	20.4
BERL-20	0.34	0.9892	0.54	0.2	3.4	9.9
BERS-100	0.17	0.9768	0.52	0.4	8.9	27.1
BERS-60	0.29	0.9938	0.52	0.2	6.3	19.2
BERS-20	0.33	0.9841	0.50	0.2	3.5	10.3
BE2-100	0.20	0.9932	0.55	0.4	7.3	21.2
BE2-60	0.29	0.9931	0.51	0.2	5.1	16.4
BE2-20	0.34	0.9825	0.56	0.2	3.4	9.7
BE5-100	0.18	0.9908	0.67	0.4	9.8	31.2
BE5-60	0.23	0.9892	0.64	0.3	7.2	22.6
BE5-20	0.29	0.9852	0.61	0.3	4.4	12.4

K- release rate constant (h^{-n}), R^2- regression coefficient, n- release exponent indicate the mechanism of drug release, $t_{10\%}$, $t_{50\%}$ and $t_{90\%}$- time taken (in h) for 10, 50 and 90 % drug release respectively.

In case of formulations containing 100 % w/w of PEO 100 kD and no ERL 100 (BP1-100), the BRT release was found to be extended for 6 h ($t_{10\%}$ of 0.3 h and $t_{90\%}$ of 6.6 h) as shown in Fig 6.10 and the release rate was found to be 0.32 $h^{-0.71}$ with 'n' value of 0.71. Various combinations of PEO 100 kD and ERL 100 were investigated in order to optimise formulations, such that the drug release is prolonged up to 24 h and at the same time sufficient mucoadhesive strength was retained. It was expected that the relative proportion of PEO in the ocular inserts matrix will have a major contribution to the mucoadhesive strength.

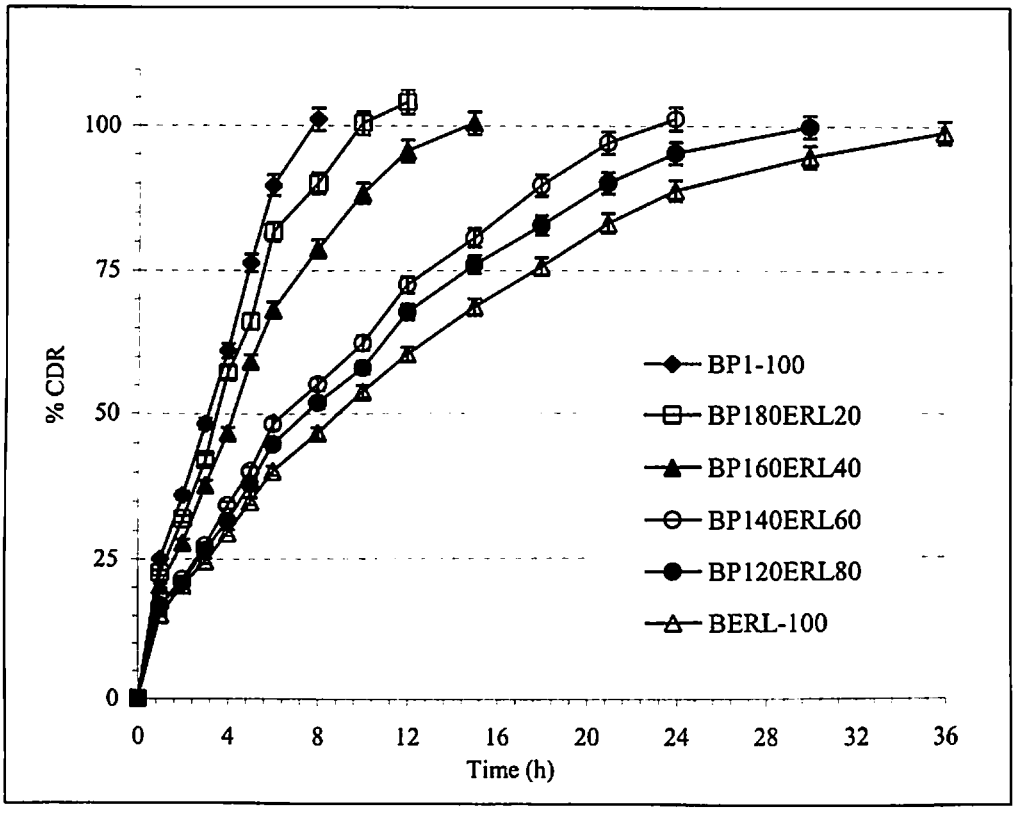

Fig 6.10: In vitro drug release profile of polymer combination (PEO 100 kD and ERL 100) based brimonidine tartrate ocular insert formulations. Each data point represents the average of two batches in triplicate with standard deviation.

When the PEO 100 kD proportion in the matrix was decreased with corresponding increase in ERL 100 proportion, $t_{90\%}$ value was found to increase (Table 6.5). A drastic increase in $t_{90\%}$ (13.5 h) and a substantial decrease in release constant (0.17 $h^{-0.61}$) were observed with duration of drug release extended in case of formulations prepared using PEO 100 kD - 40 % w/w and ERL 100 at 60 % w/w level. A further increase in relative proportion of ERL 100 up to 100 % w/w, the rate of release was found to decrease further with duration of release extending beyond 36 h. The drug release kinetic data (presented in the Table 6.5) showed that the drug release was by non-Fickian anamolous transport mechanism. Similar observation was seen in case of formulations with combination of PEO 100 kD and ERS 100 as shown in Fig 6.11.

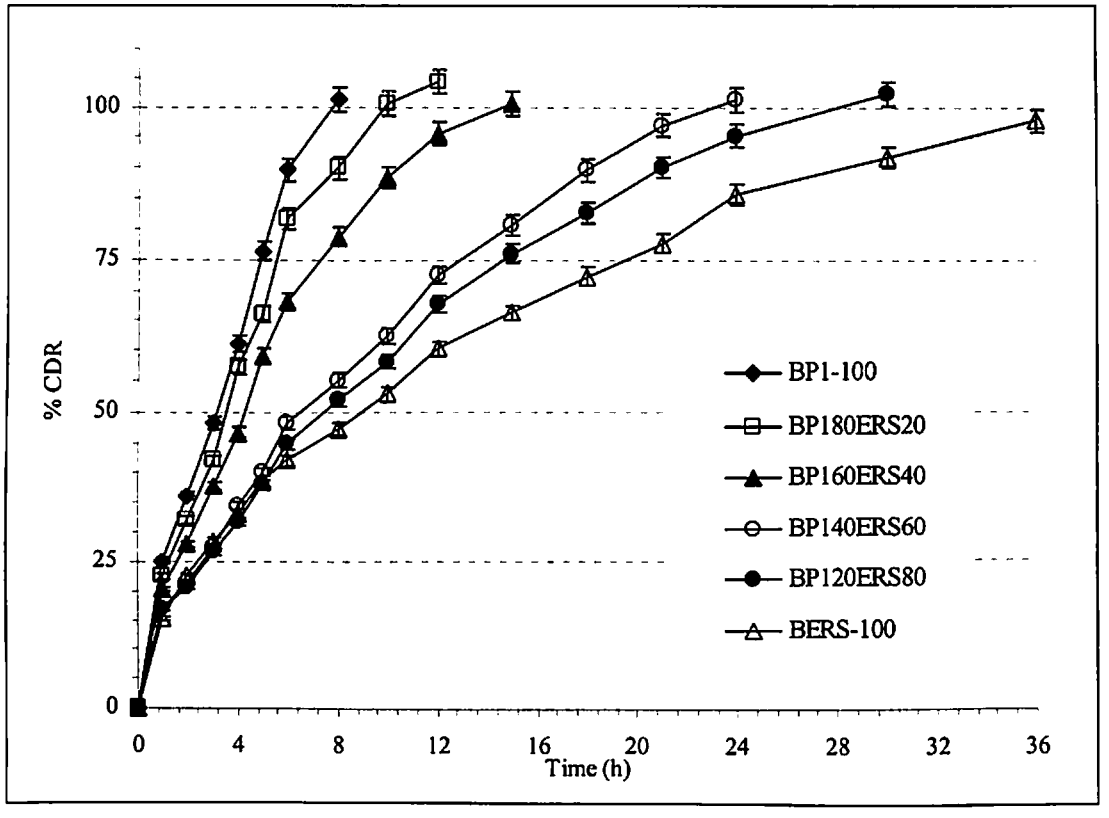

Fig 6.11: In vitro drug release profile of polymer combination (PEO 100 kD and ERS 100) based brimonidine tartrate ocular insert formulations. Each data point represents the average of two batches in triplicate with standard deviation

Both ERL 100 and ERS 100, because they exist as salts, therefore the drug release from their matrices are pH independent and very slow. In case of ERL 100, the poly (ethyl acrylate, methyl methacrylate, trimethylammonioethyl methacrylate chloride) ratio is 1 : 2 : 0.2, while ERS 100 has a poly(ethyl acrylate, methyl methacrylate, trimethyl ammonioethyl methacrylate chloride) ratio of 1 : 2 : 0.1 . The presence of trimethyl ammonio group in the salt form renders these polymers as inert or neutral in nature with pH independent fluid penetration and hence pH independent release of drug from the matrices of these polymers.

As the proportion of Eudragits increase in the formulation, the matrix tends to become harder, the drug release was found to be predominately governed by diffusion. At a lower proportion of ERL 100 and higher proportion of PEO 100 kD, a relatively higher release was observed, this could be due to the hydrophilic nature of the PEO and also due to relative decrease in the hydrophobicity of the matrix with erosion as the primary mechanism of drug release.

(b) Combination of PEO 400 kD with Eudragit

The drug release from PEO 400 kD and ERL 100 based ocular inserts formulations depends on the relative proportion of both the polymers in the matrix (Fig 6.12 and 6.13). Formulation containing 100 % w/w of PEO 400 kD released the drug for 10 h ($t_{10\%}$ of 0.2 h and $t_{90\%}$ of 7.1 h) (Table 6.5). The release rate was found to be 0.36 $h^{-0.61}$ and the releases exponent was 0.6. Different combination of PEO 400 kD and ERL 100 were investigated by varying the relative percentage of polymers. When the percentage of PEO 400 kD was decreased to 80 % w/w and ERL 100 percentage was increased to 20 % w/w, the release rate was decreased significantly (0.32 $h^{-0.62}$) and the duration of BRT release was extended to 12 h ($t_{10\%}$ of 0.24 h and $t_{90\%}$ of 8.4 h) (Table 6.5). Further decrease in PEO 400 kD and proportional increase in the percentage of ERL 100 resulted in drastic decrease in the release rate and increase in the duration of drug release.

The acceptable amount of initial drug release in case of all the formulations could be due to release of surface bound drug as well as increased porosity of the matrix due to the dissolution of hydrophilic polymer and the formation of micropores on the surface of the matrix, which also contributed for the release of drug in the later periods (Tatavarti et al, 2004).

In case of formulations with PEO 400 kD and ERS 100, when the proportion of PEO 400 kD was decreased to 80% and ERL proportion increased to 20 % (BP480ERS20), the K decreased to 0.32 $h^{-0.60}$, $t_{10\%}$ was to 0.2 h and $t_{90\%}$ increased to 8.9 h. The formulation BP460ERS40 showed a controlled release of drug with a K value of 0.28 $h^{-0.55}$, $t_{90\%}$ of 13.3 h and $t_{10\%}$ of 0.3 h. This is due to decrease in the proportion of PEO 400 kD and increase in the proportion of ERS. When the PEO 400 kD proportion was further decreased to 20 % with a increase in ERL proportion to 80%,(BP420ERS80), the K decreased to 0.2 $h^{-0.5}$, $t_{10\%}$ increased to 0.4 h and $t_{90\%}$ increased to 26 h.

Similar effects were observed in case of formulations in combination of PEO 400 kD and ERS 100. The release rate constant gradually decreased and $t_{10\%}$ and $t_{90\%}$ were increased as the proportion of PEO 400 kD was decreased and ERS was increased. The ocular insert formulation with 100 % w/w of ERL 100 retarded the release for beyond 24 h. In all the above formulations, the drug release was found to be dependent on the proportion of ERS 100 or ERL 100 in the matrix.

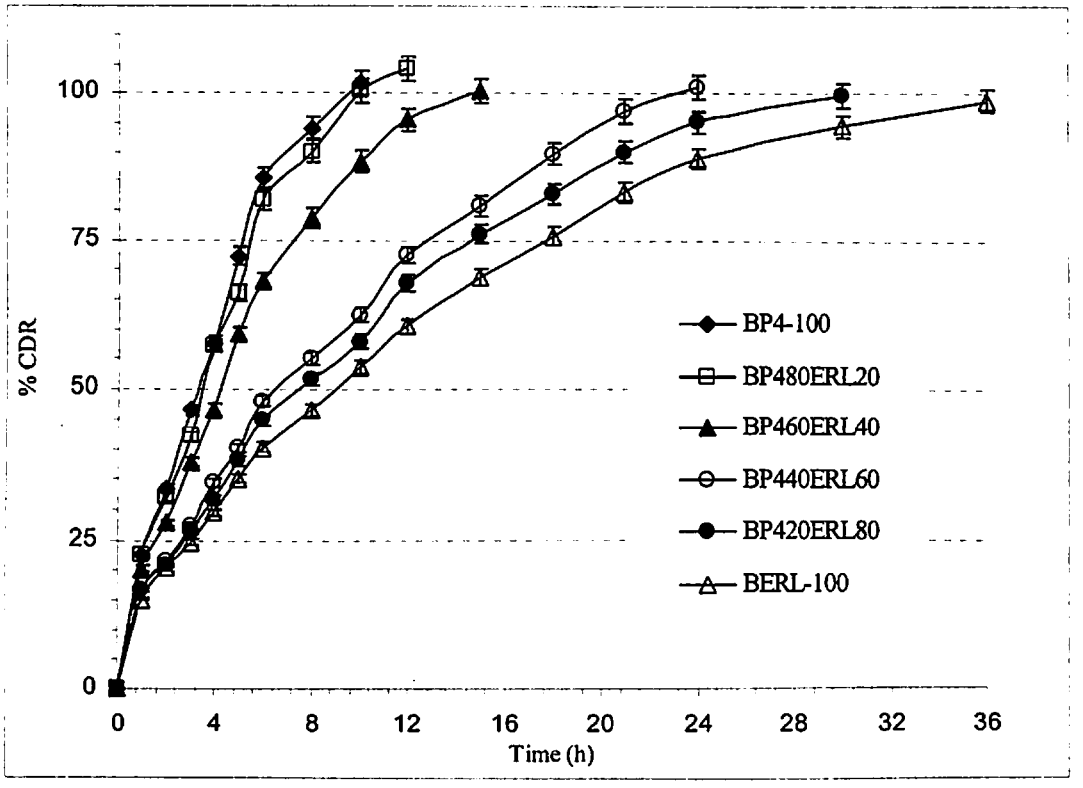

Fig 6.12: In vitro drug release profile of polymer combination (PEO 400 kD and ERL 100) based brimonidine tartrate ocular insert formulations. Each data point represents the average of two batches in triplicate with standard deviation.

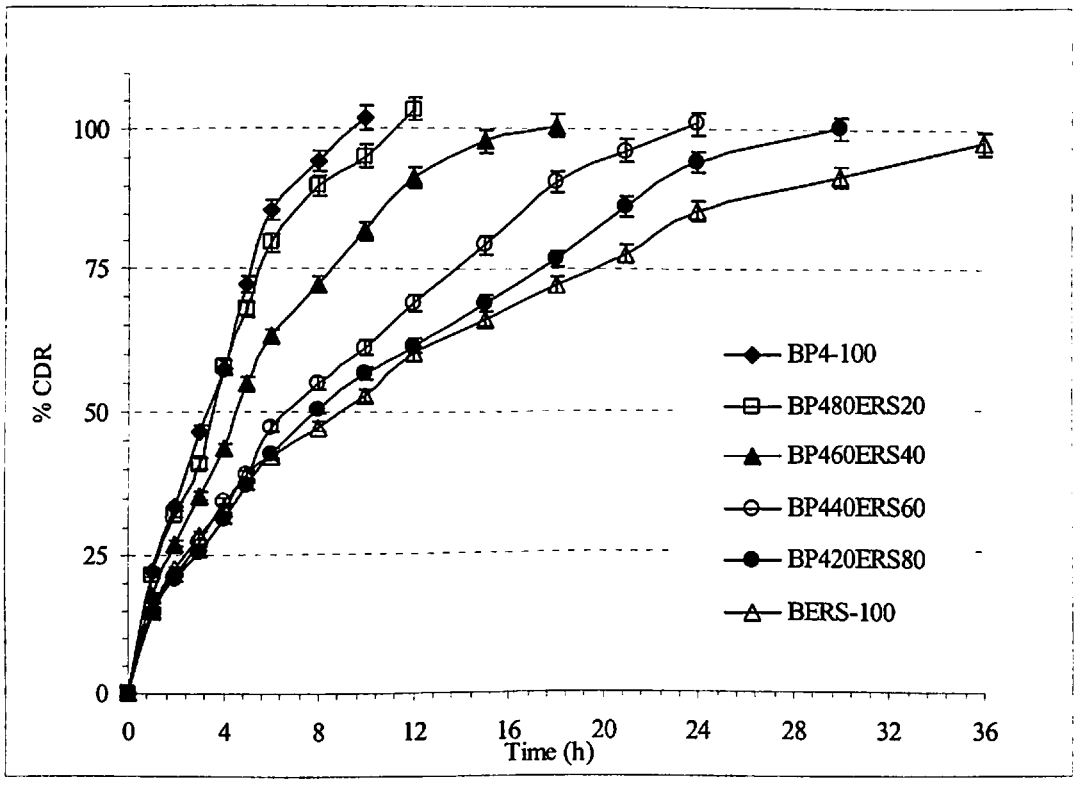

Fig 6.13: In vitro drug release profile of polymer combination (PEO 400 kD and ERS 100) based brimonidine tartrate ocular inserts formulations. Each data point represents the average of two batches in triplicate with standard deviation.

As the proportion of PEO was decreased and Eudragit proportion was increased, the release mechanism slowly shifted towards diffusion controlled. This may be due to the decreased swelling and decreased erosion of the matrix in the presence of Eudragits. The drug release kinetics data upon fitting to Korsmeyer-Peppas model has been shown in Table 6.5.

Table 6.5: Results of drug release kinetics studies for polymer combination [hydrophilic polymers (PEO 400 kD, PEO 400 kD) with inert/zwitterionic polymers (ERL 100 and ERS 100)] based brimonidine tartrate ocular inserts fitted into Korsmeyer-Peppas model.

Batch code	KP model			$t_{10\%}$ (h)	$t_{50\%}$ (h)	$t_{90\%}$ (h)
	K (h^{-n})	$R^{2\,¥}$	n #			
BP1-100	0.32	0.9725	0.71	0.3	2.9	6.6
BP180ERL20	0.29	0.9908	0.67	0.3	3.4	8.4
BP160ERL40	0.26	0.9892	0.64	0.3	4.3	10.5
BP140ERL60	0.17	0.9852	0.61	0.5	7.1	13.5
BP120ERL80	0.16	0.9932	0.61	0.5	7.3	19.4
BERL-100	0.14	0.9825	0.58	0.5	9.0	25.6
BP180ERS20	0.28	0.9918	0.67	0.3	3.5	8.4
BP160ERS40	0.26	0.9892	0.64	0.3	4.3	10.7
BP140ERS60	0.22	0.9768	0.63	0.4	5.4	13.7
BP120ERS80	0.16	0.9938	0.61	0.5	7.3	19.2
BERS-100	0.17	0.9768	0.52	0.4	8.9	27.1
BP4-100	0.36	0.9725	0.61	0.2	2.7	7.1
BP480ERL20	0.32	0.9908	0.62	0.2	3.3	8.4
BP460ERL40	0.28	0.9949	0.55	0.3	4.5	12.9
BP440ERL60	0.20	0.9852	0.53	0.4	7.5	18.4
BP420ERL80	0.19	0.9938	0.51	0.4	8.7	26.4
BP480ERS20	0.32	0.9908	0.60	0.2	3.4	8.9
BP460ERS40	0.29	0.9892	0.56	0.3	4.6	13.3
BP440ERS60	0.20	0.9852	0.53	0.4	7.7	17.5
BP420ERS80	0.20	0.9938	0.52	0.4	8.4	26.0

K- release rate constant (h^{-n}), R^2- regression coefficient, n- release exponent indicate the mechanism of drug release, $t_{10\%}$, $t_{50\%}$ and $t_{90\%}$- time taken (in h) for 10, 50 and 90 % drug release respectively.

Mucoadhesive strength determination of formulation of PEO with Eudragit

Preliminary studies performed on designed ocular inserts prepared using combination of polymers using intestinal mucosal membrane showed that mocoadhesive strength of the ocular inserts is dependent on the relative proportion of PEO in the matrix.

Adequate mucoadhesion is required for the ocular inserts to be retained in the lower cul de sac on topical administration. Lower mucoadhesive strength to the ocular inserts can cause detachment of ocular inserts resulting in the blockade of vision and subsequent chance of formulation falling off from the eye. Addition of Eudragits to PEO based formulations resulted in decrease in detachment force. The formulations containing Eudragits alone did not show any mucoadhesive strength. The force of detachment for the ocular inserts containing two grades of PEO (PEO 100 kD and 400 kD) and Eudragits (ERL 100 and ERS 100) are shown in Fig. 6.14 (a) (PEO 100 kD and ERL 100), 6.14 (b) (PEO 100 kD and ERS 100) and 6.15 (a) (PEO 400 kD and ERL 100) and 6.15(b) (PEO 400 kD and ERS 100).

Formulations with 100 % w/w of PEO showed a drastic increase in the detachment force of 0.83 N/cm^2 (PEO 100 kD) and 1.02 N/cm^2 (PEO 400 kD). Gradual decrease in PEO 100 kD proportion and increase in ERL proportion resulted in decrease in force of detachment. Interestingly with PEO 400 kD alone formulations, the force of detachment was found to be lesser than that of formulations with PEO 100 kD alone, which could be due to the fact that as the number of chains in polymer increases with the increase in the molecular weight, the possibility of polymer-polymer interaction increases which subsequently resulting in reduction in the number of penetration polymer chains per unit of mucosal volume (Bremmecker, 1983, Di Colo et al, 2001). Ocular inserts prepared using Eudragit (ERL and ERS) showed poor force of detachment.

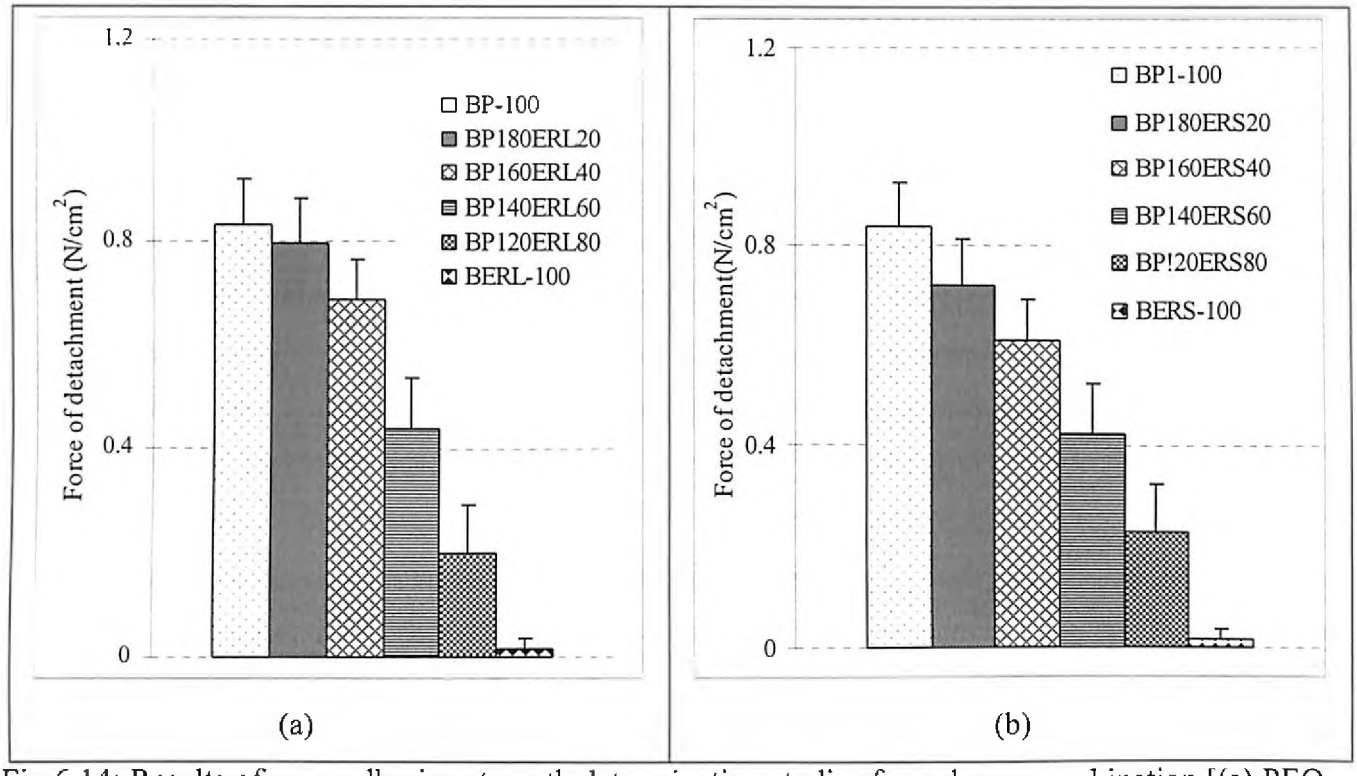

Fig 6.14: Results of mucoadhesive strength determination studies for polymer combination [(a) PEO 400 kD and ERL 100, (b) PEO 400 kD and ERS 100] based brimonidine tartrate ocular insert formulations. Each data point represents the average of two batches in triplicate with standard deviation.

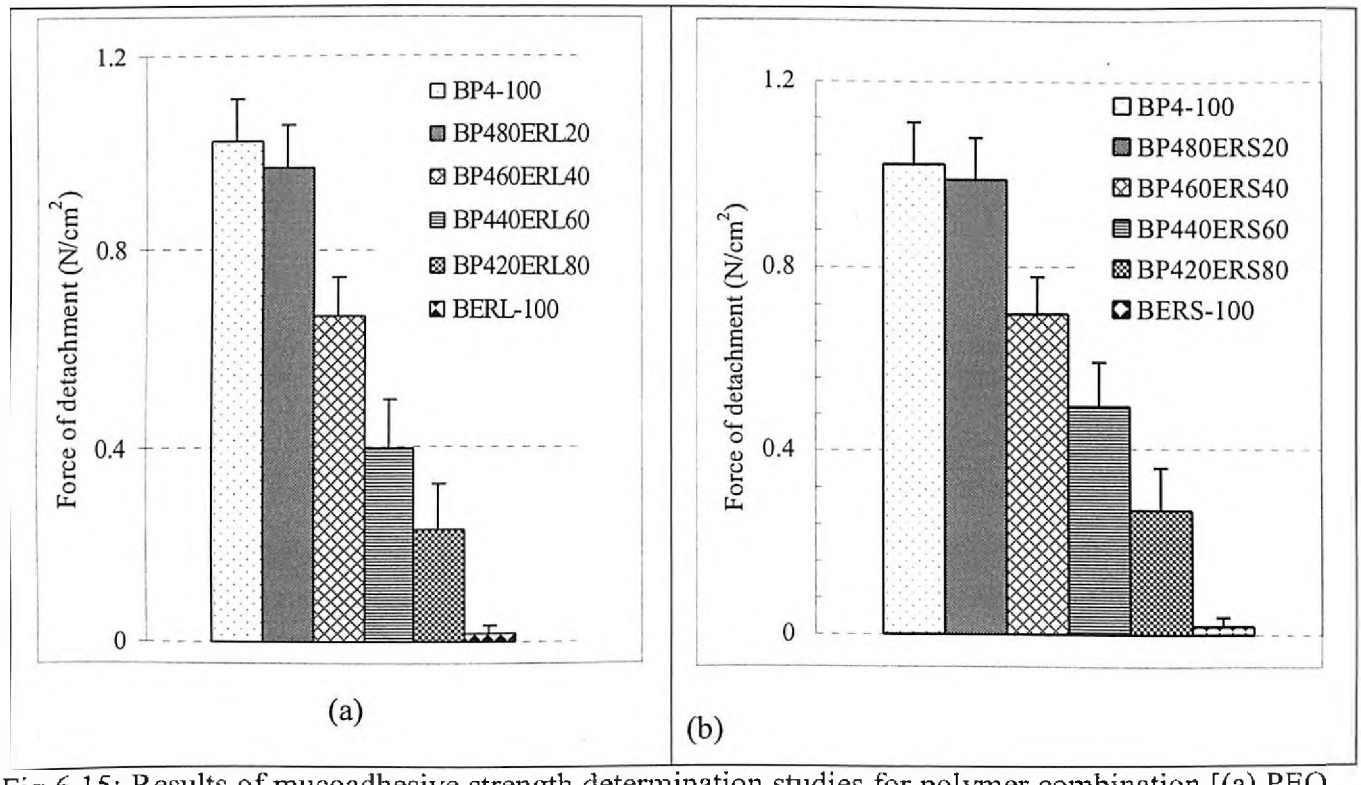

Fig 6.15: Results of mucoadhesive strength determination studies for polymer combination [(a) PEO 100 kD and ERL 100 (b) PEO 100 kD and ERS 100] based brimonidine tartrate ocular insert formulations. Each data point represents the average of two batches in triplicate with standard deviation.

(ii) Effect of combination of hydrophilic (PEO) with hydrophobic (EC) polymers

(a) Combination of PEO with EC

As discussed in the previous sections involving the PEO based ocular inserts formulations, the drug release from PEO based ocular inserts matrices were faster and lasted for 6 h only for PEO 100 kD and 8 h for PEO 400 kD. In order to sustain the extent of release to longer duration, several combinations of hydrophobic polymers were investigated, so that a prolonged release with sufficient mucoadhesive strength was obtained.

PEO has good mucoadhesive strength at its higher proportions in the ocular insert matrix, but resulted in shorter duration of drug release. Ethyl cellulose (EC), an inert hydrophobic polymer was incorporated to the ocular insert matrix in different relative proportions, so that the main objective of the formulation design was attained.

Upon decreasing the PEO 100 kD proportion to 80 % w/w and adding 20 % w/w of EC-22 (BP180E220) (Fig 6.16), the drug release rate was decreased to 0.29 $h^{-0.67}$ and $t_{90\%}$ was extended to 8.4 h. Further decrease in the relative proportions of PEO 100 kD and corresponding increase in EC-22 resulted in extension of drug release and drastic decrease in the release rate constant. The formulation with 100 % w/w of EC-22 showed a duration drug release for 30 h with a release rate constant of 0.14 $h^{-0.59}$ and $t_{90\%}$ of 23.7 h (Table 6.6).

Similarly, in the case of PEO 100 kD and EC-50 series formulations (Fig 6.17), the drug release was retarded greatly by the addition of EC-50 to the ocular insert matrix and the duration of drug release was more sustained than in the case of PEO 100 kD and EC-22 series formulations. As the relative proportion of EC-50 was increased with the decrease in the PEO 100 kD proportion, the drug release rate was decreased. In the case of PEO 100 kD at 80 % w/w proportion, the drug release rate constant was found to be 0.29 $h^{-0.66}$ with the $t_{90\%}$ found to be 8.4 h. Further decrease in relative proportion of PEO 100 kD to 60 % w/w and increase in EC-50 proportion to 40 % w/w resulted in decrease in drug release rate constant (0.26 $h^{-0.64}$) and increase in $t_{90\%}$ (10.5 h). Similar trend continued with further decrease in PEO 100 kD and increase in EC-50 proportions. The effect of relative polymer proportion variation on mucoadhesive strength has been discussed in the later sections in detail.

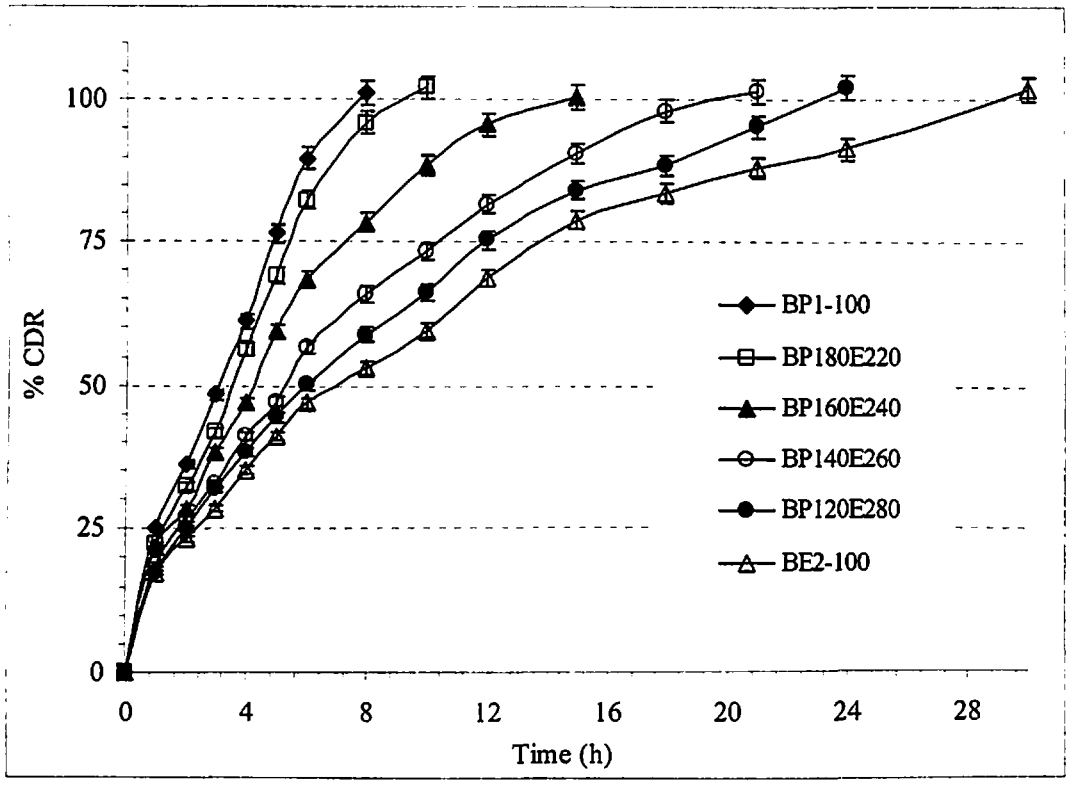

Fig 6.16: In vitro drug release profile polymer combination (PEO 400 Da and EC-22) based brimonidine tartrate ocular insert formulations. Each data point represents the average of two batches in triplicate with standard deviation.

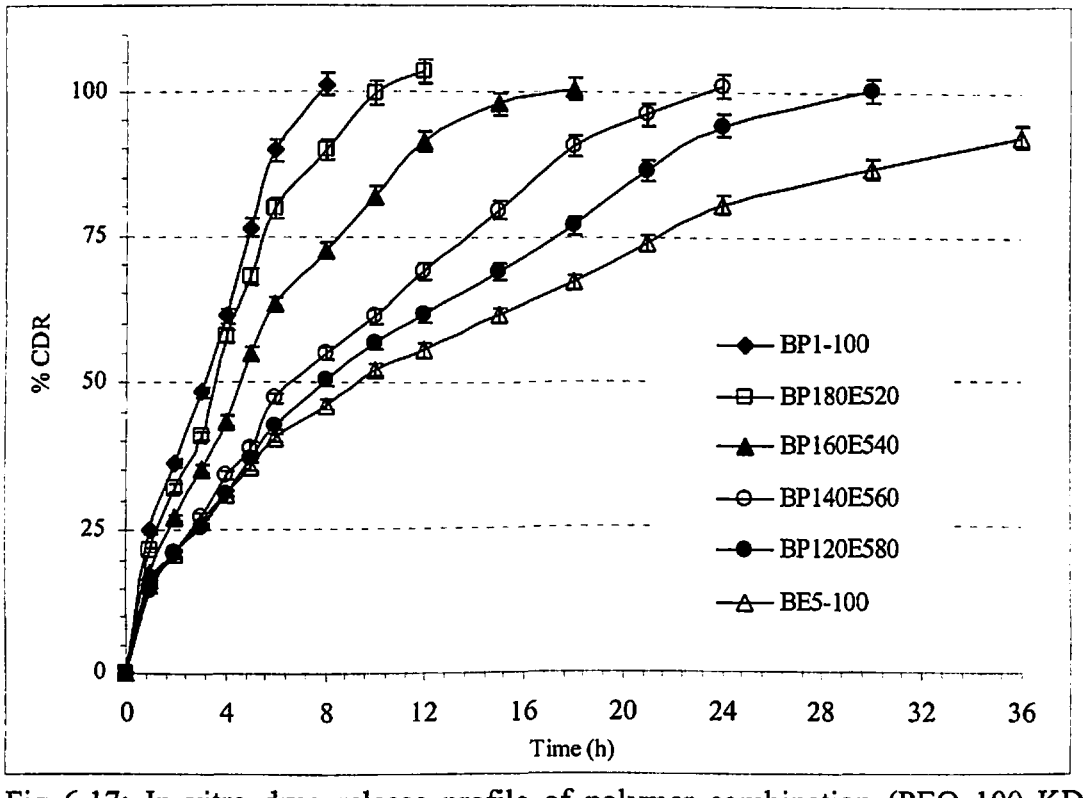

Fig 6.17: In vitro drug release profile of polymer combination (PEO 100 KD and EC- 50) based brimonidine tartrate ocular insert formulations. Each data point represents the average of two batches in triplicate with standard deviation.

In case of ocular insert formulations with PEO 400 kD and EC-22, similar observation as that of PEO 100 kD and EC-22 series ocular insert formulations was made (Fig 6.18). The drug release was much faster in case of 100 % w/w PEO 400 kD formulation. Addition of 20 % w/w of EC-22 with decrease in PEO 400 proportion to 80 % PEO 400 kD, resulted in extension of drug release. Suitable combinations of PEO 400 kD and EC-22 were investigated so that duration of release was extended and mucoadhesive strength was sufficient enough for optimal ocular administration. At a PEO 400 kD proportion of 40 % w/w and EC-22 of 60 % w/w, it was observed that the drug release was extended for 24 h with a release rate constant of 0.20 $h^{-0.53}$ and the $t_{90\%}$ of 17.5 h. Further decrease in the relative proportion of PEO 400 and increase in EC-22 proportion, resulted in sustained release of drug, but unfortunately, mucoadhesive strength decreased drastically.

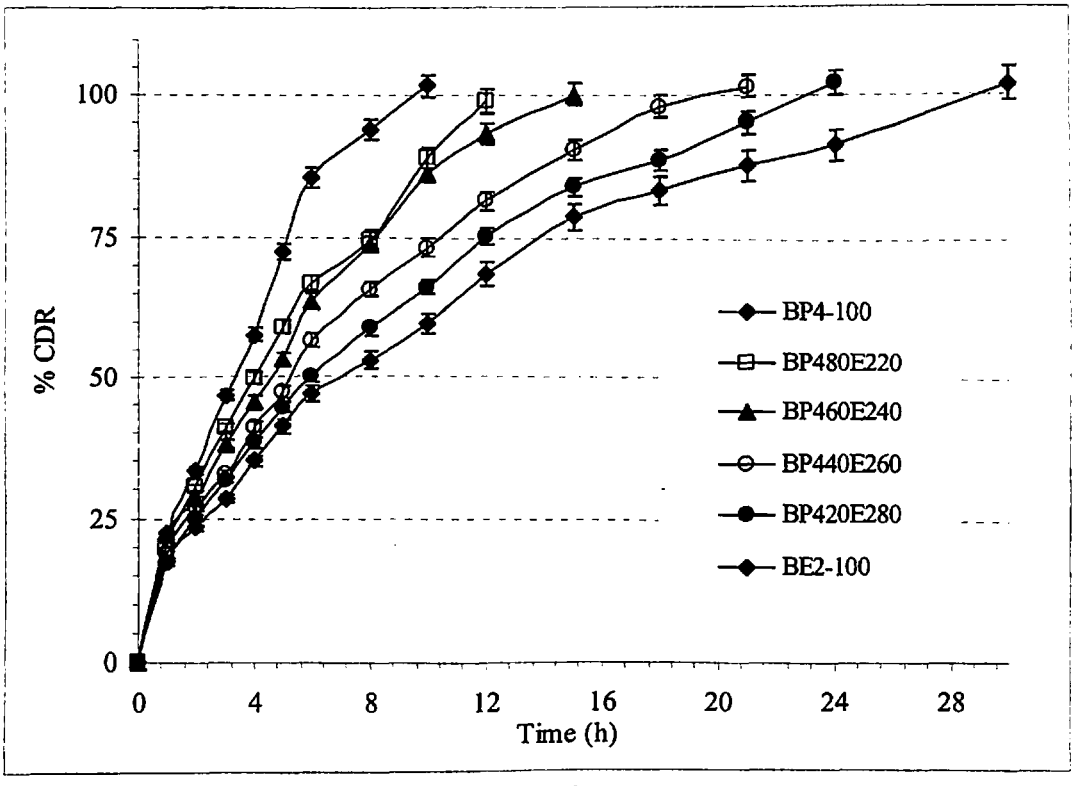

Fig 6.18: In vitro drug release profile of polymer combination (PEO 400 KDa and EC-22) based brimonidine tartrate ocular insert formulations. Each data point represents the average of two batches in triplicate with standard deviation.

Ocular inserts formulations with PEO 400 kD and EC-50, showed varying degree of drug release depending on the relative proportion of PEO 400 and EC-50 in the formulation matrix (Fig 6.19). As the relative proportion of PEO 400 was decreased and EC-50 was increased, the drug release was more prolonged with release rate of 0.31 $h^{-0.71}$ (BP1-100) to 0.16 $h^{-0.51}$ (BP420E580). The decrease in the release rate can be attributed to the relative

increase in the proportion of EC-50 and decrease in PEO 400 kD proportion. As the proportion of PEO was decreased in the ocular insert formulation with increase in the EC proportion, the release mechanism was gradually moved from non-Fickian anamolous to Fickian diffusion transport. This was further confirmed with the correlation between percent drug released vs. percent matrix erosion. The release kinetics data is shown in the Table 6.6.

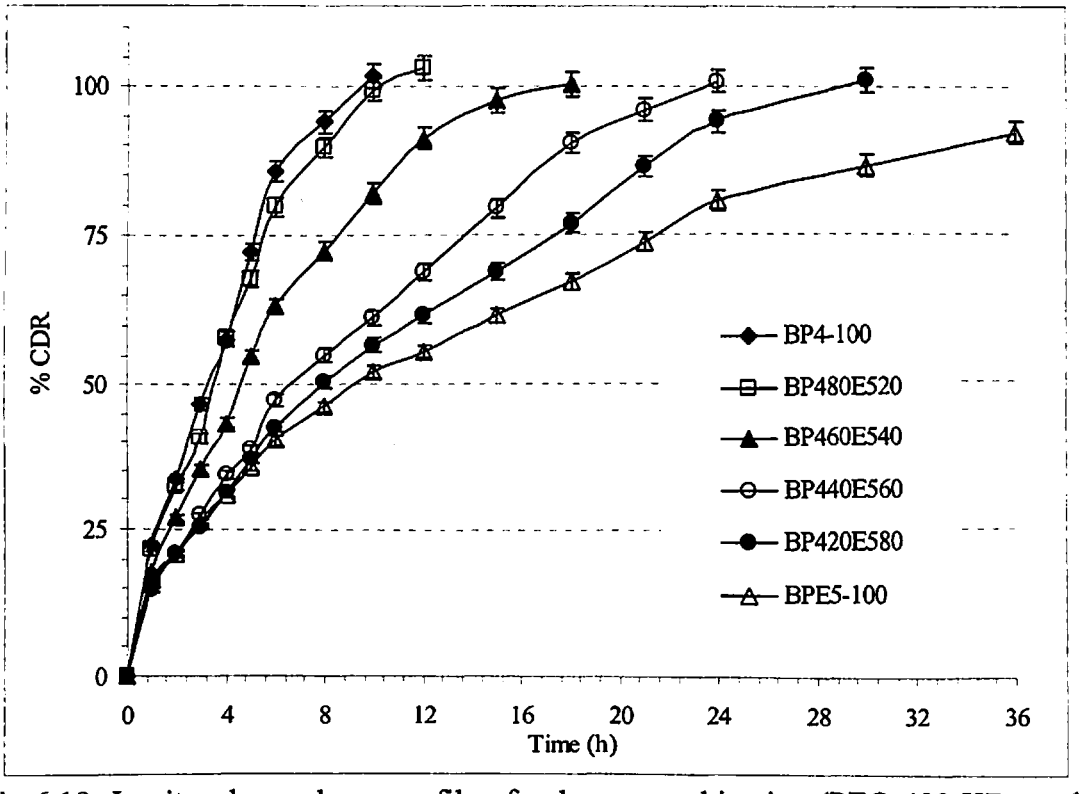

Fig 6.19: In vitro drug release profile of polymer combination (PEO 400 KDa and EC-50) based brimonidine tartrate ocular insert formulations. Each data point represents the average of two batches in triplicate with standard deviation.

Mucoadhesive strength determination

The results of mucoadhesive strength determination are presented in the Fig 6.20(a) (PEO 100 kD and EC-22) , 6.20(b) PEO 100 kD with EC-50, 6.20(c) PEO 400 kD with EC-22 and 6.20(d) PEO 400 kD with EC-50.

Decrease in the proportion of PEO in the formulation resulted in sharp decrease in the force of detachment of the ocular inserts. Ocular insert formulations with only EC showed no mucoadhesive strength.

Table 6.6: Results of drug release kinetics studies for polymer combination [hydrophilic polymers (PEO 400 kD, PEO 400 kD) with hydrophobic polymers (EC-22 and EC-50)] based brimonidine tartrate ocular inserts formulations fitted into Korsmeyer-Peppas model

Batch code	KP model			$t_{10\%}$ (h)	$t_{50\%}$ (h)	$t_{90\%}$ (h)
	K (h^{-n})	$R^{2\,¥}$	n #			
BP1-100	0.32	0.9725	0.71	0.3	2.9	6.6
BP180E220	0.29	0.9908	0.67	0.3	3.5	8.4
BP160E240	0.26	0.9892	0.64	0.4	4.3	10.7
BP140E260	0.22	0.9768	0.63	0.4	5.3	13.6
BP120E280	0.16	0.9938	0.61	0.5	7.3	19.2
BE2-100	0.14	0.9941	0.59	0.6	8.8	23.7
BP180E520	0.29	0.9908	0.66	0.3	3.4	8.4
BP160E540	0.26	0.9892	0.64	0.3	4.3	10.5
BP140E560	0.17	0.9852	0.60	0.5	7.1	13.5
BP120E580	0.16	0.9932	0.60	0.5	7.3	19.3
BE5-100	0.13	0.9931	0.59	0.6	8.7	29.8
BP4-100	0.36	0.9725	0.61	0.2	2.7	7.0
BP480E220	0.32	0.9908	0.60	0.2	3.4	8.9
BP460E240	0.29	0.9892	0.56	0.3	4.6	13.4
BP440E260	0.20	0.9852	0.53	0.4	7.7	17.5
BP420E280	0.19	0.9938	0.51	0.4	8.3	25.9
BP480E520	0.32	0.9908	0.62	0.2	3.3	8.4
BP460E540	0.28	0.9949	0.55	0.3	4.5	12.9
BP440E560	0.20	0.9852	0.53	0.4	7.5	18.4
BP420E580	0.19	0.9938	0.51	0.4	8.7	26.4

K- release rate constant (h^{-n}), R^2- regression coefficient, n- release exponent indicate the mechanism of drug release, $t_{10\%}$, $t_{50\%}$ and $t_{90\%}$- time taken (in h) for 10, 50 and 90 % drug release respectively.

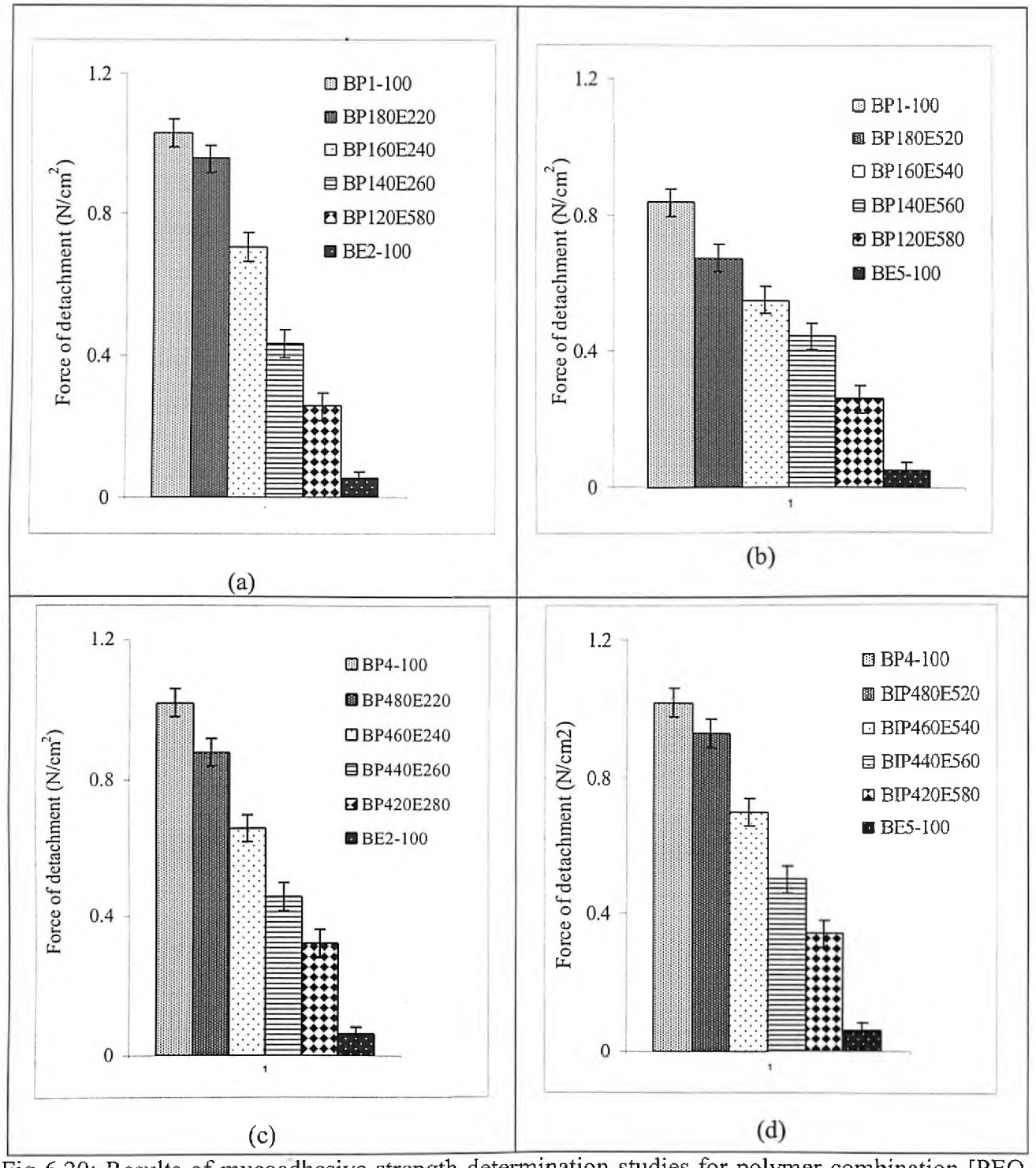

Fig 6.20: Results of mucoadhesive strength determination studies for polymer combination [PEO 100 kD and EC-22 (b) PEO 100 kD and EC-50, (c) PEO 400 kD and EC-22 and (d) PEO 400 kD and EC-50] based brimonidine tartrate ocular insert formulations. Each data point represents the average of two batches in triplicate with standard deviation.

(iii) Effect of combination of hydrophilic polymer (HPMC) with zwitterionoic polymers (Eudragits)

(a) Combination of HPMC K4M with Eudragits

The release profiles of various combinations of HPMC K4M and ERL 100 are shown in the Fig 6.21. At a HPMC K4M proportion of 80 % w/w and ERL 100 proportion of 20 % w/w, the release rate constant was found to be 0.26 $h^{-0.84}$ with $t_{90\%}$ of 8.2 h. This trend of decreasing release rate constant and increasing the duration of drug release ($t_{90\%}$) was observed with further decrease in the relative proportion of HPMC K4M in the matrix. The formulation with 40 % w/w of HPMC K4M and 60 % ERL 100 showed a release profile of 24 h with a release rate constant of 0.23 $h^{-0.78}$ and a $t_{90\%}$ of 14.2 h.

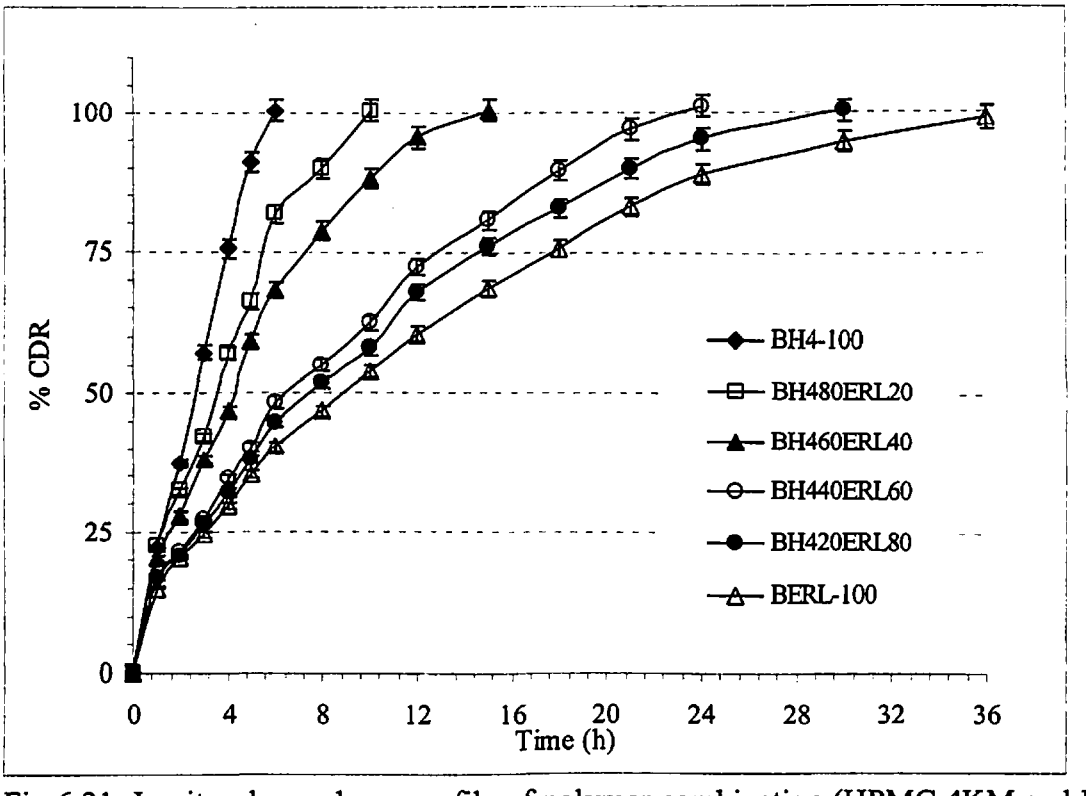

Fig 6.21: In vitro drug release profile of polymer combination (HPMC 4KM and ERL 100) based brimonidine tartrate ocular insert formulations. Each data point represents the average of two batches in triplicate with standard deviation.

Similar observations were noticed in the case of formulations with HPMC K4M and ERS 100 at various relative proportion levels. The results are shown in Fig 6.22. The release rate and the $t_{90\%}$ values varied significantly with decrease in HPMC K4M proportion and subsequent increase in ERS 100 proportion in the matrix.

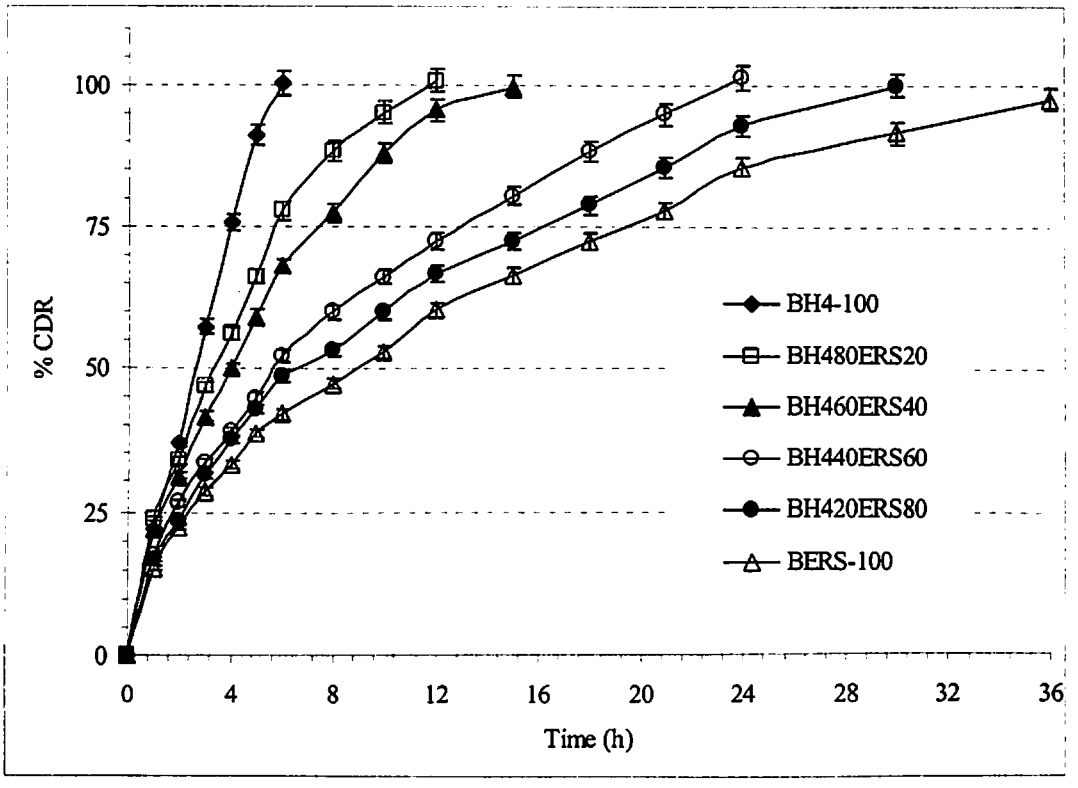

Fig 6.22: In vitro drug release profile of polymer combination (HPMC 4KM and ERS 100) based brimonidine tartrate ocular inserts formulations. Each data point represents the average of two batches in triplicate with standard deviation.

(b) Combination of HPMC K15M and Eudragits

In case of formulations with HPMC K15M and Eudragits, investigations were carried out to optimise the formulations with prolonged release and sufficient mucoadhesive strength. The drug release rate at 100 % w/w HPMC K15M was faster with release rate constant of 0.27 $h^{-0.81}$ ant the release lasted for 6-8 h with $t_{90\%}$ of 6.3 h. To enhance the duration of release, ERL 100 was incorporated to the ocular insert matrix (Fig 6.23). With the addition of 20 % w/w of ERL 100 and reduction of HPMC K15M proportion to 80 % w/w, the release rate was decreased to 0.23 $h^{-0.77}$ and $t_{90\%}$ was increased to 8.9 h. further decrease in HPMC K15M to 60 % and increase in ERL 100 to 40 % w/w resulted in reduced drug release rate to 0.21 $h^{-0.76}$ and enhanced duration of release with $t_{90\%}$ 12.9 h. Similar trend was observed with further modifications in the relative proportions of HPMC K15M and ERL 100.

Similar pattern of drug release retardation with decrease in HPMC K15M proportion and increase in ERS 100 proportion was observed with HPMC K15M with ERS 100 based ocular insert formulations (Fig 6.24).

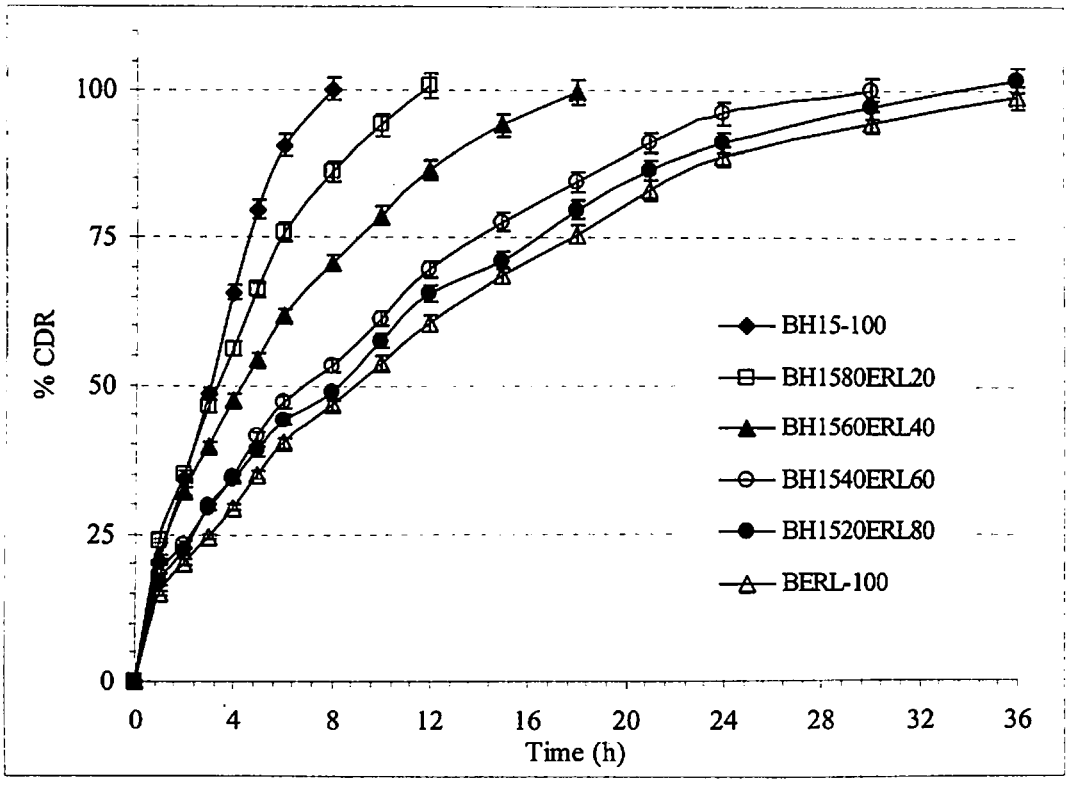

Fig 6.23: In vitro drug release profile of polymer combination (HPMC 15KM and ERL 100) based brimonidine tartrate ocular insert formulations. Each data point represents the average of two batches in triplicate with standard deviation.

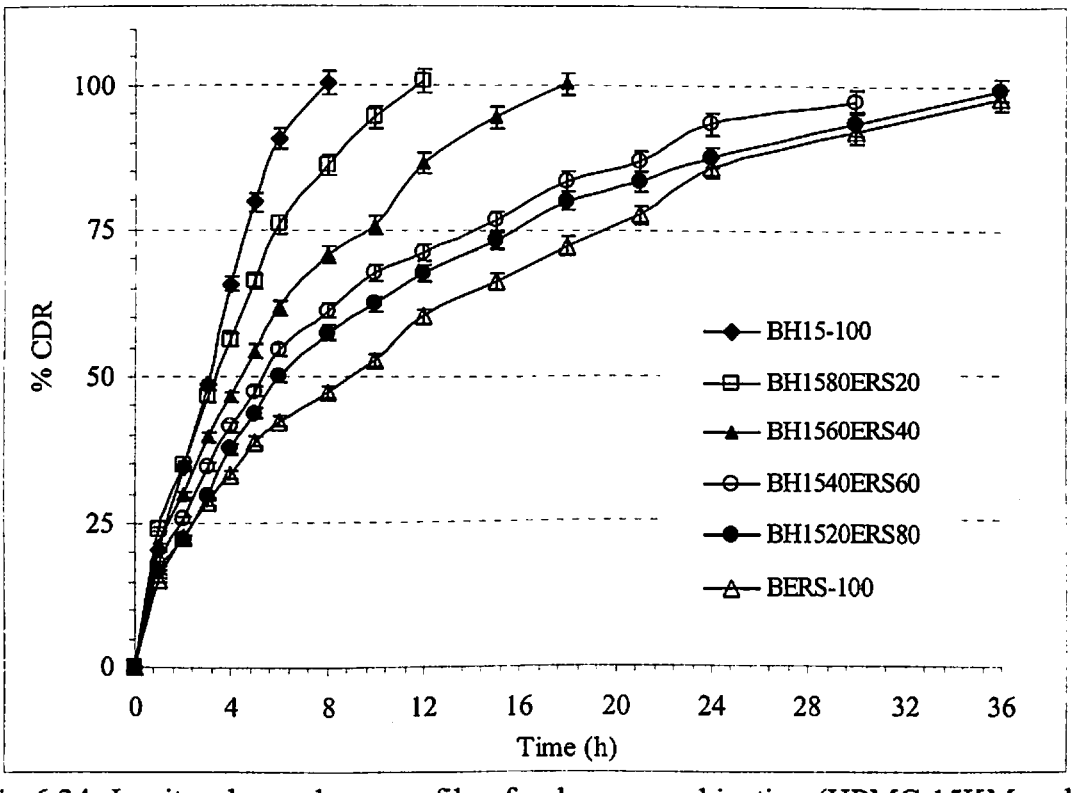

Fig 6.24: In vitro drug release profile of polymer combination (HPMC 15KM and ERS 100) based brimonidine tartrate ocular insert formulations. Each data point represents the average of two batches in triplicate with standard deviation.

(c) Combination of HPMC K100M and Eudragit

In case of HPMC K100M and Eudragit based formulations, the drug release was found to be greatly modulated by the decrease in HPMC proportion and increase in the Eudragit proportion (ERL 100 and ERS 100). Modification in the relative proportions of HPMC and Eudragits greatly enhanced the duration of release, as evident from the Fig 6.25 and 6.26. The $t_{90\%}$ values ranged from 10.2 h in case of BH1080ERL20 to 23.3 h in case of BH1020ERL80. For the corresponding HPMCK100M and ERS 100 combinations, the $t_{90\%}$ value varied from 11.2 h to 23.9 h. The mechanism of drug release was found to be non-Fickian anamolous drug transport (Table 6.7).

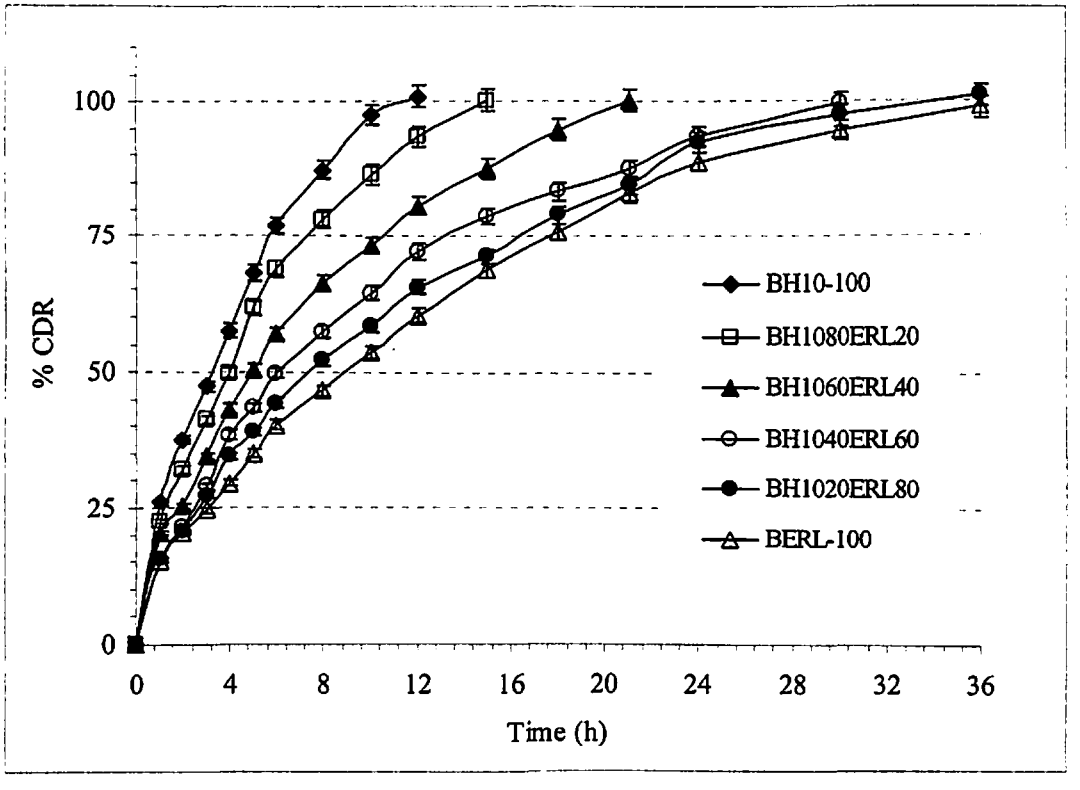

Fig 6.25: In vitro drug release profile of polymer combination (HPMC K100 M and ERL 100) based brimonidine tartrate ocular inserts formulations. Each data point represents the average of two batches in triplicate with standard deviation.

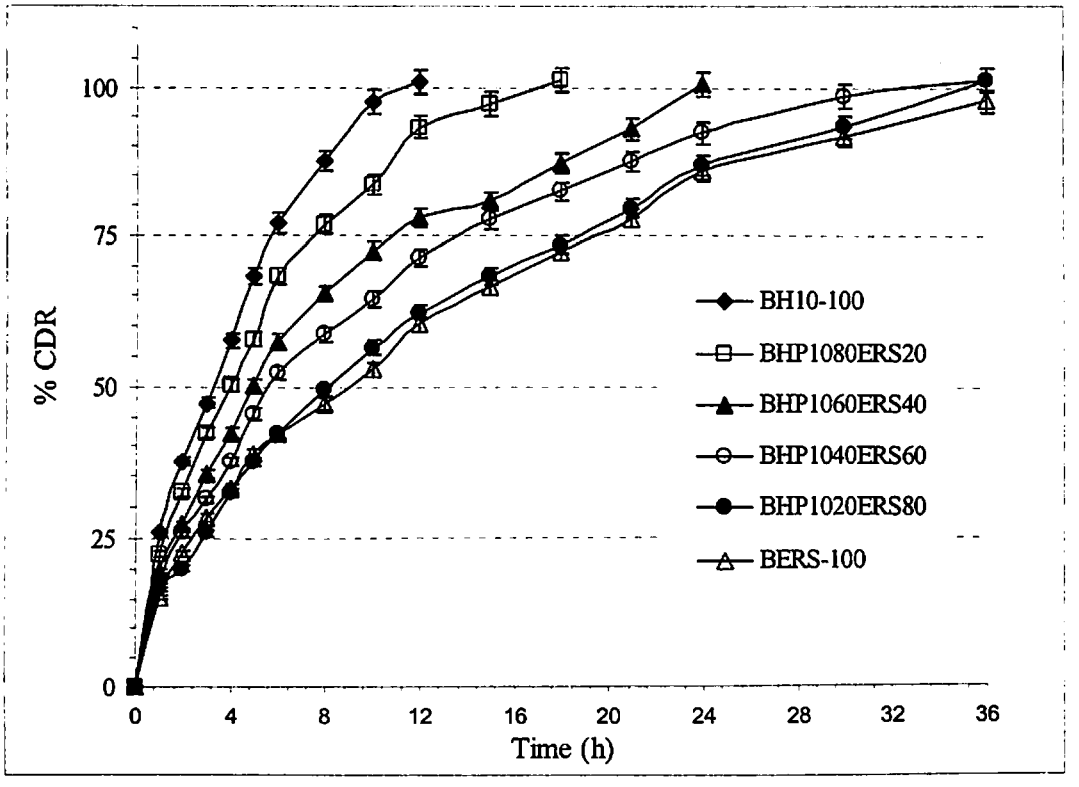

Fig 6.26: In vitro drug release profile of polymer combination (HPMC K100 M and ERS 100) based brimonidine tartrate ocular insert formulations. Each data point represents the average of two batches in triplicate with standard deviation.

Mucoadhesive strength determination

The mucoadhesive strength of the HPMC and Eudragit based ocular insert formulations greatly depended in the relative proportion of HPMC in the matrix formulation [Fig 6.27(a), (b) and (c)].

Formulations with higher proportion of HPMC showed good mucoadhesive strength. There was no much difference between mucoadhesive strength of HPMC formulations with either ERL 100 or ERS 100. Formulation with higher viscosity HPMC grades showed higher force of detachment. Hence the optimization involved the optimisation of ocular insert formulation with sufficient duration of drug release (at least for 24 h) and sufficient mucoadhesion, so that the formulation remain adhesive to the cul de sac of the eye for the duration of its drug release. In all the cases, the formulations with 40 % w/w of HPMC (K4M, K15M and K100M) and 60 % w/w of Eudragits (ERL 100 and ERS 100) yielded better results amongst the series of formulations studied, with desirable drug release and optimum mucoadhesive strength

Table 6.7: Results of drug release kinetics studies for polymer combination [hydrophilic polymers (HPMC K4M, HMPC K15M and HPMC K100M) with inert/ zwitterionic polymers (ERL 100 and ERS 100)] based brimonidine tartrate ocular insert formulations fitted into Korsmeyer-Peppas model

Batch code	KP model			$t_{10\%}$ (h)	$t_{50\%}$ (h)	$t_{90\%}$ (h)
	K (h^{-n})	$R^{2\,¥}$	n #			
BH4-100	0.29	0.9908	0.88	0.22	2.6	5.1
BH480ERL20	0.26	0.9944	0.84	0.24	3.2	8.2
BH460ERL40	0.24	0.9833	0.81	0.25	4.3	10.6
BH440ERL60	0.23	0.9783	0.78	0.28	5.2	14.2
BH420ERL80	0.18	0.9812	0.65	0.37	7.1	19.2
ERL-100	0.14	0.9825	0.57	0.53	9.1	25.6
BH480ERS20	0.25	0.9822	0.81	0.22	4.6	8.4
BH460ERS40	0.25	0.9722	0.78	0.26	4.9	11.2
BH440ERS60	0.22	0.9724	0.73	0.29	5.3	15.9
BH420ERS80	0.17	0.9829	0.54	0.36	7.3	22.2
ERS-100	0.17	0.9768	0.52	0.41	8.9	27.1
BH15-100	0.27	0.9932	0.81	0.21	3.0	6.3
BH1580ERL20	0.23	0.9811	0.77	0.25	5.2	8.9
BH1460ERL40	0.21	0.9720	0.72	0.27	5.9	12.9
BH1540ERL60	0.17	0.9753	0.66	0.39	6.8	17.8
BH1520ERL80	0.14	0.9811	0.62	0.46	8.7	24.3
BH1580ERS20	0.25	0.9830	0.81	0.26	5.7	9.3
BH1460ERS40	0.23	0.9780	0.76	0.27	6.3	13.2
BH1540ERS60	0.19	0.9644	0.72	0.30	6.8	19.3
BH1520ERS80	0.15	0.9833	0.71	0.36	8.2	24.3
BH10-100	0.26	0.9908	0.70	0.21	3.2	8.7
BH1080ERL20	0.23	0.9833	0.71	0.29	5.9	10.2
BH1060ERL40	0.21	0.9733	0.68	0.37	6.6	15.7
BH1040ERL60	0.18	0.9982	0.60	0.41	7.3	20.1
BH1020ERL80	0.15	0.9821	0.56	0.47	8.2	23.3
BH1080ERS20	0.24	0.9788	0.69	0.28	6.1	11.2
BH1060ERS40	0.22	0.9722	0.66	0.37	6.9	16.2
BH1040ERS60	0.18	0.9822	0.68	0.43	7.8	20.9
BH1020ERS80	0.14	0.9722	0.54	0.49	8.2	23.9

K- release rate constant (h^{-n}), R^2- regression coefficient, n- release exponent indicate the mechanism of drug release, $t_{10\%}$, $t_{50\%}$ and $t_{90\%}$- time taken (in h) for 10, 50 and 90 % drug release respectively.

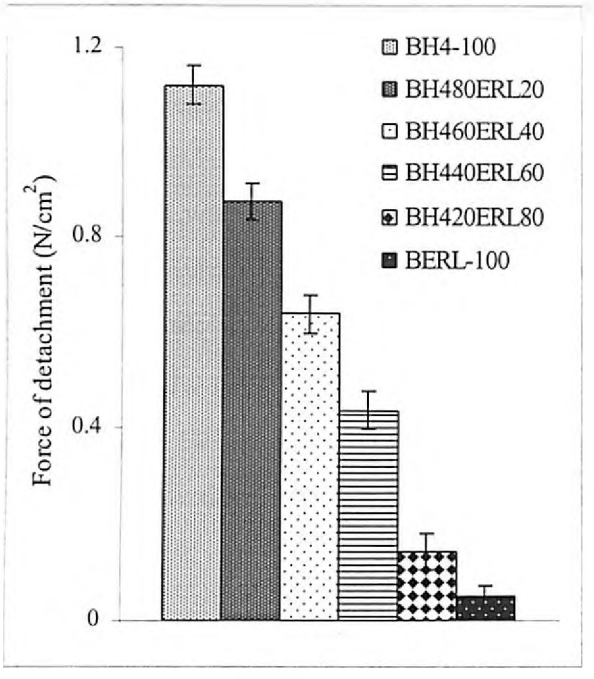

(a)

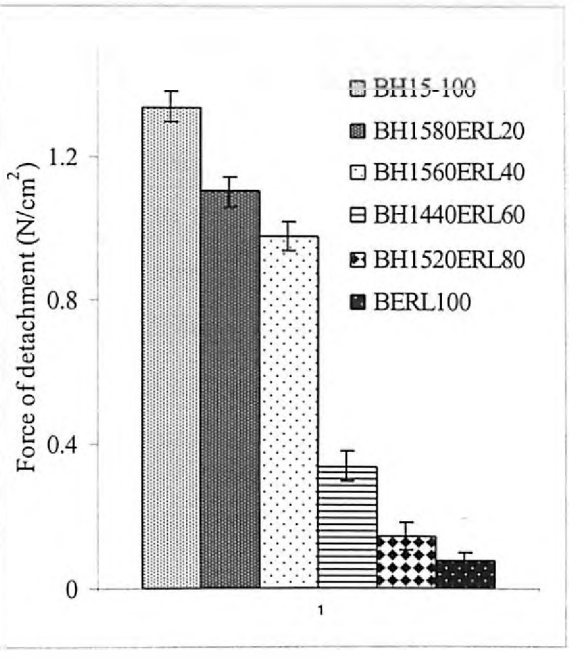

(b)

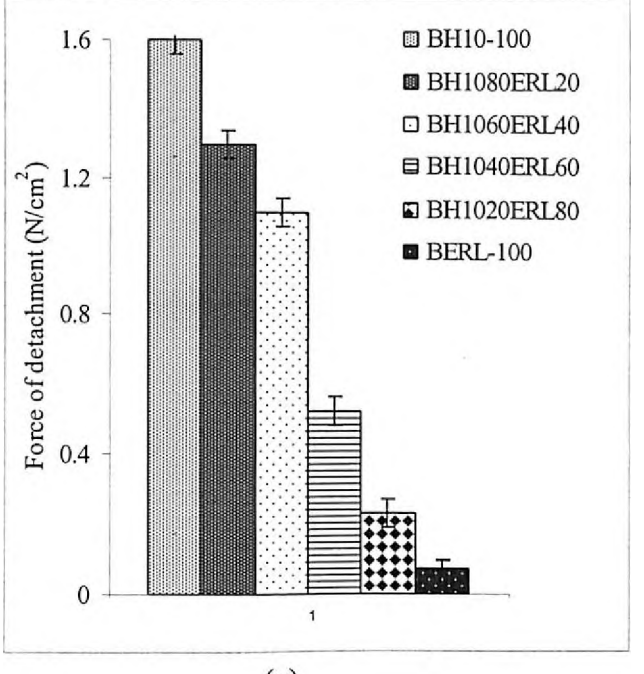

(c)

Fig 6.27: Results of mucoadhesive strength determination studies for polymer combination [(a) HPMC K4M and ERL 100 (b) HPMC K15M and ERL 100, (c) HPMC K100M and ERL 100] based brimonidine tartrate ocular insert formulations. Each data point represents the average of two batches in triplicate with standard deviation.

(iv) Effect of combination of hydrophilic (HPMC) and hydrophobic (EC) polymers

(a) HPMC K4M and EC

The drug release profile of the ocular inserts prepared using varying proportions of HPMC K4M with EC-22 is represented in the Fig 6.28. The release of drug from ocular insert formulations was greatly modulated by the addition of EC to the insert system. EC, a non swellable polymer, does not undergo any swelling while a negligible erosion upon contact with the water and alter the drug release pattern from HPMC 4KM based matrix. With decrease in the relative proportion of HPMC and subsequent increase in EC proportion, the drug release rate was decreased and the duration of drug release was enhanced. The drug release kinetic data is shown in the Table 6.8.

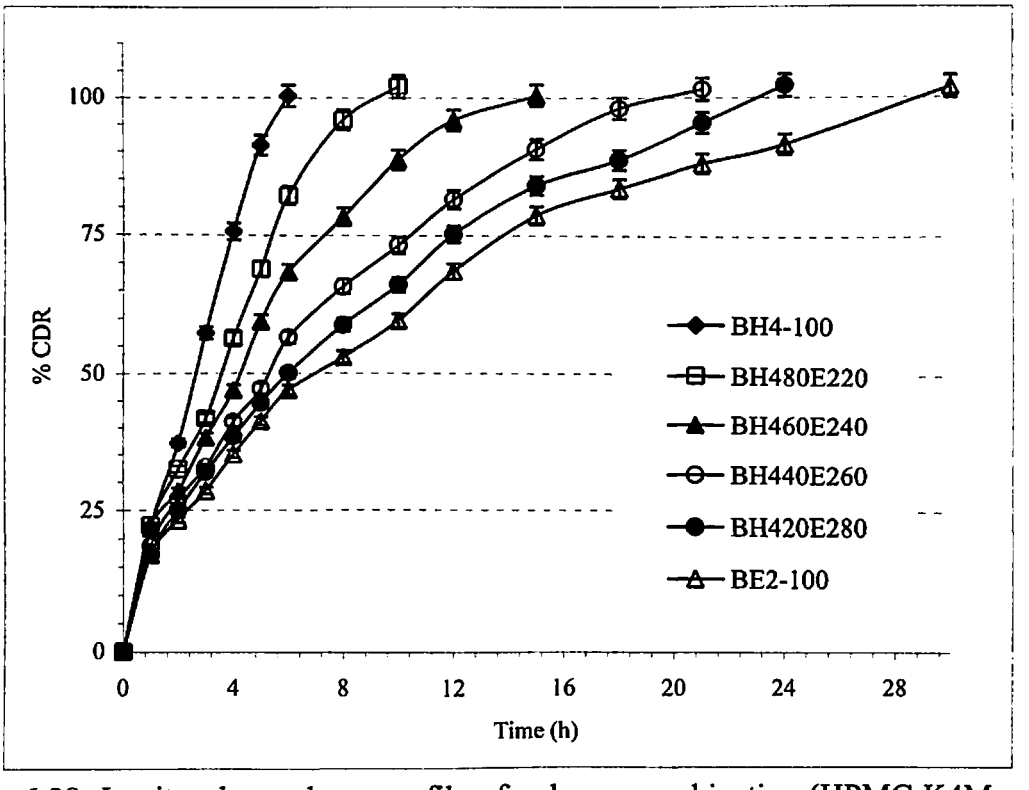

Fig 6.28: In vitro drug release profile of polymer combination (HPMC K4M and EC-22) based brimonidine tartrate ocular insert formulations. Each data point represents the average of two batches in triplicate with standard deviation.

Similarly with ocular inserts prepared with HPMC K4M and EC-50, the drug release was sustained upon increase in the relative proportions of EC in the matrix (Fig 6.29). The drug release rate was found to be 0.29 $h^{-0.88}$ for HPMC K4M alone formulations with $t_{90\%}$ of 5.1 h. Decrease in the HPMC K4M to 80 % w/w and increase of EC-50 to 20 %w/w resulting in 'K' of 0.26 $h^{-0.79}$ and $t_{90\%}$ was 8.2 h. With HPMC K4M proportion of 40 % w/w and EC-50 proportion of 60 % w/w, the 'K' was reduced to 0.21 $h^{-0.70}$ and drug release was sustained

for longer period of time with $t_{90\%}$ 15.9 h. Further decrease in hydrophilic polymer proportion and increase in EC proportion, further sustained the release of drug.

The mechanism of drug release was found to be non-Fickian anamolous transport. A combination of swelling, erosion and diffusion of drug through the diffusional layers of swollen matrix are contributing to the release of drug. But with the EC alone formulations, the release was towards Fickian diffusion. Formulation with HPMC KM (60 % w/w) and 40 % w/w of EC-22, the release rate constant was found to be 0.23 $h^{-0.70}$. Further increase in the relative proportion of EC resulted in further retardation of drug release.

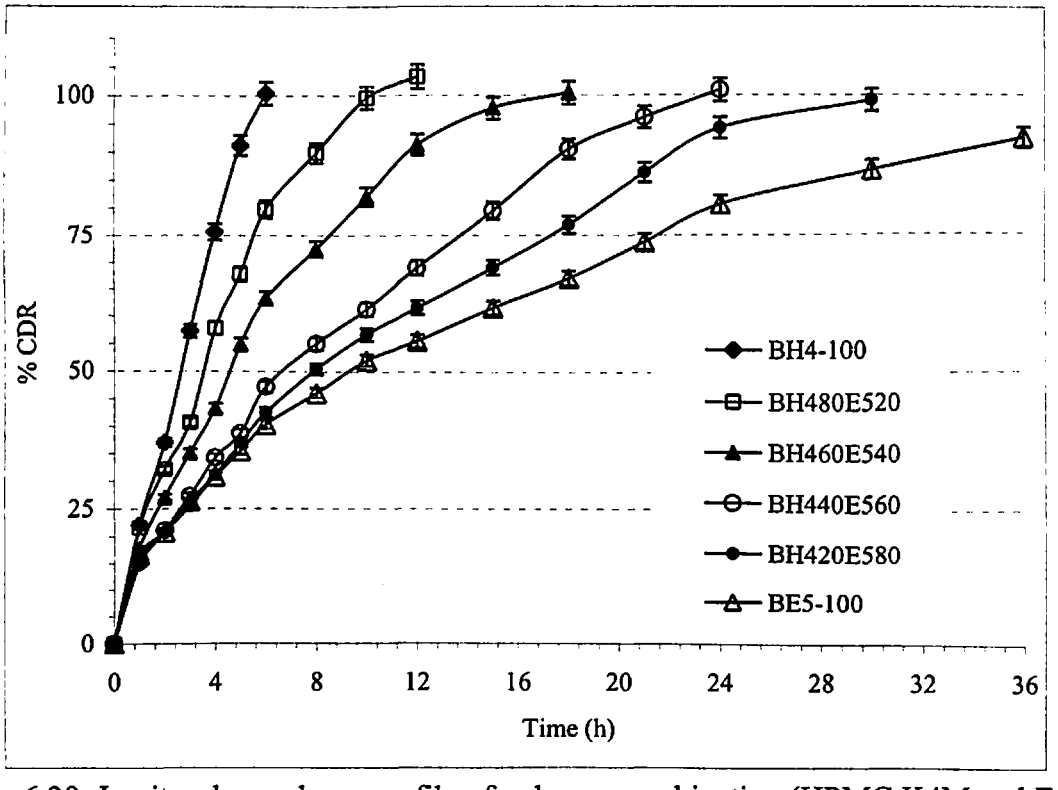

Fig 6.29: In vitro drug release profile of polymer combination (HPMC K4M and EC-50) based brimonidine tartrate ocular insert formulations. Each data point represents the average of two batches in triplicate with standard deviation.

Similar trend in terms of drug release rate and duration of drug release were observed with HPMC K15M with EC (EC-22 and EC-50) and HPMC K100M with EC (EC-22 and EC-50). The corresponding in vitro drug release profile are shown in Fig 6.30 (HPMC K15M and EC-22), 6.31 (HPMC K15M with EC-50), 6.32 (HPMC K100M with EC-50) respectively. The release mechanism for all these series of formulations was found to be non-Fickian anamolous.

Mucoadhesive strength determination

The results of mucoadhesive strength determination for HPMC and EC based ocular inserts re shown in the Fig 6.34. The optimised formulation is the one where proportion of HPMC and EC in the insert formulation matrix was optimum such that where the in vitro drug release in sufficiently longer (24 h) and the mucoadhesive strength is sufficient. As the proportion of HPMC is increased in the matrix, good mucoadhesive strength was observed. Relative decrease in the HPMC proportion, with an increase in EC proportion, gradually reduced the mucoadhesive strength, while the formulations with no HPMC and 100 w/w of EC, showed no mucoadhesion.

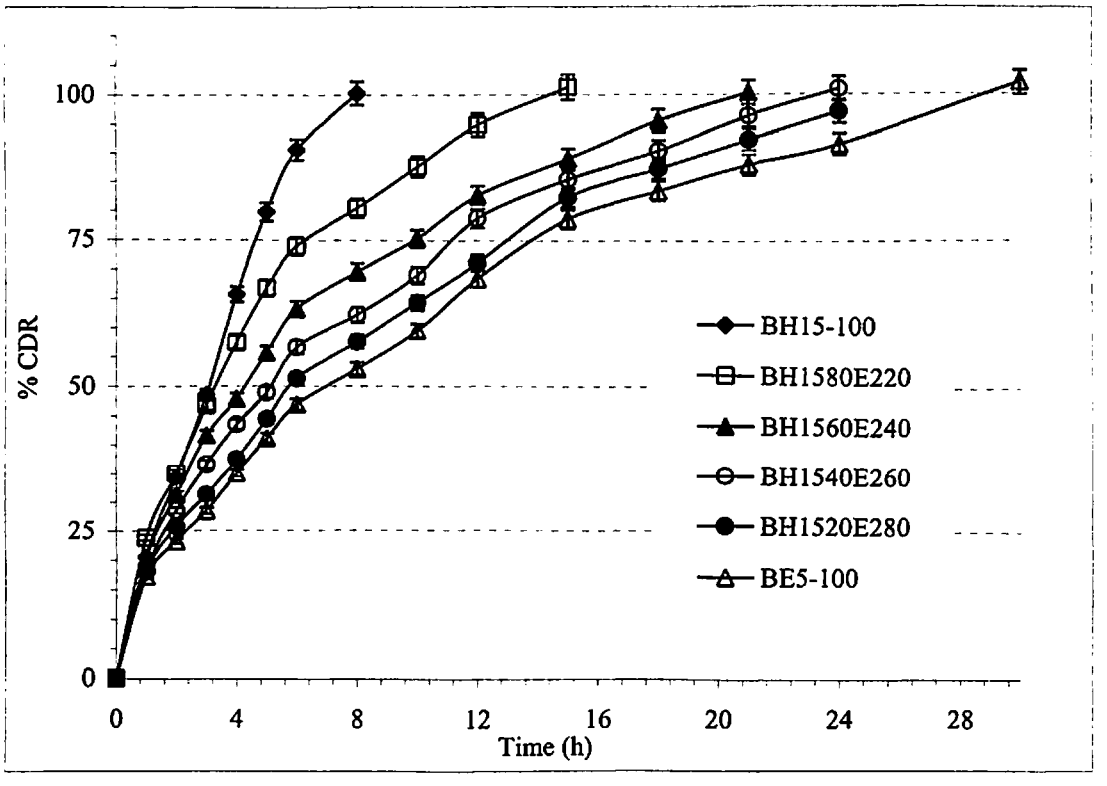

Fig 6.30: In vitro drug release profile of polymer combination (HPMC K15M and EC-22) based brimonidine tartrate ocular insert formulations. Each data point represents the average of two batches in triplicate with standard deviation.

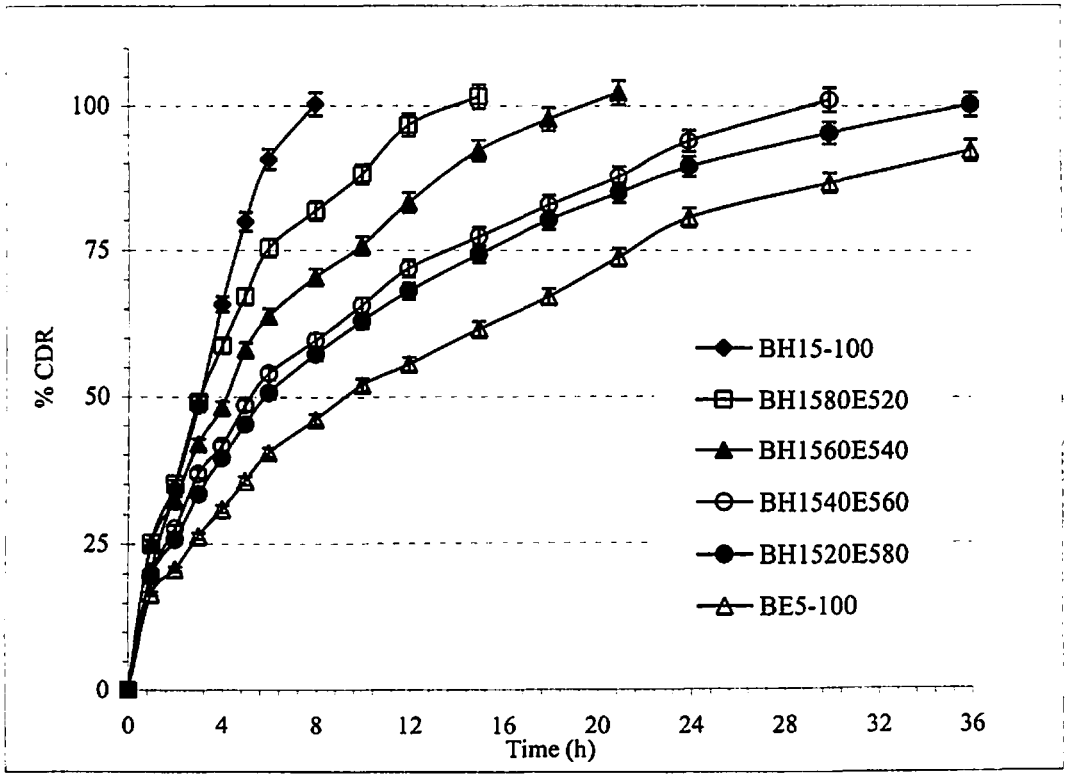

Fig 6.31: In vitro drug release profile of polymer combination (HPMC K15M and EC-50) based brimonidine tartrate ocular insert formulations. Each data point represents the average of two batches in triplicate with standard deviation.

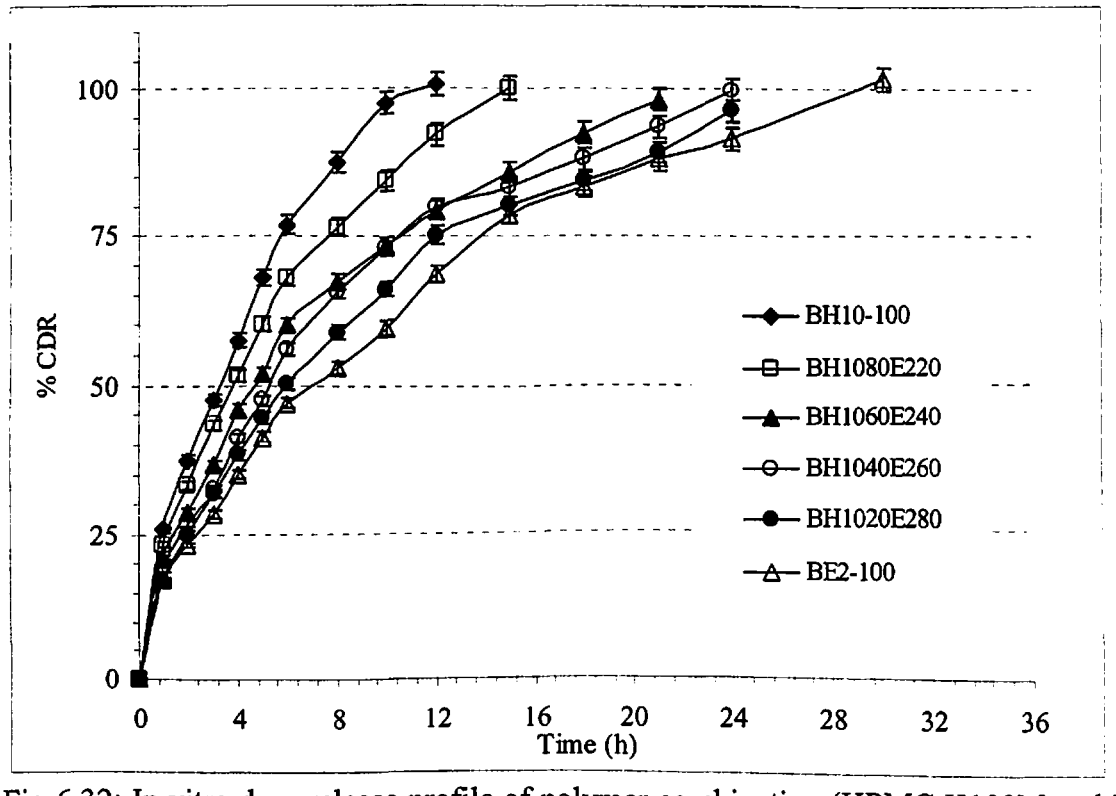

Fig 6.32: In vitro drug release profile of polymer combination (HPMC K100M and EC-22) based brimonidine tartrate ocular insert formulations. Each data point represents the average of two batches in triplicate with standard deviation.

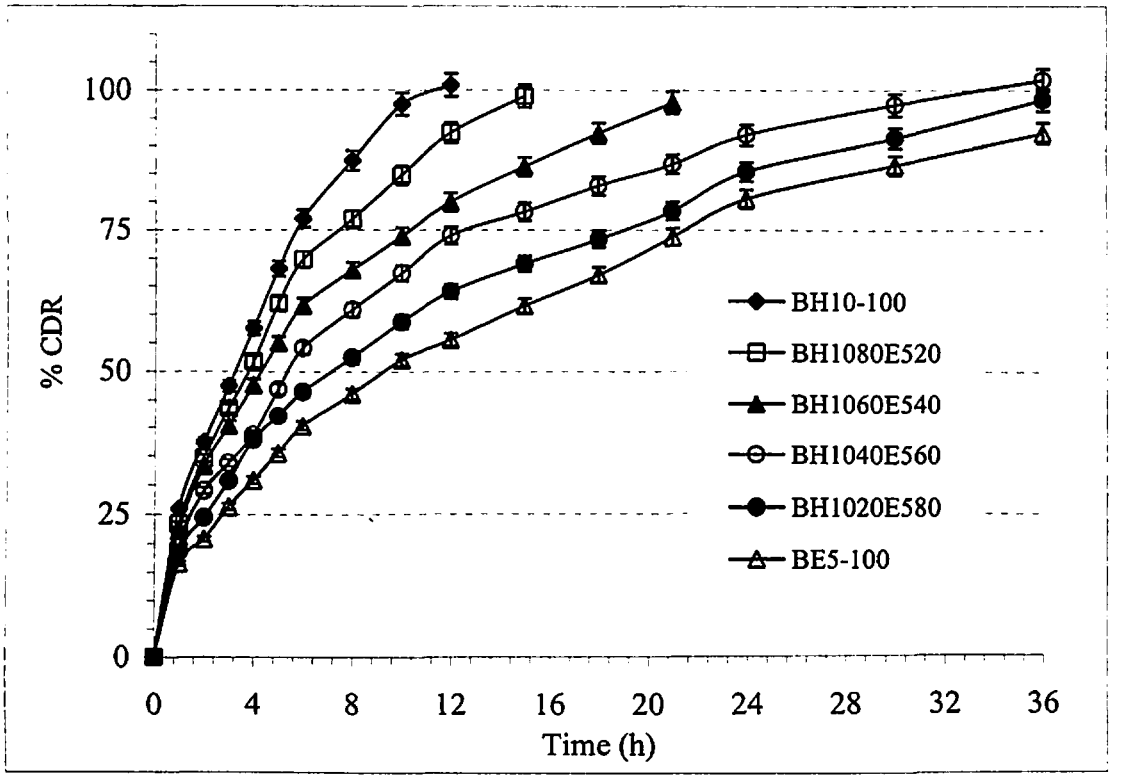

Fig 6.33: In vitro drug release profile of polymer combination (HPMC K100M and EC-50) based brimonidine tartrate ocular insert formulations. Each data point represents the average of two batches in triplicate with standard deviation.

6.4.2. Stability studies

Stability studies were performed for the selected formulations by storing the selected ocular inserts at ambient (25° C ± 2° C /60 ± 5% RH) and ATC (40° C ± 2° C/75 ± 5% RH) showed that the ocular insert formulations were stable at both the storage conditions with no significant degradation observed at accelerated conditions. The parameters like appearance, drug content, mucoadhesive strength, erosion pattern and in vitro drug release profiles remained unaltered for the entire duration of the studies. The results are shown in the Table 6.9.

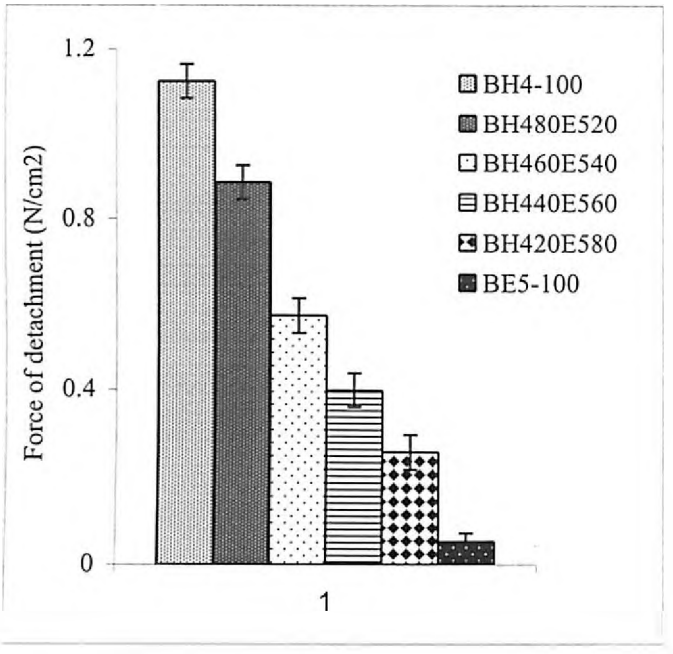

(a)

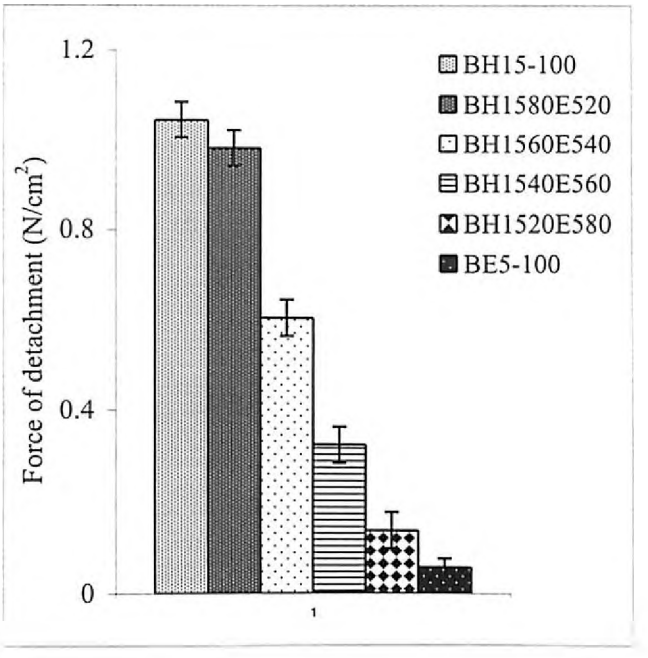

(b)

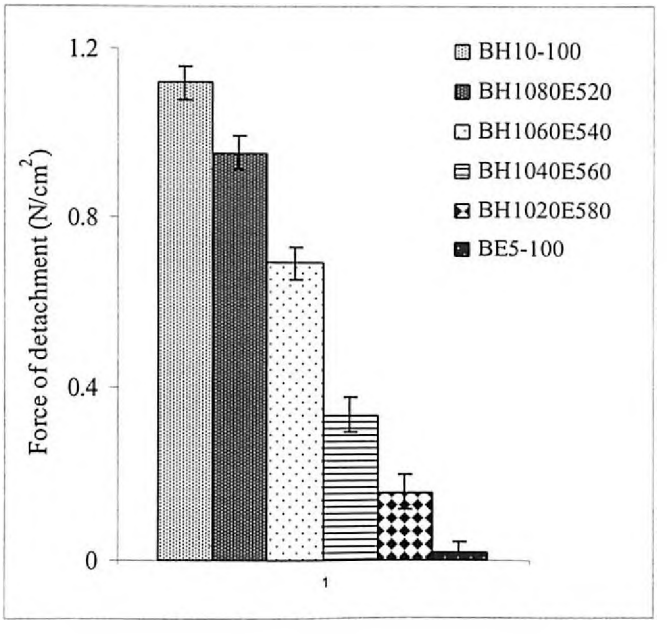

(c)

Fig 6.34: Results of mucoadhesive strength determination studies for polymer combination [(a) HPMC K4M and EC-50 (b) HPMC K15M and EC-50 (c) HPMC K100M and EC-50] based brimonidine tartrate ocular insert formulations. Each data point represents the average of two batches in triplicate with standard deviation.

Table 6.8: Results of drug release kinetics studies for polymer combination [hydrophilic polymers (HPMC K4M, HMPC K15M and HPMC K100M) with hydrophobic polymers (EC-22 and EC-50)] based brimonidine tartrate ocular insert formulations fitted into Korsmeyer-Peppas model

Batch code	KP model			$t_{10\%}$ (h)	$t_{50\%}$ (h)	$t_{90\%}$ (h)
	K (h^{-n})	$R^{2\,¥}$	n #			
BH4-10	0.29	0.9908	0.88	0.2	2.6	5.1
BH480E220	0.26	0.9944	0.79	0.3	3.2	8.2
BH460E240	0.23	0.9833	0.73	0.3	4.3	10.6
BH440E260	0.21	0.9783	0.70	0.3	5.2	14.2
BH420E280	0.16	0.9812	0.62	0.4	7.1	19.2
BE2-100	0.14	0.9941	0.59	0.6	8.81	24.6
BH480E520	0.25	0.9822	0.81	0.2	4.6	8.4
BH460E540	0.20	0.9722	0.78	0.3	4.9	11.2
BH440E560	0.22	0.9724	0.73	0.3	5.3	15.9
BH420E580	0.17	0.9829	0.54	0.4	7.3	22.2
BE5-100	0.13	0.9931	0.59	0.6	8.7	29.8
BH15-100	0.27	0.9932	0.81	0.2	3.0	6.3
BH1580E220	0.23	0.9811	0.77	0.3	5.2	8.9
BH1560E240	0.21	0.9720	0.72	0.3	5.9	12.9
BH1540E260	0.17	0.9753	0.66	0.4	6.8	17.8
BH1520E280	0.14	0.9811	0.62	0.5	8.7	24.3
BH1580E520	0.25	0.9830	0.81	0.3	5.7	9.3
BH1560E540	0.23	0.9780	0.76	0.3	6.3	13.2
BH1540E560	0.19	0.9644	0.72	0.3	6.8	19.3
BH1520E580	0.15	0.9833	0.71	0.4	8.2	24.3
BH10-100	0.26	0.9908	0.70	0.2	3.2	8.7
BH1080E220	0.22	0.9833	0.71	0.3	5.9	10.2
BH1060E240	0.18	0.9733	0.68	0.4	6.6	15.7
BH1040E260	0.15	0.9982	0.60	0.4	7.3	20.1
BH1020E280	0.15	0.9821	0.56	0.5	8.2	23.3
BH1080E520	0.24	0.9788	0.69	0.3	6.1	11.2
BH1060E540	0.22	0.9722	0.66	0.4	6.9	16.2
BH1040E560	0.18	0.9822	0.68	0.4	7.8	20.9
BH1020E580	0.14	0.9722	0.54	0.5	8.2	23.2

K- release rate constant (h^{-n}), R^2- regression coefficient, n- release exponent indicate the mechanism of drug release, $t_{10\%}$, $t_{50\%}$ and $t_{90\%}$- time taken (in h) for 10, 50 and 90 % drug release respectively.

Table 6.9: Stability study results selected brimonidine tartrate ocular insert formulations stored at various conditions.

Formulation Code	Storage condition	Drug content		K_{deg} x 10^3 (month $^{-1}$) (Mean ± SD)
		Initial	After 6 M	
BP140ERS60	Ambient	98.02 ± 2.11	97.22 ± 2.21	0.34 ± 0.03
	ATC	98.02 ± 2.11	92.01 ± 1.91	3.52 ± 0.04
BP140ERL60	Ambient	99.45 ± 3.33	96.77 ± 1.22	0.36 ± 0.02
	ATC	99.45 ± 3.33	94.33 ± 1.92	3.57 ± 0.05
BP440ERS60	Ambient	102.22 ± 1.21	99.33 ± 1.45	0.29 ± 0.07
	ATC	102.22 ± 1.21	95.33 ± 2.32	4.33 ± 0.06
BP440ERL60	Ambient	98.33 ± 2.11	95.33 ± 1.83	0.34 ± 0.03
	ATC	98.33 ± 2.11	92.33 ± 2.44	3.52 ± 0.04
BP120E280	Ambient	99.22 ± 1.96	95.22 ± 1.56	0.56 ± 0.02
	ATC	99.22 ± 1.96	92.22 ± 1.36	4.77 ± 0.05
BP140E560	Ambient	100.23 ± 2.64	97.27 ± 2.44	0.49 ± 0.07
	ATC	100.23 ± 2.64	93.23 ± 1.64	4.04 ± 0.03
BP440E260	Ambient	99.21 ± 1.22	97.21 ± 1.32	0.31 ± 0.04
	ATC	99.21 ± 1.22	94.21 ± 1.22	4.16 ± 0.04
BP460E540	Ambient	99.34 ± 0.59	97.34 ± 0.19	0.57 ± 0.05
	ATC	99.34 ± 0.59	93.34 ± 0.99	3.34 ± 0.03
BH440ERL60	Ambient	99.01 ± 3.22	95.01 ± 2.22	0.62 ± 0.04
	ATC	99.01 ± 3.22	90.01 ± 1.22	4.36 ± 0.02
BH1540ERS60	Ambient	99.42 ± 1.46	96.22 ± 1.56	0.56 ± 0.02
	ATC	99.22 ± 1.96	92.22 ± 1.36	4.77 ± 0.05
BH1040ERL60	Ambient	100.23 ± 2.64	97.27 ± 2.44	0.49 ± 0.07
	ATC	100.23 ± 2.64	93.23 ± 1.64	4.04 ± 0.03
BH440E560	Ambient	99.21 ± 1.22	97.21 ± 1.32	0.31 ± 0.04
	ATC	99.21 ± 1.22	94.21 ± 1.22	4.16 ± 0.04
BH1560E540	Ambient	99.34 ± 0.59	97.34 ± 0.19	0.57 ± 0.05
	ATC	99.34 ± 0.59	93.34 ± 0.99	3.34 ± 0.03
BH1040E560	Ambient	99.01 ± 3.22	95.01 ± 2.22	0.62 ± 0.04
	ATC	99.01 ± 3.22	90.01 ± 1.22	4.36 ± 0.02

K_{deg}: degradation rate constant, ATC: Accelerated test condition. T_{90}: shelf life in months. Each data point represents the average of two batches in triplicate with standard deviation

6.5. CONCLUSIONS

In the present study, ocular inserts were prepared by employing hydrophilic polymers such as HPMC (K4M, K15M and K100M) and PEO (PEO 100 kD and PEO 400 kD) with inert, hydrophobic (EC) and/or inert/zwitterionic polymers (ERL 100 and ERS 100) alone and in combination to attain prolonged release of drug while retaining sufficient mucoadhesive properties. The prepared ocular inserts showed good physicochemical properties, like drug content, crushing strength and friability. Mucoadhesive strength was found to be dependent on the proportion of hydrophilic polymer in the formulations. Addition of EC and/or Eudragits to the insert matrix resulted in decrease in mucoadhesive strength, but a prolongation of drug release was observed. In vitro drug release was found to extend up to about 24 h to 36 h. A shift in the mechanism of drug release from non-Fickian anamolous (swelling and erosion) to diffusion controlled was observed, when the proportion of Eudragits/ EC were increased and PEO/ HPMC proportion was decreased in the matrix. In case of formulations with PEO alone, the drug release was found to be dependent on erosion of the polymer, while in the case of Eudragit and EC alone, the drug release dependent predominately on the diffusion with very small degree of swelling. Ocular inserts formulations, which showed desirable in vitro performance (duration of drug release, high degree of mucoadhesiveness) were further evaluated for their in vivo pharmacodynamic efficacy studies.

6.6. REFERENCES

Baeyens V, Felt-Baeyens O, Rougier S, Pheulpin S, Boisrame B, Gurny R. 2002. Clinical evaluation of bioadhesive ophthalmic drug inserts (BODI) for the treatment of external ocular infections in dogs. J. Control. Release, 85; 163-168.

Bozdag S, Weyenberg W, Adriaens E, Dhondt MM, Vergote V, Vervaet C, De Prijck K, Nelis HJ, De Spiegeleer B, Ludwig A, Remon JP. 2010. In vitro evaluation of gentamicin- and vancomycin-containing minitablets as a replacement for fortified eye drops. Drug Dev. Ind. Pharm. Jun 14 [Epub ahead of print].

Bourlais CL, Acar L, Zia H, Sado PA, Needham T, Leverge R. 1998. Ophthalmic drug delivery systems-recent advances. Prog. Retin. Eye Res, 17; 33-58.

Bremecker KD. 1983. Model to determine the adhesive time of mucosal adhesive pintments in vitro. Pharm. Ind, 45; 417-419.

Chandran S. 2003. Studies on novel approaches for better ocular delivery of flurbiprofen. Ph.D Thesis, Birla Institute of Technology and Science, Pilani; 1-383.

Di Colo G, Burgalassi S, Chetoni P, Fiaschi MP, Zambito Y, Saettone MF. 2001. Relevance of polymer molecular weight to the in vitro/in vivo performances of ocular inserts based on poly (ethylene oxide). Int. J. Pharm, 220; 169-177.

Di Colo G, Zambito Y. 2002a. A study of release mechanisms of different ophthalmic drugs from erodible ocular inserts based on poly (ethylene oxide). Eur. J. Pharm. Biopharm, 54; 193-199.

.Di Colo G, Zambito Y, Burgalassi S, Serafini A, Saettone MF. 2002b. Effect of chitosan on in vitro release and ocular delivery of ofloxacin from erodible inserts based on poly(ethylene oxide). Int. J. Pharm, 248; 115-122.

Einmahl S, Zignani M, Varesio E, Heller J, Veuthey JL, Tabatabay C, Gurny R. 1999. Concomitant and controlled release of dexamethasone and 5-fluorouracil from poly(ortho ester). Int. J. Pharm, 185; 189-198.

El-Shanawany S. 1992 Ocular delivery of pilocarpine from ocular inserts, S.T.P. Pharma. Sci, 2; 337-341.

Gilhotra RM, Gilhotra N, Mishra DN. 2009. Piroxicam bioadhesive ocular inserts: physicochemical characterization and evaluation in prostaglandin-induced inflammation. Curr. Eye Res, 34; 1065-1073.

Greaves JL, Olejnik O, Wilson CG. 1992. Polymers and the precorneal tear film. S.T.P. Pharma Sci, 2; 13-33.

Gurtler F and Gurny R. 1995. Patent literature review of ophthalmic inserts, Drug Dev. Ind. Pharm, 21; 1-18.

Hornof M, Weyenberg W, Ludwig A, Bernkop-Schnürch A. 2003. Mucoadhesive ocular insert based on thiolated poly(acrylic acid): development and in vivo evaluation in humans. J. Control. Release, 89; 4194-4228.

Lee CM, Lee YH, Lee VH. 1994. Improved ocular penetration of gentamicin by mucoadhesive polymer polycarbophil in the pigmented rabbit. Invest. Ophthalmol. Vis. Sci, 35; 2809-2814.

Lee Y, Yalkowsky SH. 1999. Systemic absorption of insulin from a Gelfoam ocular device. Int. J. Pharm, 190; 35-40.

Maggi L, Segale, ML, Torre, E, Ochoa M, Conte U. 2002. Dissolution behaviour of hydrophilic matrix tablets containing two different polyethylene oxides (PEOs) for the controlled release of a water-soluble drug, A dimensionality study. Biomaterials, 23; 1113-1119.

Nadkarni SR, Yalkowsky SH. 1993. Controlled delivery of pilocarpine. 1. In-vitro characterization of Gelfoam® matrices. Pharm. Res, 10; 109-112.

Paliwal SK, Chauhan R, Sharma V, Majumdar DK, Paliwal S. 2009. Entrapment of ketorolac tromethamine in polymeric vehicle for controlled drug delivery. Ind. J Pharm. Sci, 71; 687-691.

Peppas NA, Sahlin JJ. 1989. A simple equation for the description of solute release, III. Coupling of diffusion and relaxation. Int. J. Pharm, 57; 169-172.

Pongjanyakul T, Puttipipatkhachorn S. 2007. Modulating drug release and matrix erosion of alginate matrix capsules by microenvironmental interaction with calcium ion. Eur. J. Pharm. Biopharm, 67; 187-195

Saettone MF, Salminen L. 1995. Ocular inserts for topical delivery, Adv. Drug Deliv. Rev, 16; 94-106.

Sasaki H, Tei C, Koyo N, Nakamura J. 1993. Drug release from an ophthalmic insert of a b-blocker as an ocular drug delivery system. J. Control. Rel, 27; 127-137.

Sasaki H, Nagano T, Sakanaka K, Kawakami S, Nishida K, Nakamura J, Ichikawa N, Iwashita J, Nakamura T, Nakashima M. 2003. One-side-coated insert as a unique ophthalmic drug delivery system. J. Control. Release, 92; 241-247.

Simamora P, Nadkarni SR Lee YC, Yalkowsky SH 1998. Controlled delivery of pilocarpine. 2. In-vivo evaluation of Gelfoam® device. Int. J. Pharm, 170; 209-214.

Tatavarti AS, Mehta KA, Augsburger LL, Hoag SW. 2004. influence of methacrylic and acrylic acid polymers on the release performance of weakly basic drugs from sustained release matrices. J. Pharm. Sci, 93; 2310-2331.

Verestiuc L, Nastasescu O, Barbu E, Sarvaiya I, Green KL, Tsibouklis J. 2006. Functionalized chitosan/NIPAM (HEMA) hybrid polymer networks as inserts for ocular drug delivery: synthesis, in vitro assessment, and in vivo evaluation. J. Biomed. Mater. Res. A, 77; 726-35.

Weyenberg W, Bozdag S, Foreman P, Remon JP, Ludwig A. 2006. Characterization and in vivo evaluation of ocular minitablets prepared with different bioadhesive Carbopol-starch components. Eur. J. Pharm. Biopharm, 62; 202-209.

Weyenberg W, Vermeire A, Dhondt MM, Adriaens E, Kestelyn P, Remon JP, Ludwig A. 2004. Ocular bioerodible minitablets as strategy for the management of microbial keratitis. Invest. Ophthalmol. Vis. Sci; 3229-3233.

Worthen DM, Zimmerman TJ, Wind CA. 1974. Evaluation of pilocarpine ocular insert. Invest. Ophthalmol, 13; 296-299.

CHAPTER SEVEN

LONG ACTING NANOPARTICLE FORMULATIONS

7.1. INTRODUCTION

Micro and nanoparticles represent a promising drug delivery carriers for the targeting of drugs to specific organs, tissues and cells of the body. Nanoparticles in the range of 10-1000 nm can be nanospheres or nanocapsules (Kreuter, 1994). Nanospheres are small solid monolithic spheres comprises of a dense solid polymeric network where a pharmacologically active moiety can be either incorporated or adsorbed onto its surface. Nanocapsules are small reservoir type systems with a central cavity surrounded by a polymeric membrane (Fig.7.1). When properly designed can provide a controlled and prolonged drug release without compromising the drug delivery rates and drug bioavailability provided they are retained at the site of application (Mitra, 2003).

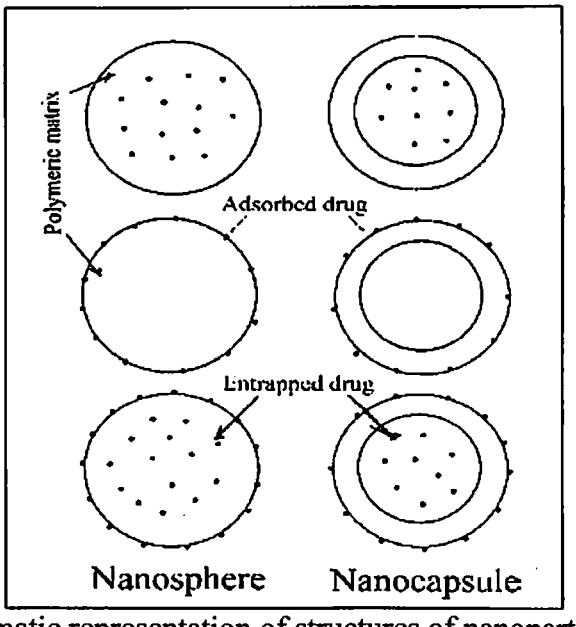

Fig 7. 1: Schematic representation of structures of nanoparticles (Mitra, 2003)

Because of the size of nanoparticles, offer enhanced therapeutic benefit and better stability profile. They offer following advantages (Svetlana et al, 2005; Sultana et al, 2006; Vandervoort and Ludwig, 2007; Hamidi et al, 2008).

a) Improved ocular penetration - The size of nanoparticles can guide them to the targeted ocular tissue by improved passage across various ocular barriers, hence a better therapeutic response.
b) Better ocular localisation and improved targeting.

Other advantages of colloidal drug carriers include high stability, high carrier capacity and, feasibility of incorporation of variety of hydrophobic and hydrophilic molecules; they are well tolerated in the ocular cavity as well as in the other body tissues. When

formulated with some mucoadhesive polymers, a prolonged contact time with the target tissue can be attained. Also a varying and improved drug entrapment can be attained by changing the nature of the polymer employed as well as the method of preparation.

7.1.1. Methods of preparation

Considering the advantages of nanoparticles, various methods are employed in the design and preparation of micro and nanoparticles for ocular drug delivery as presented in the Table 7. 1. The method of preparation and the nature of the polymer to be employed depend largely on the physicochemical properties of the drug. A method which yields high drug incorporation and which renders the system more suitable to attain the desired attributes like targeted/ sustained release for a desired length of time is always the choice in the ocular delivery. Some of the literature reports on the nanoparticle formulations, drugs and polymer employed have been presented in the Table 1.6 (Chapter I- Introduction).

In the current research work, nanoparticles were prepared using Eudragit RS 100/ Eudragit RL 100 and chitosan by multiple emulsion solvent evaporation method and ionotropic gelation method respectively.

(a) Multiple emulsion - solvent evaporation method

In this method, polymer dissolved in an organic solvent is suspended in an aqueous or oily medium to form an emulsion system. The organic solvent is then extracted from the droplets by stirring resulting in the formation of nanoparticles. These particles are then separated by centrifugation, filtration or lyophilization. The size of the emulsion droplets that are formed in the emulsion system mainly determines the diameter of the resultant particles. Barichello et al (1999) compared the encapsulation efficiency using this method for a range of hydrophilic and hydrophobic drugs and concluded that lipophilic drugs can be better encapsulated than the hydrophilic drugs using solvent evaporation technique. The hydrophilic drugs have a poor affinity for the polymer with the drug movement from organic to aqueous phase during emulsification process. Subconjunctival micro and nanoparticles of budesonide have been prepared using polylactic acid polymer by using this method (Kompella et al, 2003).

Table 7.1: Various methods of preparation of nanoparticles employed in ocular drug delivery.

Method of preparation	Polymers employed	Advantages	Disadvantages
Precipitation/coacervation	Bovine serum albumin (Merodio et al, 2002), Poly lactic acid (Bourges et al, 2003), Poly caprolactone (Foucher et al, 2002), Poly-d,l-lactic acid (Giannavola et al, 2003).	• Size of particle can be controlled by varying air pressure or spray-nozzle diameter. • Hardening of particles can be done by using cross linking to that control drug release. • Involves aqueous solvents and mild processing conditions and therefore ideal for maintaining the stability of proteins and peptides	Not suitable for water soluble drugs. Cross linking agent is required such as glutaraldehyde /alcohol.
Emulsification/solvent evaporation	Poly lactic acid (Kompella et al, 2003); Carrasquillo et al, 2003) Poly lactide-co-glycolic acid (Santos et al, 2006; Ayalasomayajula et al, 2005)	• Particle size can be controlled by emulsion droplet size. • Water used as non-solvent simplifies and improves process economics • Applicable to only lipids soluble drugs. • Minimized agglomeration. • High encapsulation efficiency • Reduced encapsulating efficiency. • High batch to batch reproducibility. • Narrow size distribution. • Efficient in encapsulating lipophilic drugs.	• High volumes of water to be eliminated from the suspension. • Leakage of water-soluble drug into the saturated aqueous external phase during emulsification, • High energy requirements in homogenization. • Toxicity due to organic solvent.

Table 7.1 (contd).

Method of preparation	Polymers employed	Advantages	Disadvantages
Microemulsion/ polymerization	Poly cyanoacrylates (Heussler et al 1990; Heussler et al 1992; Zimmer et al, 1991, Zimmer et al, 1994; Zimmer et al, 1995). Methyl methacrylate and sulphopropyl methacrylate (Langer et al, 1997; Salgueiro et al, 2004, De et al, 2003, De et al, 2004)	• pH has to be maintained at critical levels for higher yields. • Addition of drug into the system is critical issue (if added before or during polymerisation, gets incorporated into the particles, after poymerisation-gets adsorbed onto the surface.	• Initiator is required for polymerisation
Ionic gelation method	Chitosan (Calvo et al, 1997; Campos et al, 2001; Cleland et al, 2001; Motwani et al, 2008; Papadimitriou et al, 2008)	• Use of non toxic reagents and simpler method. • Ionic interaction can be controlled by charge density of TPP and chitosan. • Suitable for water soluble drugs and polymers	• Particle separation is difficult, high rpm is required. • Redispersion is difficult; ultrasonication is required • Efficiency of the method is dependent upon the deacetylation of CS. Sometimes aggregation on storage occurs.
Quasi emulsion solvent diffusion.	Chitosan (Kawashima et al, 1993), Acrylates (Pignatello et al, 2002a & b; Pignatello et al, 2006)	• Avoidance of toxic organic solvents commonly used in micro and nanoparticle solvent evaporation techniques	Particle morphology and size is dependent on agitation speed, polymer concentration in the initial ethanol solution and volume and injection rate of the latter.

Nanosized complex of antisense oligonucleotide of transforming growth factor β-2 with polyethylenimine when formulated using PLGA into microspheres by double emulsion solvent evaporation method, showed better intracellular penetration of the oligonucleotide in conjunctival cells and improved bleb survival in a rabbit model after filtration surgery (Santos et al, 2006).

In case of multiple emulsion solvent evaporation technique (Rosa et al, 2002) an emulsion either water in oil or oil in water is dispersed in an aqueous solution containing an emulsifier to form a multiple emulsion and the organic solvent was evaporated at room temperature. Non aqueous solvents can also be used for simple emulsion dispersion (Carrasquillo et al, 2003; Ayalasomayajula et al, 2005). Emulsification/spray drying method was reported by Gavini et al (2004) wherein the emulsion of the drug and the polymer was sprayed through a nozzle resulting in the formation of microspheres.

(b) Ionic gelation method

This method is based on the interaction between the positively charged macromolecules such as tripolyphosphate (TPP) (Fig 7.2) and negatively charged chitosan molecule (Fig 7.3).The interaction is mainly dependent on the charge density of TPP and chitosan, which in turn depends on the pH of the solution (Boonsongrit et al, 2006).

Chitosan nanoparticles were formulated by ionic gelation method for cyclosporine (Campos et al, 2001 &2004) and fluorescine (Cleland et al, 2001). In this method nanoparticles were formed by the interaction of negative groups of tripolyphosphate with the positively charged amino groups of the polymer like chitosan at room temperature. This method has some advantages such as

a) Use of non toxic reagents and simpler method.

This method does not need use of any organic solvent or chemical, hence this method can be widely applied in encapsulating biological molecules.

b) Suitable for water soluble drugs and polymers

In this case particle separation and redipersibility is difficult and therefore requires processing at high rpm and ultrasonication. Efficiency of the method is dependent upon the deacetylation of chitosan. Sometimes aggregation on storage occurs.

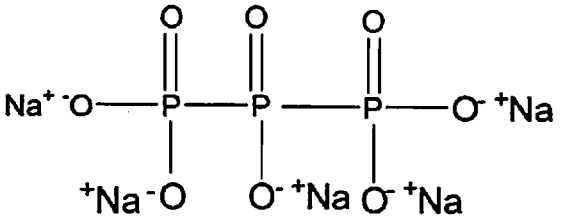

Fig 7. 2: Chemical structure of tripolyphosphate (TPP)

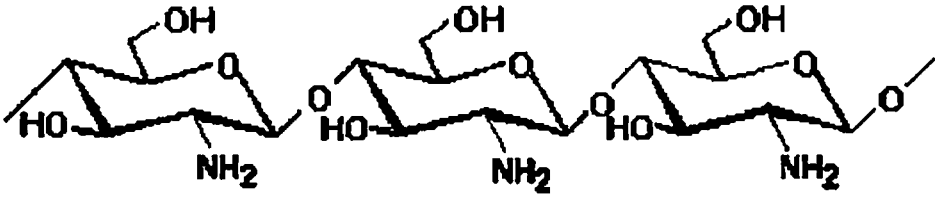

Fig 7.3: Chemical structure of chitosan (Roberts, 1992)

7.1.2. Mechanisms of drug release from micro and nanoparticles

Depending on the polymer employed and composition of the delivery system the release of entrapped drug from the micro and nanoparticles can occur by different mechanisms; (a) diffusion of the drug across the polymer network or across pores filled with fluid, (b) erosion of the matrix, (c) ion exchange process and (d) hydrolysis of the polymer or combination. The polymer employed, its rate of degradation, drug solubility, drug loading, method employed in the preparation determines the release kinetics of the drug from the micro and nanoparticles (Wada et al, 1990; Izumikawa et al, 1991; Ramirez et al, 1999; Burkersroda et al, 1999).

Bioerodible polymers like polyesters and polyanhydrides release the entrapped or encapsulated drug by diffusion or hydrolysis with the rate of diffusion depending on the hydrolysis of the ester or anhydride linkage (Miller et al, 1977). In the case of PLGA and PLA, the drug release occurs by hydrolytic degradation of the polymer chain with the formation of low molecular weight polymers. Rate of degradation in cases of copolymers varies with the lactic and glycolic acid content in the polymer chain (Faisant et al, 2002).

Erosion process can be bulk (homogeneous) or surface (heterogeneous). In case of bulk erosion which usually occurs in polymers having less reactive functional groups, the entire system gets wetted and polymer chain cleavage occurs throughout the system. In contrast, surface erosion is characterized by rapid polymer degradation and occurs mainly within

the outermost layers of the system. Polymers like PLGA are known to erode by bulk erosion process (Miller et al, 1977). Drug release from PLGA microparticles was shown to be biphasic (with initial burst followed by zero order release) and reported to be controlled by diffusion process (Faisant et al, 2002). In case of polycyanoacrylate polymers, the rate of degradation of the polymer and thereby the drug release is governed by alkyl chain length with release occuring by surface erosion mechanism. (Miller et al, 1977; Muller et al, 1990). Addition of ingredients such as dextrose has shown to increase the porosity of the matrix and therefore enhanced disintegration rate with a modified liberation of the drug. Other important mechanism include desorption of the drug from the polymer surface and then diffusion.

Eudragits are a class of synthetic cationic and anionic polymers of dimethyl aminoethyl methacrylates, methacrylic acid, and methacrylic acid esters in varying ratios. They are widely used for coating in the oral formulations to achieve a time-controlled delivery of the drug incorporated in it. Eudragit RS 100 (ERS 100) and Eudragit RL 100 (ERL 100) are inert polymeric resin copolymers of poly (ethacrylate, methylmethacrylate and chlorotrimethyl ammonioethyl methacrylayte) containing an amount of quaternary ammonium groups ranging between 4.5 % to 6.8 % w/w and 8.8 to 12 % w/w or RS and RL respectively. Since they are insoluble in water at physiological pH conditions, and capable of slight swelling, they form good carriers for the dispersion of active compounds (Kawashima et al, 1993; Perumal et al, 1999).

Several reports are available in the literature on the application of ERS 100 and ERL 100 as polymeric carriers for the delivery of drugs. Pignetello et al (2002a) reported the preparation of ERS 100 and ERL 100 based nanosupsensions and studied the effects of these nanoparticles on the ocular tissues to determine the presence of any ocular toxicity. It was concluded that the ERS 100 and ERL 100 based nanosuspensions were well tolerated without any irritability or toxicities. In another study by Pignetello et al (2002b), ERS 100 and ERL 100 based nanoparticles have been prepared for flurbiprofen to improve the bioavailability and to prevent myosis induced during extracapsular cataract surgery. The results showed that the flurbiprofen nanoparticles enhanced the antagonising activity against myosis and increased its active concentration in the aqueous humour.

Eudragit microparticles were reported for gentamicin, a water soluble drug (Al-Kassas, 2004). Microparticles were prepared by multiple emulsion-solvent evaporation method with minor modifications. Various approaches were investigated in order to improve the

drug loading. Anti- microbial efficacy of released drug against Gram-positive and negative organisms were improved by the formulation of drug into microparticulate formulations.

Eudragit RS 100 microspheres containing chitosan were prepared by the solvent evaporation method and their properties were compared with Eudragit RS 100 microspheres without chitosan and studied the effect of process variables on the characteristic of nanoparticles (Krinzar et al, 2003). It was suggested that the process variables have drastic influence on the characteristics such as size and surface of nanoparticles.

Gibaud et al (2004) studied poly (ε-caprolactone) and Eudragit microparticles of fludrocortisone acetate. The study was done with different polymers (poly (ε-caprolactone), Eudragit (RS 100 and RL 100) and different processes (o/w solvent evaporation methods and s/o/w (suspension-in-oil-in-water) evaporation methods. It was observed that all the parameters investigated in the study showed to have improved the encapsulation of drug into the particles.

Esposito et al (1999) reported the preparation of cationic microspheres based on Eudragit RS and cationic agents (i.e. cationic acrylic polymer and three different cationic surfactants) for the delivery of nucleic acids. The type of cationic agents used determined the morphological and dimensional characteristics of microparticles. The designed microparticles displayed very low cytotoxicity on cultured human cell line K562 DDAB18 model.

The main objective of the present work is to formulate nanoparticles of ERS 100 and ERL 100 combination and chitosan by multiple emulsion solvent evaporation method and ionic gelation methods respectively. The effect of various formulation and process variables on the characteristics of the obtained nanoparticles in terms of average particle size, drug loading and loading efficiency were investigated. The in vitro drug release profile of the prepared nanoparticles were studied. Few of the selected formulations were selected for the in vivo studies to ascertain and compare the efficacy of the nanoparticles in animal models.

7.2. MATERIALS AND EQUIPMENTS

7.2.1 Materials

Brimonidine tartrate was obtained as a gift sample from FDC Ltd, Mumbai, India. Eudragit RL 100 and Eudragit RS 100 were obtained from Evonik Degussa, Mumbai, India. Chitosan (deacetylation value of 91.2%) was obtained from Marine Chemicals, Delhi. Soya lecithin, Pluronic PF-68, dialysis membrane (12-14 kDa,) tripolyphosphate

were purchased from Sigma Aldrich, Bangalore, India. Poly (vinyl) alcohol, Tween- 80, acetic acid were purchased from SD Fine Chemicals, Mumbai. India. All other chemicals and reagents used were of analytical grade.

7.2.2. Equipments

The emulsification was carried out using Ultrasonicator (Microsons Probe sonicator (Microsons probe sonicator, Micronix Inc. NY, USA)). Magnetic shaker with heater (MAC Instruments, India) was used for the preparation polymer solution. For all the analytical studies, UV-Visible spectrophotometer, (Jasco, Tokyo, Japan, model V-570) connected to computer loaded with spectra manager® software, with automatic wavelength accuracy of 0.1 nm, a 10 mm matched quartz cells was used. The solvent evaporation was carried out using Rotavapor (Buchi® Rotavapor R-210, Switzerland). Obtained nanoparticles were lyophilized using Heto gel dryer and lyophilizer (Freeze dryer (Maxi Dry Lyo, Heto, Germany). For the characterisation of nanoparticles, Zetasizer (3000HS-Zetasizer, Malvern Instruments Inc. Malvern, UK), scanning electron microscopy (SEM, JSM 840A, Jeol, Japan.) and transmission electron microscopy (TEM, 200CX, Jeol, Japan) were used. In vitro release studies were carried out using USP Type I dissolution apparatus (basket type, Electrolab TDT-08L, Mumbai, India). A pH meter (Eutech, pH Tutor) fitted with glass electrode, filled with potassium chloride solution was used for all the pH measurements.

7.3. METHODS

7.3.1. Preparation of nanoparticles

(i) Preparation of Eudragit based nanoparticles

The procedure involves two steps.

(a) Formation of primary emulsion

The primary emulsion was prepared by dispersing the aqueous phase containing specified amount of drug and organic phase (chloroform, dichloromethane, ethyl acetate) containing varying proportions of polymers (ERL 100 and ERS 100) and surfactants (lecithin). The dispersion was homogenized by ultrasonication (Microsons probe sonicator) at 10 kW energy for 2 minutes in pulsed mode (30 sec per cycle) under controlled temperature (4° C) to reduce the emulsion globule size, resulting in the formation of primary emulsion (w/o).

(b) Preparation of double emulsion

The primary emulsion (w/o) was then slowly injected by an fine syringe into a secondary aqueous phase containing varying proportions of secondary surfactants (PVA, Pluronic PF-68) in phosphate buffer (pH 7.4, 100 mM) under vigorous stirring and ultrasonication (10 kW, RT, 15 min) to form double emulsion (w/o/w).

The resulting double emulsion was allowed to stir for 2 h and the organic phase was evaporated under vacuum in Rotavapor (Buchi® Rotavapor) at room temperature over a period of 30 mins. The obtained nanoparticles were centrifuged, washed with TDW and finally lyophilised at -20° C after adding suitable cryoprotectants (1% w/v mannitol) in glass ampoules for 24 h at 1 mbar pressure and -110 °C temperature to obtain free flowing powder. The thus prepared products were stored in tightly sealed containers under refrigeration.

(ii) Preparation of chitosan based nanoparticles

BRT loaded chitosan nanoparticles were prepared by ionotropic gelation method (Calvo et al, 1997; Campos et al, 2001; Campos et al, 2004; Csaba et al, 2009). Weighed amounts of chitosan was dispersed in water containing 1 % w/v acetic acid in a beaker on a magnetic stirrer and stirred for 4 h till chitosan was completely dissolved. Separately tripolyphosphate solution was prepared in TDW. Nanoparticles were obtained upon addition of TPP solution (0.2 % w/v, 2ml) into a solution of chitosan in 1 % w/v acetic acid on a magnetic stirrer with stirring at high speed and unltrasonication. The resulting dispersion was allowed to stand for 1 h in order to harden the formed nanoparticles. The obtained nanoparticles were separated by centrifugation, washed with water to remove non-entrapped free drug and finally lyophilised.

Different proportions of chitosan and TPP solutions were prepared in order to investigate the optimum ratio resulting in the formation of spherical and narrow sized nanoparticles. Different amounts of drug was used in order to study the effect of initial drug amount on the characteristics of nanoparticles. The effect pH of TPP solution on the characteristics and in vitro release behaviour of nanoparticles was also studied.

7.3.2 Study of effect of formulation and process variables

In case of nanoparticles formulated with ERL 100 and ERS 100, formulation variables investigated include, initial amount of drug, primary emulsifiers and stabilizers (type and proportion), internal phase (volume and pH), external phase (volume and pH), secondary emulsifier (type and proportion) and polymer proportion on the average particle size, drug

loading and entrapment efficiency and in vitro drug release profile. The process variables include emulsification (intensity and duration), evaporation rate (duration and intensity), lyophilisation conditions (type and proportion of cryoprotectants and lyophilisation duration).

In case of chitosan based formulations, variables such as effect of chitosan to TPP ratio, effect of PF-68 proportion, effect of TPP solution pH and effect of initial drug amount on the average particle size, drug loading and entrapment efficiency and in vitro drug release profile were investigated.

The formulation composition and effect of formulation and process variables on each of the selected formulations are shown in the Table 7.2 and in Table 7.3.

7.3.3. Characterisation of nanoparticles

The formulated nanoparticles were evaluated for following characteristics.

(i) Drug content estimation

For ERL 100 and ERS 100 based nanoparticles, the drug content estimation was carried out by dispersing accurately weighed freeze-dried formulations in selected organic solvent (methylene chloride, ethyl acetate) in a calibrated tube under ultrasonication for 10 mins at room temperature. The drug was the extracted by adding phosphate buffer (pH 7.4) and shaking for 10 mins at room temperature. The aqueous layer was separated and diluted suitably and analysed at 248 nm for the drug content using UV-Visible analytical method (as described in Chapter III-Analytical method development).

For chitosan nanoparticles, an accurately weighed amount of nanoparticles were dispersed in 1.0 % v/v acetic acid solution in calibrated tubes under ultrasonication for 15 mins at room temperature. The resulting dispersion was centrifuged (12000 rpm, 25° C), supernatant was collected and diluted suitably with phosphate buffer pH 7.4 and analysed at 248 nm using UV-Visible analytical method (Chapter III).

Table 7.2: Formulation composition for Eudragit based brimonidine tartrate nanoparticle formulations

Formulation code	BRT (mg)*	Org. Phase	ERS:ERL (mg)	LCT (% w/v)	PVA (% w/v)	PF-68 (% w/v)	Internal Phase (ml)	External Phase (ml)	pH (Int. phase/ Ext. phase)
Effect of initial drug amount									
BENP-D10	10	EtOAc	100:100	0.1	-	1.0	3	30	7.4/ 7.4
BENP-D20	20	EtOAc	100:100	0.1	-	1.0	3	30	7.4/ 7.4
BENP-D30	30	EtOAc	100:100	0.1	-	1.0	3	30	7.4/ 7.4
BENP-D40	40	EtOAc	100:100	0.1	-	1.0	3	30	7.4/ 7.4
BENP-D60	60	EtOAc	100:100	0.1	-	1.0	3	30	7.4/ 7.4
Effect of Lecithin proportion									
BENP-L0.05	30	EtOAc	100:100	0.05	-	1.0	3	30	7.4/ 7.4
BENP-L0.10	30	EtOAc	100:100	0.15	-	1.0	3	30	7.4/ 7.4
BENP-L0.15	30	EtOAc	100:100	0.10	-	1.0	3	30	7.4/ 7.4
BENP-L0.20	30	EtOAc	100:100	0.20	-	1.0	3	30	7.4/ 7.4
Effect of internal phase volume									
BENP-IP1	30	EtOAc	100:100	0.10	-	1.0	1	30	7.4/ 7.4
BENP-IP2	30	EtOAc	100:100	0.10	-	1.0	2	30	7.4/ 7.4
BENP-IP3	30	EtOAc	100:100	0.10	-	1.0	3	30	7.4/ 7.4
BENP-IP4	30	EtOAc	100:100	0.10	-	1.0	4	30	7.4/ 7.4
Effect of external phase volume									
BENP-EP20	30	EtOAc	100:100	0.10	-	1.0	3	20	7.4/7.4
BENP-EP30	30	EtOAc	100:100	0.10	-	1.0	3	30	7.4/7.4
BENP-EP40	30	EtOAc	100:100	0.10	-	1.0	3	40	7.4/7.4
BENP-EP60	30	EtOAc	100:100	0.10	-	1.0	3	60	7.4/7.4

BRT- Brimonidine tartrate, (*amount per 200 mg of polymer) EtOAc- ethyl acetate, ERS- Eudragit RS 100, ERL- Eudragit RL 100, LCT- lecithin, PVA- poly vinyl alcohol, PF-68 – Ploxamer pluronic 68.

Table 7. 2: Formulation composition for Eudragit based brimonidine tartrate nanoparticle formulations (contd.)

Formulation code	BRT (mg)*	Org. Phase	ERS:ERL (mg)	LCT (% w/v)	PVA (% w/v)	PF-68 (% w/v)	Internal Phase (ml)	External Phase (ml)	pH (Int. phase/ Ext. phase)
Effect of Secondary emulsifier (PVA)									
BENP-PVA0.5	30	EtOAc	100:100	0.10	0.5	-	3	30	7.4/ 7.4
BENP-PVA1.0	30	EtOAc	100:100	0.10	1.0	-	3	30	7.4/ 7.4
BENP-PVA1.5	30	EtOAc	100:100	0.10	1.5	-	3	30	7.4/ 7.4
BENP-PVA2.0	30	EtOAc	100:100	0.10	2.0	-	3	30	7.4/ 7.4
Effect of secondary emulsifier (PF-68)									
BENP-PF0.5	30	EtOAc	100:100	0.10	-	0.5	3	30	7.4/ 7.4
BENP-PF1.0	30	EtOAc	100:100	0.10	-	1.0	3	30	7.4/ 7.4
BENP-PF1.5	30	EtOAc	100:100	0.10	-	1.5	3	30	7.4/ 7.4
BENP-PF2.0	30	EtOAc	100:100	0.10	-	2.0	3	30	7.4/ 7.4
Effect of Internal phase pH									
BENP-IpH2	30	EtOAc	100:100	0.10	-	0.5	3	30	2.0/ 7.4
BENP-IpH4	30	EtOAc	100:100	0.10	-	1.0	3	30	4.0/ 7.4
BENP- IpH6	30	EtOAc	100:100	0.10	-	1.5	3	30	6.0/ 7.4
BENP- IpH7.4	30	EtOAc	100:100	0.10	-	1.5	3	30	7.4/ 7.4
BENP-IpH8.5	30	EtOAc	100:100	0.10	-	2.0	3	30	8.5/ 7.4

BRT- Brimonidine tartrate, (*amount per 200 mg of polymer) EtOAc- ethyl acetate, ERS- Eudragit RS 100, ERL- Eudragit RL 100, LCT- lecithin, PVA- poly vinyl alcohol, PF-68 – Ploxamer pluronic 68.

Table 7. 2: Formulation composition for Eudragit based brimonidine tartrate nanoparticle formulations (contd.)

Formulation code	BRT (mg)*	Org. Phase	ERS:ERL (mg)	LCT (% w/v)	PVA (% w/v)	PF-68 (% w/v)	Internal Phase (ml)	External Phase (ml)	pH (Int. phase/ Ext. phase)
Effect of external phase pH									
BENP-EpH6	30	EtOAc	100:100	0.10	-	1.0	3	30	7.4/ 6.0
BENP-EpH7.4	30	EtOAc	100:100	0.10	-	1.0	3	30	7.4/ 7.4
BENP- EpH6	30	EtOAc	100:100	0.10	-	1.0	3	30	7.4/ 8.0
BENP-EpH8.5	30	EtOAc	100:100	0.10	-	1.0	3	30	7.4/ 9.0
Effect of polymer proportion									
BENP-P50	30	EtOAc	1:1 (50)	0.10	-	1.0	3	30	7.4/ 7.4
BENP-P100	30	EtOAc	1:1(100)	0.10	-	1.0	3	30	7.4/ 7.4
BENP-P510	30	EtOAc	1:1(150)	0.10	-	1.0	3	30	7.4/ 7.4
BENP-P200	30	EtOAc	1:1(200)	0.10	-	1.0	3	30	7.4/ 7.4
BENP-P100	30	EtOAc	1:2	0.10	-	1.0	3	30	7.4/ 7.4
BENP-P100	30	EtOAc	2:1	0.10	-	1.0	3	30	7.4/ 7.4

BRT- Brimonidine tartrate, (*amount per 200 mg of polymer) EtOAc- ethyl acetate, ERS- Eudragit RS 100, ERL- Eudragit RL 100, LCT- lecithin, PVA- poly vinyl alcohol, PF-68 – Poloxamer Pluronic 68.

Table 7.3: Formulation composition of chitosan based brimonidine tartrate nanoparticle formulations

Formulation code	BRT (mg)	Chitosan (mg)	TPP (mg)	PF-68 (% w/v)	TPP solution pH
(a) Effect of Chitosan to TPP ratio					
BCHN01	60	60	60	0.5	8.4
BCHN02	60	120	60	0.5	8.4
BCHN03	60	180	60	0.5	8.4
BCHN04	60	240	60	0.5	8.4
BCHN05	60	300	60	0.5	8.4
BCHN06	60	360	60	0.5	8.4
(b) Effect of PF-68 proportion					
BCHN07	60	300	60	0.25	8.4
BCHN05	60	300	60	0.5	8.4
BCHN08	60	300	60	0.75	8.4
BCHN09	60	300	60	1.0	8.4
(c) Effect of TPP solution pH					
BCHN10	60	300	60	0.5	2.0
BCHN11	60	300	60	0.5	4.0
BCHN12	60	300	60	0.5	6.0
BCHN05	60	300	60	0.5	8.4
(b) Effect of initial drug amount					
BCHN13	30	300	60	0.5	2.0
BCHN14	90	300	60	0.5	2.0
BCHN15	120	300	60	0.5	2.0
BCHN16	180	300	60	0.5	2.0

BRT- Brimonidine tartrate, TPP- tripolyphospahte, PF-68- Poloxamer pluronic F68,

The drug loading efficiency (LE) was calculated as percentage of the amount of drug encapsulated in comparison to the unit weight of nanoparticle formulation product obtained.

$$\text{Drug Loading Efficiency} = \frac{\text{Drug content in the product obtained (mg)}}{\text{Total product weight (mg)}} \times 100$$

The drug entrapment efficiency (EE) was calculated as percentage of amount of drug encapsulated or entrapped in the nanoparticles in comparison to the initial amount of drug added in the preparation of the formulation.

$$\text{Drug Entrapment Efficiency} = \frac{\text{Drug content in the product obtained (mg)}}{\text{Initial total amount of drug added (mg)}} \times 100$$

(iii) Particle size and size distribution

The particle size analysis of prepared nanoparticle formulations were performed by photon correlation spectroscopy using Malvern Zetasizer (3000HS-Zetasizer, Malvern Instruments Inc. Malvern, UK), The freeze dried nanoparticle formulations were dispersed in Milli-Q water and samples were analysed by particle size analyser at a 90° angle in respect to the incident beam.

(iii) Surface morphology and shape

The surface morphology and shape was studied by scanning electron microscopy (SEM) (JSM 840A, Jeol, Japan.) and transmission electron microscopy (TEM, 200CX, Jeol, Japan). The samples for the study were prepared by dispersing a known amount of nanoparticulate formulations in Milli-Q water and ultrasonicated for 10 mins at room temperature.

Samples for SEM were prepared by mounting the particles in solid state on a carbon mould followed by gold sputtering (two cycles) under vacuum, for 30 mins. The resultant gold coated sample with the holder was mounted under electron microscope camera.

For TEM, the dispersed samples were diluted with 0.02 % w/v phosphotungstic acid in water and mounted on carbon coated copper grid of TEM instrument and was allowed stand for 5 mins. The excess liquid was blotted out and the grid was allowed to dry at room temperature for 30 mins. The samples were then mounted and micrographed at 80-100 kV on a digital TEM station.

(iv) In vitro drug release studies

The in vitro drug release studies of prepared formulations were performed in USP Type I dissolution apparatus (basket type) with modifications. Dialysis membrane (12-14 kD) were used. The studies were carried out in 25 ml of freshly prepared STF (pH 7.4) at 37° C ± 0.5° C, while agitation in the media was maintained by stirring the media at 75 rpm. Accurately weighed nanoparticle formulations were dispersed in 1 ml of STF (pH 7.4). This dispersion was then introduced into a previously treated dialysis membrane pouch with three ends sealed. Following the introduction of dispersion sample, the pouch was sealed at the fourth end and immediately suspended into dissolution medium. Samples (2 ml), were withdrawn at predetermined time intervals, diluted suitably and analysed by previously developed and validated UV- Visible analytical method (Chapter III- Analytical method development). At each sample time point, 2 ml of fresh media was replaced into the release media in order maintain sink conditions and to maintain constant volume of media throughput the study.

Percent drug released was determined based on the initial amount of nanoparticles taken for the studies and were plotted as a function of time (h).

The drug release was then fitted into various drug release kinetic models [(zero order, first order, Higuchi square root model, Korsmeyer- Peppas model (KP)] to ascertain the release kinetics and mechanism of drug release from the formulation matrix. The KP model was employed for the first 60 % drug release and was used to determine the mechanism of drug release form the nanoparticulate matrices.

The KP model is given by

$$M_t / M_\infty = K\, t^n$$

Where K is kinetic constant incorporating structural and geometric characteristics of the matrix, M_t is the amount of drug released at time t and M_∞ is the amount of drug released at infinite time and n is the release exponent, indicative of release mechanism. The values of 'n', 'K' and 'R^2' were used to determine the release rate mechanism and a best fit model. The parameters like $t_{20\%}$ (to ascertain the release of loading dose or burst release from the formulations), $t_{50\%}$ (to compare the formulations in terms of drug release) and $t_{90\%}$ (indicator for the complete release) were computed from best fit models.

(v) Freeze drying and redispersibility

The prepared freeze dried nanoparticle formulations were subjected to physical stability and redipersibility studies. About 20 ml of aliquots of samples were frozen at -40 °C and freeze dried using lyophiliser and gel dryer for 24 h at -110 °C at 1 mbar pressure. At an interval of 1 month, the freeze dried samples, stored at room temperature were rehydrated with the original volume of TDW to restore the initial polymer concentration in small screw capped tubes. The size and size distribution were determined by procedures described earlier earlier.

(vi) Stability studies

The stability studies of selected optimised formulations in dispersed and in freeze dried states were carried out as per ICH guidelines after storage of the formulations for 24 months. The storage conditions employed were ambient (25° C ± 2° C), refrigeration (5° C ± 3° C), and freezed (-20° C ± 5° C) and in ambient (25° C ± 2° C/60 ± 5% RH) conditions At predetermined time intervals, samples were withdrawn, and studied for the characteristics such as loading and entrapment efficiency, particle size and size distribution, in vitro drug release profile.

7.4. RESULTS AND DISCUSSION

7.4.1. Eudragit based nanoparticles

The multiple-emulsion solvent evaporation technique was found to be suitable for the preparation of BRT loaded ERS 100 - ERL 100 nanoparticles. The particles obtained with ERS-ERL were of low mean particle size and well suited for ocular application. The nanoparticles obtained showed improved drug loading and entrapment compared to other reported literatures, but it was still low. The low drug incorporation may be attributed to the water soluble nature of BRT. A rapid diffusion of the drug into the aqueous phase during secondary emulsion formation resulted in a low drug incorporation. Various investigations were carried out by varying the different formulation as well as process variables to improve nanoparticle characteristics.

(a) Effect of initial amount of drug

The initial amount of drug employed in the preparation of nanoparticles did not show any significant effect on the average particle size of the nanoparticle obtained. The particle size remained constant with varying initial amount of drug but a significant change in LE and EE was observed with change in initial drug amount (Table 7.4 and Fig.7.4).

Table 7.4: Effect of initial drug loading on the characteristics of Eudragit based brimonidine tartrate nanoparticle formulations.

Batch code	Initial drug amount (mg)	Nanoparticle characteristics		
		PS (nm)	LE (% w/w)	EE (% w/w)
BENP-D10	10	278 ± 5	4.8 ± 0.4	31.3 ± 1.2
BENP-D20	20	262 ± 5	5.1 ± 0.3	32.2 ± 1.3
BENP-D30	30	299 ± 5	5.2 ± 0.2	34.6 ± 1.2
BENP-D40	40	250 ± 6	8.9 ± 0.8	33.3 ± 0.9
BENP-D60	60	247 ± 3	8.8 ± 0.3	27.9 ± 0.8

PS- average particle size (in nm), LE- Loading efficiency (in % w/w), EE- Entrapment efficiency. Each data represents the average of two batches in triplicate with standard deviation.

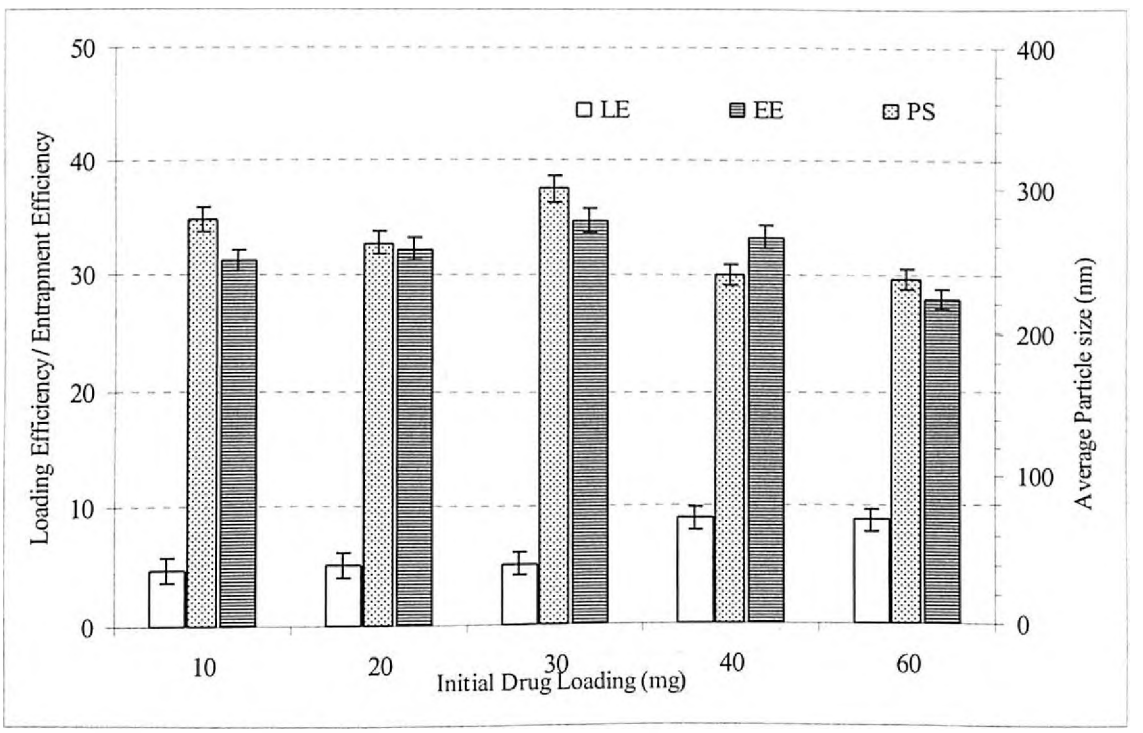

Fig 7.4: Effect of initial drug amount on the characteristics of Eudragit based brimonidine tartrate nanoparticle formulations. Each data represents the average of two batches in triplicate with standard deviation.

A decrease in the initial drug amount from 30 mg to 20 mg resulted in decrease in LE from 5.2 % to 5.1 % w/w, further decrease to 4.8 % with 10 mg of initial drug loading was

also observed. The increase in initial drug amount resulted in increase in LE and EE till 30 mg of initial drug amount. It followed a sigmoidal trend, with further increase in initial drug loading did not result further increase in LE and EE. Both LE and EE increased with increase in initial drug amount till 40 mg, further increase resulted in no change in LE and EE.

(b) Effect of lecithin proportion

Lecithin, used as surfactant and stabilizer in forming w/o emulsion was found to have significant effect on the characteristics of obtained nanoparticles. Lecithin was used as a primary emulsifier in the formation of w/o emulsion which was subsequently emulsified to secondary w/o/w emulsion. From the preliminary studies, it was found that lecithin containing formulations showed a narrow particle size, in comparison to other emulsifiers like Span-80.

Lecithin at a conc. of 0.1 % w/v of primary emulsion produced nanoparticles with average particle size of 299 nm and LE and EE of 5.2 % and 34.6 % respectively. Decrease in lecithin proportion to 0.05 % w/v resulted in increase in average particle size to 312 nm and LE and EE of 7.6 % and 39.9 % respectively (Table 7.5 and Fig 7.5).

Table 7.5: Effect of lecithin proportion on the characteristics of Eudragit based brimonidine tartrate nanoparticle formulations.

Batch code	Lecithin proportion (%)	Nanoparticle characteristics		
		PS (nm)	LE (% w/w)	EE (% w/w)
BENP-L0.05	0.05	312 ± 3	7.6 ± 0.3	39.9 ± 1.0
BENP-L0.10	0.10	299 ± 5	5.2 ± 0.2	34.6 ± 1.2
BENP-L0.15	0.15	254 ± 3	4.8 ± 0.3	20.6 ± 0.9
BENP-L0.20	0.20	237 ± 4	2.5 ± 0.2	18.2 ± 0.8

PS- average particle size (in nm), LE- Loading efficiency (in % w/w), EE- Entrapment efficiency. Each data represents the average of two batches in triplicate with standard deviation.

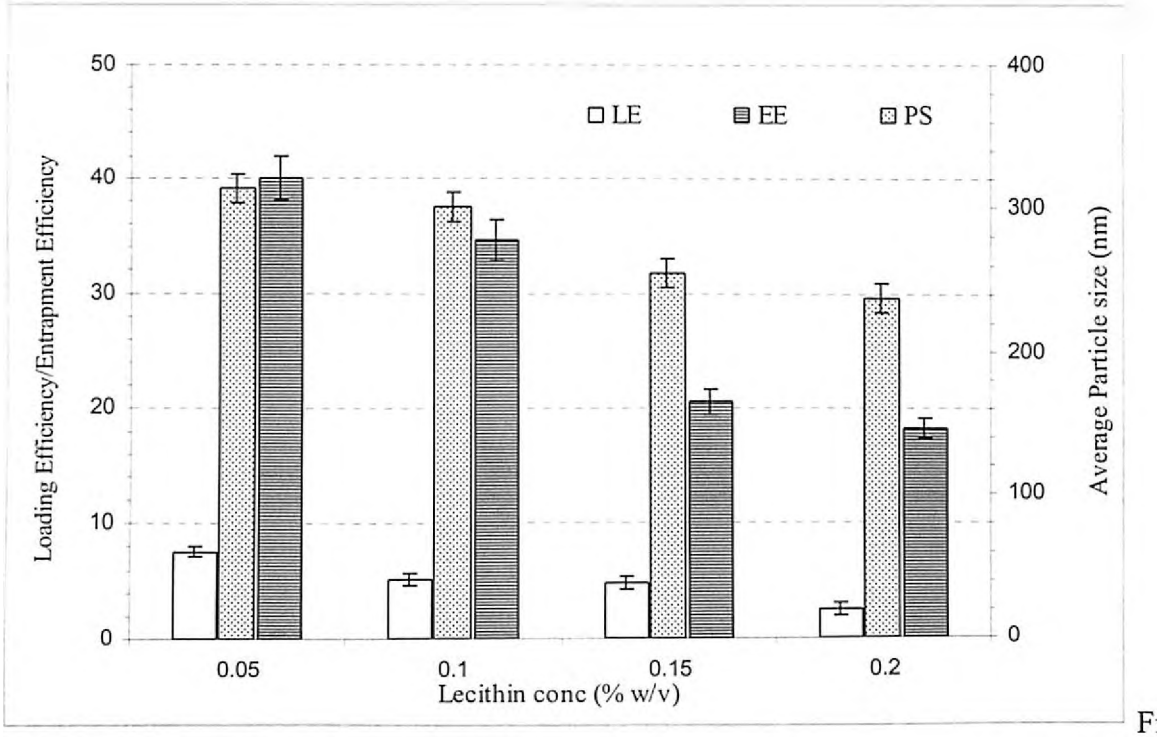

Fig. 7.5: Effect of proportion of lecithin on the characteristics of Eudragit based brimonidine tartrate nanoparticle formulations. Each data represents the average of two batches in triplicate with standard deviation.

Increase in lecithin proportion to above 0.1 % w/v, caused a decrease in average particle size. With increase in proportion of 0.15% w/v, the average particle size, LE and EE were found to be 254 nm, 4.8 % and 20.6 % respectively. Further increase in lecithin (0.2 % w/v) resulted in further decrease in particle size to 237 nm with LE decreased to 2.5 % and EE to 18.2 %.

(c) Effect of phase volume

The phase volume ratio in the emulsion preparation greatly influenced the formation of emulsion and hence on the characteristics of the nanoparticles obtained. The results are presented in the Table 7.6 and in Fig.7.6. Decrease in the internal aqueous phase volume in primary emulsion from 4 ml (BENP-IP4) to 1 ml (BENP-IP1) resulted in decreased average particle size from 311 nm to 220 nm. With an internal phase volume of 3 ml (BENP-IP3), the average particle size was found to be 299 nm, LE and EE of 5.2 % and 34.6 % respectively. Increase in internal phase volume to 4 ml (BENP-IP4) resulted in increased average particle size (311 nm) with increased LE (5.9 %) and improved EE (40.1 %). The increase in internal phase volume resulted in decreased the drug concentration in the internal aqueous phase and therefore decreases the loss of drug through diffusion.

Table 7.6: Effect of internal/external phase volume on the characteristics of Eudragit based brimonidine tartrate nanoparticles. Each data represents the average of two batches in triplicate with standard deviation.

Batch code	Internal phase volume (ml)	Ext. Phase volume (ml)	Nanoparticle characteristics		
			PS (nm)	LE (% w/w)	EE (% w/w)
Effect of internal phase volume					
BENP-IP1	1	30	220 ± 2	2.0 ± 0.2	6.8 ± 0.2
BENP-IP2	2	30	258 ± 4	2.9 ± 0.3	5.8 ± 0.4
BENP-IP3	3	30	299 ± 5	5.2 ± 0.2	34.6 ± 1.2
BENP-IP4	4	30	311 ± 5	5.9 ± 0.4	40.1 ± 0.9
Effect of external phase volume					
BENP-EP20	3	20	358 ± 5	7.6 ± 0.2	44.3 ± 2.2
BENP-EP30	3	30	299 ± 5	5.2 ± 0.2	34.6 ± 1.2
BENP-EP40	3	40	245 ± 5	4.2 ± 0.2	31.3 ± 1.3
BENP-EP60	3	60	234 ± 4	4.1 ± 0.2	29.9 ± 2.1

PS- average particle size (in nm), LE- Loading efficiency (in % w/w), EE- Entrapment efficiency. Each data represents the average of two batches in triplicate with standard deviation.

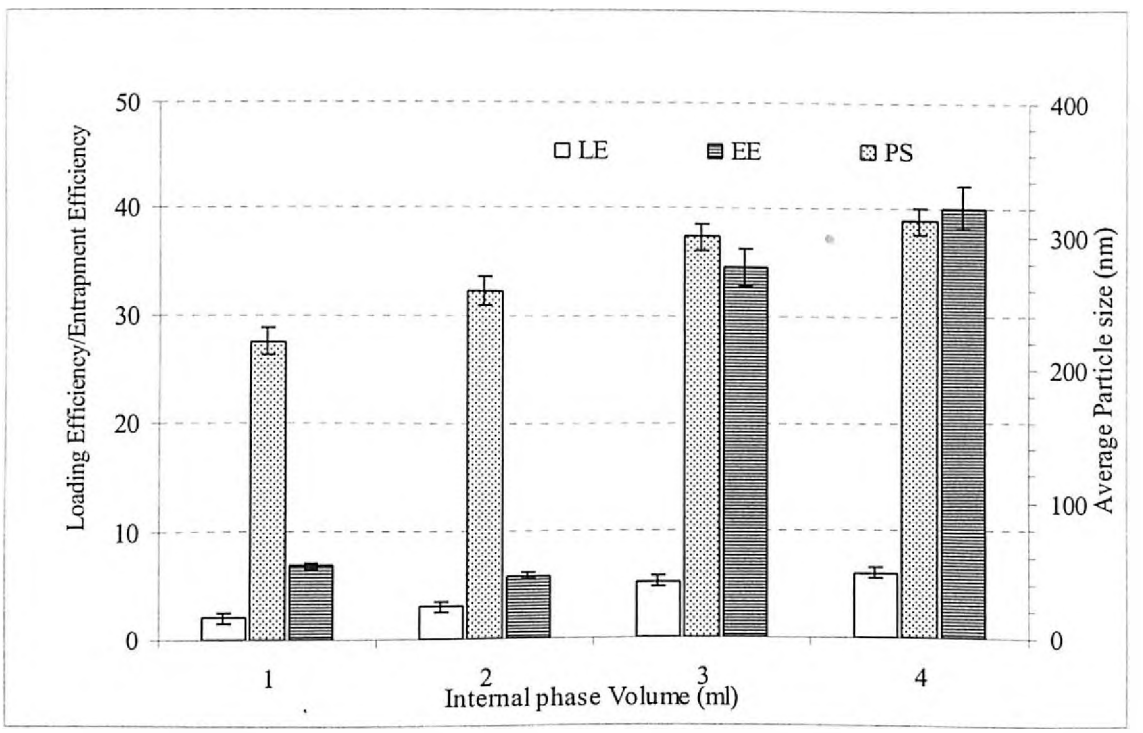

Fig. 7.6: Effect of varying internal phase volume on characteristics of Eudragit based brimonidine tartrate nanoparticle formulations. Each data represents the average of two batches in triplicate with standard deviation.

Decrease in internal phase volume resulted in the formation of concentrated drug solution, hence a decrease in LE and EE were observed with decrease in internal phase volume.

Also during emulsification process, with constant energy and duration, decrease in internal phase volume resulted in decrease in droplet size of primary emulsion, resulting in decrease in average particle size. The increase in number of droplets with smaller size, also contributed to the loss of drug by diffusion.

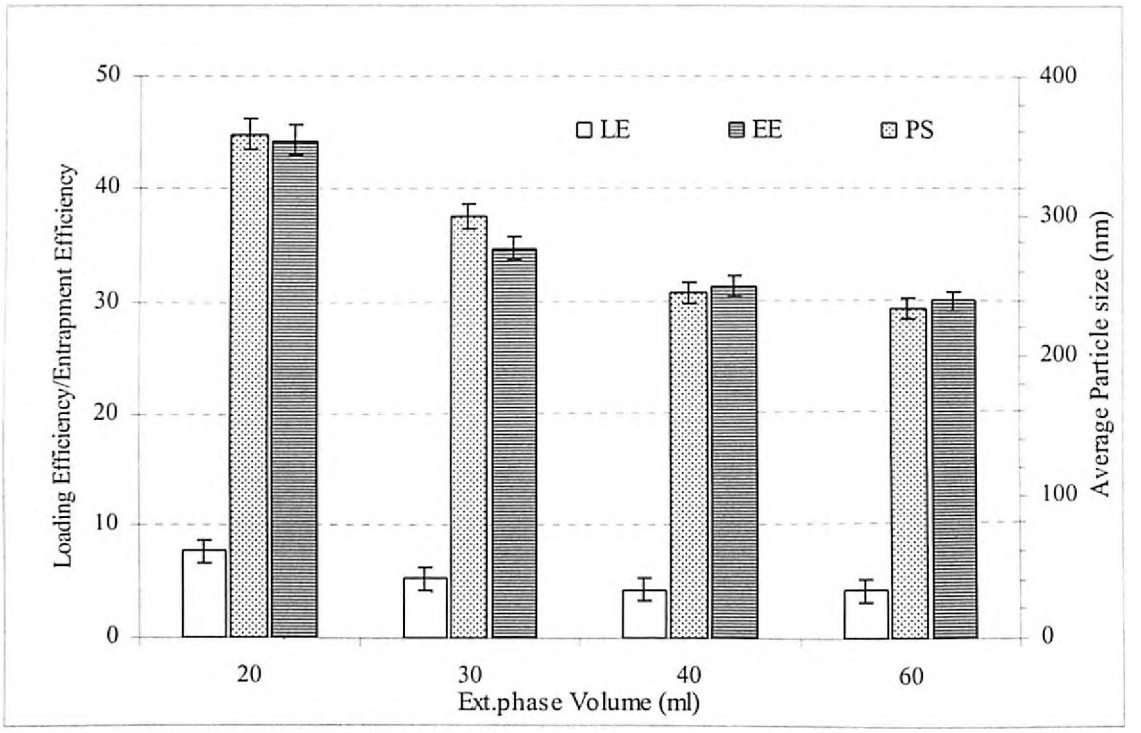

Fig 7.7: Effect of varying external phase volume on the characteristics of Eudragit based brimonidine tartrate nanoparticle formulations. Each data represents the average of two batches in triplicate with standard deviation.

External phase volume (the volume of secondary phase in multiple emulsion) also played a important role in the characteristics of nanoparticles. From the Table 7.6 and Fig 7.7, it is clear that the formulation with 30 ml of external phase showed an avg. particle size of 299 nm, LE of 5.2 % and EE of 34.6 %. Decrease in external phase volume to 10 ml increased average particle size to 358 nm. The LE and EE increased significantly with decrease in the volume of external aqueous phase. The decreased volume might have caused decrease in the loss of drug due to diffusion. An increase in the volume from 30 ml (BENP01) to 60 ml (BENP14) resulted in average particle size of 234 nm.

(d) Effect of aqueous phase pH

As shown in the Table 7.7 and Fig 7.8, the aqueous phase pH was found exhibit a tremendous influence on nanoparticle characteristics and in vitro drug release profiles. The pH of both internal phase and external phase at 7.4 resulted in narrow particles size range

and good LE and EE. Decrease in the internal phase pH, increased the average particle size and increased LE and EE considerably.

Table 7.7: Effect of phase pH (internal and external) on the characteristics of Eudragit based brimonidine tartrate nanoparticle formulations.

Batch code	Internal phase pH	External phase pH	Nanoparticle characteristics		
			PS (nm)	LE (% w/w)	EE (% w/w)
Effect of internal phase pH					
BENP-IpH2	2.0	7.4	389 ± 4	12.4 ± 0.3	51.2 ± 1.2
BENP-IpH4	4.0	7.4	354 ± 4	9.6 ± 0.4	44.6 ± 2.1
BENP- IpH6	6.0	7.4	324 ± 3	7.3 ± 0.3	39.6 ± 2.7
BENP- IpH7.4	7.4	7.4	299 ± 5	5.2 ± 0.2	34.6 ± 1.2
BENP-IpH8.5	8.5	7.4	279 ± 4	3.2 ± 0.3	23.6 ± 2.3
Effect of external phase pH					
BENP-EpH6	7.4	6.0	243 ± 5	4.0 ± 0.1	34.2 ± 1.42
BENP-EpH7.4	7.4	7.4	299 ± 5	5.2 ± 0.2	34.6 ± 1.2
BENP-EpH8	7.4	8.0	321 ± 4	8.9 ± 0.2	49.6 ± 1.1
BENP-EpH9	7.4	9.0	345 ± 4	13.2 ± 0.2	59.3 ± 2.1

PS- average particle size (in nm), LE- Loading efficiency (in % w/w), EE- Entrapment efficiency. Each data represents the average of two batches in triplicate with standard deviation.

The pH of the solution governed the ionisation of the drug and hence its solubility. BRT, a weakly basic drug with pKa of 7.22, exhibits predominately in ionised form at acidic pH ranges where its solubility is higher. Therefore at acidic pH, the drug loss due to rapid diffusion into external phase was diminished and hence entrapment of drug into the nanoparticle was found to increase (Fig. 7.8).

Increase in internal phase pH largely determines the ionisation of drug from 2.0 to 7.4. Ionisation of the drug decreases with increase in pH and therefore resulted in a decrease in average particle size while drug loading and entrapment decreased. The decrease in LE and EE could be due to the fact that increase in pH decreases the solubility of drug in the internal phase, hence higher trend for diffusion of drug into the external phase (Fig. 7.8).

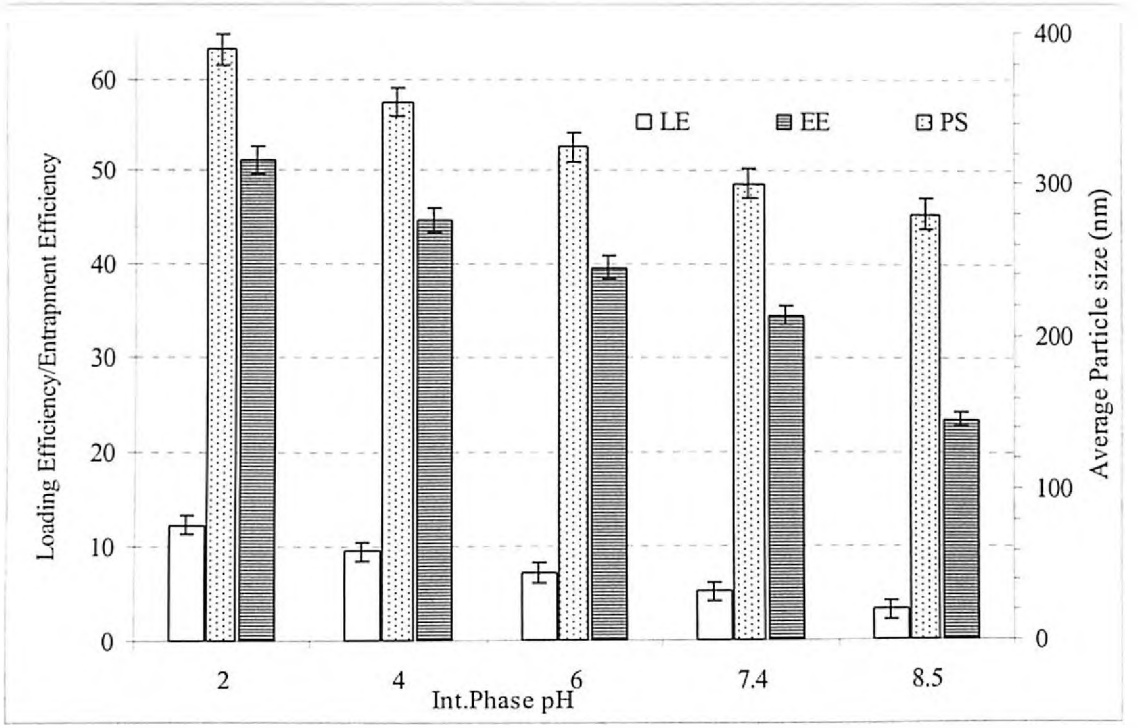

Fig 7.8: Effect of varying internal phase pH on characteristics of Eudragit based brimonidine tartrate nanoparticle formulations. Each data represents the average of two batches in triplicate with standard deviation.

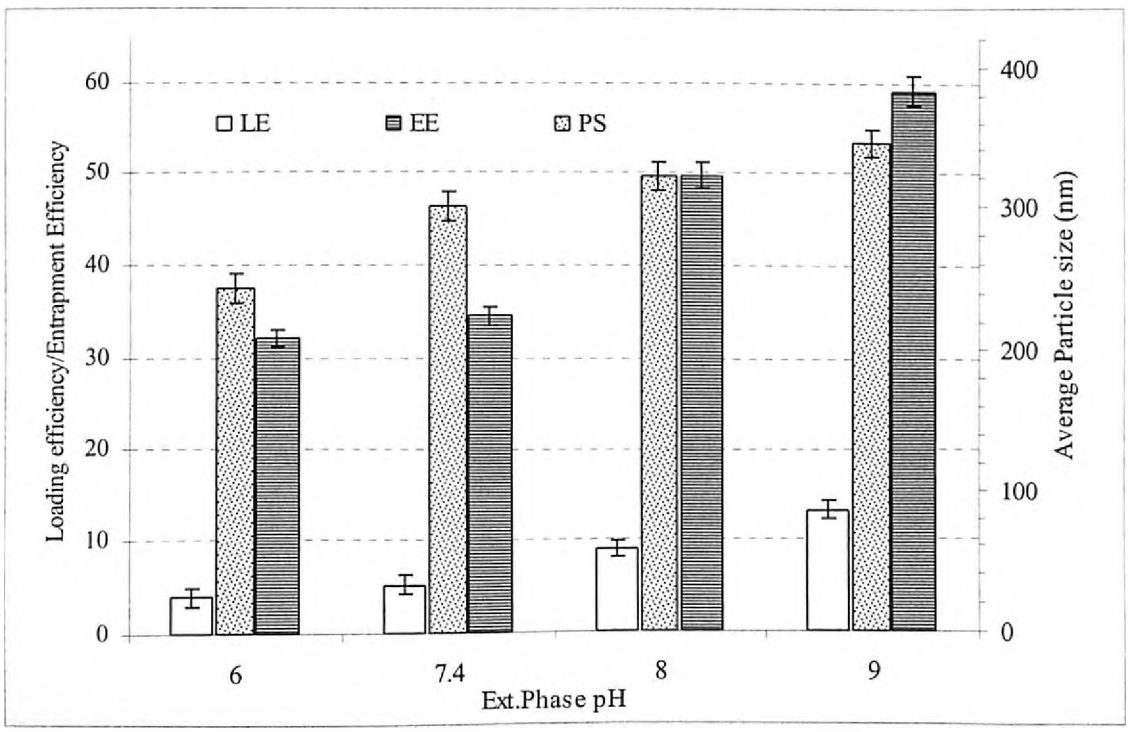

Fig 7.9: Effect of varying external phase pH on characteristics of Eudragit based brimonidine tartrate nanoparticle formulations. Each data represents the average of two batches in triplicate with standard deviation.

As shown in Fig 7.9, at higher pH values of external phase, an increase in average particle size, increase in drug loading and entrapment efficiency was observed. At lower pH of external phase where solubility of drug was higher, increased diffusion drive for drug

diffusion, but at higher pH the solubility decreased, hence LE and EE increased. At external phase pH of 7.4, a loading of 13.2% and entrapment of 59.3% was observed.

(e) Effect of secondary emulsifier (type and proportion)

Modification in the type and proportion of secondary emulsifier influenced the characteristics of nanoparticles. A steady decrease in the average particle size was observed with an increase in the PVA concentration. PVA being surfactant aligns itself in the oil/water interface and greatly reduces interfacial tension between the phases and helps in reducing the droplet size of secondary emulsion. This also contributed to decreased agglomeration of formed nanoparticles resulting in formation of small sized particles with narrow size range. Increase in concentration of PVA in the formulation resulted in nanoparticles of BRT with decreased size and narrow size range. The results are represented in the Table 7.8 and in Fig. 7.10.

Table 7.8: Effect of different proportion of PVA/ PF-68 on the characteristics Eudragit based brimonidine tartrate nanoparticle formulations.

Batch code	PVA proportion (% w/v)	PF-68 proportion (% w/v)	Nanoparticle characteristics		
			PS (nm)	LE (% w/w)	EE (% w/w)
Effect of PVA proportion					
BENP-PVA0.5	0.5	-	325 ± 4	5.21 ± 0.2	35.9 ± 2.8
BENP-PVA1.0	1.0	-	289 ± 4	7.0 ± 0.3	38.4 ± 2.1
BENP-PVA1.5	1.5	-	268 ± 5	9.0 ± 0.3	46.0 ± 2.0
BENP-PVA2.0	2.0	-	258 ± 4	10.9 ± 0.2	51.2 ± 2.9
Effect of PF-68 proportion					
BENP-PF0.5	-	0.5	368 ± 4	4.9 ± 0.2	31.2 ± 1.8
BENP-PF1.0	-	1.0	299 ± 5	5.2 ± 0.2	34.6 ± 1.2
BENP-PF1.5	-	1.5	241 ± 4	8.0 ± 0.2	42.0 ± 2.0
BENPPF-2.0	-	2.0	221 ± 3	11.0 ± 0.2	49.6 ± 2.1

PS- average particle size (in nm), LE- Loading efficiency (in % w/w), EE- Entrapment efficiency. Each data represents the average of two batches in triplicate with standard deviation.

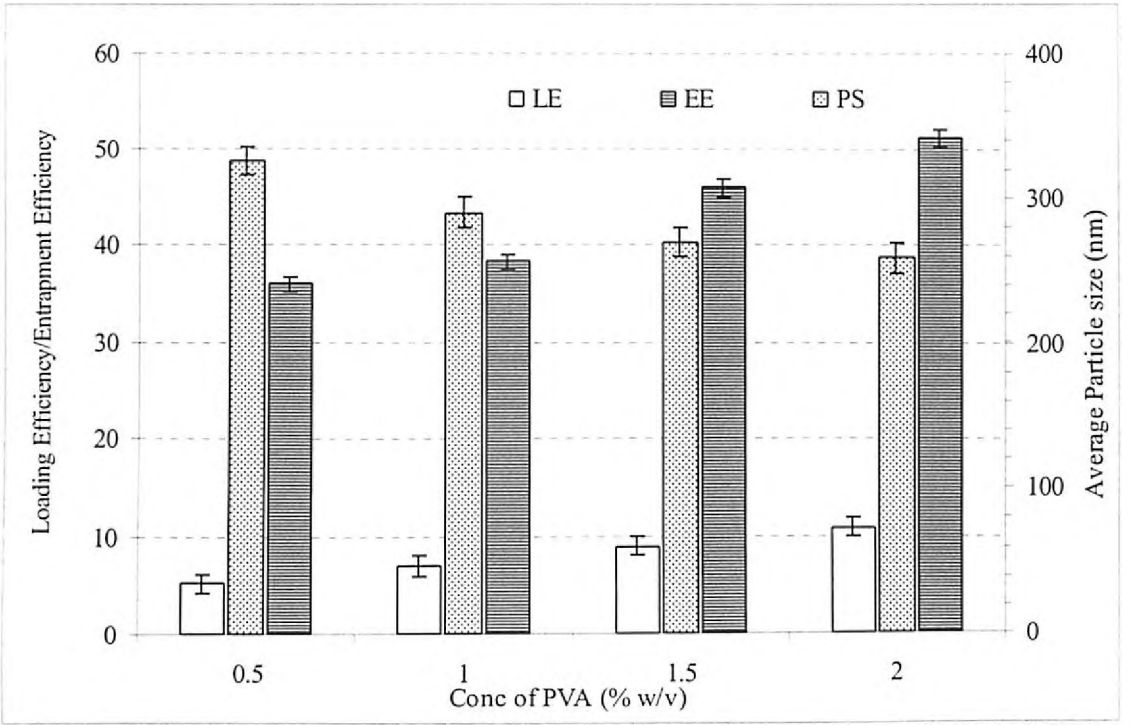

Fig. 7.10: Effect of varying PVA proportion on the characteristics of Eudragit based brimonidine tartrate nanoparticle formulations. Each data represents the average of two batches in triplicate with standard deviation.

The LE and EE increased with increase in the PVA concentration. At lower concentration the LE and EE were found to be 5.2 % and 35.9% for formulations with 0.5% PVA. Increasing the PVA concentration to 2 % resulted in increase in LE and EE to 10.8 % and 45.9 % respectively. At higher proportion of PVA, due to the formation of stable secondary emulsion and uniform dispersion of the drug, probably decreased the drug loss and hence increased drug encapsulation.

When PF-68 was used as secondary emulsifier, as shown in Table 7.8 and Fig.7.11, similar trends were observed. With PF-68 concentration of 1.0 % w/v, the average particle size was 299 nm, LE and EE were found to be 5.2 % and 34.6 % respectively. Decrease in PF-68 concentration, increased average particle size and correspondingly LE and EE decreased. Like PVA, PF-68 has emulsion stabilising property, did not incorporate viscosity to the solution, hence net shear during emulsification would be higher than that of PVA, which ultimately contributed to smaller as well as narrower average particle size when compared to PVA based formulations.

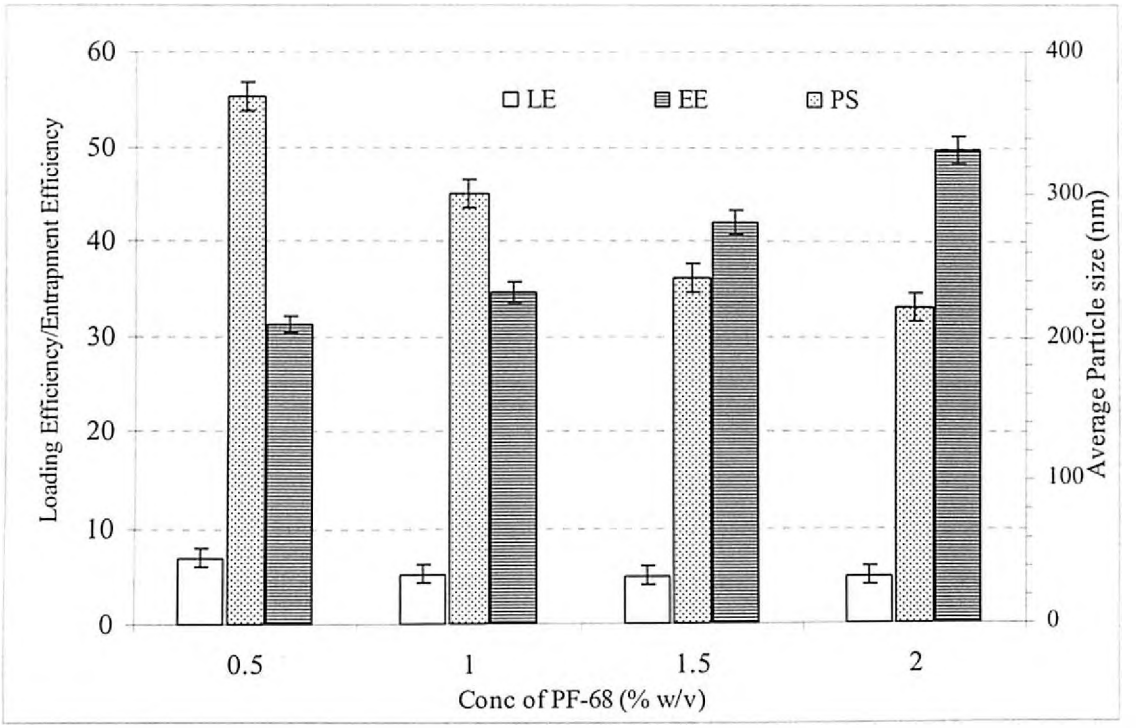

Fig. 7.11: Effect of varying PF-68 proportion on the characteristics of Eudragit based brimonidine tartrate nanoparticle formulations. Each data represents the average of two batches in triplicate with standard deviation.

The in vitro drug release profiles of varying proportions of PVA is shown in Fig. 7.12.

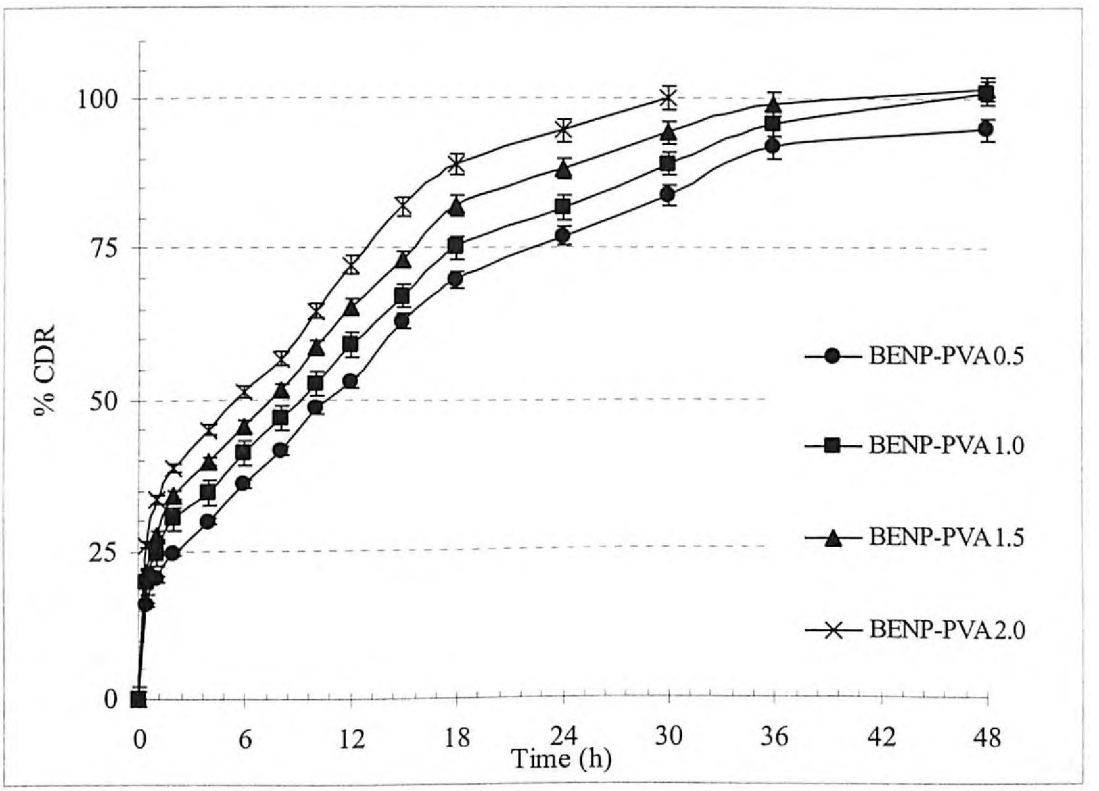

Fig.7.12: In vitro release profiles of Eudragit based brimonidine tartrate nanoparticle formulations prepared with different proportions of PVA. Each data point represents the average of two batches in triplicate with standard deviation.

It is evident that the formulations with higher proportion of PVA resulted in higher initial burst release and drug release was faster than the formulations with lower proportion of PVA. The dissolution and release of surface bound PVA molecules in the nanoparticles caused the initial high release. The formulations with lower proportion of PVA found to prolong the release of drug for a longer period of time.

Similar drug release profile was observed for formulations with PF-68 as secondary emulsifier, with the rate of drug release increased and duration of release decreased with increase in PF-68 concentration (Fig 7.13). The data for the drug release kinetic models is presented in Table 7.10.

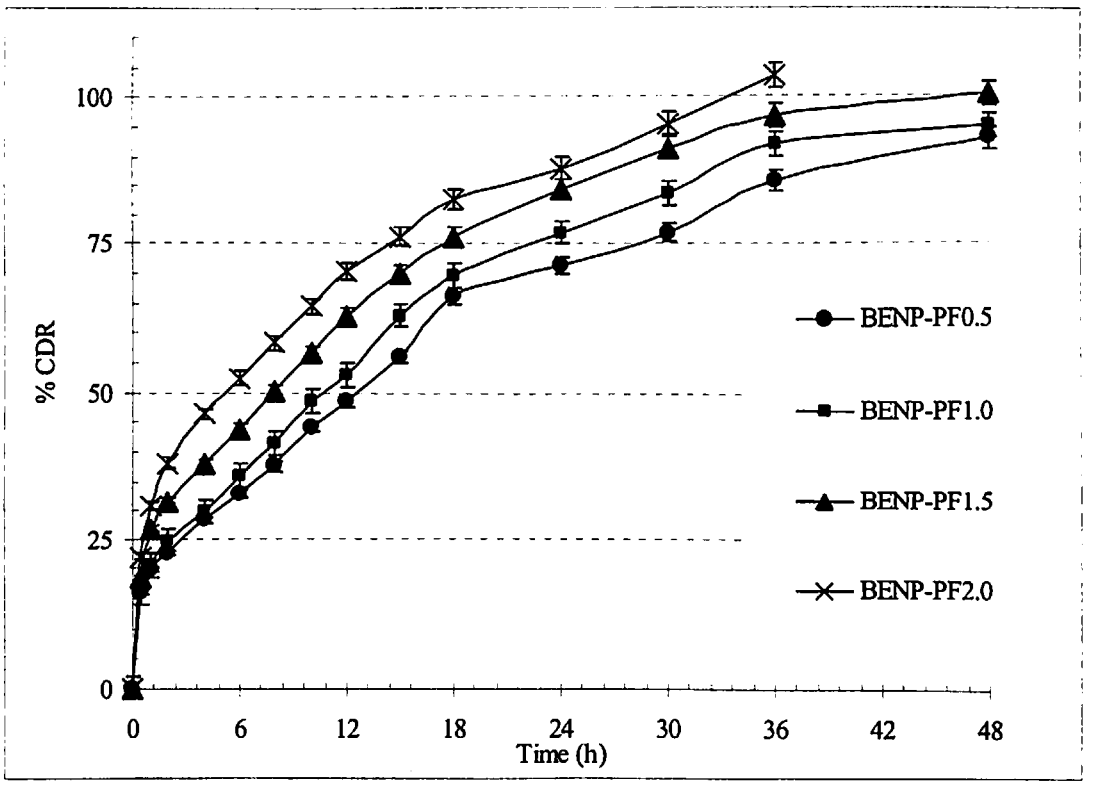

Fig 7.13: In vitro release profiles of Eudragit based brimonidine tartrate nanoparticle formulations prepared with different proportions of PF-68. Each data point represents the average of two batches in triplicate with standard deviation.

(f) Effect of polymer proportion

The polymer proportion-either individual or in combination, was found to have profound effect on the characteristics of obtained nanoparticles. The average particle size, LE and EE and in vitro release were found to be largely dependent (Table 7.9 and Fig 7.4) on the polymer proportion in the formulation. Increase in total amount of polymer (ERL 100 and ERS 100 used in the ratio 1:1) from 100 mg to 400 mg showed a significant increase in the average particle from 245 nm to 410 nm. This increase can attributed to the fact that increased polymer percentage resulted in increased extent of agglomeration of formed

particles under constant net shear of emulsification. Formation of high viscous polymer solution and consequent increase in droplet size of emulsion caused an increase in particle size.

Table 7.9: Effect of polymer proportion on the characteristics of Eudragit based brimonidine tartrate nanoparticle formulations.

Batch code	Polymer proportion (ERL:ERS)	Nanoparticle characteristics		
		PS (nm)	LE (% w/w)	EE (% w/w)
BENP-1:1(50)	1:1 (50:50)	245 ± 4	4.1 ± 0.2	30.1 ± 2.0
BENP-1:1(100)	1:1(100:100)	299 ± 5	5.2 ± 0.2	34.6 ± 1.2
BENP-1:1(150)	1:1(150:100)	312 ± 3	4.8 ± 0.1	40.2 ± 1.7
BENP-1:1(200)	1:1(200:200)	410 ± 5	3.4 ± 0.3	59.1 ± 2.1
BENP-1:2	1:2(100:200)	366 ± 4	4.3 ± 0.2	51.2 ± 1.9
BENP-2:1	2:1(200:100)	399 ± 5	4.2 ± 0.5	47.6 ± 1.4

PS- average particle size (in nm), LE- Loading efficiency (in % w/w), EE- Entrapment efficiency. Each data represents the average of two batches in triplicate with standard deviation.

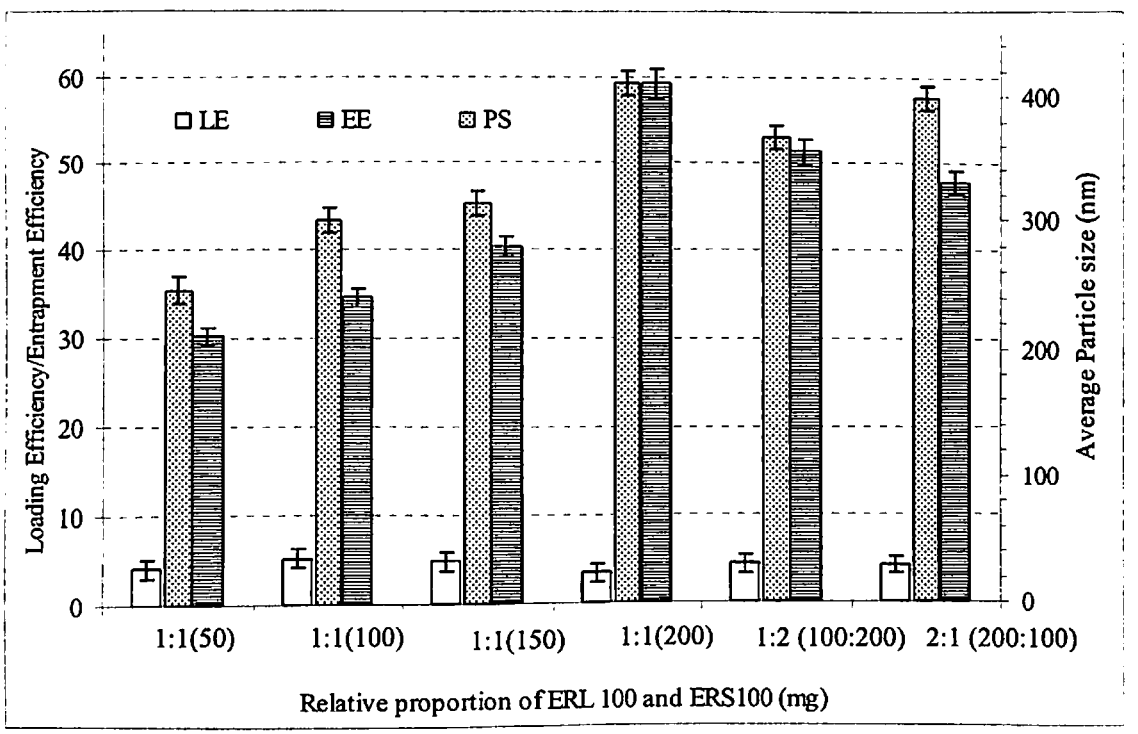

Fig. 7.14: Effect of polymer proportion on characteristics Eudragit based brimonidine tartrate nanoparticle formulations. Each data represents the average of two batches in triplicate with standard deviation.

Entrapment efficiency increased from 30 % [in case of BENP-1:1(50)] to 59.1 % in case of [BENP-1:1(200)], as the total amount of polymer was increased from 100 mg to 400 mg.

The in vitro drug release profile of formulations with varying polymer proportions showed a decreased rate of drug release with increase in total polymer proportion (Fig 7.15). The polymer proportion played major role in determining the burst release, duration of release along with having impact on characteristics of nanoparticles.

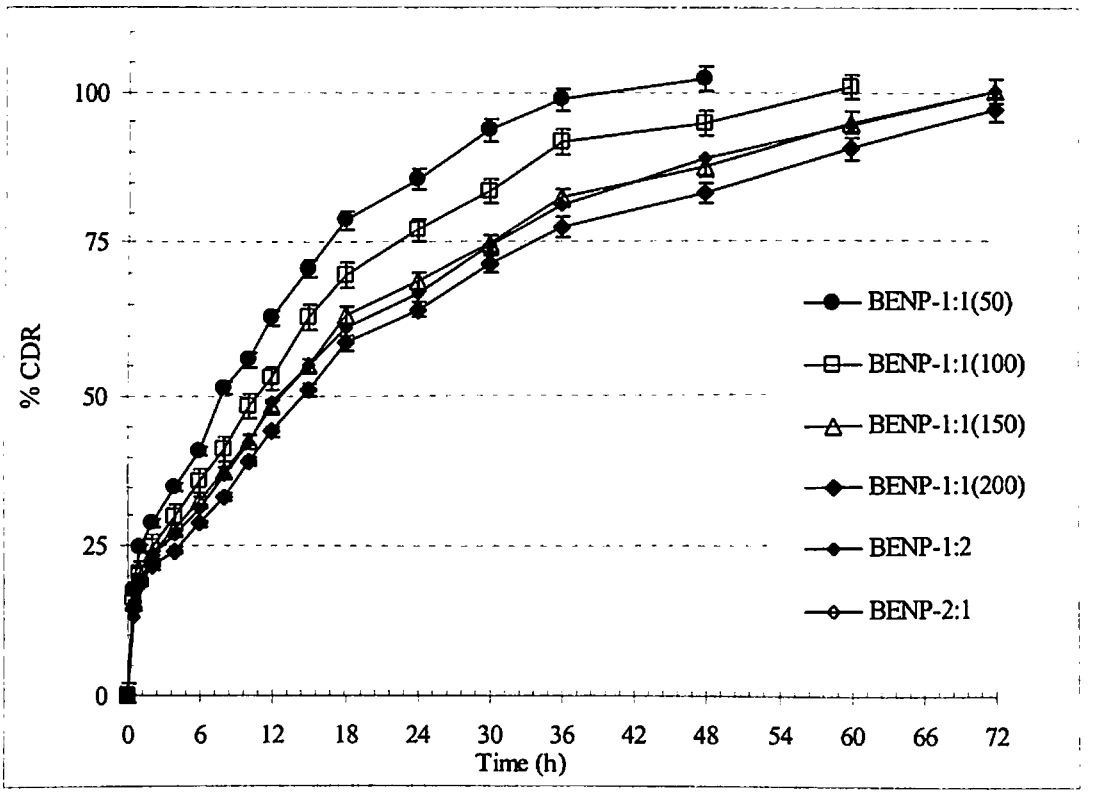

Fig 7.15: In vitro release profiles of Eudragit based brimonidine tartrate nanoparticle formulations prepared with varying proportions of polymer. Each data point represents the average of two batches in triplicate with standard deviation.

Increase in the proportion of ERL 100 and ERS 100 from 1:1 (50: 50) mg to 1:1 (200: 200) mg resulted in tremendous decrease in burst effect from 28.4% [BENP-1:1(50)] to about 15.0% in the case of formulation BENP-1:1(200)). At higher proportions of polymer, the formation of compact matrix and higher degree of encapsulation of drug into the matrix would have resulted in the decreased burst release.

The $t_{20\%}$ for BENP-1:1(50) was found to be 1.4 h while for the formulation BENP-1:1(200) it was found to be 3.7 h. The duration of drug release was also greatly affected by the proportion of polymers in the formulations. As the polymer quantity was increased, the drug release was found to be more sustained for a longer period of time. In the case of formulation BENP-1:1(50), the $t_{90\%}$ value was found to be 25.4 h, while increasing the total polymer amount to 200 mg in BENP-1:1(100:100) resulted in increase of $t_{90\%}$ to 33.9 h. Further increase in total polymer amount to 300 mg in BENP-1:1 (150:150) and to 400

mg in BENP-1:1 (200:200) resulted in further controlled release of the entrapped drug with $t_{90\%}$ values of 45.2 h and 59.4 h respectively with complete release by 72 h.
Variations in the relative proportions of ERL 100 and ERS 100 did not alter the release profile significantly.
The drug release mechanisms for the formulations with varying proportions of PVA, PF-68 and varying amount and proportions of polymer is shown in Table 7.10. In case of formulations with varying PVA proportions, the release exponent 'n' varied from 0.60 to 0.67, suggesting a non-Fickian anamolous drug transport mechanism in the release of drug. Multiple mechanisms such as swelling, erosion, polymer relaxation etc might play a role in drug release. As the proportion of PVA was increased, a gradual decrease in release exponent values was observed. This could be because rapid dissolution of PVA from the surface of the nanoparticles created pores or channels and further drug release might have been through these pores or channels rather than by erosion.
Similar results were also observed in the case of formulations with varying PF-68 as secondary emulsifier. The drug release was by non-Fickian anamolous mechanism.
Formulations with varying amount and proportions of polymer showed drug release mechanism by non-Fickian anamolous transport. Increase in the polymer proportion did not alter the drug release mechanism. The SEM image of representative batch (BENP-1:1(200)) is shown in Fig 7.16.

(g) Freeze drying and redipersibility

Based on the studies on the effect of formulation and process variables, it is evident that increase in stabiliser/surfactant proportion increased the redipersibility of the nanoparticle dispersions. PF-68 demonstrated better average particle size, and also nanoparticle formulation dispersions of PF-68 as surfactant were better redispersible compared to PVA. After some preliminary investigations with and without cryoprotectants, it was observed that use of mannitol as cryoprotectants helped in minimising the effect of vacuum on nanoparticles, thus no significant effect of freeze drying was observed. In the studies of varying formulation and process variables, a constant amount of cryoprotectants was used in all the formulations during the freeze drying process.

Table 7.10: Results of drug release kinetics studies for the Eudragit based brimonidine tartrate nanoparticle formulations fitted into Korsmeyer-Peppas kinetics model.

Batch code	K P model			
	n	$t_{20\%}$ (h)	$t_{50\%}$ (h)	$t_{90\%}$ (h)
Effect of varying proportions of PVA				
BENP-PVA0.5	0.66	3.2	12.1	42.2
BENP-PVA1.0	0.59	2.8	9.2	34.4
BENP-PVA1.5	0.59	2.2	7.9	30.2
BENP-PVA2.0	0.57	1.9	6.6	27.3
Effect of varying proportions of PF-68				
BENP-PF0.5	0.63	2.9	13.0	41.0
BENP-PF1.0	0.49	2.5	10.2	33.9
BENP-PF1.5	0.68	2.1	8.3	31.1
BENPPF-2.0	0.58	1.2	6.8	25.8
Effect of varying amount and proportions of polymer				
BENP-1:1(50)	0.64	1.4	7.3	25.4
BENP-1:1(100)	0.49	2.5	10.2	33.9
BENP-1:1(150)	0.57	3.0	12.8	45.2
BENP-1:1(200)	0.58	3.7	17.3	59.4
BENP-1:2	0.59	2.9	15.7	42.4
BENP-2:1	0.55	2.7	14.1	41.3

n- Release exponent indicator of drug release mechanism, $t_{20\%}$, $t_{50\%,and}$ $t_{90\%}$- time taken (in h) for 20, 50 and 90 % drug release respectively.

(h) Effect of emulsification energy

The intensity and duration of emulsification energy was found to have significant effect on average particle size and drug loading and entrapment efficiency and also on the morphology of nanoparticle surface. A change of sonication energy from 10 to 20 kW resulted in a significant decrease in average particle size from 299 nm to 225 nm, while loading and entrapment efficiency decreased slightly from 5.2 to 4.0 % and entrapment efficiency dropped slightly from 34.6 to 30.0% similar trend was also observed with the increase in the duration of sonication. The decrease in the average particle size with increase in the sonication treatment could be attributed to formation of primary emulsion with smaller dispersed phase droplets. The decrease in drug loading and entrapment

efficiency could be due to slight rise in the temperature of the emulsification system, which could cause enhanced drug diffusion process from the particles.

7.4.2. Chitosan nanoparticles

The preparation of chitosan nanoparticles is based on the pH dependent solubility behaviour of chitosan. It is poorly soluble in water. Solubility of chitosan can be improved by the addition of acids due to the protonation of amino groups present in the structure. Chitosan based nanoparticles were prepared by the ionotrpic gelation method. The nanoparticles were obtained by the interaction between positively charged amino group of chitosan and a negatively charged counter ion of TPP, which eventually resulted in the reduction of aqueous solubility of chitosan. The interaction between chitosan and TPP is greatly dependent on the charge density of chitosan and TPP, which is governed by the pH of solution in which they are present. The effects of these parameters on the characteristics of obtained nanoparticles were investigated extensively. The effects of various formulation variables investigated on the characteristic of obtained nanoparticles are presented in Table 7.11(a) (effect of chitosan to TPP ratio) 7.11(b) [effect of stabilizer proportion (PF-68)], 7.11(c) (effect of TPP solution pH) and 7.11(d) (effect of initial drug amount).

(i) Effect of chitosan to TPP ratio

The formation of nanoparticles by ionotropic gelation method found to depend mainly on the interaction of chitosan and TPP. The ratio between chitosan and TPP was found to be critical on the characteristics of nanoparticles such as the average particle size, drug loading and in vitro release profile. The particle size of the nanoparticles is very critical as it affects the in vitro and in vivo performance of the obtained nanoparticles. The effect of chitosan to TPP ratio on the characteristics of nanoparticles obtained was investigated. The results are shown in Table 7.11(a) and in Fig 7.17. The goal was to determine the optimum ratio that produces nanoparticles of lower particle size with sufficient drug loading.

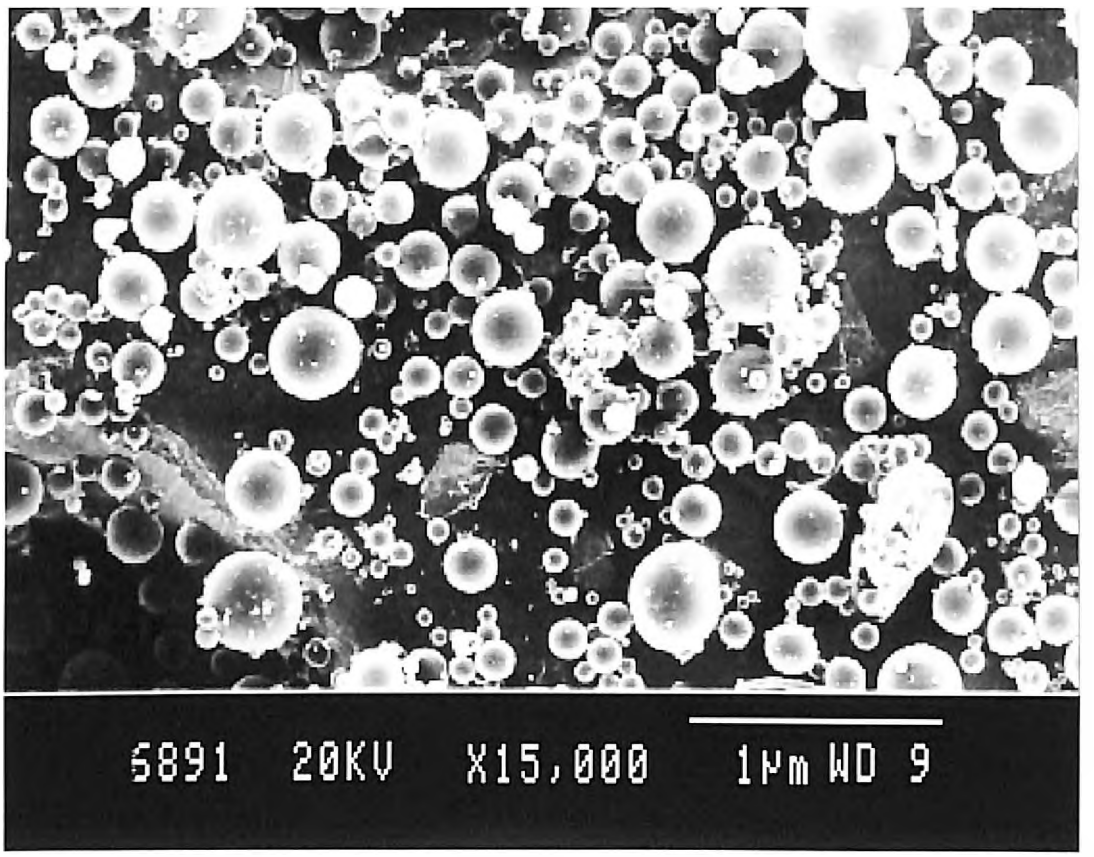

Fig.7.16: Representative scanning electron microscopic image of Eudragit based brimonidine tartrate nanoparticles (Batch Code: BENP-1:1(150)).

Table 7.11(a): Effect of chitosan: TPP ratio on the characteristics of chitosan based brimonidine tartrate nanoparticle formulations.

Batch code	Chitosan : TPP ratio	Nanoparticle characteristics		
		PS (nm)	LE (% w/w)	EE (% w/w)
BCHN01	1:1	411 ± 5	6.8 ± 0.2	34.3 ± 2.0
BCHN02	2:1	377 ± 6	7.3 ± 0.2	39.4 ± 1.2
BCHN 03	3:1	341 ± 4	6.9 ± 0.1	42.1 ± 1.7
BCHN 04	4:1	311 ± 5	7.1 ± 0.3	43.3 ± 2.1
BCHN05	5:1	281 ± 6	7.9 ± 0.2	53.3 ± 1.9
BCHN06	6:1	274 ± 4	7.3 ± 0.5	51.3 ± 1.4

PS- average particle size (in nm), LE- Loading efficiency (in % w/w), EE- Entrapment efficiency. Each data represents the average of two batches in triplicate with standard deviation.

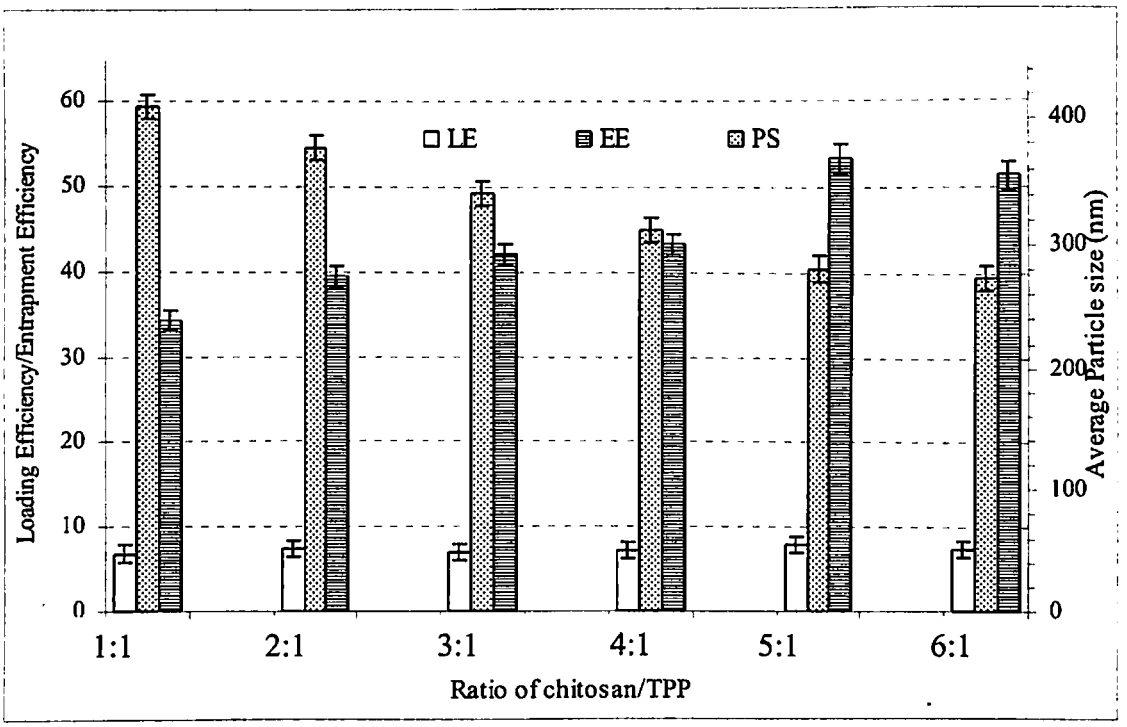

Fig 7.17: Effect of chitosan/TPP ratio on the characteristics of chitosan based brimonidine tartrate nanoparticle formulations. Each data represents the average of two batches in triplicate with standard deviation.

As shown in the Fig 7.17, the average particle size of nanoparticles obtained was found to decrease with an increase in the ratio of chitosan to TPP. At a chitosan to TPP ratio of 1:1, the particles formed had an average particle size of 411 nm. At chitosan to TPP ratio of 5:1, nanoparticles of average particle size 281 nm were obtained. As the ratio was increased, the average particle size decreased significantly. It was found that the optimum chitosan: TPP ratio was 5:1, which might be due to the fact that TPP (Fig 7.2) is a poly-functional cross-linking agent and can create five ionic cross-linking points with amino

groups of chitosan. As a result, the chitosan: TPP ratio of 5:1 led to most efficient cross-linking of amino groups producing the most compact particle structure (Zhang et al, 2004). The LE of nanoparticles prepared at varying chitosan: TPP ratios remained constant while the EE increased with the increase in the ratio. This could be due to formation of spherical particles and hence more drug could get entrapped within the polymeric matrix.

The in vitro release profile of developed chitosan nanoparticles showed BRT release from the chitosan nanoparticles followed a biphasic pattern, characterized by an initial rapid release period (burst release) followed by a period of slower release (Fig 7.18). This is in agreement with reported studies on drug-loaded chitosan nanoparticles (Boonsongrit et al, 2006). The initial fast release might due to the rapid dissolution of the drug located at or close to the surface of the nanoparticles or from the incompletely formed nanoparticles at lower polymer proportions.

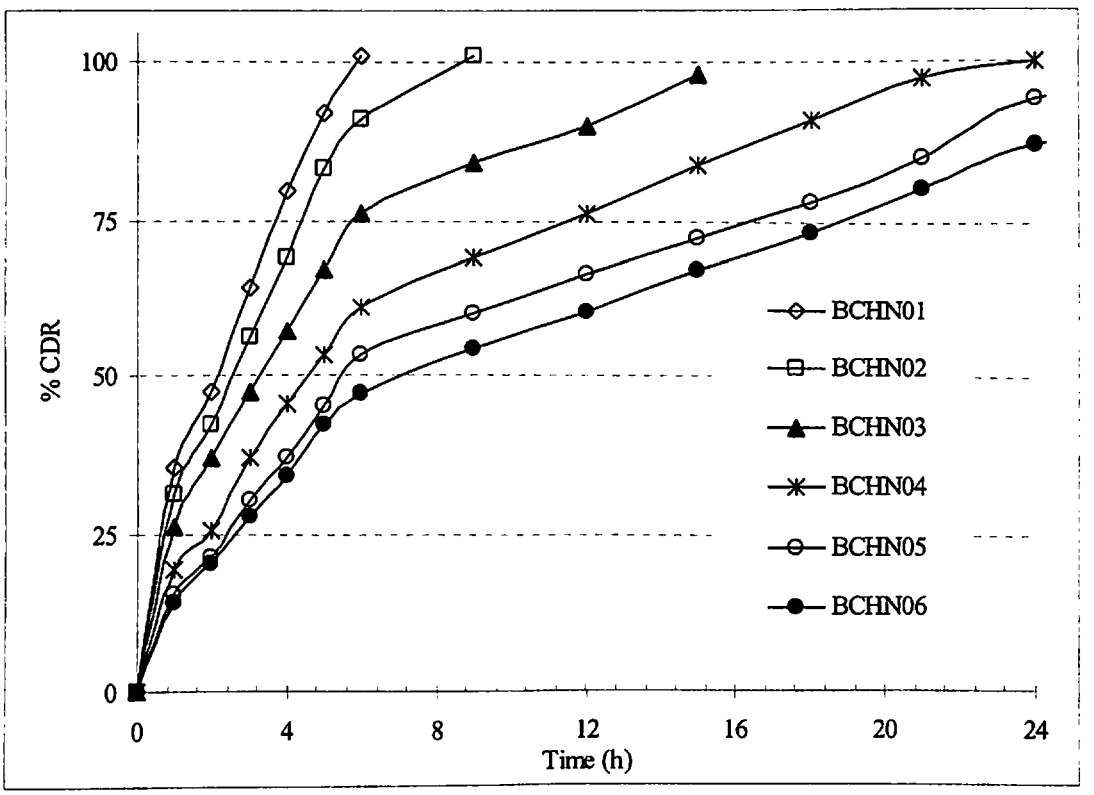

Fig 7.18: In vitro drug release profiles of chitosan based brimonidine tartrate nanoparticle formulations prepared with varying amounts of chitosan to TPP ratios. Each data point represents the average of two batches in triplicate with standard deviation.

As the ratio was increased, the formation of spherical particles were observed and at a chitosan to TPP ratio of 5:1, spherical and narrow sized particles were formed. This formulation showed a controlled release of drug for 30 h ($t_{90\%}$ of 22.4 h) with reduced rapid initial release ($t_{20\%}$ of 2.4 h). The drug release from the chitosan nanoparticles

followed non-Fickian anamolous type drug transport mechanism from the chitosan nanosphere matrices (Table 7.12). Increase in the chitosan proportion with respect to TPP resulted in shifting of 'n' value from 0.83 (CHN01) to 0.64 (BCHN06).

(ii) Effect of stabiliser (PF-68)

The prepared chitosan based nanoparticles showed high degree of agglomeration upon hardening and on standing. The surface of the nanoparticles tends to swell upon contact with water and gradually caused agglomeration. Also when higher proportion of chitosan was used, due to the increase in viscosity of the solution, the homogenous distribution of TPP was not possible. This leads to the formation of agglomerates in the nanoparticles and increased degradation of formed particles. In order to prevent this PF-68 (hydrophilic surfactant and a stabiliser) was used. Use of PF-68 can also prevent the formation of agglomerates and improve stability. As shown in Table 7.11 (b) and as depicted in Fig 7.19, at a PF-68 proportion of 0.5 % w/v, the average particle size of the nanoparticles was found to be 281 nm. With increase in PF-68 proportion in the formulation, particle size was found to be slightly decreasing from 298 nm at 0.25 % w/v to 270 nm at 1.0 % w/v (Fig 7.19). The LE and EE increased gradually with an increase in PF-68 proportion. This could be due to the fact that increase in stabilizer proportion increased the surface properties of nanoparticles with lesser tendency for particle aggregation and leaching of the drug out of matrices. But beyond 0.75 % w/v proportion, no significant increase in LE and EE were observed.

However the in vitro dissolution profile for the formulations with varying amounts of Pf-68 remained unaffected (data not presented).

Table 7.11(b): Effect of stabilizer (PF-68) proportion on the characteristics of chitosan based brimonidine tartrate nanoparticle formulations.

Batch code	PF-68 (% w/v)	Nanoparticle characteristics		
		PS (nm)	LE (% w/w)	EE (% w/w)
BCHN07	0.25	298 ± 6	6.0 ± 0.5	47.4 ± 2.3
BCHN05	0.50	281 ± 4	7.9 ± 0.7	53.3 ± 2.5
BCHN 08	0.75	272 ± 6	8.2 ± 0.7	56.4 ± 2.0
BCHN 09	1.00	270 ± 5	8.6 ± 0.4	58.3 ± 1.9

PS- average particle size (in nm), LE- Loading efficiency (in % w/w), EE- Entrapment efficiency. Each data represents the average of two batches in triplicate with standard deviation.

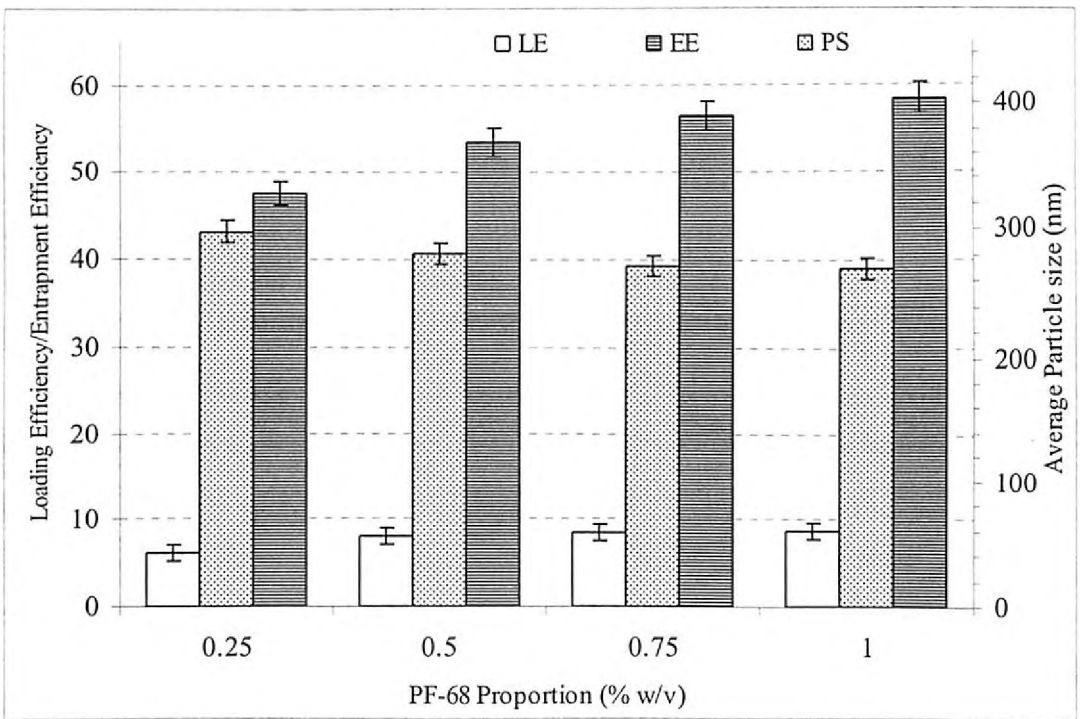

Fig 7.19: Effect of stabilizer (PF-68) proportion on the characteristics of chitosan based brimonidine tartrate nanoparticle formulations. Each data represents the average of two batches in triplicate with standard deviation.

(iii) Effect of TPP solution pH

TPP-chitosan nanoparticles were prepared by the ionic interaction between a positively charged amino group of chitosan and a negatively charged counter ion of TPP. As shown in Table 7.11(c) and in Fig 7.20, the particles obtained at the TPP solution pH of 8.4 were comparatively larger in size and were not spherical. As the pH of the solution was lowered, the formation of smaller particles with more spherical shape were observed. The pH of the TPP solution is of great importance as it decides the degree of ionization of TPP. At higher pH (original TPP solution pH of 8.42), TPP dissociates into OH^- and TPP ions

($HP_3O_{10}^{4-}$ and $P_3O_{10}^{5-}$). However in low pH, only $P_3O_{10}^{5-}$ is formed. Also due to the weak polybasic nature of chitosan, the ionisation of amine group in chitosan increases at lower pH ranges. The nanoparticles formed in the higher TPP solution pH are dominated by deprotonation of chitosan resulting in partial ionic interaction, while at lower pH a complete ionic interaction results. The results are in agreement with some of the previous reports (Mi et al, 1999a; Mi et al, 1999b; Shu and Zhu 2000; Shu and Zhu 2001; Lee et al, 2001).

Table 7.11(c): Effect of TPP solution pH on the characteristics of chitosan based brimonidine tartrate nanoparticle formulations.

Batch code	TPP solution pH	Nanoparticle characteristics		
		PS (nm)	LE (% w/w)	EE (% w/w)
BCHN10	2.0	211 ± 5	4.3 ± 0.3	59.2 ± 2.2
BCHN 11	4.0	243 ± 4	5.7 ± 0.5	55.4 ± 2.9
BCHN 12	6.0	267 ± 6	6.3 ± 0.6	54.4 ± 2.4
BCHN05	8.4	281 ± 4	7.9 ± 0.7	53.3 ± 2.5

PS- average particle size (in nm), LE- Loading efficiency (in % w/w), EE- Entrapment efficiency. Each data represents the average of two batches in triplicate with standard deviation.

The chitosan nanoparticles were not completely spherical in shape, and had a rough surface. At lower pH (2.0), the formed nanoparticles were more spherical in shape and had smoother surface than those prepared at higher pH values. This might be due to high density of matrix. The results are shown in Fig 7.20. The LE decreased and EE steadily increased when the pH of the TPP solution was lowered to acidic range. At pH 8.4 the LE and EE were found to be 7.9 % and 53.3 % respectively. When the pH was brought to acidic range the LE and EE were found to be 4.3 and 59.2% respectively.

The in vitro release profiles of formulations with varying TPP solution pH showed high dependence on pH of the TPP solution (Fig.7.21). As pH of TPP solution was decreased, the drug release rate was decreased. The results obtained were similar to the some earlier reports describing evaluation of chitosan nanoparticles for other drugs (Mi et al. 1999a; Mi et al. 1999b; Shu and Zhu, 2000; Shu and Zhu, 2001; Lee et al, 2001). The duration of release as represented by $t_{90\%}$ decreased from 33.9 h at TPP solution pH of 2.0 to 22.4 h at pH 8.4. The release mechanism of was found to be non-Fickian anamolous indicating a combination of diffusion and erosion mechanism (Table 7.12).

Fig 7.20: Effect of TPP solution pH on the characteristics of chitosan based brimonidine tartrate nanoparticle formulations. Each data represents the average of two batches in triplicate with standard deviation.

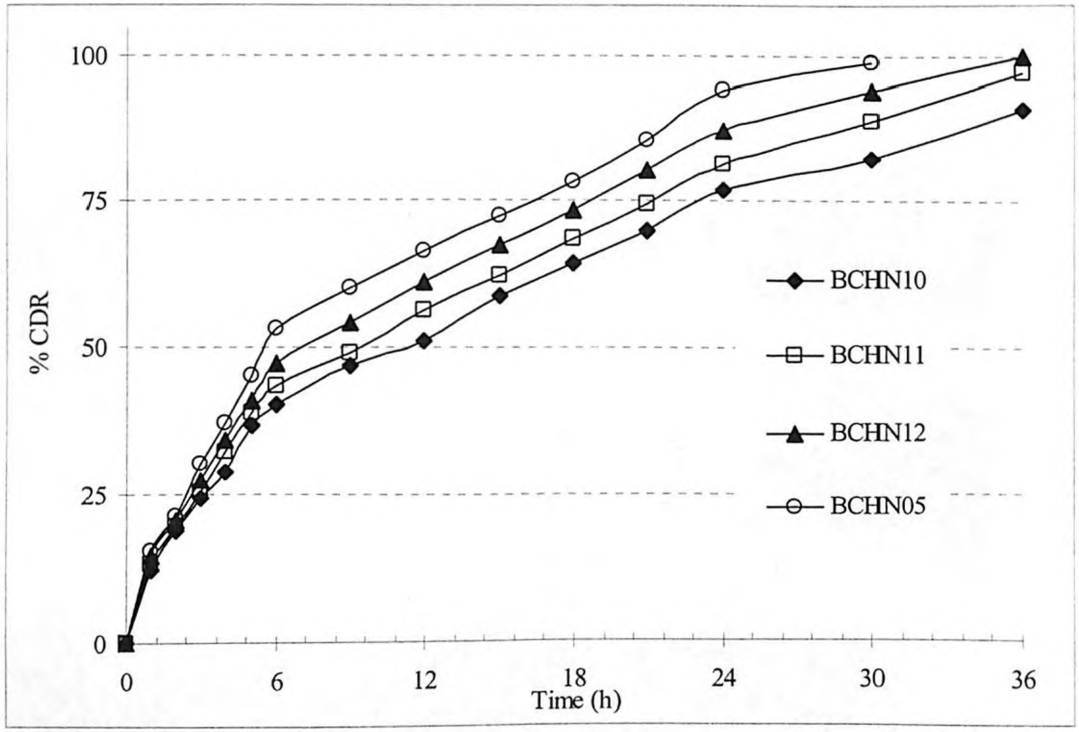

Fig 7.21: In vitro drug release profiles of chitosan based brimonidine tartrate nanoparticle formulations prepared with varying TPP solution pH. Each data point represents the average of two batches in triplicate with standard deviation.

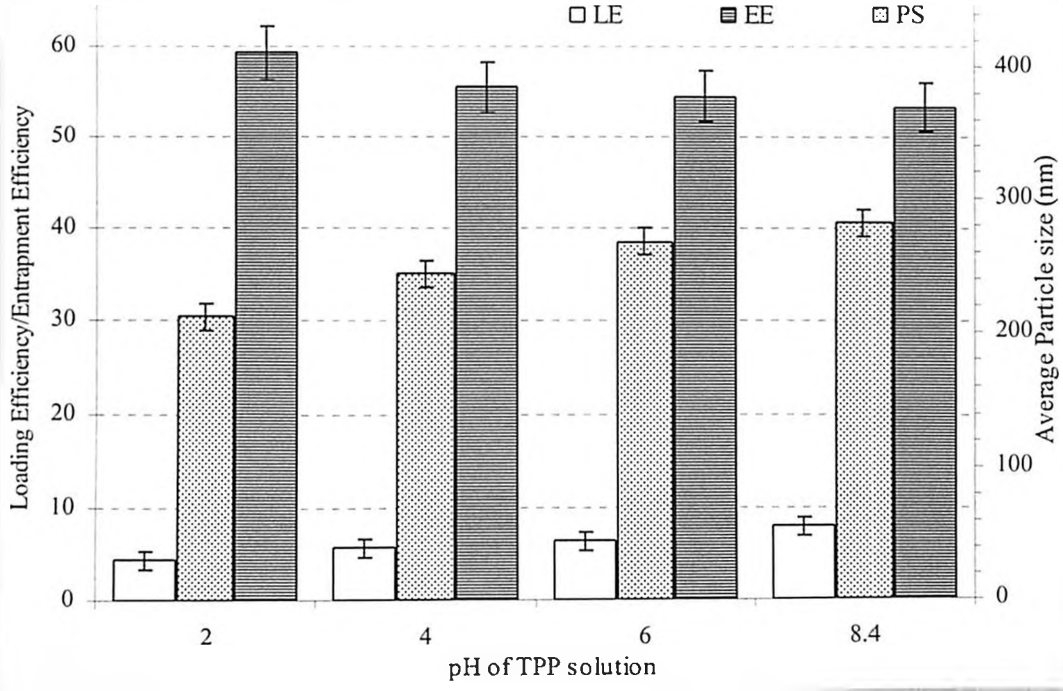
LE
EE
PS
Loading Efficiency/Entrapment Efficiency
Average Particle size (nm)
0
10
20
30
40
50
60
0
100
200
300
400
2
4
6
8.4
pH of TPP solution

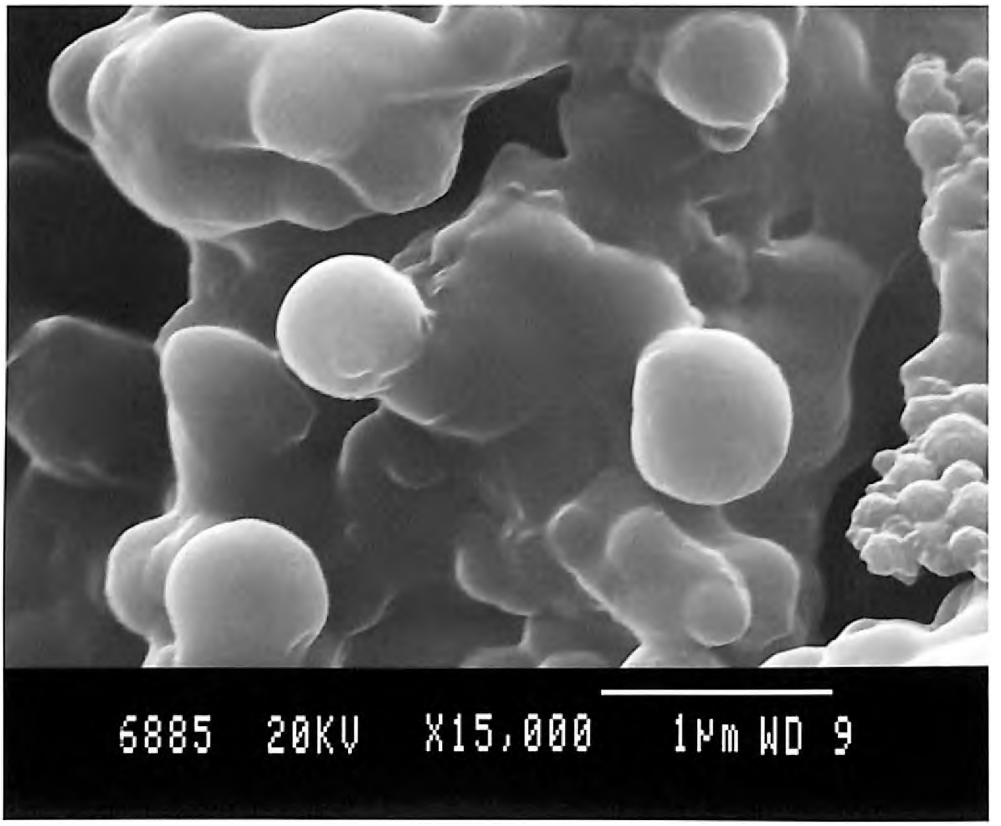

Fig 7.22(a): Scanning electron microscopic image of chitosan based brimonidine tartrate nanoparticle formulations prepared at TPP solution pH of 2.0.

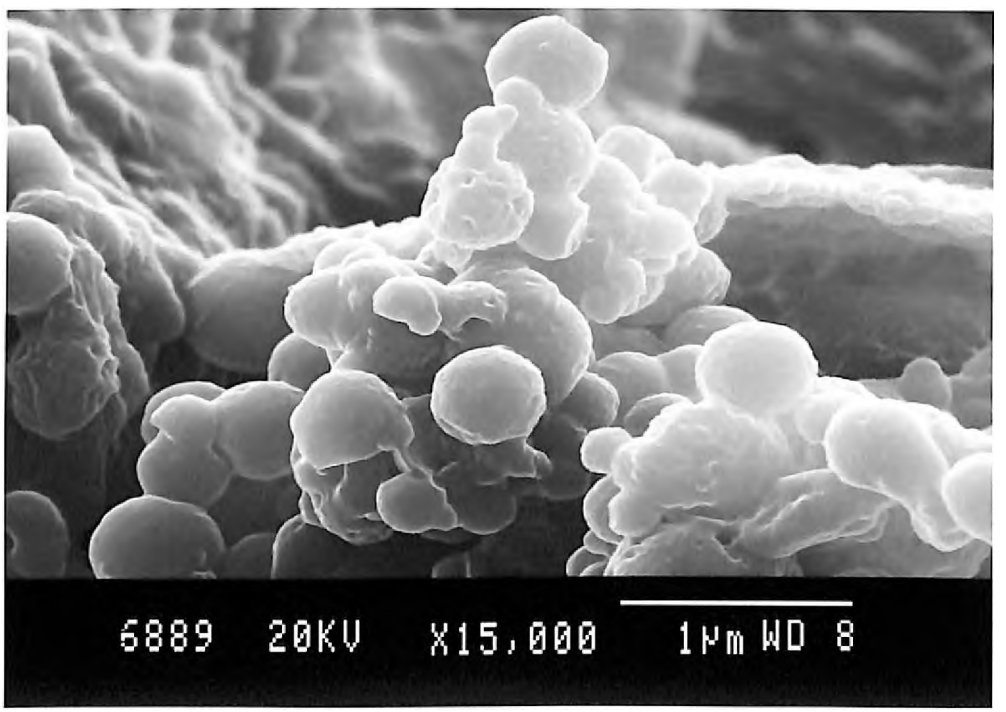

Fig 7.22(b): Scanning electron microscopic image of chitosan based brimonidine tartrate nanoparticle formulations prepared at TPP solution pH of 6.0

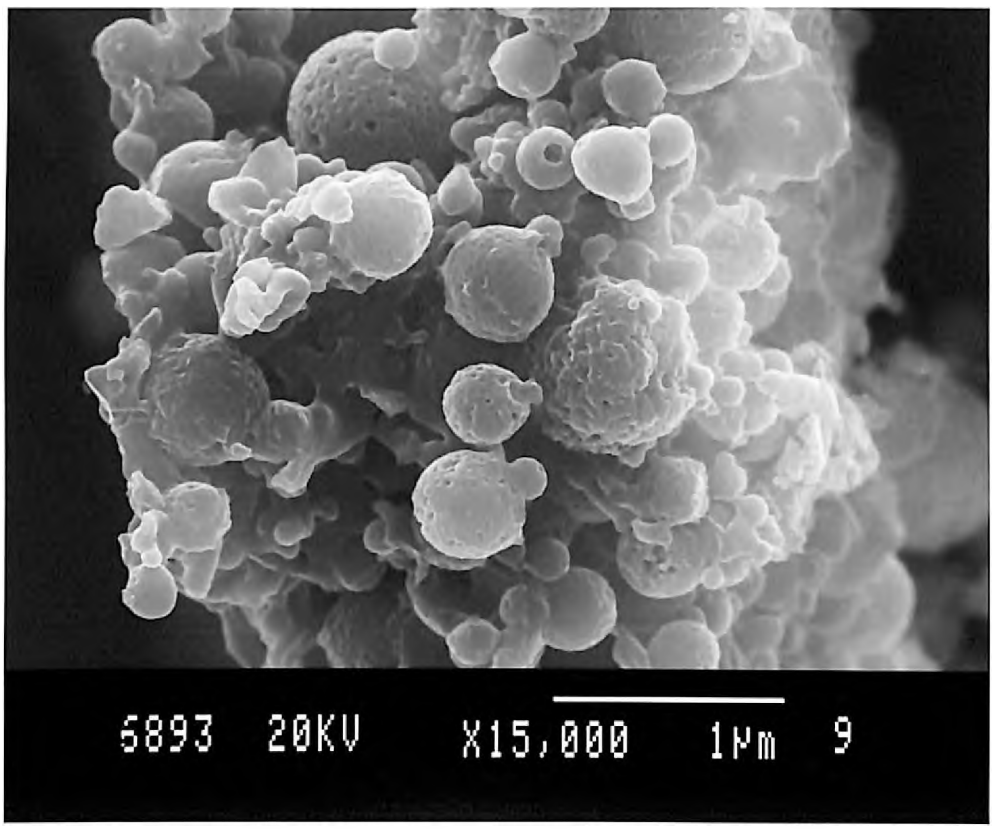

Fig 7.22(c): Scanning electron microscopic image of chitosan based brimonidine tartrate nanoparticle formulations prepared at TPP solution pH of 8.4

(iv) Effect of initial drug amount

The initial drug amount employed in the preparation of nanoparticles showed no effect on the particle size with the particle size remaining unaffected with the increase in the amount of drug (Fig 7.23). But the LE and EE increased significantly with an increase in the initial drug amount. This could be due to increased availability of drug molecules for entrapment when the concentration of drug was higher.

Table 7.11(d): Effect of initial drug amount on the characteristics of chitosan based brimonidine tartrate nanoparticle formulations.

Batch code	Initial amount of drug (mg)	Nanoparticle characteristics		
		PS (nm)	LE (% w/w)	EE (% w/w)
BCHN13	30	277 ± 6	6.0 ± 0.4	43.4 ± 1.9
BCHN05	60	281 ± 4	7.9 ± 0.7	53.3 ± 2.5
BCHN 14	90	289 ± 5	8.6 ± 0.4	58.3 ± 3.2
BCHN 15	120	288 ± 6	9.0 ± 0.5	64.3 ± 2.9
BCHN 16	180	309 ± 5	8.7 ± 0.5	68.3 ± 2.3

PS- average particle size (in nm), LE- Loading efficiency (in % w/w), EE- Entrapment efficiency. Each data represents the average of two batches in triplicate with standard deviation.

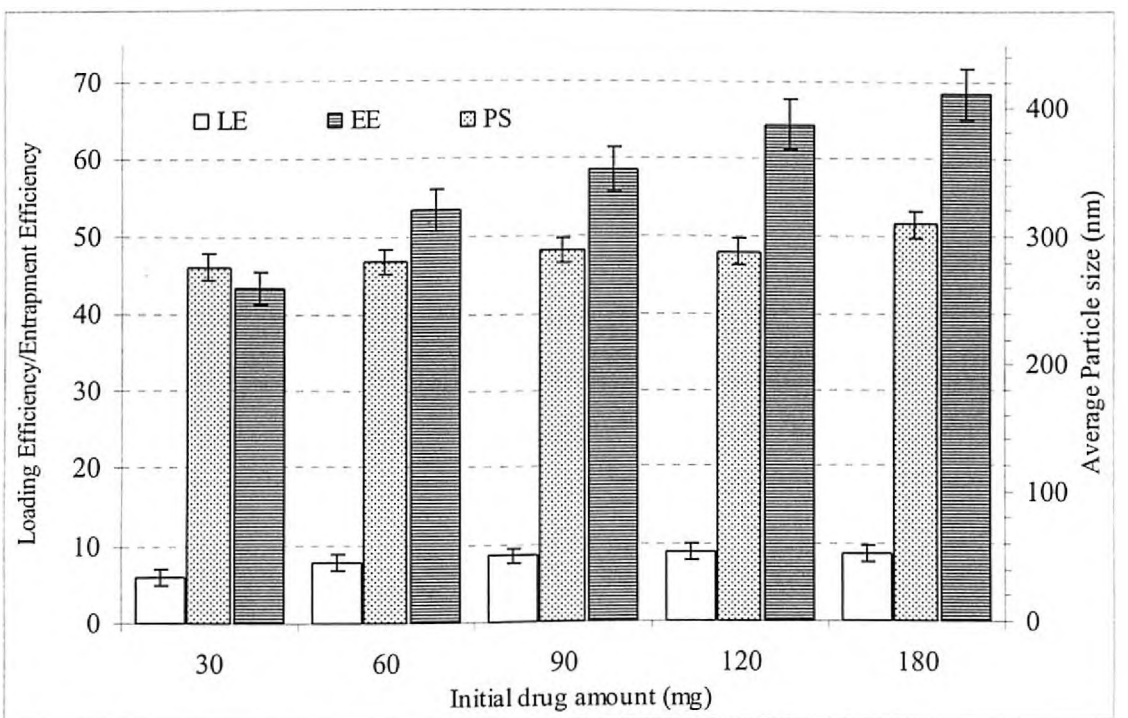

Fig 7.23: Effect of varying initial drug amount on the characteristics of chitosan based brimonidine tartrate nanoparticle formulations. Each data point represents the average of two batches in triplicate with standard deviation.

Table 7.12: Results of drug release kinetics studies for chitosan based brimonidine tartrate nanoparticle formulations fitted into Korsmeyer-Peppas model.

Batch code	KP model				
	K (h^{-n})	n	$t_{20\%}$ (h)	$t_{50\%}$ (h)	$t_{90\%}$ (h)
Effect of ration of chitosan and TPP					
BCHN01	0.2538	0.83	1.0	3.1	6.4
BCHN02	0.2218	0.79	1.2	3.7	7.7
BCHN 03	0.1826	0.72	1.4	4.9	11.0
BCHN 04	0.1078	0.68	1.9	7.3	17.1
BCHN05	0.0482	0.67	2.3	9.3	22.4
BCHN06	0.0318	0.64	2.62	10.9	27.3
Effect of Varying pH of TPP solution					
BCHN 10	0.0298	0.64	3.2	13.3	33.3
BCHN11	0.0328	0.62	2.9	12.1	30.3
BCHN12	0.0464	0.66	2.6	10.4	25.3
BCHN 05	0.0482	0.67	2.3	9.3	22.3

K- Release rate constant (h^{-n}), n- release exponent indicator of drug release mechanism, $t_{20\%}$, $t_{50\%}$, $t_{90\%}$- time taken (in h) for 10, 50 and 90 % drug release respectively

7.4 Stability studies

The stability studies performed at various storage conditions; refrigerated (5° C ± 3° C), and deep freezed (-20° C ± 5° C) and ambient (25° C ± 2° C /60 ± 5 % RH) conditions to determine the effect of these conditions on selected nanoparticles formulations, in terms of degree of aggregation, drug content, particle size and ease of redispersibility. The results are shown in Table 7.13, Table 7.14 and Table 7.15. Nanoparticle batches showed detectable aggregation at ambient while at refrigerated (5° C ± 3° C) and freeze (-20° C ± 5° C) conditions, negligible aggregation was observed.

The physicochemical changes observed were much lesser in case on freeze dried preparations. The formulations stored at freezed conditions (-20° C ± 5° C) showed no significant change in the drug content and average particle size after 3 and 6 months of storage.

Table 7.13: Stability study results for the selected Eudragit based brimonidine tartrate nanoparticle formulations stored at various conditions (3 months)

Formulation		Initial		Ambient		Refrigerated		Freezed	
		Assay (LE)	PS (nm)	Assay (LE)	PS (nm)	Assay (LE)	PS (nm)	Assay (LE)	PS (nm)
Dispersion	BENP-D30	5.2 ± 0.2	289 ± 3	4.9 ± 0.1	311 ± 4	5.0 ± 0.18	303 ± 2	5.1 ± 0.2	303 ± 3
	BENP-PF20	10.9 ± 0.2	221 ± 3	9.5 ± 0.6	249 ± 3	10.0 ± 0.3	281 ± 3	10.2 ± 0.3	274 ± 3
	BENP-1:1(150)	4.8 ± 0.1	312 ± 3	3.6 ± 0.1	332 ± 4	4.2 ± 0.10	325 ± 3	4.4 ± 0.1	322 ± 4
Freeze dried	BENP-D30	5.2 ± 0.2	289 ± 3	4.9 ± 0.2	305 ± 3	4.9 ± 0.12	309 ± 3	5.1 ± 0.1	300 ± 3
	BENP-PF20	10.9 ± 0.2	221 ± 3	9.2 ± 0.3	243 ± 3	9.9 ± 0.48	257 ± 3	9.4 ± 0.7	272 ± 2
	BENP-1:1(150)	4.8 ± 0.1	312 ± 3	3.9 ± 0.1	325 ± 3	4.3 ± 0.13	317 ± 3	4.6 ± 0.1	313 ± 3

PS-average particle size (in nm), LE-Loading efficiency (in % w/w). Each data point represents the average of two batches in triplicate with standard deviation.

Table 7.14: Stability study results for the selected Eudragit based brimonidine tartrate nanoparticle formulations stored at various conditions (6 months)

Formulation		Initial		Ambient		Refrigerated		Freezed	
		Assay (LE)	PS (nm)	Assay (LE)	PS (nm)	Assay (LE)	PS (nm)	Assay (LE)	PS (nm)
Dispersion	BENP-D30	5.2 ± 0.2	289 ± 3	4.2 ± 0.2	324 ± 4	4.8 ± 0.3	339 ± 4	5.0 ± 0.2	312 ± 3
	BENP-PF20	10.9 ± 0.2	221 ± 3	8.0 ± 0.4	260 ± 3	9.6 ± 0.7	282 ± 3	9.8 ± 0.5	288 ± 3
	BENP-1:1(150)	4.8 ± 0.1	312 ± 3	3.0 ± 0.2	341 ± 3	3.9 ± 0.2	334 ± 3	4.0 ± 0.1	333 ± 4
Freeze dried	BENP-D30	5.2 ± 0.2	289 ± 3	4.2 ± 0.2	322 ± 4	4.1 ± 0.1	312 ± 2	4.9 ± 0.2	309 ± 3
	BENP-PF20	10.9 ± 0.2	229 ± 3	8.9 ± 0.5	254 ± 2	9.4 ± 0.5	239 ± 2	9.0 ± 0.3	299 ± 3
	BENP-1:1(150)	4.8 ± 0.1	312 ± 3	3.0 ± 0.2	336 ± 3	4.0 ± 0.2	325 ± 4	4.3 ± 0.2	321 ± 4

PS-average particle size (in nm), LE-Loading efficiency (in % w/w). Each data point represents the average of two batches in triplicate with standard deviation.

Table 7.15: Stability study results for the selected chitosan based brimonidine tartrate nanoparticle formulations stored at various conditions (3 months)

Formulation		Initial		Ambient		Refrigerated		Freezed	
		Assay (LE)	PS (nm)	Assay (LE)	PS (nm)	Assay (LE)	PS (nm)	Assay (LE)	PS (nm)
Dispersion	BCHN05	7.9 ± 0.3	281 ± 6	5.4 ± 0.1	321 ± 4	6.0 ± 0.2	313 ± 2	7.0 ± 0.2	301 ± 3
	BCHN10	4.3 ± 0.2	211 ± 3	3.5 ± 0.3	249 ± 3	3.4 ± 0.3	231 ± 3	3.9 ± 0.2	234 ± 3
	BCHN15	8.9 ± 0.1	288 ± 3	5.6 ± 0.1	332 ± 4	6.2 ± 0.1	325 ± 3	6.9 ± 0.2	322 ± 4
Freeze dried	BCHN05	7.9 ± 0.3	281 ± 6	5.9 ± 0.2	315 ± 3	5.9 ± 0.2	309 ± 3	6.1 ± 0.1	300 ± 3
	BCHN10	4.3 ± 0.2	211 ± 3	3.2 ± 0.3	283 ± 3	3.9 ± 0.5	257 ± 3	3.9 ± 0.2	242 ± 2
	BCHN15	8.9 ± 0.1	288 ± 3	5.9 ± 0.1	325 ± 3	6.4 ± 0.1	317 ± 3	7.6 ± 0.1	303 ± 3

PS-average particle size (in nm), LE-Loading efficiency (in % w/w). Each data point represents the average of two batches in triplicate with standard deviation

7.5. CONCLUSIONS

The BRT nanoparticles were designed and formulated using ERS and ERL as polymers by multiple emulsion solvent evaporation method. The multiple emulsion solvent evaporation method was found to be suitable for the preparation of BRT nanoparticles of narrow average particle size range, high drug loading and entrapment efficiency, prolonged and controlled release of drug. Various formulations and process variables were investigated to study the effect on the characteristics of nanoparticles. The effect of phase volume ratio, surfactant concentration, initial drug loading, aqueous phase pH, secondary surfactants and polymer proportion showed varying effects of particle size, drug loading and entrapment efficiency and in-vitro drug release. The optimized formulations showed higher drug loading and entrapment efficiency and extended release of drug over 48-72 h which could be useful for designing long acting BRT ophthalmic nanoparticle based formulations. The stability studies showed that the selected formulations were found to be more stable at refrigerated and in freezed condition than at room temperature.

Chitosan based nanoparticles were prepared by ionic gelation method. The obtained particles had a narrow size range. The nanoparticles were found to retard the drug release beyond 24 hours. BRT because of its high water solubility, showed low drug loading and low entrapment efficiency in the designed nanoparticles preparation but by carefully varying formulation and process parameters, considerable improvement in drug loading and entrapment efficiency was achieved in the present work. Further, because of the low and narrow average particle size of the nanoparticles obtained, it can be concluded that this could be promising carriers for improved drug delivery to the eye.

7.6. REFERENCES

Al-Kassas R. 2004. Design and in vitro evaluation of gentamicin-Eudragit microspheres intended for intra-ocular administration. J. Microencapsul, 21; 71-81.

Ayalasomayajula SP, Kompella UB. 2005. Subconjunctivally administered celecoxib-PLGA microparticles sustain retinal drug levels and alleviate diabetes-induced oxidative stress in a rat model. Eur. J. Pharmacol, 511; 191-198.

Barichello JM, Morishita M, Takayama K, Nagai T. 1999. Encapsulation of hydrophilic and lipophilic drugs in PLGA nanoparticles by the nanoprecipitation method. Drug Dev. Ind. Pharm, 25; 471-476.

Bourges JL, Gautier SE, Delie F, Bejjani RA, Jeanny JC, Gurny R, Benezra D, Behar-Cohen FF. 2003. Ocular drug delivery targeting the retina and retinal pigment epithelium using poly lactide nanoparticles. Invest. Ophthalmol. Vis. Sci, 44; 3562-3569.

Boonsongrit Y, Mitrevej A, Mueller BW. 2006. Chitosan drug binding by ionic interaction. Eur. J. Pharm. Biopharm, 62; 267-274.

Burkersroda F, Goepferich A. 1999. An approach to classify degrad- able polymers. In: Neenan, T., Marcolongo, M.,Valentini, R.F. (Eds.),Biomedical Materials—Drug Delivery, Implants and Tissue Engineering. Symp. Proceed. 550, Mat. Res. Soc; 17-22.

Calvo P, Vila-Jato JL, Alonso MJ. 1997. Evaluation of cationic polymer-coated nanocapsules as ocular drug carriers. Int. J. Pharm, 153; 41-50.

Campos AMD, Sanchez A, Alonso MJ. 2001. Chitosan nanoparticles: a new vehicle for the improvement of the delivery of drugs to the ocular surface. Application to Cyclosporine A. Int. J. Pharm, 224; 159-168.

Campos AM, Diebold Y, Carvalho ELS, Sánchez A, Alonso MJ. 2004. Chitosan nano particles as new ocular drug delivery systems: in vitro stability, in vivo fate, and cellular toxicity. Pharm. Res, 21; 803-810.

Carrasquillo KG, Ricker JA, Rigas IK, Miller JW, Gragoudas ES, Adamis AP. 2003. Controlled delivery of the anti- VEGF aptamer EYE001 with poly (lactic-*co*-glycolic) acid microspheres. Invest. Ophthalmol. Vis. Sci, 44; 290-299.

Cleland JL, Duenas ET, Park A, Daugherty A, Kahn J, Kowalski J, Cuthbertson A. 2001. Development of poly-(D,L-lactide–coglycolide) microsphere formulations containing recombinant human vascular endothelial growth factor to promote local angiogenesis. J. Control. Release, 72; 13-24.

Csaba N, Koping-Hoggard M, Alonso MJ. 2009. Ionically crosslinked chitosan/ tripolyphosphate nanoparticles for oligonucleotide and plasmid DNA delivery. Int. J. Pharm, 382; 205-214.

De TK, Rodman DJ, Holm BA, Prasad PN, Bergey EJ. 2003. Brimonidine formulation in polyacrylic acid nanoparticles for ophthalmic delivery. J. Microencapsul, 20; 361-374.

De TK, Bergey EJ, Chung SJ, Rodman DJ, Bharali DJ, Prasad PN. 2004. Polycarboxylic acid nanoparticles for ophthalmic drug delivery: an ex vivo evaluation with human cornea. J. Microencapsul, 21; 841-855.

Esposito E, Sebben S, Cortesi R, Menegatti E, Nastruzzi C. 1999. Preparation and characterization of cationic microspheres for gene delivery. Int. J. Pharm, 189; 29-41.

Faisant N, Siepmann J, Benoit JP. 2002. PLGA-based microparticles: elucidation of mechanisms and a new, simple mathematical model quantifying drug release. Eur. J. Pharm. Sci, 15; 355-366.

Foucher SB, Gref R, Russo P, Guechot J, Bochot A. 2002. Design of poly epsilon caprolactone nanospheres coated with bioadhesive hyaluronic acid for ocular delivery. J. Control. Release, 83; 365-375.

Gavini E, Chetoni P, Cossu M, Alvarez MG, Saettone MF, Giunchedi P. 2004. PLGA microspheres for the ocular delivery of a peptide drug, vancomycin using emulsification/spray dring as the preparation method: in vitro/in vivo studies. Eur. J. Pharma. Biopharm, 57; 207-212.

Giannavola C, Bucolo C, Maltese A, Paolino D, Vandelli A M, Puglisi G, Vincent H. LL, Fresta M. 2003. Influence of preparation conditions on acyclovir-loaded poly-d,l-lactic acid nanospheres and effect of PEG coating on ocular drug bioavailability. Pharm. Res, 20; 584-590.

Gibaud S, Al Awwadi NJ, Ducki C, Astier A. 2004. Poly(ε-caprolactone) and Eudragit® microparticles containing fludrocortisone acetate. Int. J. Pharm. 269; 491-508.

Hamidi M, Azadi A, Rafiei P. 2008. Hydrogel nanoparticles in drug delivery. Adv. Drug Deliv. Rev. 60; 1638-1649.

Heussler ML, Fessi H, Devissaguet JP, Hoffman M, Maincent P. 1992. Colloidal drug delivery systems for the eye: A comparison of the efficacy of three different polymers: Polyisobutyl cyanoacrylate, polylactic-co-glycolic acid, polyepsilon-caprolactone, STP. Pharma. Sci, 2; 98-104.

Heussler ML, Maincent P, Hoffman M, Spittler J, Couvreur P. 1990. Antiglaucomatous activity of betaxolol chlorhydrate sorbed onto different isobutylcyanoacrylate nanoparticle preparations. Int. J. Pharm, 58; 115-122.

Izumikawa S, Yoshioka S, Aso Y, Takeda Y. 1991. Preparation of poly (l-lactide) microspheres of different crystalline morphology and effect of crystalline morphology on drug release rate. J. Control. Release, 15; 133-140.

Kawashima Y, Iwamoto T, Niwa T, Takeuchi H, Hino T. 1993. Size control of ibuprofen microspheres with an acrylic polymer by changing the pH in an aqueous dispersion medium and its mechanism. Chem. Pharm. Bull, 41; 191-195.

Kompella UB, Bandi N, Ayalasomayajula SP. 2003. Subconjunctival nano- and microparticles sustain retinal delivery of budesonide, a corticosteroid capable of inhibiting VEGF expression. Invest. Ophthalmol. Vis. Sci, 44; 1192-1201.

Kreuter J. 1994. Nanoparticles. In J.Swarbrick and J.C.Boylan (Ed). Encyclopedia of pharmaceutical technology. Marcel Dekker, New York; 165-190.

Krinzar B, Mateovic T, Bogataj M, Mrhar A . 2003. The influence of chitosan on in vitro properties of eudragit RS microspheres. Chem. Pharm. Bull, 51; 359-364.

Langer K, Mutschler E, Lambrecht G, Mayer D, Troschau G, Stieneker F, Kreuter J 1997. Methylmethacrylate sulfopropylmethacrylate copolymer nanoparticles for drug delivery Part III: Evaluation as drug delivery system for ophthalmic applications. Int. J Pharm, 158; 219-231.

Lee ST, Mi FL, Shen YJ, Shyu SS. 2001. Equilibrium and kinetic studies of copper (II) ion uptake by chitosan tripolyphosphate chelating resin. Polymer, 42; 1879-1892.

Merodio M, Espuelas MS, Mirshahi M, Arnedo A, Irache JM. 2002. Efficacy of Ganciclovir-loaded Nanoparticles in Human Cytomegalovirus (HCMV)-infected Cells. J. Drug Target, 10; 231-238.

Mi FL, Shyu SS, Kuan CY, Lee ST, Lu KT, Jang SF. 1999a. Chitosan- polyelectrolyte complexation for the preparation of gel beads and controlled release of anticancer drug. I. Effect of phosphorous polyelectrolyte complex and enzymatic hydrolysis of polymer. J. Appl. Polym. Sci, 74; 1868-1879.

Mi FL, Shyu SS, Lee ST, Wong TB. 1999b. Kinetic study of chitosan- tripolyphosphate complex reaction and acid-resistive properties of the chitosan-tripolyphosphate gel beads prepared by in-liquid curing method. J. Polym. Sci: Polym. Phys, 37; 1551-1564.

Mitra AK. 2003. Ophthalmic drug delivery systems. 2nd edition.New York. Marcel Dekker, Inc.

Miller RA, Brady JM, Cutright DE. 1977. Degradation rates of oral resorbable implants (polylactates and polyglycolates): Rate modification with changes in PLA/PGA copolymer ratios. J. Biomed. Mater. Res, 1; 711-719.

Motwani SK, Chopra S, Talegaonkar S, Kohli K, Ahmad FJ, Khar RK. 2008. Chitosan-sodium alginate nanoparticles as submicroscopic reservoirs for ocular delivery: formulation, optimisation and in vitro characterisation. Eur. J. Pharm. Biopharm, 68; 513-525.

Muller RH, Lherm C, Herbert J, Couvreur P. 1990. In vitro model for the degradation of alkylcyanoacrylate nanoparticles. Biomaterials, 11; 590-595.

Papadimitriou S, Bikiaris D, Avgoustakis K, Karavas E, Georgarakis M. 2008. Chitosan nanoparticles loaded with dorzolamide and pramipexole. Carbohydr. Polymers, 73; 44-54

Perumal D, Dangor CM, Alcock RS, Hurbans N, Moopanar KR. 1999. Effect of formulation variables on in vitro drug release and micromeritic properties of modified release ibuprofen microspheres. J. Microencapsul, 16; 475-487.

Pignatello R, Bucolo C, Puglisi G. 2002a. Ocular tolerability of Eudragit RS100 and RL100 nanosuspensions as carriers for ophthalmic controlled drug delivery. J. Pharm. Sci, 91; 2536-2641

Pignatello R, Bucolo C, Spedalieri G, Maltese A, Puglisi G. 2002b. Flurbiprofen-loaded acrylate polymer nanosuspensions for ophthalmic application. Biomaterials, 23; 3247-3255.

Pignatello R, Ricupero N, Bucolo C, Maugeri F, Maltese A, Puglisi G. 2006. Preparation and characterization of Eudragit retard nanosuspensions for the ocular delivery of cloricromene. AAPS PharmSciTech, 7; E27.

Rosa GD, Quaglia F, Rotonda ML, Besnard M, Fattal E. 2002. Boidegradable microparticles for the controlled delivery of oligonucleotides. Int. J. Pharm, 242; 225-228.

Ramirez L, Pastoriza P, Vanrell RH. 1999. Biodegradable poly(DL-lactic-co-glycolic acid) microspheres containing tetracaine hydrochloride. In-vitro release profile. J. Microencapsul, 16; 105-115.

Roberts GAF. 1992. Chitin Chemistry. Mac Millian Press, Houndmills; 1-50.

Salgueiro A, Egea MA, Espina M, Valls O, Garcia ML. 2004. Stability and ocular tolerance of cyclophosphamide-loaded nanospheres. J. Microencapsul, 21; 213-223.

Santos ALG, Bochot A, Doyle A, Tsapis N, Siepmann J, Siepmann F, Schmaler J, Besnard M, Behar-Cohen F, Fattal E. 2006. Sustained release of nanosized complexes of polyethylenimine and anti-TGF-β2 oligonucleotide improves the outcome of glaucoma surgery. J. Control. Release, 112; 369-381.

Shu XZ, Zhu KJ. 2000. A novel approach to prepare tripolyphosphate/chitosan complex beads for controlled drug delivery. Int. J. Pharm, 201; 51-58.

Shu XZ, Zhu KJ. 2001. Chitosan/gelatin microspheres prepared by modified emulsification and ionotropic gelation. J. Microencapsul, 18; 237-245.

Sultana Y, Jain R, Aqil M, Ali A. 2006. Review of ocular drug delivery. Curr. Drug Deliv, 3; 207-217.

Svetlana G, Kevin K, Michael D, Leonid H. 2005. The Potential Advantages of Nanoparticle Drug Delivery Systems in Chemotherapy of Tuberculosis. Am. J. Resp. Crit. Care Med, 172; 1487-1490.

Vandervoort J, Ludwig A. 2007. Ocular drug delivery: nanomedicine applications. Nanomed, 2; 11-21.

Wada R, Hyon SH, Ikada Y. 1990. Lactic acid oligomer microspheres containing hydrophilic drugs. J. Pharm. Sci, 79; 919-924.

Zimmer A, Kreuter, J, Robinson JR. 1991. Studies on the transport pathway of PBCA nanoparticles in ocular tissues, J. Microencapsul, 8; 497-504.

Zimmer AK, Zerbe H, Kreuter J. 1994. Evaluation of pilocarpine-loaded albumin particles as drug delivery systems for controlled delivery in the eye, I. In vitro and in vivo characterisation. J. Control. Release, 32; 57-70.

Zimmer AK, Saettone MF, Zerbe H, Kreuter J. 1995. Evaluation of pilocarpine-loaded albumin particles as drug delivery systems for controlled delivery in the eye II. Coating of pilocarpine-loaded albumin nanoparticles with bioadhesive and viscous polymers. J. Control. Release, 33; 31-46.

Zhang H, Oh M, Allen C, Kumacheva E. 2004. Monodisperse chitosan nanoparticles for mucosal drug delivery. Biomacromolecules, 5; 2461-2468.

CHAPTER EIGHT

IN VIVO STUDIES

8.1. INTRODUCTION

The in vivo studies are an essential part in the development of ocular drug delivery systems. Design of modern ocular drug delivery systems requires a sound understanding of the drug disposition pathways in the eye and the overall ocular pharmacokinetic/ pharmacodynamic profile (Urtti and Salminen, 1993).

It is not always possible to conduct ocular in vivo studies in humans as it is not possible to sample ocular tissues or fluids. It is also difficult to measure pharmacodynamic response without adopting invasive procedure that are painful and may cause painful injury. For this reason, various animal models have been developed and optimized. Though the anatomical or physiological parameters are different, still animal models can give reliable results which could be extrapolated to humans. There exist some differences between anatomy and physiology of human and rabbit eye, mainly in terms of blinking rate, pH. Because rabbit models are relatively inexpensive and easy to handle, rabbits have been used as an animal model in most ocular experiments. The differences in physiological and pharmacokinetic factors between the rabbit and human eyes are presented in Table 8.1.

The study of the mechanisms of optic nerve damage in human open-angle glaucoma and its treatment has been impeded by the lack of a naturally occurring glaucoma in a species whose eye anatomy is similar to that of the human. Animals employed to study the effect of drugs on intra ocular pressure (IOP) are rabbits, rats (Ahmed et al, 2001; Urcola et al, 2006; Soldati et al, 1993; Saettone et a, 1982), mice (Ruiz-Ederra et al, 2006) and pigs (Johnson and Tomarev, 2010; Ruiz-Ederra et al, 2005).

For the evaluation of formulations, both pharmacokinetic and pharmacodynamic parameters are derived to assess the in vivo performance of the drug dosage forms. However, when the measurement of appropriate ocular pharmacodynamic responses in suitable animal models is possible without using invasive procedures and if the drug levels in intraocular tissues/fluids correspond to the pharmacodynamic effect, the pharmacodynamic model is preferred. This approach is more preferred when collecting ocular tissue or fluid involves invasive procedures.

Table 8.1: Comparison of pharmacokinetic factors between the rabbit and the human eye (Worakul and Robinson, 1997).

Pharmacokinetic factors	**Human**	**Rabbit**
Bowman's membrane	present	partially absent
Nictitating membrane	absent	present
Lacrimal punctum/puncta	2	1
Spontaneous blinking rate	6-15 times/min	4-5 times/h
Tear volume (µl)	7-30	5-10
Tear turnover rate (µl/min)	0.5-2.2	0.5-0.8
Protein content of tear fluid (%)	0.7	0.5
pH of lacrimal fluids	7.3-7.7	7.3-7.7
Lacrimal volume (µl)	7.0	7.5
Turnover rate of lacrimal fluids (%/min)	16	7
Buffering capacity of lacrimal fluids	poor	poor
Osmolarity of tear fluid (mOsm/l)	305	305
Initial drainage rate constant (min^{-1})	1.6	0.55
pH of aqueous humor	7.1-7.3	8.2
Aqueous humor volume (ml)	0.1-0.25	0.25-0.3
Aqueous humor turnover rate (µl/min)	2-3	3-4.7
Protein content of aqueous humor (mg/ml)	30	0.5
Corneal thickness (mm)	0.52-0.54	0.35-0.45
Corneal diameter (mm)	11-12	15
Corneal surface area (cm^2)	1.04	1.5-2.0
Ratio of conjunctival and corneal surface	17	9

The pharmacokinetic parameters such as precorneal absorption and transport, ocular disposition, metabolism, elimination from the eye, ocular bioavailability are employed for the evaluation of novel ocular formulations. This involves the measurement of drug concentration at the site of action, mostly at aqueous humor and its distribution pattern across various ocular tissues.

Pharmacodynamic responses such as miosis, light reflex inhibition and intra ocular pressure have been employed as parameters for investigating the effectiveness of antiglaucoma formulations.

Many studies have been reported in literature suitable animal models were selected for induction of glaucoma and subsequently the ability of the dosage form to decrease the elevated IOP and prevention of degeneration of RCG cells have been investigated (Himber et al, 1989; Fernandez et al, 1991; Percicot et al, 1996). This would help in deciding optimal dosage regimen and assessing the toxicities, if any, of the drug and dosage forms, without the invasive intervention in humans. Moreover many anti-glaucoma drugs are potent drugs, their concentration in ocular fluids and tissues would be too low to measure accurately, necessitating very sensitive methods of analysis. The only drawback associated with pharmacodynamic response measurement is that individual variations can give rise to erroneous results. But with a suitable dose response optimisation, this could be minimised. Several literatures have been reported wherein IOP lowering was used as a parameter in investigating the effectiveness of the developed antiglaucoma formulations (Fridriksdottir et al, 1997; Kaur et al, 2000; Hathout et al, 2007; Anumolu et al, 2009; Palma et al, 2009).

In the present study the selected formulations were subjected for ocular toxicity studies on healthy rabbits to determine the ocular irritability of the formulations. The pharmacodynamic response in terms of intra ocular pressure lowering capacity of the designed formulations was measured in glaucomatous rabbits by alpha-chymotrypsin injection against conventional eye drops as the reference (marketed preparation).Based on the in vitro studies, few formulations were selected based on their in vitro performance and were subjected to in vivo IOP lowering efficacy studies.

8.2. MATERIALS, INSTRUMENTS & ANIMALS

8.2.1. Materials

Brimonidine tartrate eye drops (Iobrim® E/D, FDC, Mumbai, India) was procured from Pilani market. Ciprofloxacin eye drops (Ciplox® Cipla, India), dexamethasone eye drops (Dexacip®, Cipla India) and diclofenac sodium eye drops (Voltaren®, Novartis, India) were purchased from the Pilani market. Alpha-chymotrypsin (Type II, lyophilized powder, ≥40 units/mg protein) was purchased from Sigma Aldrich, Bangalore, India. All the buffer salts were procured from CDH (Mumbai, India), Qualigens (Mumbai, India) and S.D Fine Chemicals (Mumbai, India). Alpha-chymotrypsin (4500 IU) in lyophilised powder form was purchased from Sigma-Aldrich India.

8.2.2. Instruments

The water for the preparation of phosphate buffer saline (pH 7.4) was prepared from in-house Millipore purification system (Millipore, Model Elix SA 67120, Molsheim, France). The IOP was measured using calibrated Schiotz tonometer (Scope medical, Mohali, India) provided with standard weights. The rabbit restrainer boxes were provided by Central Animal House Facility of BITS Pilani.

8.2.3. Animals

New Zealand white rabbits, weighing 2.5-3.5 kg were provided by the Central Animal House Facility of BITS Pilani and were housed under controlled and standardised conditions. They were fed a normal pellet diet and water was given ad libitum. The animals were acclamatised to light and dark cycles for 12 h. All the animals met following criteria; (i) both the eyes were completely healthy with no injury or history of injury, (ii) the basal IOP was in the range of 22 ± 3 mm Hg, (iii) the IOP difference between contralateral eyes were not exceeding 2 mm Hg. The animal handling and studies were conducted in accordance with the Principles of Laboratory Animal Care (NIH publication No 92-93, revised in 1985) and in conformation to Association for Research in Vision and Ophthalmology (ARVO) and was approved by the Institutional Animal Ethics Committee of BITS, Pilani (protocol No: IAEC/RES/12-04).

8.3. METHODS

(i) Ocular irritation studies

The main objective of the ocular irritation studies was to assess qualitatively as well as quantitatively the ocular tolerance and irritability/toxicity of selected formulation upon administration to eye. Ocular irritation studies were performed on selected formulations showing promising in vitro results, according to Draize technique (Draize et al, 1944) on healthy New Zealand white rabbits each weighing 2.5 to 3.5 kg, divided into following three groups. The solutions (saline, marketed eye drop) and developed formulations (selected in situ gels, ocular inserts and nanoparticles) were administered once a day for a period of 7 days. At the time of formulation instillation, the animals were maintained in restrainer boxes, but allowed to move their heads freely. The evaluation was performed according to the Draize technique (Draize et al, 1944) by periodically observing for ocular redness, swelling and watering conjunctival chemosis, discharge, corneal lesions). The standard scoring system was followed to ascertain the outcome of the experiment.

(ii) In vivo pharmacodynamic efficacy studies

Induction of glaucoma

Rabbits were anaesthetized by intramuscular injection of 4 mg/ kg of Xylazine, 35 mg/ kg of Ketamine. Chronic ocular glaucoma was induced by a single posterior injection of alpha-chymotrypsin (10 mg/ ml, 0.1 ml) into posterior segment of eye in rabbits (Percicot et al, 1996). Care was taken to avoid the contact of alpha-chymotrypsin with the surface of the eye. A daily ocular examination was followed for few days. After 2-3 days of injection, one drop of ciprofloxacin eye drop (Ciplox® Cipla, India), dexamethasone eye drop (Dexacip®, Cipla India) and a drop of diclofenac sodium eye drop (Voltaren®, Novartis, India) were instilled to prevent topical inflammation. Animals that showed cases of severe inflammation and erratic or inconsistent IOP increase were excluded from the study. When the IOP was stabilised to 39 ± 3 mm Hg, for three successive days, the pharmacodynamic response studies were initiated.

For IOP lowering studies, the selected ocular formulations and conventional ophthalmic drops (2-3 drops) were instilled carefully into the lower cul de sac of the left eye of the rabbits (n = 3), while to the right eye 2-3 drops of normal saline was administered. The saline treated eye acted as control in the experiments. Immediately after instillation, eye lid was closed for 10 seconds in order to avoid spillage or movement of the preparation. IOP was measured by using calibrated Schiotz tonometer (Scope medical, Mohali, India) at different time intervals. The change in IOP (ΔIOP) at each time point from the stabilised IOP (zero time) was determined by

$$\Delta IOP = IOP_{\text{zero time}} - IOP_{\text{time t}}$$

ΔIOP is reported as mean (± SEM) of three animals (n=3) for each treatment at each time point. The ΔIOP vs. time curve was plotted to compare the efficacy of prepared formulations with the conventional ophthalmic drops and the comparison was done in terms of; (i) I_{max}: peak decrease in IOP, (ii) t_{max}: time to reach peak IOP decrease, (iii) $AUC_{(\Delta IOP\ vs.\ t)}$: Area under the ΔIOP vs. time curve, (iv) Duration of IOP decrease and (v) slope of terminal linear portion of the decrease in IOP vs. time curve (Anumolu et al, 2009). The $AUC_{(\Delta IOP\ vs.\ t)}$ of ΔIOP vs. time curve was calculated using trapezoid rule (also calculated using Graph Pad Prism 4 software). The AUC_{Rel} was calculated using the following equation,

$$AUC_{Rel} = \frac{AUC_{(\Delta IOP\ vs.\ t)}\ \text{Test (designed formulations)}}{AUC_{(\Delta IOP\ vs.\ t)}\ \text{Reference (marketed eye drops)}}$$

8.4. RESULTS AND DISCUSSION

(a) Ocular irritation and tolerability studies

The results of ocular irritability and tolerability studies of selected in situ gels (gellan gum and PNIAA based), ocular inserts (combination of hydrophilic and hydrophobic/ inert/ zwitterionic polymeric systems) and nanoparticles (ERL 100-ERS 100 and chitosan based) suggested that all the formulations investigated were well tolerated without any signs of irritation or toxicity. The scores for all the selected formulations were found to be as same that of marketed preparation, which shows the potential of the developed formulations as ocular drug delivery systems.

(b) In vivo pharmacodynamic efficacy studies

The glaucoma induction by alpha-chymotrypsin is primarily because of lysis of zonular material and trabecular meshwork which serves to drain the aqueous humour in and out of the eye, lysis of which results in accumulation of it and subsequent increase in IOP. This model has been found suitable for the studies involving comparison of effect of drugs on IOP reduction and can thus be extrapolated into human glaucoma (Himber et al, 1989; Fernandez et al, 1991). Two animals developed severe topical inflammation were excluded from the study.

(i) In situ gel formulations

Three gellan gum based in situ gel formulations selected based on their physicochemical characteristics, mucoadhesive strength, gelation and viscosity, in vitro release profile and absence of any ocular irritability and toxicity in animal models.

The pharmcodynamic efficacy of selected in situ gel formulations were compared with the marketed preparation of BRT. The comparative IOP reduction profile of selected formulation with that of marketed preparation has been shown in the Fig 8.1 and the comparative parameters are summarized in the Table 8.2.

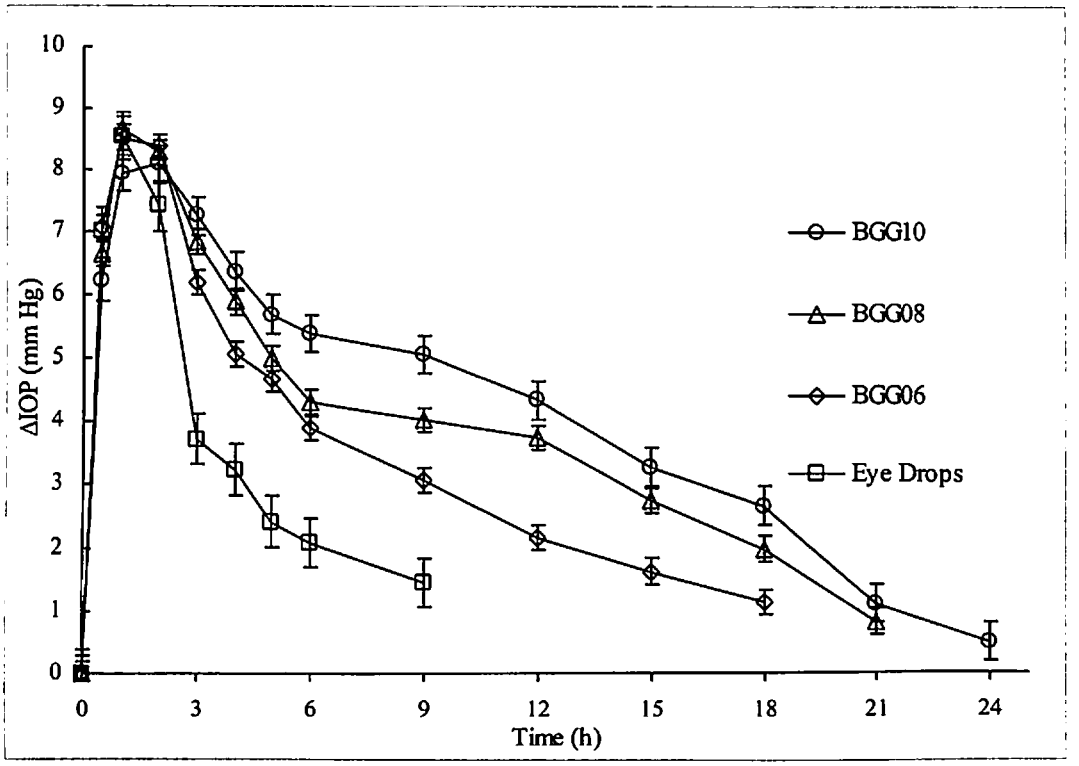

Fig 8.1: Comparative IOP reduction profile for the selected gellan gum based brimonidine tartrate in situ gel formulations in comparison with commercial BRT eye drops (Iobrim® E/D) in glaucomatous rabbits. Each data point represents the average of three measurements per animal (no. of animals = 3) with standard deviation.

Table 8.2: Results of in vivo pharmacodynamic efficacy studies of selected gellan gum based brimonidine tartrate in situ gel formulations in comparison with commercial BRT eye drops (Iobrim® E/D) in glaucomatous rabbits.

Formulation	**I_{max} (mm Hg)**	**t_{max} (h)**	**$AUC_{(\Delta IOP\ vs.\ t)}$ (h.mm Hg)**	**Slope**	**Duration (h)**	**AUC_{Rel}**
Eye drops (Iobrim® E/D)	8.55 ± 0.21	1	38.40 ± 4.21	0.4763	6	-
BGG06	8.45 ± 0.31	2	65.85 ± 3.28	0.2719	15	1.7
BGG08	8.67 ± 0.24	2	87.22 ± 3.01	0.2356	18	2.3
BGG10	8.08 ± 0.24	2	102.11 ± 3.22	0.2102	18	2.7

I_{max} : Maximum reduction in IOP (mm Hg), t_{max} : time taken for maximum reduction in IOP (h), $AUC_{(\Delta IOP\ vs.\ t)}$: Area under the ΔIOP vs. time curve, Slope: slope of terminal linear portion of ΔIOP vs. time curve, AUC_{Rel}: Ratio of AUC $_{(\Delta IOP\ vs.\ t)}$ Test (designed formulations) to AUC $_{(\Delta IOP\ vs.\ t)}$ Reference (marketed eye drops). Each data point represents the average of three measurements per animal (no. of animals = 3) with standard deviation.

From the results it was evident that all the selected formulations showed better IOP reduction ability that the marketed preparation. The IOP lowering effect was more prolonged and lasted much longer in case of designed gellan gum based formulations. In

the case of BGG06 formulation the I_{max} was found to be 8.45 mm Hg where as in case of marketed preparation it was found to be 8.55 mm Hg. The t_{max} (the time taken for maximum IOP reduction) was 2 h for all the formulations, suggested that the rapid absorption of drug when it is present in soluble form. The Area under the in ΔIOP vs. time curve ($AUC_{(\Delta IOP\ vs.\ t)}$) values indicated a significant increase in IOP reduction efficacy of designed formulations. The $AUC_{(\Delta IOP\ vs.\ t)}$ for formulations were found to be 65.85 h.mm Hg (BGG06), 87.22 h.mm Hg (BGG08), 102.11 h.mm Hg (BGG10), while for the marketed preparation, it was found to be 38.40 h.mm Hg. The AUC_{Rel} showed a 2-3 fold increase in IOP reduction ability of the designed formulations in comparison to that of marketed preparation. The overall duration of action was prolonged and more sustained. The slope of terminal part of ΔIOP vs. time curve showed that the in situ gel preparations were more slowly eliminated with sustained IOP reduction.

The temperature activated PNIAA based in situ gel formulations which showed promising in vitro characteristics such as mucoadhesive strength, gelation temperature near to topical eye temperature, prolonged in vitro release profile and better stability were selected for in vivo studies. The results of in vivo pharmacodynamic efficacy studies are shown in Fig 8.2 and the comparative parameters are presented in Table 8.3.

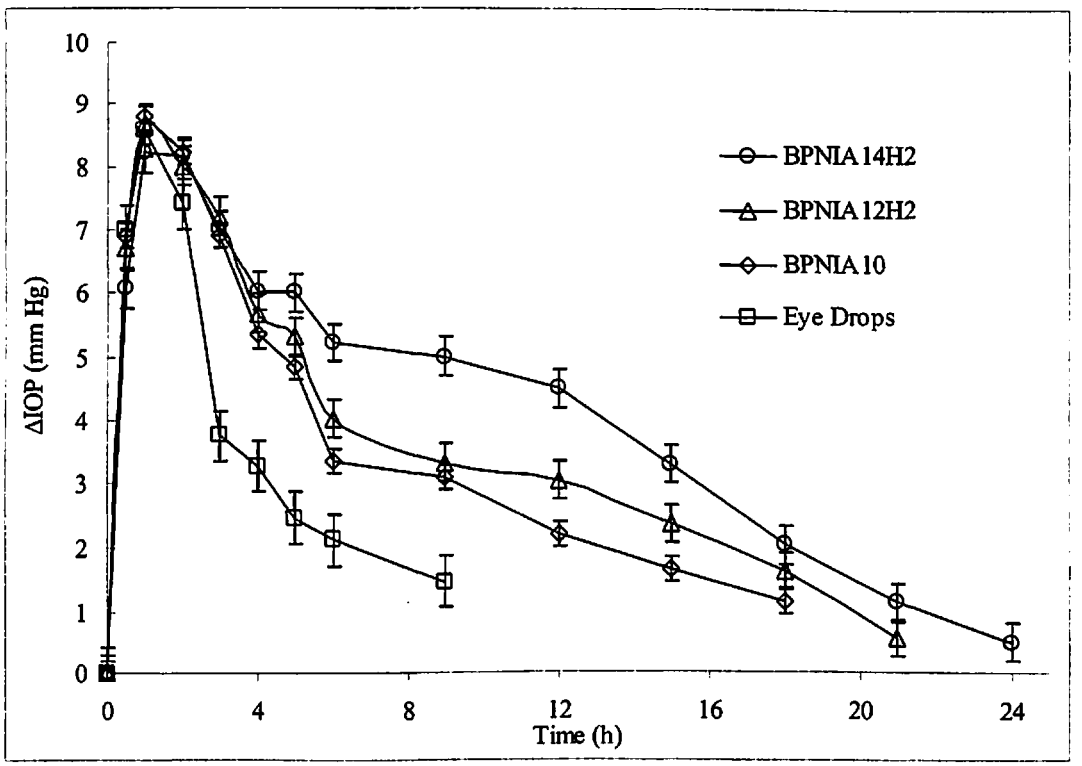

Fig 8.2: Comparative IOP reduction profile for the selected PNIAA based brimonidine tartrate in situ gel formulations in comparison with commercial BRT eye drops (Iobrim® E/D) in glaucomatous rabbits. Each data point represents the average of three measurements per animal (no. of animals = 3) with standard deviation.

Table 8.3: Results of in vivo pharmacodynamic efficacy studies of selected PNIAA based brimonidine tartrate in situ gel formulations in comparison with commercial BRT eye drops (Iobrim® E/D) in glaucomatous rabbits.

Formulation	I_{max} (mm Hg)	t_{max} (h)	$AUC_{(\Delta IOP\ vs.\ t)}$ (h.mm Hg)	Slope	Duration (h)	AUC_{Rel}
Eye drops (Iobrim® E/D)	8.55 ± 0.21	1	38.40 ± 4.21	0.4763	6	-
BPNIA10	8.45 ± 0.14	2	66.84 ± 3.98	0.2965	15	1.7
BPNIA12H2	8.67 ± 0.27	2	77.22 ± 3.11	0.2614	18	2.0
BPNIA14H2	8.08 ± 0.17	2	97.69 ± 3.22	0.2242	21	2.5

I_{max} : Maximum reduction in IOP (mm Hg), t_{max} : time taken for maximum reduction in IOP (h), $AUC_{(\Delta IOP\ vs.\ t)}$: Area under the ΔIOP vs. time curve, Slope: slope of terminal linear portion of ΔIOP vs. time curve, AUC_{Rel}: Ratio of $AUC_{(\Delta IOP\ vs.\ t)}$ Test (designed formulations) to $AUC_{(\Delta IOP\ vs.\ t)}$ Reference (marketed eye drops). Each data point represents the average of three measurements per animal (no. of animals = 3) with standard deviation.

The results indicated that the developed in situ gel formulations of PNIAA showed better IOP reduction efficacy than marketed preparation. The I_{max} and t_{max} remained almost same for all the formulations investigated. The $AUC_{(\Delta IOP\ vs.\ t)}$ of developed formulations showed significant increase in IOP lowering efficacy of designed formulations with respect to marketed preparation. Increase in polymer proportion in the in situ gel formulations resulted in increased in $AUC_{(\Delta IOP\ vs.\ t)}$ indicating that polymer at higher proportions can increase the retention time of the in situ gel due to increased mucoadhesive strength and increased ability to prolong the drug release in vivo. The addition of HPMC K4M to the PNIAA formulations, increased the duration of drug release in vitro, improved mucoadhesive strength and hence improved the IOP reduction duration for a longer period of time in vivo. The AUC_{Rel} for formulation BPNIA10 it was found to be 1.7, while for BPNIA12H2 it was 2.0 and for BPNIA14H2 it was 2.5. The higher AUC_{Rel} suggested that the developed formulations have improved IOP reduction ability compared to eye drops, which is sustained beyond 15-21 h.

(ii) Ophthalmic nanoparticle formulations

The Eudragit (ERL 100 and ERL 100) based nanoparticle formulations with improved in vitro characteristics (BENP-D30, BENP-IP4, BENP-PF20 and BENP-1:1(150) were selected for in vivo studies. The selected nanoparticle formulations showed narrow particle size, high drug loading and entrapment efficiency, prolonged release of drug and were found to be stable. The results are shown in Fig 8.3 and presented in Table 8.4.

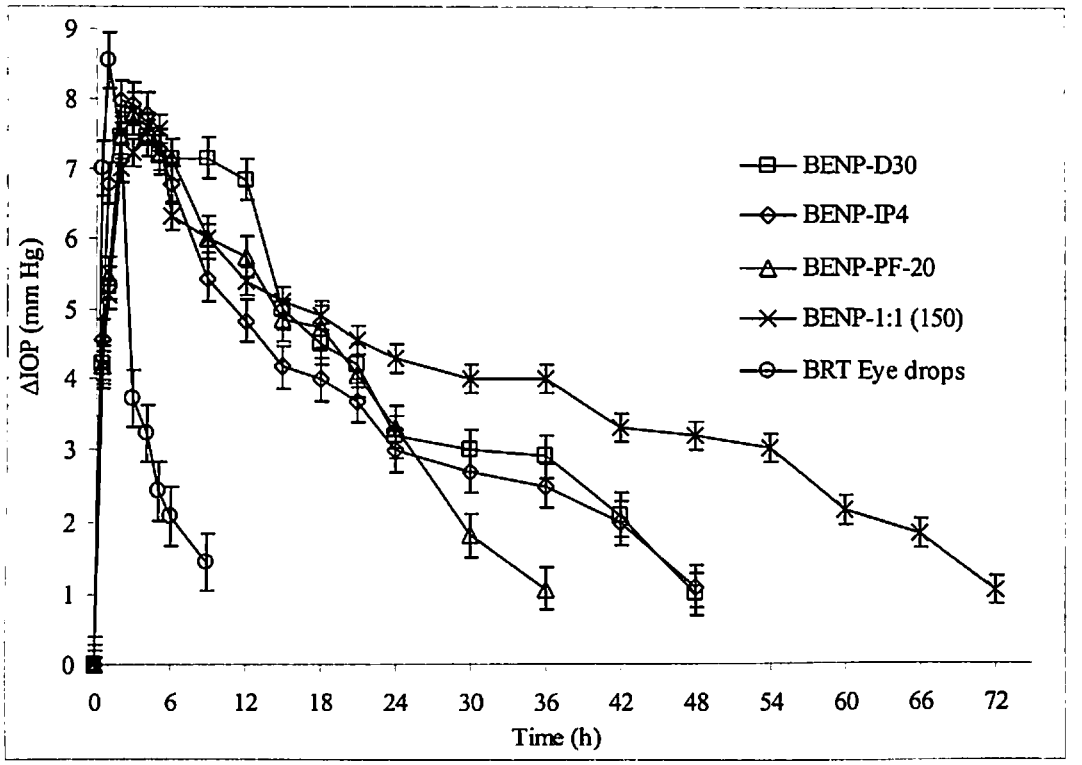

Fig 8.3: Comparative IOP reduction profile for the selected Eudragit (ERL 100 and ERS 100) based brimonidine tartrate nanoparticle formulations in comparison with commercial eye drops (Iobrim® E/D) in glaucomatous rabbits. Each data point represents the average of three measurements per animal (no. of animals = 3) with standard deviation.

Table 8.4: Results of in vivo pharmacodynamic efficacy studies of selected Eudragit (ERL 100 and ERS 100) based brimonidine tartrate nanoparticle formulations in comparison with commercial BRT eye drops (Iobrim® E/D) in glaucomatous rabbits.

Formulation	**I_{max} (mm Hg)**	**t_{max} (h)**	**$AUC_{(\Delta IOP\ vs.\ t)}$ (h.mm Hg)**	**Slope**	**Duration (h)**	**AUC_{Rel}**
Eye drops (Iobrim® E/D)	8.55 ± 0.21	1	38.40 ± 4.21	0.4763	6	-
BENP-D30	7.77 ± 0.32	3	204.93 ± 5.33	0.1022	48	5.3
BENP-IP4	7.97 ± 0.21	2 - 3	151.73 ± 4.98	0.1055	48	4.0
BENP-PF20	7.71 ± 0.19	3	136.33 ±5.12	0.1244	36	3.6
BENP-1:1(150)	7.69 ± 0.24	3	268.09 ± 4.89	0.0855	72	7.0

I_{max} : Maximum reduction in IOP (mm Hg), t_{max} : time taken for maximum reduction in IOP (h), $AUC_{(\Delta IOP\ vs.\ t)}$: Area under the ΔIOP vs. time curve, Slope: slope of terminal linear portion of ΔIOP vs. time curve, AUC_{Rel}: Ratio of AUC $_{(\Delta IOP\ vs.\ t)}$ Test (designed formulations) to AUC $_{(\Delta IOP\ vs.\ t)}$ Reference (marketed eye drops). Each data point represents the average of three measurements per animal (no. of animals = 3) with standard deviation.

As shown in Fig 8.3 and in Table 8.4, the I_{max} for all the selected Eudragit based nanoparticles was lesser in comparison to eye drop preparation. I_{max} was 7.77 mm Hg for BENP-D30, 7.97 mm Hg for BENP-IP4, 7.71 mm Hg for BENP-PF20 and 7.6 mm Hg for BENP-1:1(150) in comparison to 8.55 mm Hg for eye drop preparation. The t_{max} was about 2-3 h for nanoparticles, while for marketed eye drop preparation, it was 1 h. This suggested that the drug has to get dissoluted and then absorbed into the eye while eye drop preparation had drug in dissolved form, hence a rapid absorption occurred.

The formulation BENP-D30 (initial drug loading of 30 mg) showed an $AUC_{(\Delta IOP\ vs.\ t)}$ of 204.93 h.mm Hg. When the internal phase in BENP-D30 formulation was increased to 4 ml (BENP-IP4), the $AUC_{(\Delta IOP\ vs.\ t)}$ was decreased to 151.73 h.mm Hg. From the in vitro studies, it was evident that with an increase in internal phase volume, the particle size, drug loading and loading efficiency were increased. Therefore slow release of entrapped drug would have resulted decreased $AUC_{(\Delta IOP\ vs.\ t)}$ in case of BENP-IP4.

Formulation BENP-PF20 (PF-68 proportion of 2.0% w/w) when compared to 1% w/w in case of BENP-D30, the particle size was found to be decreased with corresponding increase in drug loading, entrapment efficiency and in vitro drug release rate. In vitro observations correlated with in vivo effect as seen by reduced duration of IOP reduction effect to 36 h (in case of BENP-PF20) compared to 48 h in case of BNP-D30. The $AUC_{(\Delta IOP\ vs.\ t)}$ was found to be decreased to 136.33 h.mm Hg compared to 204.93 h.mm Hg for BENP-D30.

When the polymer proportion was increased from 100:100(ERS: ERL) (BENP-D30) (total amount 200 mg) to 150:150 (ERS: ERL) [BENP-1:1(150)], (total amount 300 mg), the particle size was found to be increased, in vitro drug release was more prolonged and the corresponding in vivo effect lasted for 72 h. The $AUC_{(\Delta IOP\ vs.\ t)}$ was increased to 268.09 h.mm Hg. The AUC_{Rel} in comparison to eye drop formulations was found to be 5.3 for BENP-D30, 4.0 for BENP-IP4, 3.6 for BENP-PF20 and 7.0 for the formulation BENP-1:1(150). The lower value of slope for the terminal portion of the ΔIOP vs. time curve for all the selected Eudragit nanoparticles compared to eye drop preparations suggested that nanoparticle formulations were slowly eliminated compared to eye drops.

The chitosan based nanoparticles of BRT showing improved drug loading and entrapment efficiency and prolonged release and better stability profile were selected for the in vivo studies. The IOP reduction efficacy of chitosan based nanoparticles were prolonged and lasted up to 36 h. Results of in vivo IOP reduction efficacy studies is shown in the Fig 8.4 and comparative parameters in Table 8.5.

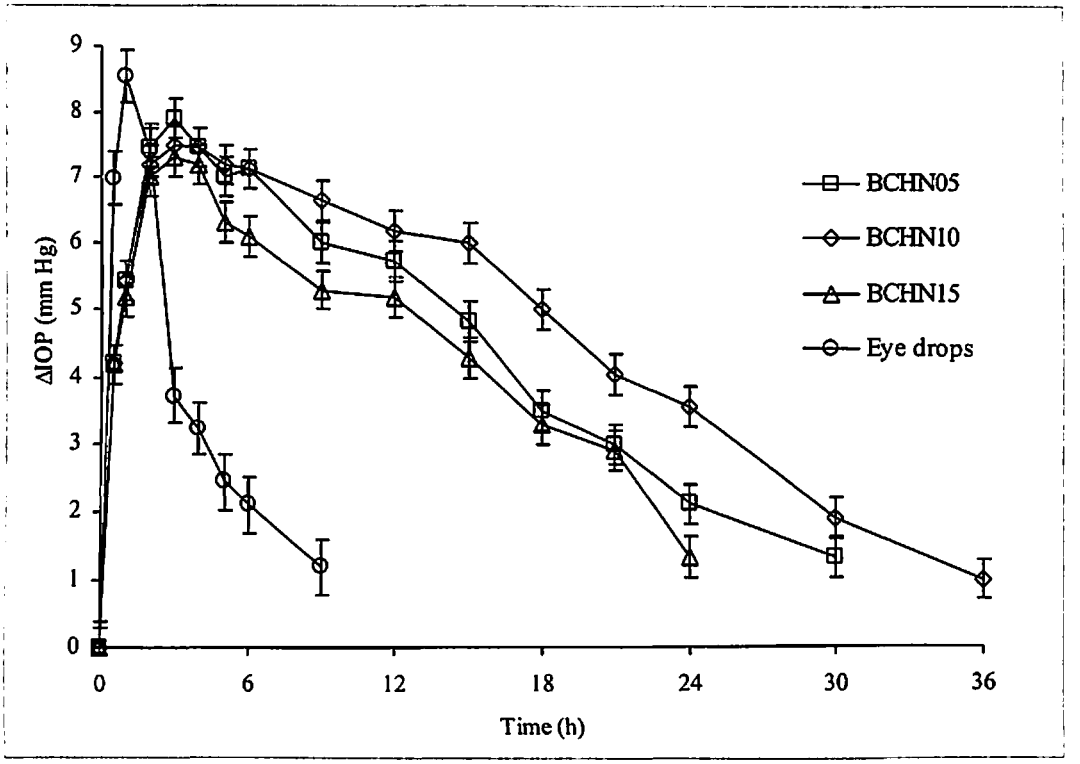

Fig 8.4: Comparative IOP reduction profile for the selected chitosan based brimonidine tartrate nanoparticle formulations in comparison to commercial eye drop (Iobrim® E/D) in glaucomatous rabbits. Each data point represents the average of three measurements per animal (no. of animals = 3) with standard deviation.

Table 8.5: Results of in vivo pharmacodynamic efficacy studies of selected chitosan based brimonidine tartrate nanoparticle formulations in comparison with commercial BRT eye drops (Iobrim® E/D) in glaucomatous rabbits

Formulation	**I_{max} (mm Hg)**	**t_{max} (h)**	**$AUC_{(\Delta IOP\ vs.\ t)}$ (h.mm Hg)**	**Slope**	**Duration (h)**	**AUC_{Rel}**
Eye drops (Iobrim® E/D)	8.55 ± 0.21	1	38.40 ± 4.21	0.4761	6	-
BCHN05	7.91 ± 0.27	3	113.06 ± 5.33	0.1320	30	2.9
BCHN10	7.61 ± 0.21	3	144.10 ± 4.78	0.1121	36	3.8
BCHN15	7.30 ± 0.18	3	95.27 ± 5.88	0.1160	24	2.5

I_{max}: Maximum reduction in IOP (mm Hg), t_{max} : time taken for maximum reduction in IOP (h), $AUC_{(\Delta IOP\ vs.\ t)}$: Area under the ΔIOP vs. time curve, Slope: slope of terminal linear portion of ΔIOP vs. time curve, AUC_{Rel}: Ratio of AUC $_{(\Delta IOP\ vs.\ t)}$ Test (designed formulations) to AUC $_{(\Delta IOP\ vs.\ t)}$ Reference (marketed eye drops). Each data point represents the average of three measurements per animal (no. of animals = 3) with standard deviation.

As shown in Table 8.5, the I_{max} was found to be 7.91 mm Hg (BCHN05), 7.61 mm Hg (BCHN10) and 7.30 mm Hg (BCHN15) for the selected formulations. All the three chitosan based nanoparticle formulations showed t_{max} of 3 h.

In the case of formulations BCHN05, the $AUC_{(\Delta IOP\ vs.\ t)}$ was found to be 113.06 h.mm Hg and the duration of IOP reduction lasted for 30 h. This formulation had a TPP solution pH of 8.4 (original TPP solution pH). When the pH of TPP solution was decreased to 2.0 (BCHN10), the particle size was found to decrease significantly. The drug release was found to be more controlled and prolonged than formulation BCHN05. Similar findings were observed in vivo, where the IOP reduction efficacy was found to be more prolonged and $AUC_{(\Delta IOP\ vs.\ t)}$ was increased to 144.1 h.mm Hg with the AUC_{Rel} found to be 3.8.

In the case of formulation BCHN15, where the initial drug loading was doubled compared to BCHN10 (keeping the TPP solution pH constant at 2.0), the particle size of the nanoparticles increased, with the increase in the drug loading and loading efficiency. The drug release in vitro was found to be faster than BCHN10 formulation due to increased drug binding to the surface of the particles. The in vivo IOP reduction was less prolonged as it lasted for 24 h and the $AUC_{(\Delta IOP\ vs.\ t)}$ was found to be 95.27 h.mm Hg. The AUC_{Rel} was found to be 2.5 in comparison to eye drop formulation.

The drug release from chitosan nanoparticles were faster compared to Eudragit nanoparticles. This could be due the fact that drug is water soluble and chitosan which is a hydrophilic swellable polymer is less effective in controlling drug release compared to Eudragit. On the other hand, Eudragit (ERL 100 and ERS 100) are inert, non swellable polymer that controlled the release of drug for a longer period of time. The IOP reduction efficacy was much lesser for chitosan nanoparticles in comparison to Eudragit nanoparticles due to rapid elimination of chitosan particles from the eye due to its swelling and erosion in the cul de sac of the eye

(iii) Ocular insert formulations

The ocular insert formulations for in vivo studies were selected based on their in vitro performance such as physicochemical characteristics, mucoadhesive strength, in vitro release profile and stability. The criteria of selection was; (i) Prolonged duration of release (up to 24 h), (ii) Adequate mucoadhesive strength and (iii) Absence of any ocular irritability and toxicity.

(a) PEO and Eudragit based formulations

The selected ocular insert formulations containing PEO 100 kD and Eudragit (BP140ERS60 & BP140ERL60) and PEO 400 kD and Eudragit (BP440ERS60 & BP440ERL60) prolonged in vitro BRT release for 24 h and mucoadhesive strength was sufficiently high and was found to be stable. Ocular irritability and toxicity studies

ensured that these formulations were found to be non-irritant and free from any ocular toxicity. The ΔIOP vs. time curve for combination of PEO 100 kD or PEO 400 kD with ERL 100 or ERS 100 based ocular inserts is shown in the Fig 8.5(a) and 8.5(b) respectively.

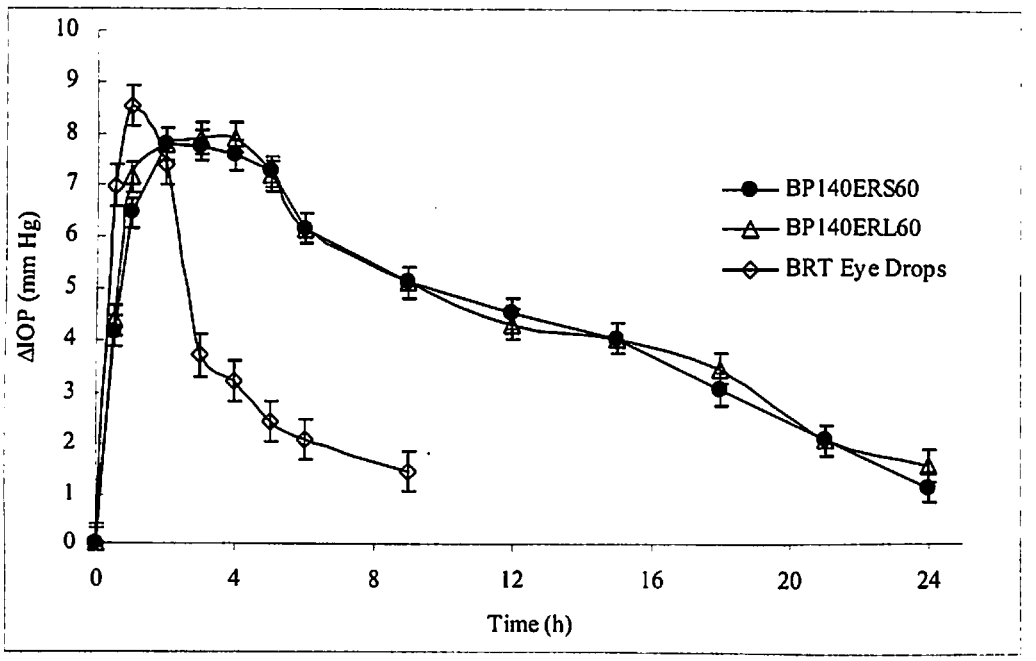

(a)

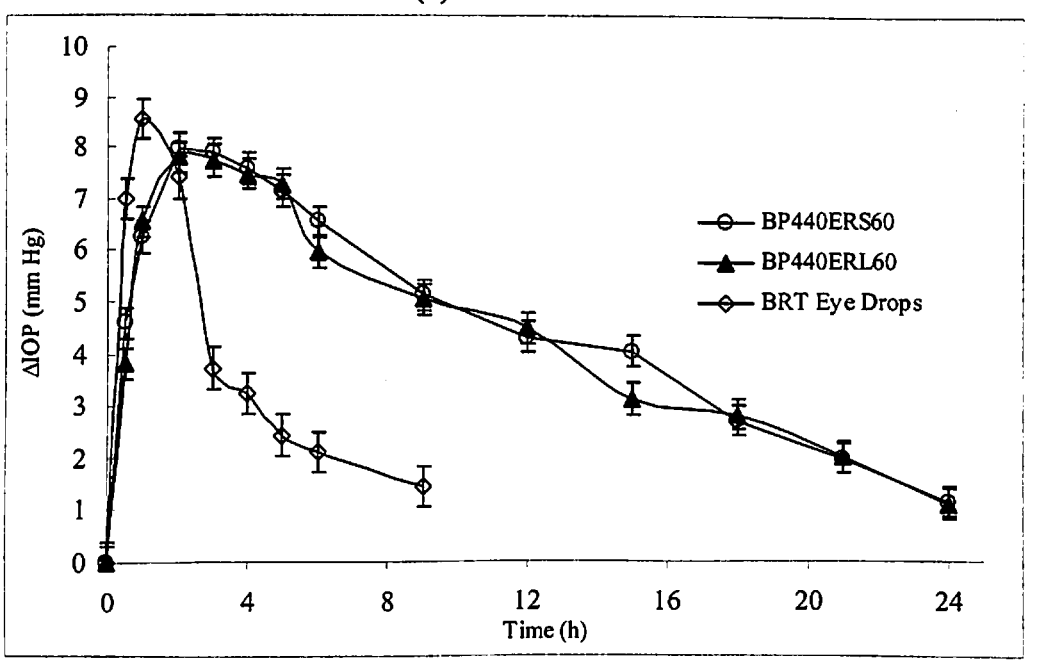

(b)

Fig 8.5: Comparative IOP reduction profile for the selected brimonidine tartrate ocular insert formulations (a) PEO 100 kD with ERS 100 and ERL 100 (b) PEO 400 kD with ERS 100 or ERL 100 in comparison to commercial eye drops (Iobrim® E/D) in glaucomatous rabbits. Each data point represents the average of three measurements per animal (no. of animals = 3) with standard deviation.

Table 8.6: Results of in vivo pharmacodynamic efficacy studies of brimonidine tartrate ocular insert formulations (PEO 100 kD or PEO 400 kD and ERS 100 or ERL 100) in comparison to commercial BRT eye drops (Iobrim® E/D) in glaucomatous rabbits.

Formulation	I_{max} (mm Hg)	t_{max} (h)	$AUC_{(\Delta IOP\ vs.\ t)}$ (h.mm Hg)	Slope	Duration (h)	AUC_{Rel}
Eye drops (Iobrim® E/D)	8.55 ± 0.21	1	38.40 ± 4.22	0.4763	6	-
BP140ERS60	7.80 ± 0.30	3	93.14 ± 5.54	0.1674	24	2.4
BP140ERL60	7.94 ± 0.30	3	90.23 ± 3.54	0.1667	24	2.3
BP440ERS60	7.97 ± 0.32	3	92.35 ± 6.21	0.1756	24	2.4
BP440ERL60	7.97 ± 0.22	3	89.42 ± 4.21	0.1674	24	2.3

I_{max}: Maximum reduction in IOP (mm Hg), t_{max} : time taken for maximum reduction in IOP (h), $AUC_{(\Delta IOP\ vs.\ t)}$: Area under the ΔIOP vs. time curve, Slope: slope of terminal linear portion of ΔIOP vs. time curve, AUC_{Rel}: Ratio of $AUC_{(\Delta IOP\ vs.\ t)}$ Test (designed formulations) to $AUC_{(\Delta IOP\ vs.\ t)}$ Reference (marketed eye drops). Each data point represents the average of three measurements per animal (no. of animals = 3) with standard deviation.

As shown in Table 8.6, the I_{max} was found to be 7.8 mm Hg and 7.94 mm Hg for the selected formulations, while the t_{max} was 3 h for all the selected formulations.

The $AUC_{(\Delta IOP\ vs.\ t)}$ was significantly increased for the ocular inserts preparations in comparison to marketed eye drop preparation. It was found to be 93.14 h.mm Hg for BP140ERS60 and 90.23 h.mm Hg for BP140ERL60. The AUC_{Rel} was found to be 2.4 and 2.3 respectively for BP10ERS60 and BP140ERL60 ocular insert formulations. The duration of IOP reduction lasted for 24 h in comparison to 6 h for eye drops.

Similarly for PEO 400 kD and ERS 100 or ERL 100 based formulations, the $AUC_{(\Delta IOP\ vs.\ t)}$ for the selected formulations was drastically enhanced with 92.35 h.mm Hg for BP40ERS60 and 89.42 h.mm Hg for BP440ERL60. The duration of IOP reduction was observed for 24 h. The AUC_{Rel} was found to be 2.4 and 2.3 for BP440ERS60 and BP440ERL60. No difference in terms of IOP reduction was seen between formulations with ERS 100 and ERL 100 in combination with PEO 100 kD and PEO 400 kD. All the selected formulations were found to be retained in the cul de sac for the entire length of the study, suggesting that mucoadhesive strength of the formulations was sufficiently high for topical ocular administration.

(b) PEO and EC based formulations

The ΔIOP vs. time profiles for the selected PEO and EC based ocular insert formulations are shown in the Fig 8.6 and comparative parameters in Table 8.7.

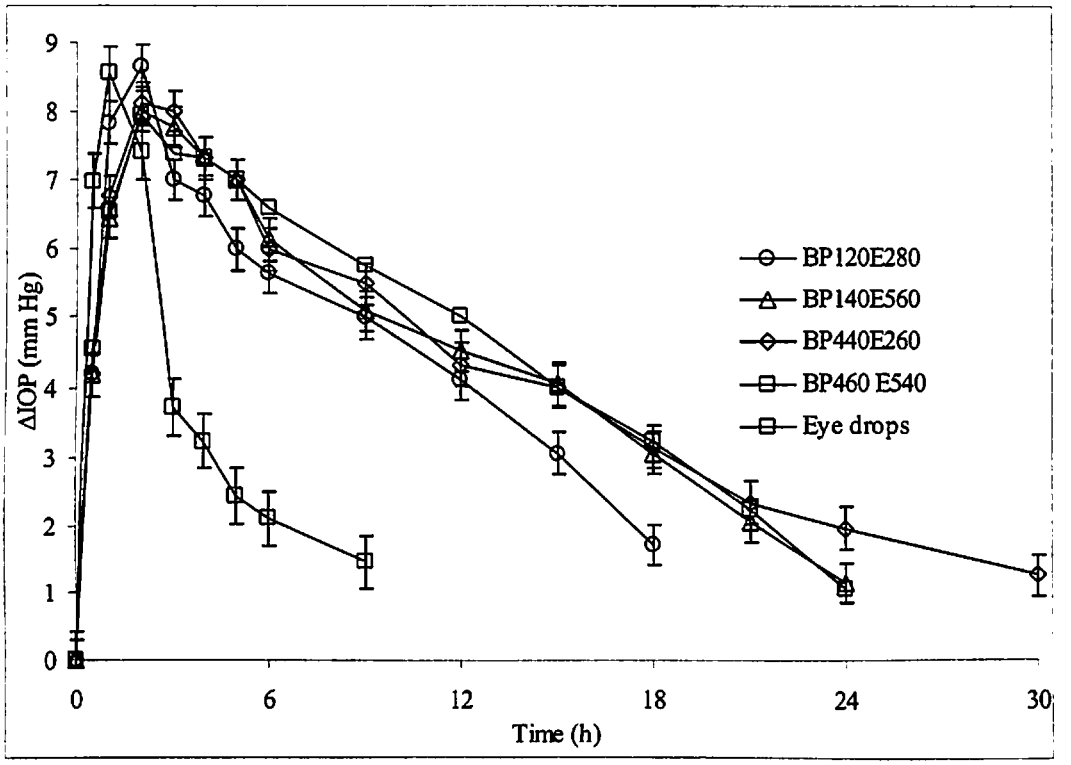

Fig 8.6: Comparative IOP reduction profile for the selected brimonidine tartrate ocular insert formulations (PEO 100 kD or PEO 400 kD with EC22 or EC 50) in comparison to commercial eye drops (Iobrim® E/D) in glaucomatous rabbits. Each data point represents the average of three measurements per animal (no. of animals = 3) with standard deviation.

Table 8.7: Results of in vivo pharmacodynamic efficacy studies of selected brimonidine tartrate ocular insert formulations (PEO and EC based) in comparison to commercial BRT eye drops (Iobrim® E/D) in glaucomatous rabbits in glaucomatous rabbits

Formulation	I_{max} (mm Hg)	t_{max} (h)	$AUC_{(\Delta IOP\ vs.\ t)}$ (h.mm Hg)	Slope	Duration (h)	AUC_{Rel}
Eye drops (Iobrim® E/D)	8.55 ± 0.21	1	38.40 ± 4.22	0.4763	6	-
BP120E280	8.66 ± 0.32	3	86.66 ± 4.54	0.1732	18	2.3
BP140E560	8.00 ± 0.38	3	92.79 ± 3.74	0.1662	24	2.4
BP440E260	8.12 ± 0.22	3	118.58 ± 6.51	0.1589	24	3.0
BP460E540	7.93 ± 0.32	3	99.86 ± 4.11	0.1677	30	2.6

I_{max}: Maximum reduction in IOP (mm Hg), t_{max} : time taken for maximum reduction in IOP (h), $AUC_{(\Delta IOP\ vs.\ t)}$: Area under the ΔIOP vs. time curve, Slope: slope of terminal linear portion of ΔIOP vs. time curve, AUC_{Rel}: Ratio of AUC $_{(\Delta IOP\ vs.\ t)}$ Test (designed formulations) to AUC $_{(\Delta IOP\ vs.\ t)}$ Reference (marketed eye drops). Each data point represents the average of three measurements per animal (no. of animals = 3) with standard deviation.

The selected formulations showed an I_{max} of 8.66, 8.0, 8.12, and 7.93 mm Hg for the formulations BP120E280, BP140E560, BP440E260, BP460E540 respectively (Table 8.7). In case of all the ocular insert formulations, the t_{max}, time for maximum IOP reduction, was found to be 3 h. The $AUC_{(\Delta IOP\ vs.\ t)}$ for all the selected formulations was significantly high compared to eye drop preparations, with 86.66 h.mm Hg (BP120E280), 92.79 h.mm Hg (BP140E560), 118.58 h.mm Hg (BP460E540) and 99.86 h.mm Hg (BP460E540). Formulation BP440E260 [PEO 400kD (60 % w/w) and EC-22 (40 % w/w)] showed highest $AUC_{(\Delta IOP\ vs.\ t)}$ amongst the selected formulations.

AUC_{Rel} for BP120E280 formulation was found to be 2.3, while it was 2.4 for BP140E560, 3.0 for BP440E260 and 2.6 for BP460E540 in comparison to eye drops preparation. This suggested that the selected eye drop preparations have greater ability to reduce IOP and for a more prolonged period of time compared to eye drops preparation.

(c) HPMC and ERS 100/ ERL 100 based formulations

The IOP reduction time profile for the selected HPMC (K4M, K15M and K100M) and ERS 100 or ERL 100 formulations has been shown in Fig 8.7 and pharmacodynamic response parameters are presented in Table 8.8.

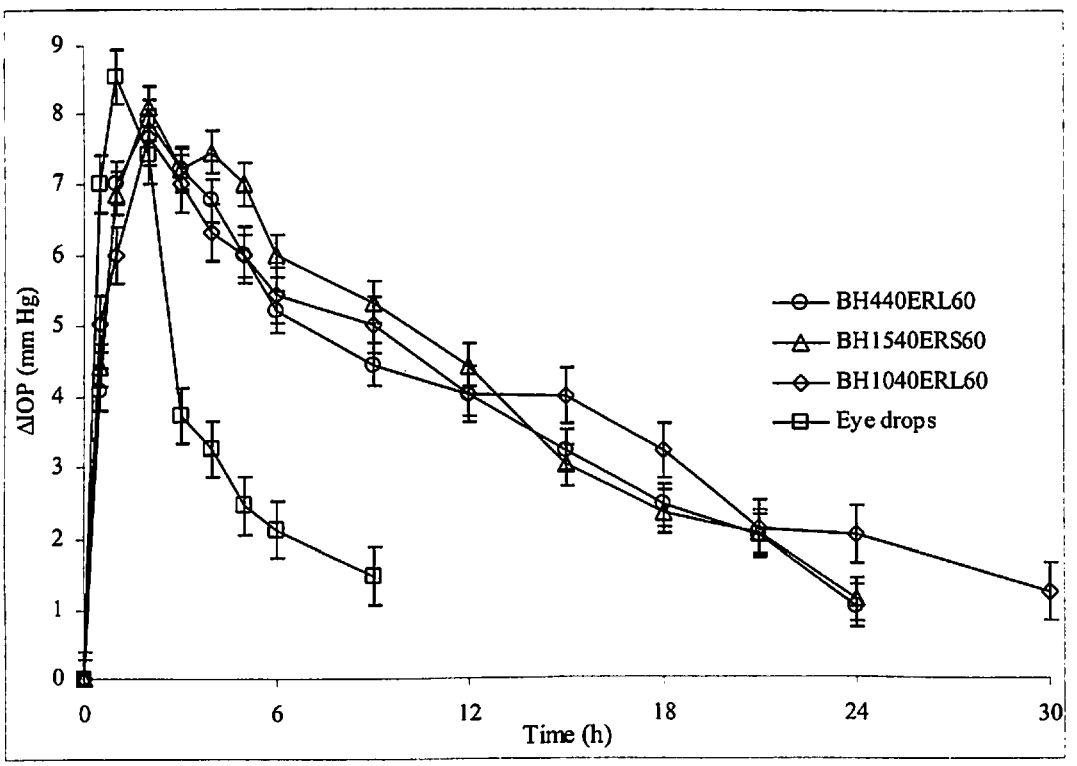

Fig 8.7: Comparative IOP reduction profile for the selected brimonidine tartrate ocular insert formulations (HMPC with ERL 100 and ERS 100) in comparison to commercial eye drop (Iobrim® E/D) in glaucomatous rabbits. Each data point represents the average of three measurements with standard deviation.

Table 8.8: Results of in vivo pharmacodynamic efficacy studies selected brimonidine tartrate ocular insert formulations (HPMC and ERS/ERL) in comparison to commercial BRT eye drops (Iobrim® E/D) in glaucomatous rabbits.

Formulation	I_{max} (mm Hg)	t_{max} (h)	$AUC_{(\Delta IOP\ vs.\ t)}$ (h.mm Hg)	Slope	Duration (h)	AUC_{Rel}
Eye drops (Iobrim® E/D)	8.55 ± 0.21	1	38.40 ± 4.22	0.4763	6	-
BH440ERL60	7.89 ± 0.32	2	99.32 ± 4.54	0.1733	24	2.6
BH1540ERS60	8.10 ± 0.35	3	88.80 ± 3.34	0.1667	24	2.3
BH1040ERL60	7.67 ± 0.42	3	111.25 ± 5.21	0.1544	30	2.9

I_{max}: Maximum reduction in IOP (mm Hg), t_{max} : time taken for maximum reduction in IOP (h), $AUC_{(\Delta IOP\ vs.\ t)}$: Area under the ΔIOP vs. time curve, Slope: slope of terminal linear portion of ΔIOP vs. time curve, AUC_{Rel}: Ratio of $AUC_{(\Delta IOP\ vs.\ t)}$ Test (designed formulations) to $AUC_{(\Delta IOP\ vs.\ t)}$ Reference (marketed eye drops). Each data point represents the average of three measurements per animal (no. of animals = 3) with standard deviation.

The plot showed that the IOP reduction profiles for the ocular insert formulations with HPMC and ERS 100 or ERL 100 were more prolonged and the efficacy of selected formulations in IOP reduction was more pronounced than eye drop preparations. From the Table 8.8, it was evident that the formulation BH440ERL60 (HPMC K4M- 40 % w/w and ERL 100-60 % w/w) showed an I_{max} of 7.89 mm Hg, while BH1540ERS60, it was found to be 8.1 mm Hg (I_{max}). Both formulations showed t_{max} of 3 h. For other selected formulations the I_{max} was more or less comparable to eye drops preparation. The $AUC_{(\Delta IOP\ vs.\ t)}$ for the selected formulations was found to be significantly enhanced and AUC_{Rel} was found to be 2.6 for BH440ERL60, 2.3 for BH1540ERS60 and 2.9 for BH1040ERL60 respectively.

(d) HPMC and EC based formulations

The IOP reduction time profile for the selected formulations from combination of HPMC and EC is shown in Fig 8.8 and the comparative parameters are presented in Table 8.9.

The results suggested that the selected ocular insert formulations showed a greater ability to reduce IOP in glaucoma induced rabbits. The I_{max} for the selected ocular inserts was found to be 7.65 mm Hg (BH440E560), 7.33 mm Hg (BH1560E540) and 7.67 mm Hg (BH1040E560), while t_{max} was 3 h for all the ocular inserts in comparison to 1 h for eye drops preparation. The $AUC_{(\Delta IOP\ vs.\ t)}$ for the ocular inserts was found to be 94.32 h.mm Hg for BH440E560, 84.80 h.mm Hg for BH1560E540 and 105.25 h.mm Hg for

BH1040E560 while that for eye drops preparation was 38.40 h-mm Hg. The AUC_{Rel} was found to be in the range of 2.2 - 2.7, suggesting that the IOP reduction ability of selected formulations was drastically higher and more prolonged compared to eye drops.

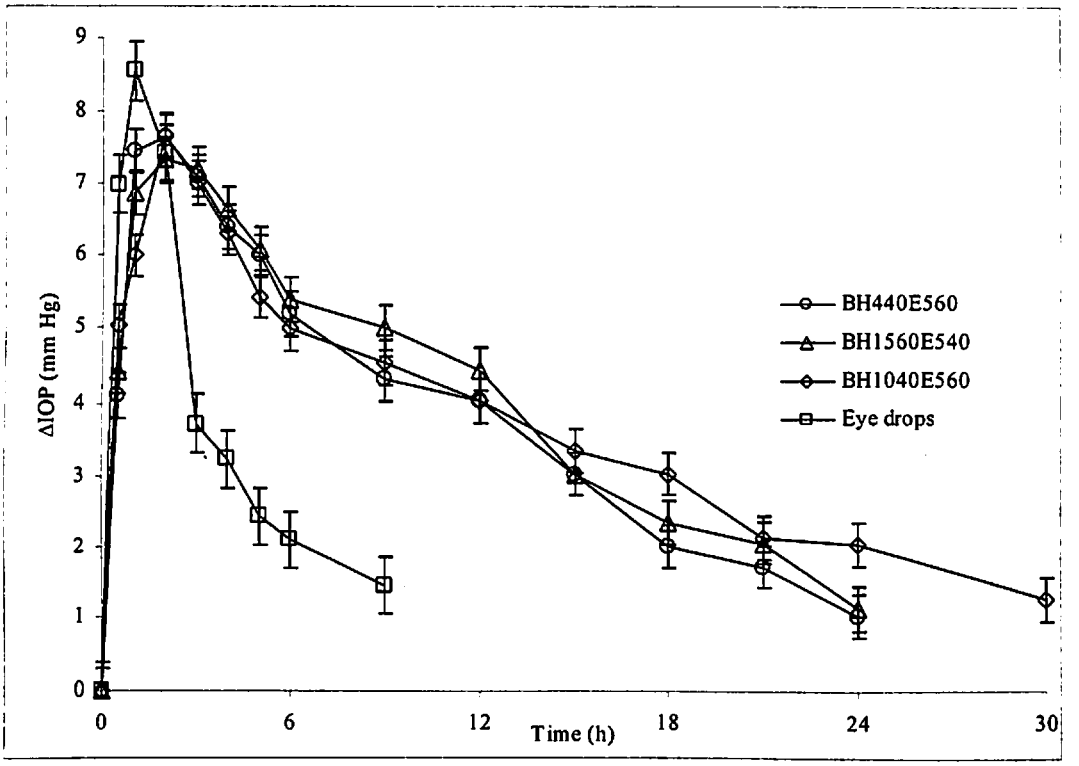

Fig 8.8: Comparative IOP reduction profile for the selected brimonidine tartrate ocular insert formulations HPMC (K4M, K15M, K100M) and EC 50 in comparison to commercial eye drop (Iobrim® E/D) in glaucomatous rabbits. Each data point represents the average of three measurements per animal (no. of animals = 3) with standard deviation.

Table 8.9: Results of in vivo pharmacodynamic efficacy studies of selected brimonidine tartrate ocular insert formulations (HPMC and EC) in comparison to commercial BRT eye drops (Iobrim® E/D) in glaucomatous rabbits.

Formulation	I_{max} (mm Hg)	t_{max} (h)	$AUC_{(\Delta IOP\ vs.\ t)}$ (h.mm Hg)	Slope	Duration (h)	AUC_{Rel}
Eye drops (Iobrim® E/D)	8.55 ± 0.21	1	38.40 ± 4.22	0.4763	6	-
BH440E560	7.65 ± 0.42	3	94.32 ± 4.54	0.1754	24	2.5
BH1560E540	7.33 ± 0.35	3	84.80 ± 3.34	0.1762	24	2.2
BH1040E560	7.67 ± 0.42	3	105.25 ± 5.21	0.1622	30	2.7

I_{max}: Maximum reduction in IOP (mm Hg), t_{max} : time taken for maximum reduction in IOP (h), $AUC_{(\Delta IOP\ vs.\ t)}$: Area under the ΔIOP vs. time curve, Slope: slope of terminal linear portion of ΔIOP vs. time curve, AUC_{Rel}: Ratio of AUC $_{(\Delta IOP\ vs.\ t)}$ Test (designed formulations) to AUC $_{(\Delta IOP\ vs.\ t)}$ Reference (marketed eye drops). Each data point represents the average of three measurements per animal (no. of animals = 3) with standard deviation.

8.4. CONCLUSIONS

All the formulations selected for the in vivo studies based on their in vitro performance parameters showed no ocular irritability and toxicity. All the selected formulations were well tolerated and no reflex tearing or lacrymation was observed in any of the formulations.

In case of ocular in situ gel formulations, both ion activated in situ gelling system (gellan gum based) and temperature activated system [poly-(N isopropylacrylamide)] based showed improved pharmacodynamic responses in comparison to the eye drops preparation of BRT. The IOP reduction profile and the AUC $_{(\Delta IOP\ vs.\ t)}$ of ΔIOP vs. time plots for selected in situ gel formulations suggested that the IOP reduction efficacy of in situ gels were more and lasted for a longer period of time. This could in turn improve the therapeutic response in glaucoma treatment with reduced frequency of administration.

The nanoparticle formulations (Eudragit based and chitosan based) were found to decrease the elevated IOP in rabbits for a longer period of time. The AUC $_{(\Delta IOP\ vs.\ t)}$ for the selected formulations were about 3-7 times higher than that of eye drops preparation. The slow elimination of administered particles from the eye with controlled release of encapsulated drug makes them a potential carrier for the delivery of drug in the treatment of glaucoma. Eudragit based nanoparticles showed IOP reduction ability up to 72 h (BENP-1:1(150)), thus can potentially decrease the frequency of administration to once in three days.

Ocular inserts, on the other hand based on combination of hydrophilic/ erodible with hydrophobic/ inert/ zwitterionoic polymers showed improved pharmacodynamic response in terms of AUC $_{(\Delta IOP\ vs.\ t)}$ for decrease in ΔIOP vs. time profile and slower rate of elimination from the eye. All the selected ocular insert formulations showed a 2-3 times increase in the AUC $_{(\Delta IOP\ vs.\ t)}$ in comparison to eye drops preparation. Hence the designed ocular insert formulations have been found to improve the therapeutic response in glaucoma and can decrease the frequency of administration of BRT and potentially improve patient compliance.

All the selected formulations were found to have improved IOP reduction efficacy in glaucoma induced rabbit model. Since the study was carried our in rabbits with the optimised conditions of glaucoma induction and model optimisation, the out come of the study can be used in the potential development of better formulations for BRT.

8.5. REFERENCES

Ahmed FAKM, Chaudhary P, Sharma SC. 2001. Effects of increased intraocular pressure on rat retinal ganglion cells. Int. J. Dev. Neurosci, 19; 209-218.

Anumolu SS, Singh Y, Gao D, Stein S, Sinko JP. 2009. Design and evaluation of novel fast forming pilocarpine-loaded ocular hydrogels for sustained pharmacological response. J. Control. Release, 137; 152-159.

Draize JH, Woodard G, Calvery HO. 1944. Methods for the study of irritation and toxicity of substances applied topically to the skin and mucous membranes. J. Pharmacol. Exp. Ther, 82, 377-390.

Fernandez DR, Ramirez JM, Trivino A, Sanchez D, Paraiso P, Garcia DLM, Ramirez A, Salazar JJ, Fernandez CA, Gutkowska J. 1991. Experimental glaucoma significantly decreases atrial natriuretic factor (ANF) receptors in the ciliary processes of the rabbit eye. Exp. Eye Res, 53; 591-596.

Fridriksdottir H, Loftsson T, Stefansson E. 1997. Formulation and testing of methazolamide cyclodextrin eye drop solutions. J. Control. Release, 44; 95-99.

Hathout RM, Mansour S, Mortada ND, Guinedi AS. 2007. Liposomes as an ocular delivery system for acetazolamide: in vitro and in vivo studies. AAPS PharmSciTech, 8; E1-E11.

Himber J, De Burlet G, Andermann G. 1989. Effects of adrenergic agents on alpha-chymotrypsin induced ocular hypertension in albino and pigmented rabbits: A comparative study. J. Ocul. Phurmacol, 5; 93-98.

Johnson TV, Tomarev IS. 2010. Rodent models of glaucoma. Brain Research Bulletin, 81; 349-358.

Kaur IP, Singh M, Kanwar M. 2000. Formulation and evaluation of ophthalmic preparations of acetazolamide. Int. J. Pharm, 199; 119-127.

Palma SD, Tartara LI, Quinteros D, Allemandi DA, R. Longhi MR, Granero GE. 2009. An efficient ternary complex of acetazolamide with HP-ß-CD and TEA for topical ocular administration. J. Control. Release, 138; 24-31.

Percicot CL, Schnell, CR. Debon C, Hariton C. 1996. Continuous Intraocular Pressure Measurement by Telemetry in Alpha-Chymotrypsin-Induced Glaucoma Model in the Rabbit: Effects of Timolol, Dorzolamide, and Epinephrine. J. Pharmacol. Toxicol. Methods, 36; 223-228.

Ruiz-Ederra J, Garcia M, Hernandez M, Urcola H, Hernandez EB, Araiz J, Vecino E. 2005. The pig eye as a novel model of glaucoma. Exp. Eye Res, 81; 561-569.

Ruiz-Ederra J, Verkman AS. 2006. Mouse model of sustained elevation in intraocular pressure produced by episcleral vein occlusion. Exp. Eye Res, 82; 879-884.

Saettone MF, Giannaccini B, Barattini F, Tellini N. 1982. The validity of rabbits for investigations on ophthalmic vehicles: A comparison of four different vehicles containing tropicamide in humans and rabbits. Pharm. Acta. Helv, 57; 47-55.

Soldati L, Gianesello V, Galbiati I, Gazzaniga A, Virno M. 1993. Ocular pharmacokinetics and pharmacodynamics in rabbits of ibopamine: a new mydriatic agent. Exp. Eye. Res, 56; 247-254.

Urcola JH, Hernandez M, Vecino E. 2006. Three experimental glaucoma models in rats: Comparison of the effects of intraocular pressure elevation on retinal ganglion cell size and death. Expt. Eye Res, 83; 429-437.

Urtti A, Salminen L. 1993. Animal Pharmacokinetic Studies. In A. K. Mitra (Ed.), Ophthalmic drug delivery systems, New York, Marcel Dekker; 121-136.

Worakul N, Robinson JR. 1997. Ocular pharmacokinetics/pharmacodynamics. Eur. J. Pharm. Biopharm, 44; 71-83.

CHAPTER NINE

CONCLUSIONS

CONCLUSIONS

Glaucoma, characterized by rise in IOP, is the second largest cause of blindness worldwide. The increased incidence of glaucoma and its complications necessitates better therapeutic understanding of the disease with improved delivery systems for antiglaucoma agents. The formulations which are currently available are mostly solution formulations, which either suffer from poor bioavailability or pose a serious systemic toxicity as majority of anti glaucoma drugs are potent and have severe cardiovascular effects. They also have poor patient compliance due to requirement of frequent instillation of 3-4 times a day.

In order to overcome the drawbacks, it was envisaged to design and develop novel ophthalmic delivery systems which can improve ocular bioavailability and minimise systemic adverse effects. Brimonidine tartrate is a selective alpha-2 agonist, used in the treatment of open angle glaucoma. It has been shown to have neuroprotective action on the degenerating RCG cells in glaucoma. The improvement of drug delivery could be attained either by improving the residence time of the dosage form in the eye or by improving the precorneal absorption along with imparting prolonged release characteristics.

To fulfil the above objectives, it was envisaged to prepare long acting novel ocular drug delivery systems such as in situ gels, ocular inserts and nanoparticles of BRT with improved precorneal residence time and prolonged drug release characteristics.

For the purpose of drug estimation in designed formulations, in vitro drug release and stability samples, an analytical method based on UV-Visible spectrophotometry was developed and validated as per ICH guidelines. The analytical method developed was found to be rapid, simple, accurate, precise, selective for the drug and robust.

Preformulation studies were carried out to determine the solubility, solution state stability, partition coefficient, dissociation constant and drug excipient compatibility. The drug was water soluble and was found have a pH dependent solubility. The pKa was found to be 7.22. DSC studies confirmed that the drug was compatible with the selected excipient.

In situ gels were prepared using ion activated in situ gelling polymer (gellan gum) and temperature activated in situ gelling systems [poly (N isopropyl acrylamide)]. The prepared gellan gum based in situ gels gelated upon contact with monovalent and/or divalent cations present in the tear fluid and upon contact with eye temperature in case of PNIAA based in situ gels. The prepared in situ gels were found to be mucoadhesive. The rheological studies showed that the in situ gels were pseudoplastic in nature with viscosity

decreasing with increase in shear, thus making them suitable for ocular administration. The in vitro drug release was prolonged and controlled for a longer period of time. The selected formulations, upon in vivo pharmacodynamic efficacy studies were found to be more efficacious in terms of IOP reduction efficacy compared to marketed preparations. The AUC_{Rel} was increased by about 3 folds, indicating that the developed in situ gels have a potential for improving the therapeutic efficacy.

Ocular inserts, prepared using hydrophilic/ swellable/ erodible polymers and hydrophobic/ inert/zwitterionoic polymers, either alone or in combinations showed good physicochemical characteristics. The addition of hydrophilic polymer (PEO or HPMC) to the ocular inserts increased the mucoadhesion. The in vitro release of BRT was found to be more prolonged and controlled. The addition of hydrophobic (EC) and inert/ zwitterionoic polymer (ERL 100 and ERS 100) to the ocular insert matrix greatly prolonged the release of drug. In vivo studies revealed that the selected ocular insert formulations showed better IOP reduction capacity with respect to eye drops. The IOP reduction profile was more prolonged and was maintained for a longer period of time. The AUC_{Rel} was found to be 2.5 to 3 times more than the eye drop formulations.

Nanoparticle formulations of brimonidine tartrate were prepared by using ERL 100 and ERS 100 by multiple emulsion solvent evaporation method and chitosan by ionotropic gelation method. The particle size, drug loading and encapsulation efficiency were found to be dependent on various formulation and process variables. The particle size of the optimised formulations were found to be in the range of 250-350 nm and the drug loading was sufficiently high. The in vivo studies showed that the selected nanoparticle formulations showed much better IOP reduction profile and the duration effectiveness was extended up to 48-72 h with AUC_{Rel} showing 5-7 fold increase.

Thus, the developed formulations have a potential to improve the drug delivery in glaucoma with improved therapy and reduced dose and dosing frequency.

Future prospects

This research work may be further extended by using several other polymers in case of ocular inserts such as hydrophilic/hydrophobic polymers reported recently. The in situ gels formulations may be further optimized by carrying out studies on understanding human ocular contact times and evaluating the therapeutic efficacy in higher primates. More approaches can be investigated to further improve the drug loading in nanoparticles.

Formulation optimization and process validation studies need to be conducted to scale-up the manufacturing process to industrial scale. Proof of concept clinical study in glaucomatous patients also need to be performed.

List of Publications and Presentations

Publications

1. **Prakash Bhagav**, Sajeev Chandran, Sujitha Vattikonda. Formulation and in-vitro evaluation of sustained release ophthalmic gels of rebamipide for treating dry eye syndrome; AAPS Journal, 9 (S2), 2007, Abstract M1214.
2. **Prakash Bhagav**, Pandurang Deshpande, Saurabh Pandey, Sajeev Chandran. Development and validation of stability indicating UV spectrophotometric method for the estimation of brimonidine tartrate in pure form, formulations and preformulation Studies. Der Pharmacia Lettre, 2010, 2(3): 106-122.
3. **Prakash Bhagav**, Sajeev Chandran. Novel Sustained Release Ocuserts of Brimonidine Tartrate for Better Treatment in Open Angle Glaucoma. Drug Delivery and Translational Research (Accepted).
4. **Prakash Bhagav**, Hari Om Upadhyay, Sajeev Chandran. Design and Evaluation of Brimonidine Tartrate-Eudragit Long Acting Nanoparticle Formulations for the Improved Treatment Glaucoma. AAPS Pharmascitech (Communicated)
5. **Prakash Bhagav**, Durlabh Sharma, Sajeev Chandran. Novel ocular in Situ Gel Preparations of Brimonidine Tartrate: Formulation, Optimization, in Vitro and in Vivo Evaluation. Drug Delivery (Communicated).
6. **Prakash Bhagav**, Luv Bagga, Sajeev Chandran. Chitosan Nanoparticles of Brimonidine Tartrate for Ocular Delivery: Formulation, Optimization, in Vitro and in Vivo Evaluation. Journal of Drug Targetting (Communicated)

Paper presentations

1. **Prakash Bhagav**, Vinay Kumar, Mohammad Imran, Sajeev Chandran. Studies on solubilization and stabilization of viscous ophthalmic gels of cyclosporine and 5-fluorouracil at 7th International Symposium on Advances in Technology and Business Potential of New Drug Delivery Systems, Organized by Controlled Release Society Inc. USA, Indian Chapter, 13-14 Feb. 2007, Mumbai, India.**[Received best poster award]**

2. **Prakash Bhagav**, Sujitha Vattikonda. Sajeev Chandran. Preparation and in vitro evaluation of sustained release mucoadhesive ophthalmic gels of brimonidine tartrate for treating glaucoma; 59th Indian Pharmaceutical Congress, 20-23 Dec, 2007, Varanasi. India.

3. **Prakash Bhagav**, Sajeev Chandran. Design and development of matrix based ocular controlled release inserts of brimonidine tartrate; 59th Indian Pharmaceutical Congress, 20-23 Dec, 2007, Varanasi, India.

4. **Prakash Bhagav**, Vinay Kumar, Mohammad Imran, Sajeev Chandran. Studies on viscous emulsion type formulations of 5-Fluorouracil and Cyclosporine for improved ocular delivery; 13th National Conference on "Surfactants, Emulsions and Biocolloids with special focus on Biomimetic Systems (NATCOSEB XIII-BIMS)" Organized by Chemistry Group, BITS, Pilani, 22-24 Feb, 2007, Pilani, India.

5. **Prakash Bhagav**, Sujitha Vattikonda, Sajeev Chandran. Controlled release ophthalmic formulations of rebamipide for improved efficacy in dry eye syndrome; 8th International Symposium on Advances in Technology and Business Potential of New Drug Delivery Systems, Organized by Controlled Release Society Inc. USA, Indian Chapter, 26-27 Feb, 2008, BV Patel PERD Centre, Ahmadabad, India

6. **Prakash Bhagav**, Hari Om Upadhyay, Sajeev Chandran. Design and evaluation of brimonidine tartrate-Eudragit nanoparticles for ophthalmic delivery. AAPS annual meeting and exposition. Nov 8-12, 2009. Los Angeles. CA. USA.

7. **Prakash Bhagav**, Sajeev Chandran. Development, design and evaluation of in-situ gels for improved ophthalmic delivery of brimonidine tartrate in glaucoma. AAPS Conference AAPS annual meeting and exposition. Nov 8-12, 2009. Los Angeles. CA. USA.

8. **Prakash Bhagav**, HariOm Upadhyay, Sajeev Chandran. Design And Evaluation Of Long Acting Eudragit Nanoparticles For Topical Ophthalmic Delivery Of Brimonidine Tartrate. 37th Annual Meeting & Exposition of the Controlled Release Society. July10-14, 2010, Oregon Convention Center Portland, Oregon, U.S.A.

Biography of Prakash Bhagav

Mr. Prakash Bhagav has completed his bachelor degree in Pharmacy (B.Pharm) from Manipal College of Pharmaceutical Sciences, Manipal, Karnataka in the year 2003 and Post Graduation (M.Pharm) in Pharmaceutics from Government College of Pharmacy, Bangalore, Karnataka in the year 2005. He has been carrying out his research as research scholar at Pharmacy Group, BITS, Pilani from 2006 to 2010 in the institute under the supervision of Dr. Sajeev Chandran. He has published 02 research papers in peer reviewed journals. Several of his research papers are under review with international peer reviewed journals. He has also presented/ co-authored 08 research papers at national and international conferences.

Biography of Dr. Sajeev Chandran

Dr. Sajeev Chandran is currently working as Sr. Manager, Advanced Drug Delivery Systems- R & D, Pharma R & D, Lupin Research Park, Lupin Ltd, Pune since Dec 2008. Prior to joining Lupin Dr. Sajeev Chandran served as Assistant Professor of Pharmacy & Assistant Dean, Engineering Services Division at Birla Institute of Technology and Science, Pilani. He completed his B. Pharm. from Institute of Technology, Banaras Hindu University, Varanasi in 1996 and M. Pharm. from Birla Institute of Technology & Science, Pilani in 1998. He earned his Ph.D. degree in Pharmaceutics (Novel Drug Delivery System Design) from Birla Institute of Technology & Science, Pilani in 2003 and a M.B.A. in Operation Management in 2004. Dr. Sajeev Chandran is recipient of *'Young Pharmacy Teacher of the Year Award- 2008'* from Association of Pharmaceutical Teachers of India (APTI), and *'Young Scientist Award'* in 2005 from Dept. of Science & Technology, Govt. of India. He has also received national awards like, Professor M. L. Khorana Memorial Award, Aruna & Malviya Gold medal, Professor G. P. Srivastava memorial award and G. P. Nair IDMA award.

Dr. Chandran has 11 years of UG and PG level teaching experience and more than 5 years of administrative experience at BITS, Pilani and 03 years of combined experience of working in Pharmaceutical R&D. He is presently engaged in research in the area of 'Design and development of advanced drug delivery systems'. He has supervised one PhD doctoral work and currently one candidate is pursuing his doctoral research work under his supervision from BITS, Pilani. He has supervised more than 50 M. Pharm projects/ dissertations and around 100 undergraduate projects. He has authored one laboratory manual and has more than 40 research papers in peer reviewed journals of international repute. He has 07 patent applications in the area of advanced drug delivery system under various stages of evaluation. He has presented or co-authored more than 75 research papers in various national and international conferences. At BITS- Pilani, he has participated as Principal or Co-investigator in around 08 major research projects from Industries and Govt. agencies.

Modeling of dissolution data and release rate kinetics

I. Korsmeyer-Peppas model

$$M_t / M_\infty = Kt^n$$

Where, M_t / M_∞ is fraction of drug released at any time 't', K is release rate constant incorporating the structural and geometric characteristics of the tablets and n is the diffusional exponent, indicative of the release mechanism.

Type of release mechanism	Cylinder[a]		Sphere	
	Non-swellable system	Swellable system	Non-swellable system[b]	Swellable system
Quasi-Fickian	n<0.45	n<0.45	n<0.43	n<0.43
Fickian (Case-I)[c]	n = 0.45	n = 0.45	n = 0.43	n = 0.43
Non-Fickian (anomalous)[e]	0.45<n<1.0	0.45<n<0.89	0.43<n<1.0	0.43<n<0.85
Case-II (zero order)[f]	n=1.0	n=0.89	n=1.0	n=0.85
Super case I I[g]	n>1.0	n>0.89	n>1.0	n>0.85

[a] : Applicable to tablet based formulations

[b] : Applicable to microsphere based systems

[c] : Refers to pure Fickian based diffusion mechanism with negligible polymer relaxation

[d]: Combination of both diffusion process and polymer relaxation controls the transport of molecules

[f] : Polymer relaxation predominantly controls the movement of molecules with negligible diffusion

[g] : Release mechanism is erosion controlled.